JAERI 1344

JAERI 1344

JP0250127

JENDL Dosimetry File 99 (JENDL/D-99)

January 2002

日 本 原 子 力 研 究 所

Japan Atomic Energy Research Institute

JAERIレポートは，日本原子力研究所が研究成果編集委員会の審査を経て不定期に公刊している研究報告書です。

入手の問合わせは，日本原子力研究所研究情報部研究情報課（〒319-1195　茨城県那珂郡東海村）あて，お申し込み下さい。なお，このほかに財団法人原子力弘済会資料センター（〒319-1195　茨城県那珂郡東海村日本原子力研究所内）で複写による実費頒布をおこなっております。

JAERI reports are reviewed by the Board of Editors and issued irregularly.

Inquiries about availability of the reports should be addressed to Research Information Division, Department of Intellectual Resources, Japan Atomic Energy Research Institute, Tokai-mura, Naka-gun, Ibaraki-ken 319-1195, Japan.

編集兼発行　日本原子力研究所

JENDL Dosimetry File 99 (JENDL/D-99)

Katsuhei KOBAYASHI[*1], Tetsuo IGUCHI[*2], Shin IWASAKI[*3], Takafumi AOYAMA[*4], Satoshi SHIMAKAWA[+], Yujiro IKEDA[++], Naoteru ODANO[*5], Kiyoshi SAKURAI[+++], Keiichi SHIBATA, Tsuneo NAKAGAWA and Masaharu NAKAZAWA[*6]

Department of Nuclear Energy System
Tokai Research Establishment
Japan Atomic Energy Research Institute
Tokai-mura, Naka-gun, Ibaraki-ken

(Received September 4, 2001)

Abstract

The JENDL Dosimetry File 99 (JENDL/D-99), which is a revised version of the JENDL Dosimetry File 91 (JENDL/D-91), has been compiled and released for the determination of neutron flux and energy spectra. This work was undertaken to remove the inconsistency between the cross sections and their covariances in JENDL/D-91 since the covariances were mainly taken from IRDF-85 although the cross sections were based on JENDL-3. Dosimetry cross sections have been evaluated for 67 reactions on 47 nuclides together with covariances. The cross sections for 34 major reactions and their covariances were simultaneously generated, and the remaining 33 reaction data were mainly taken from JENDL/D-91. Latest measurements were taken into account in the evaluation. The resultant evaluated data are given in the neutron energy region below 20 MeV in both of point-wise and group-wise files in the ENDF-6 format. In order to confirm the reliability of the evaluated data, several integral tests have been carried out: comparisons with average cross sections measured in fission neutron fields, fast/thermal reactor spectra, DT neutron fields and Li(d,n) neutron fields. It was found from the comparisons that the cross sections calculated from JENDL/D-99 are generally in good agreement with the measured data. The contents of JENDL/D-99 and the results of the integral tests are described in this report. All of the dosimetry cross sections are shown in a graphical form in the Appendix.

Keywords: Dosimetry, Cross Section, Covariance, JENDL/D-99, ENDF-6 Format, Integral Test, Average Cross Section, Standard Neutron Field, Cf-252 Spontaneous Fission Spectrum, U-235 Fission Spectrum, DT Neutron Field, Li(d,n) Neutron Field, ISNF, CFRMF, ΣΣ, YAYOI, JOYO, JMTR.

+ Department of HTTR Project, Oarai Research Establishment
++ Center for Neutron Science
+++ Nuclear Safety Research Center
*1 Research Reactor Institute, Kyoto University
*2 Faculty of Engineering, Nagoya University
*3 Faculty of Engineering, Tohoku University
*4 Oarai Engineering Center, Japan Nuclear Cycle Development Institute
*5 Nuclear Technology Division, National Maritime Research Institute
*6 Faculty of Engineering, University of Tokyo

JENDL ドシメトリーファイル 99 (JENDL/D-99)

日本原子力研究所東海研究所エネルギーシステム研究部

小林 捷平[*1]・井口 哲夫[*2]・岩崎 信[*3]・青山 卓史[*4]・島川 聡司[+]・池田 裕二郎[++]
小田野 直光[*5]・桜井 淳[+++]・柴田 恵一・中川 庸雄・中沢 正治[*6]

(2001 年 9 月 4 日受理)

要　旨

中性子束及びエネルギースペクトルの決定のために、JENDL ドシメトリーファイル 91 (JENDL/D-91) の改訂版である JENDL ドシメトリーファイル 99 (JENDL/D-99) を編集し、公開した。JENDL-91 では断面積は JENDL-3、共分散は IRDF-85 をベースにしており、一貫性を欠いていたため、今回の改訂作業を行った。47 核種、67 反応のドシメトリー断面積及びその共分散を評価した。主たる 34 反応の断面積及び共分散は同時に評価され、残りの 33 反応のデータは主に前版 JENDL/D-91 から採用した。評価に際しては、最新の測定データを考慮した。評価データは、20MeV 以下のエネルギー範囲において、ENDF-6 フォーマットで point-wise ファイルと group-wise ファイルの 2 種類で与えられている。データの信頼性を確認するために、核分裂中性子場、高速/熱中性子炉の中性子場、DT 中性子場及び Li(d,n) 中性子場での平均断面積値との比較による積分テストを行った。これらの比較から JENDL/D-99 による計算結果は測定値と一般的に良く一致していることが分かった。本報告では、JENDL/D-99 ファイルの内容と積分テストの結果について述べる。また、付録に評価したドシメトリー断面積の図を掲載する。

東海研究所：〒319-1195 茨城県那珂郡東海村白方白根 2 - 4
+　大洗研究所高温工学試験研究炉開発部
++　中性子科学研究センター
+++　安全性試験研究センター
*1　京都大学原子炉実験所
*2　名古屋大学大学院工学研究科
*3　東北大学大学院工学研究科
*4　核燃料サイクル開発機構大洗工学センター
*5　海洋技術安全研究所原子力技術部
*6　東京大学大学院工学系研究科

Contents

目　次

List of Tables

List of Figures

This is a blank page.

1. Introduction

A dosimetry file is a data set of neutron reaction cross sections which are basically used for the determination of neutron flux/fluence and energy spectrum at specific neutron fields. While the IRDF-85 dosimetry file[1] mainly based on ENDF/B-V[2] was so far used widely as the standard in various research fields, it was a strong request for the dosimetry applications to make a Japanese dosimetry file in the framework of the Japanese Evaluated Nuclear Data Library Version 3 (JENDL-3)[3]. Corresponding to this requirement, the Dosimetry Integral Test Working Group (DITWG) of the Japanese Nuclear Data Committee was organized to endeavor to issue the first Japanese dosimetry file named JENDL Dosimetry File (JENDL/D-91)[4]. After the first version of the dosimetry file was compiled and released, it was expected to have a more consistent dosimetry cross section data set, because the cross sections were mainly taken from the JENDL-3 file and the covariance data from IRDF-85. The IAEA developed a dosimetry file referred to as IRDF-90V2[5] which included various evaluations available up to 1991. This file contains cross sections for 58 dosimetry reactions as well as covariances. The quality of the IRDF-90V2 was uncertain although it has been widely used. Under such circumstances, the DITWG started re-evaluating the dosimetry cross sections together with the covariance data for the revised version, JENDL Dosimetry File 99 (JENDL/D-99), using the GMA code[6] or the spline fitting method[7] from the basic experimental data in EXFOR[8]. In the evaluation for JENDL/D-99, latest measurements were taken into account, and the cross sections and covariances for major reactions were simultaneously generated in a consistent way. The evaluated data contains cross sections for 67 reactions on 47 nuclides together with covariances. Intending that the file is useful not only for reactor dosimetry but also for neutron dosimetry in the higher energy region, some of the (n,2n) and (n,γ) reactions have been newly included in the file.

In general, higher accuracy and reliability are required for cross sections in the dosimetry file. Moreover, various applications need appropriate cross sections sensitive to the specific neutron energy spectra depending on the field characteristics. In this context, extensive efforts have been devoted to the integral test of the cross sections included in this dosimetry file by using available neutron fields, verifying adequacy of the data in terms of reliability and consistency.

In Chapter 2, given is the documentation of the JENDL Dosimetry File 99 (JENDL/D-99) with the list of the reactions included and the data structure. Graphs of evaluated cross sections are shown in the Appendix. In Chapters 3 and 4, average cross sections calculated with the JENDL/D-99 and/or -91 files are compared with the measurements in the various benchmark neutron fields relating to fission reactors and fusion reactors, and the present status of the integral test of the file is discussed.

Sixty-seven nuclear reactions have been considered in the present JENDL/D-99 and they are selected mainly for dosimetry applications to fission reactor fields, 14 MeV neutronic experiments and spallation neutron fields, as in the cases of IRDF-85[1] and JENDL/D-91[4]. This is a reason why many reactions are common to the JENDL/D and IRDF. Precise comparisons with the integral tests have been summarized in Chapter 5.

2. Compilation of JENDL Dosimetry File 99

2.1 Activities of Dosimetry File Integral Test Working Group

2.1.1 General Description of the Working Group

To compile and test the first Japanese Dosimetry File (JENDL/D-91)[4], a working group was organized in 1987 in the framework of JENDL-3[3] nuclear data evaluation. At the moment to start the tasks of compilation of data, dosimetry files available, such as IRDF-85[1] and ENDF/B-V[2], were referred to get basic idea for the JENDL/D-91. The first step was to identify and select the reactions to be included regarding the importance, availability and coverage for the energy of extending interest. In the first file, JENDL/D-91, since the covariance data were not produced simultaneously in the cross section evaluation, the covariance matrices were mainly taken from the IRDF-85.

After the first file was released, there were discussions that the covariance matrices should be produced together with the evaluated cross section values. In order to get the consistency between the cross sections and their covariance matrices for the main dosimetry reactions, in 1996, the working group started again the evaluation work to revise JENDL/D-91.

2.1.2 Selection of Dosimetry Reactions

The basic idea was to provide a dosimetry cross section set based on JENDL-3.2[9]. Whatever the reactions of importance were in the JENDL-3.2 general purpose file, the JENDL-3.2 data were suited in the dosimetry file so that fully consistent data set could be provided. However, there should have been various useful reactions but not included in the JENDL-3.2 general purpose file, because the reactions were highly specific to the dosimetry purpose. They are ^{64}Zn(n,p)^{64}Cu, ^{93}Nb(n,2n)^{92m}Nb, ^{115}In(n,γ)^{116m}In, ^{169}Tm(n,2n)^{168}Tm, ^{197}Au(n,2n)^{196}Au, ^{197}Au(n,γ) ^{198}Au, ^{199}Hg(n,n')^{199m}Hg. The covariance matrices of natural Ti cross sections were newly obtained from the isotopic contributions in this evaluation work. The reactions of ^{93}Nb(n,n') and ^{199}Hg(n,n') seemed attractive due to considerably low threshold energies below 1 MeV. These two reaction cross sections were evaluated in the framework of the JENDL/D-91 file compilation[4]. It has been considered of importance to include those reactions because the deficiency of such low threshold reactions has been so often quoted. The reaction of ^{169}Tm(n,2n)^{168}Tm, which is not included in IRDF-90V2[5], is one of the attractive dosimetry cross sections in the high energy region.

Four capture reactions, namely, ^{109}Ag(n,γ)^{110m}Ag, ^{151}Eu(n,γ)^{152}Eu, ^{181}Ta(n,γ)^{182}Ta and ^{186}W(n,γ)^{187}W, were included in view of the importance in the thermal reactor dosimetry although the latter three reactions were not included in IRDF-90V2[5] .

2.1.3 Scenario of the Integral Test

Comparison with IRDF

Preliminary consistency check on a prototype file was made through comparing with the cross sections in IRDF-90V2 by calculating spectrum-averaged cross sections in 12 kinds of benchmark neutron spectra, numerical data for ten of which were available in IRDF-90. The results of comparison will be given in detail in section 3.1.

Neutron Fields

In order to assure the quality of the reaction cross sections in JENDL/D-99, integral tests have been performed.

We have used four neutron fields for the integral test as follows:

(1) ^{252}Cf and ^{235}U fission neutron fields,

(2) ISNF/CFRMF/BIG-TEN/ΣΣ/ORR/YAYOI/NEACRP/JOYO/JMTR reactor neutron fields,

(3) D-T fusion neutron field,

(4) D-Li neutron field.

These have been selected as the testing fields because many experimental data of dosimetry reaction rates are available with reasonable accuracy. The neutron spectra are different from each other, covering wide sensitive energy range from thermal to the energy higher than 15 MeV.

Integral Test

Comparison between the experimental data and the calculations of spectrum-averaged cross sections was carried out by considering uncertainties estimated from covariance matrices. The covariance matrices for most of the dosimetry cross sections in JENDL/D-99 were simultaneously produced in the cross section evaluation. However, the matrices which were not produced in JENDL/D-99 were tentatively taken from the JENDL/D-91 data file. The covariance between fluxes in different energies for the benchmark neutron spectrum was generated on the assumption that diagonal and off-diagonal elements were 5 and 2%, respectively[10]. Details of the treatment of the error will be described in the corresponding section.

2.2 Contents of JENDL Dosimetry File 99

Table 2.2.1 shows the 67 reactions of which cross section data are stored in JENDL/D-99. Thirty-four dosimetry cross sections and the covariance matrices have been generated through the present evaluation work for the JENDL/D-99 file. Other reaction data in the file were taken from the JENDL/D-91 file. Table 2.2.1 lists the MAT numbers, reactions, threshold energies, half-lives of reaction products, and sources of cross section data and covariance matrices. In addition to the data of the reactions listed in Table 2.2.1, the total cross section is given for the nuclides whose capture and/or fission cross sections are stored, in order to calculate self-shielding factors. No covariance matrix is given for the total cross section. The data were compiled in the ENDF-6 format[19].

In compilation of JENDL/D-99, evaluation of cross section was performed at 0 K and then the point-wise data file was generated. In the point-wise data file, the fission and capture cross sections in the resolved and unresolved resonance regions were reconstructed from resonance parameters with RESENDD[20]. The group-wise data file was obtained by averaging the point-wise cross sections in the SAND-II[21] type energy intervals listed in **Table 2.2.2.** This structure is the same as that of IRDF. The calculation of average cross sections was simply carried out as follows by using CRECTJ5[22] which is a program to edit the ENDF format data,

$$\sigma_i(E) = \int_{E_i^{min}}^{E_i^{max}} \sigma(E)dE / (E_i^{max} - E_i^{min}),$$

where E_i^{min} and E_i^{max} are boundary energies of the i-th energy interval.

Followings are brief description of cross section data newly evaluated and stored in JENDL/D-99 and modified data from JENDL/D-91[4].

$^{19}F(n,2n)^{18}F$

Evaluation of the cross section and covariance data was performed with the GMA code[6] using Gauss-Markov-Aitoken least-squares method based on the selected experimental data in NESTOR-2[23], which was converted from the experimental data base EXFOR[8]. The GMA code, which is a program to derive covariance data from a set of experimental data, was often used in the present work.

$^{23}Na(n,2n)^{22}Na$

The cross section and covariance data were evaluated using the spline fitting method[7] to a set of selected experimental data taken from NESTOR-2. The evaluation was mainly based on the experimental data of Adamski et al.[24]

$^{24}Mg(n,p)^{24}Na$

The cross section and covariance data were evaluated using the GMA code from the experimental data in NESTOR-2.

$^{27}Al(n,p)^{27}Mg$

The cross section and covariance were evaluated using the GMA code from the experimental data in NESTOR-2.

$^{31}P(n,p)^{31}Si$

The cross section and covariance data were evaluated using the GMA code from the experimental data in NESTOR-2 and the nuclear model calculation by Strohmaier et al.[25]

^{46}Sc, ^{47}Sc and ^{48}Sc production from natural Ti

The cross sections were obtained from each isotope data in JENDL/D-99 as follows:

$\sigma(^{46}Sc \text{ production}) = \sigma(^{46}Ti(n,p)) \times 0.0825 + \sigma(^{47}Ti(n,np)) \times 0.0744$

$\sigma(^{47}Sc \text{ production}) = \sigma(^{47}Ti(n,p)) \times 0.0744 + \sigma(^{48}Ti(n,np)) \times 0.7372$

$\sigma(^{48}Sc \text{ production}) = \sigma(^{48}Ti(n,p)) \times 0.7372 + \sigma(^{49}Ti(n,np)) \times 0.0541$

As is described later, MT numbers are not assigned for such reactions in the ENDF-6 format. Therefore, MT's of 220, 221 and 222 were tentatively used for ^{46}Sc, ^{47}Sc and ^{48}Sc production cross sections, respectively. Covariance matrices were also obtained from each isotope data in JENDL/D-99.

$^{46}Ti(n,2n)^{45}Ti$

This cross section was not considered in JENDL/D-91. The cross section and covariance were evaluated using the GMA code from the experimental data in NESTOR-2.

$^{46}Ti(n,p)^{46}Sc$

The cross section and covariance data were evaluated using the GMA code from the

experimental data in NESTOR-2.

^{47}Ti(n,np)^{46}Sc and ^{47}Ti(n,p)^{47}Sc

The cross section was evaluated by eye-guide based on the experimental data. The covariance was evaluated by the KALMAN code system[12], which was designed to calculate cross-section covariances from uncertainties in parameters required as input to nuclear model codes.

^{48}Ti(n,np)^{47}Sc

The cross section and covariance data were evaluated using the KALMAN code from the experimental data in NESTOR-2.

^{48}Ti(n,p)^{48}Sc

The cross section and covariance data were evaluated using the GMA code from the experimental data in NESTOR-2.

^{49}Ti(n,np)^{48}Sc

The cross section and covariance data were evaluated using the GMA code from the experimental data in NESTOR-2.

^{50}Cr(n,γ)^{51}Cr

The cross section was not considered in JENDL/D-91. The cross section was taken from JENDL-3.2 [9] and the covariance was taken from the latest version of the U.S. library ENDF/B-VI[14].

^{52}Cr(n,2n)^{51}Cr

The cross section was not considered in JENDL/D-91. The cross section and covariance data were evaluated using the GMA code from the experimental data in NESTOR-2.

^{55}Mn(n,2n)^{54}Mn

The cross section and covariance data were evaluated using the spline fitting method to a set of the selected experimental data taken from NESTOR-2.

^{54}Fe(n,p)^{54}Mn

The cross section and covariance data were evaluated using the GMA code from the experimental data in NESTOR-2.

^{58}Fe(n,γ)^{59}Fe

In the resonance region, the variance of cross section was estimated from standard deviations of the resonance parameters. The standard deviations were taken from the experimental data which were considered in the parameter evaluation. For the resonance parameters determined from the capture area, their errors were estimated from the error of capture area. An error of 10 % was assumed for other cases. No off-diagonal elements were given in the covariance matrix. Above 350 keV, covariance matrix was obtained by using the KALMAN. Errors of the following parameters were considered: the optical potential and level density parameters, and the normalization cross section. In order to connect the two covariance matrices, an artificial covariance matrix was given in

the energy range from 250 to 700 keV.

$^{59}Co(n,2n)^{58}Co$

The cross section and covariance data were evaluated using the spline fitting method to a set of the selected experimental data taken from NESTOR-2.

$^{58}Ni(n,2n)^{57}Ni$ and $^{58}Ni\ (n,p)^{58}Co$

The cross sections and their covariance data were evaluated using the GMA code from the experimental data in NESTOR-2.

$^{60}Ni(n,p)^{60}Co$

The cross section and covariance data were evaluated using the spline fitting method to a set of the selected experimental data taken from NESTOR-2.

$^{63}Cu(n,2n)^{62}Cu$ and $^{63}Cu\ (n,\alpha)^{60}Co$

The cross section and covariance data were evaluated using the GMA code from the experimental data in NESTOR-2.

$^{65}Cu(n,2n)^{64}Cu$

The cross section and covariance data were evaluated using the GMA code from the experimental data in NESTOR-2.

$^{64}Zn(n,p)^{64}Cu$

The cross section and covariance data were evaluated using the GMA code from the experimental data in NESTOR-2.

$^{89}Y(n,2n)^{88}Y$

The cross section was not considered in JENDL/D-91. The cross section and covariance were evaluated using the GMA code from the experimental data in NESTOR-2.

$^{90}Zr(n,2n)^{89}Zr$

The cross section and covariance were evaluated using the GMA code from the experimental data in NESTOR-2.

$^{93}Nb(n,n')^{93m}Nb$

The cross section and covariance data were evaluated based on the experimental data using the least-squares method[26].

$^{93}Nb(n,2n)^{92m}Nb$

The cross section and covariance data were evaluated using the spline fitting method to a set of the selected experimental data taken from NESTOR-2.

$^{109}Ag(n,\gamma)^{110m}Ag$

The cross section was not considered in JENDL/D-91. The cross section data were taken from

EAF-99[15] whose evaluation is based on JENDL-3.2 capture cross sections and systematics on the isomeric ratio. The covariance data were taken from IRDF-90V2.

$^{127}I(n,2n)^{126}I$

The cross section and covariance data were evaluated using the GMA code from the experimental data in NESTOR-2.

$^{169}Tm(n,2n)^{168}Tm$

The cross section was not considered in JENDL-D/91. The cross section and covariance data were evaluated using the GMA code from the experimental data in NESTOR-2.

$^{186}W(n,\gamma)^{187}W$

Resolved resonance parameters at –65.4 and 18.83 eV were modified from JENDL-3.2. The calculated 2200 m/sec cross section is 37.88 b and the resonance integral is 476.1 b. The variance data were estimated by comparing with experimental data.

$^{197}Au(n,2n)^{196}Au$

The cross section and covariance data were evaluated using the GMA code from the experimental data in NESTOR-2.

$^{237}Np(n,f)$

The cross section data below 30 keV were taken from JENDL-3.2 while data above 30 keV were evaluated using the GMA code from the experimental data in NESTOR-2. The covariance data were evaluated by the GMA code.

2.3 Format of JENDL Dosimetry File 99

The JENDL/D-99 file was compiled in the ENDF-6 format[19]. In this section, a basic part of the format is briefly described. An example of the group-wise data file is given in **Fig. 2.3.1**.

In the ENDF-6 format, one record consists of the following 80 columns:

column	description
1 – 11	numerical data field 1
12 – 22	numerical data field 2
23 – 33	numerical data field 3
34 – 44	numerical data field 4
45 – 55	numerical data field 5
56 – 66	numerical data field 6
67 – 70	MAT number
71 – 72	MF number
73 – 75	MT number
76 – 80	sequential number

The MAT number in the columns from 67 to 70 identifies a nuclide or material. The MAT numbers adopted in JENDL/D-99 are determined as follows and given in Table 2.2.1.

$$MAT = atomic\ number \times 100 + 25 + 3*(N-1)$$

where N is a number corresponding to an order of isotopes. In the case of natural elements, the lower two digits are set to zero. The MF numbers are as follows.

MF	description
1	descriptive information on the data.
2	resonance parameters.
3	cross sections.
33	covariance matrices.

In MF=2 of both of the point-wise and group-wise files, only scattering radius and spin of the nuclide are given. For nuclides whose original data have the unresolved resonance parameters, the parameters are stored in the point-wise files. These parameters must be used only for self-shielding factor calculation, because the contributions from the unresolved resonance parameters have been already added to the cross sections.

The MT numbers in columns from 73 to 75 represent reaction types. The following MT numbers are used in JENDL/D-99.

MT	reactions
1	total cross section
16	(n,2n) reaction
18	fission
28	(n,np) reaction
51	inelastic scattering to the 1-st level
57	inelastic scattering to the 7-th level
102	capture
103	(n,p) reaction
107	(n,α) reaction
205	t production
207	α production
220	^{46}Sc production (used in the data of Ti)
221	^{47}Sc production (used in the data of Ti)
222	^{48}Sc production (used in the data of Ti)

The first record of the file is a tape ID record. The data are stored from the second record. A set of records with the same MT number is called as a section. Just after a certain MT section, a 'section-END record', whose MT number is set to zero, follows. If there are various MT sections, data are arranged in the increasing order of MT numbers. The set of records with the same MF number ends with an 'MF END record' (MF=0, MT=0). The last record of certain MAT data is a 'MAT END record' (MAT=0, MF=0, MT=0). After this record, the data of the next nuclide are stored. The last record of the file is a 'tape END record' (MAT=-1, MF=0, MT=0). The followings are explanations of MF's of 1, 3 and 33. MF=2 is not important for usual use of the JENDL/ D-99.

1) Descriptive data and list of contents

In the beginning of each nuclide data, descriptive information on the evaluation and compilation is given in the following format.

ZA	AWR	LRP	LFI	0	NMOD	MAT	1	451
0.0	0.0	0	0	0	6	MAT	1	451
1.0	0.0	0	0	10	3	MAT	1	451
0.0	0.0	0	0	NWD	NDC	MAT	1	451
						MAT	1	451
	descriptive data (NWD records)					MAT	1	451
						MAT	1	451
		MF_I	MT_I	NCD_I	MOD_I	MAT	1	451
						MAT	1	451
		MF_{NDC}	MT_{NDC}	NCD_{NDC}	MOD_{NDC}	MAT	1	451
						1	0	

ZA represents a nuclide as Z × 1000 + A, and AWR is weight of the nuclide in a neutron mass unit. LRP is a flag for resonance parameters. In the group-wise data file, LRP is zero for all the nuclides, which means no resonance parameters are given. For many nuclides in the point-wise data file, LRP is also zero. In only the case where the unresolved resonance parameters are given for the calculation of self-shielding factors, LRP is set to 2. LFI indicates whether this material includes fission cross sections. NMOD is the status of the evaluation. NWD is the number of descriptive information records which follow the fourth record. Just after the descriptive data records, NDC records of a content list are given. In the content list, MF, MT numbers are given with the number of records (NCD) and a modification number (MOD).

2) Cross Section Data

Cross section data are given in the following format.

ZA	AWR	0	0	0	0	MAT	3	MT
QM	QI	0	0	NR	NP	MAT	3	MT
NBP(1)	INT(1)	..	..			MAT	3	MT
E(1)	S(1)	E(2)	S(2)	E(3)	S(3)	MAT	3	MT
E(4)	S(4)	E(5)	S(5)	..	..	MAT	3	MT
..	..	E(NP)	S(NP)			MAT	3	MT
						MAT	3	0

QM : mass difference Q-value (eV).
QI : reaction Q-value (eV).
NR : number of interpolation ranges.
NP : number of energy points.
NBP, INT : interpolation method (INT) to be used up to the NBP-th energy point. The following interpolation methods can be used.

INT	description
1	S is constant in E (constant)
2	S is linear in E (linear-linear)
3	S is linear in log(E) (linear-log)
4	Log(S) is linear in E (log-linear)
5	Log(S) is linear in log(E) (log-log)

E and S are values of energy (eV) and cross section (barns). In the group-wise file, they are given at a lower limit of an energy interval, and the cross section in an interval is constant and equal to S. Therefore, only constant interpolation is used: NR= 1, NBP=NP and INT=1 (constant).

3) Covariance

The covariance data for cross sections are given in MF=33. The format for covariance data is more complicated than that for cross section data. In the JENDL/D-99 file, covariance matrices between different reactions are not given. Therefore, the description here is restricted to the explicit covariance (NI-type) and the options used in the JENDL/D-99 file. Full description of the format can be found in Ref. 19.

The MF=33 starts with the following record, and NL sub-sections follow it:

ZA AWR 0 0 0 NL MAT 33 MT

NL sets of sub-section

Each sub-section represents the covariance matrix between the cross sections for (MAT, 3, MT) and (MAT1, 3, MT1). In the JENDL/D-99 file, only one sub-section is given to describe the covariance matrix for the cross section (MAT, 3, MT) itself. Therefore NL=1, and in this case MAT1=0. The value of MT1 is given in the first record of the sub-section. The sub-section has the following structure.

0.0 0.0 0 MT1 0 NI MAT 33 MT

NI sets of sub-sub-section

The covariance matrix is a sum of those matrices described in NI sub-sub-sections. The

sub-sub-section starts with the following record.

0.0 0.0 LT LB NT NP MAT 33 MT

LB is a flag on covariance representation and NT is the number of values following this record. NP is the number of pairs of values in the arrays given in the following records. Let σ_i refer to an average cross section at energy x_i. Then,

$$COV(\sigma_i,\sigma_j) = \sum_{n=1}^{NI} COV(\sigma_i,\sigma_j)_n .$$

An element of covariance matrix described in the n-th sub-sub-section, $COV(\sigma_i, \sigma_j)_n$, is written as follows depending on the flag LB:

LB = 0 $COV(\sigma_i, \sigma_j)_n = F(x_i)$ if i=j; otherwise 0,
LB = 1 $COV(\sigma_i, \sigma_j)_n = F(x_i)\,\sigma_i\,\sigma_i$ if i=j; otherwise 0,
LB = 2 $COV(\sigma_i, \sigma_j)_n = F(x_i)\,F(x_j)\,\sigma_i\,\sigma_j$.

For these cases, NP pairs of (E, F) are given just after this record (NT=2×NP). $F(x_i)$ means the value in the energy interval containing x_i.

LB = 3 $COV(\sigma_i, \sigma_j)_n = F^k(x_i)\,F^l(x_j)\,\sigma_i\,\sigma_j$.

In this case, sets of (E, F^k) and (E, F^l) are given in this order. LT represents the number of (E, F^l) pairs, and NP is the total number of (E, F^k) and (E, F^l) pairs (NT=2×NP).

Another LB used in the JENDL/D-99 file is LB=5 where elements of covariance matrix are written as

LB = 5 $COV(\sigma_i, \sigma_j)_n = F(x_i,x_j)\,\sigma_i\,\sigma_j$,

where $F(x_i,x_j)$ denotes the value in the energy interval which contains both of x_i and x_j. In this case, if LT=0, an asymmetric matrix F is given, and if LT=1, a symmetric matrix F is given. NP is the number of energy points (NP=the number of energy interval + 1), and NT is the number of total elements. The use of LB=5 allows the representation of more complicated correlation than that of LB=3, since the two-dimensional array $F(x_i,x_j)$ is employed.

3. Integral Tests for Fission Reactors

3.1 Comparison with IRDF-90V2

3.1.1 Resonance Integral

Resonance integrals calculated from the JENDL Dosimetry File 99 (JENDL/D-99) are compared with the recommended values by Mughabghab et al.[27], those obtained from JENDL/D-91[4] and IRDF-90V2[5], and the measured data by Kobayashi et al.[28] The calculation was made above a cutoff energy of 0.5 eV, and the results are given in **Table 3.1.1**.

The resonance integrals calculated from the JENDL/D-99 are in good agreement with Mughabghab's recommendation except for the ^{55}Mn(n,γ) and ^{58}Fe(n,γ) reaction cross sections.

3.1.2 Average Cross Sections in Fission Neutron Fields

In this section, JENDL/D-99 is compared with IRDF-90V2 by calculating average cross sections using the ten standard group-wise spectra stored in IRDF-90[16], all of which are related to the fission neutron fields. In addition, in the present report, two neutron spectra of JOYO and JMTR have been used.

No.	spectra
1	^{252}Cf spontaneous fission spectrum (NBS evaluation)[29]
2	^{235}U thermal fission spectrum (NBS evaluation)[30]
3	^{235}U thermal fission spectrum (ENDF/B-V)[2]
4	Intermediate-Energy Standard Neutron Field (ISNF)[31]
5	Coupled Fast Reactivity Measurement Facility (CFRMF)[32]
6	10% ^{235}U-enriched uranium cylindrical critical assembly (BIG-TEN)[33]
7	Coupled thermal/fast uranium and boron carbide spherical assembly (ΣΣ)[34] (E < 15 MeV)
8	ORR[35] (E < 20 MeV)
9	YAYOI[36] (E < 20 MeV)
10	NEACRP benchmark spectrum[37] (E < 10.5 MeV)
11	Neutron spectrum in the core of JOYO[38]
12	Neutron spectrum in the core of JMTR[39]

The neutron spectra from 1 to 10 are given in the energy range from 10^{-4} eV to 18 MeV, except that the ΣΣ, ORR, YAYOI and NEACRP benchmark spectra are defined below 15, 20, 20 and 10.5 MeV, respectively. The neutron spectra of 11 and 12 (JOYO and JMTR) are given between 10^{-3} eV and 20 MeV and between 3.3×10^{-5} eV and 16.5 MeV, respectively. **Figures 3.1.1(a), (b), (c) and (d)** show these 12 spectra. More detailed descriptions of ISNF, CFRMF, ΣΣ, YAYOI, JOYO and JMTR are given in Section 3.3 together with comparison with experimental data.

The average cross sections were calculated from the group-wise data file in the energy range from 10^{-4} eV to 20 MeV where the spectra are given:

$$\bar{\sigma} = \sum_i \bar{\sigma}(E_i)\phi(E_i)\Delta E_i, \qquad (1)$$

where $\overline{\sigma}(E_i)$ and $\phi(E_i)$ are group-wise cross section and spectrum in the i-th energy group, and ΔE_i is an energy width of the i-th energy interval. The spectrum is normalized as follows:

$$\sum_i \phi(E_i)\Delta E_i = 1. \tag{2}$$

Error of the average cross section was estimated as:

$$(\delta\overline{\sigma})^2 = \sum_i \sum_j \{COV(\sigma(E_i)\sigma(E_j))\phi(E_i)\phi(E_j) + \sigma(E_i)\sigma(E_j)COV(\phi(E_i)\phi(E_j))\}\Delta E_i \Delta E_j, \tag{3}$$

where $COV(\sigma(E_i)\ \sigma(E_j))$ and $COV(\phi(E_i)\ \phi(E_j))$ are components of covariance matrices for the cross section and the spectrum, respectively. Since covariance matrices of spectra are not given in the IRDF-90 spectrum file, we assumed that the diagonal and off-diagonal elements for the neutron spectra would be 5% and 2%, respectively, considering the results obtained by Mannhart[40] and Kobayashi et al.[41] The following covariance matrix was assumed for all the spectra:

diagonal parts : $COV(\phi(E_i)\ \phi(E_j)) = (0.05)^2\ \phi(E_i)^2$,
off-diagonal parts : $COV(\phi(E_i)\ \phi(E_j)) = (0.02)^2\ \phi(E_i)\ \phi(E_j)$.

The average cross sections obtained with JENDL/D-99 are compared with those by IRDF-90V2 in **Tables 3.1.2 – 3.1.13**. For each spectrum, the average cross sections calculated from the JENDL/D-99 and IRDF-90V2 are given in the unit of mb. Calculated errors which include both contributions from cross section and spectrum uncertainties are given only for JENDL. The contributions from spectrum uncertainties are about 2 or 3 %. The NEACRP benchmark spectrum is defined below 10.5 MeV, and therefore the average cross sections are zero for the reactions with threshold energies larger than 10.5 MeV.

Differences between JENDL/D-99 and IRDF-90V2 were obtained as:

$$Diff. = \frac{(IRDF-90V2)-(JENDL/D-99)}{JENDL/D-99} \times 100. \tag{4}$$

They are given in the last column of each table. Furthermore, an asterisk is written at the right end of each cross section in the case where the discrepancy is larger than 5 %, 2 asterisks in the cases discrepant more than 10 %, 3 asterisks in the cases discrepant more than 20 %, and 4 asterisks in the cases discrepant more than 40 %.

As the results of comparison of the average cross sections, a large discrepancy is found for the following threshold reaction cross section:

^{47}Ti(n,np)^{46}Sc.

The following five capture cross sections are also discrepant:

$^{23}Na(n,\gamma)^{24}Na$, $^{45}Sc(n,\gamma)^{46}Sc$, $^{58}Fe(n,\gamma)^{59}Fe$, $^{109}Ag(n,\gamma)^{110m}Ag$, and $^{115}In(n,\gamma)^{116m}In$.

Other reaction cross sections are almost consistent with each other. Discrepancies among group-wise cross sections for these reactions can be seen in the figures in Appendix.

3.2 Integral Test with Fission Neutron Fields

3.2.1 Standard Neutron Fields

Standard neutron spectrum fields and neutron benchmark fields are important not only for the development of accurate and reliable reactor dosimetry techniques and surveillance programs but also for dosimetry cross section measurements and neutron detector calibrations. The standard neutron field is required to fulfill the following conditions:

1) The neutron spectrum should be known as precisely as possible.
2) Its shape should be gently-sloping without resonant peaks and dips.
3) The spectrum is reproducible in inter-laboratories.
4) The neutron flux should be flat for position and angle.
5) The absolute value of the flux should be obtained precisely.

A pure ^{235}U fission neutron field is apt to be hampered by perturbation effects arising from epithermal neutron background, wall returned and scattered neutrons. Due to these inherent disadvantages, the ^{235}U fission neutron field is superseded by the ^{252}Cf spontaneous fission neutron field. With a compact form of a ^{252}Cf source and a high specific neutron yield (2.3×10^9 n/mg/sec), the ^{252}Cf spontaneous fission neutron field can be realized to be almost free of spectrum distortion effects.

At the IAEA Consultants Meeting in 1976, the classification of benchmark neutron fields was carried out[42]. In the fast neutron energy region, the spontaneous fission neutron spectrum of ^{252}Cf was classified as belonging to the standard neutron field in category I. The thermal neutron-induced fission spectrum of ^{235}U was identified as a reference neutron field. These standard and reference neutron fields make the spectrum-averaged data very useful for the validation of energy dependent cross section evaluations.

^{252}Cf Spontaneous Fission Neutron Field

In 1970s, it was regarded that most of the ^{252}Cf spontaneous fission neutron spectrum data between 250 keV and 8 MeV were in agreement with each other. The uncertainties of the spectrum in the lower and higher energy regions were, however, still considerably large. Much effort has been concentrated on new experiments and theoretical attempts in order to investigate and resolve the data discrepancies in the ^{252}Cf fission neutron spectrum[43,44]. Although a large number of measurements of the ^{252}Cf spontaneous fission neutron spectrum were made for more than 35 years, old experiments lack a detailed description that was needed for an estimate of corrections or re-analysis of the data. In order to evaluate the ^{252}Cf fission neutron spectrum precisely, Mannhart[45] selected six differential experimental data between 25 keV and 19.8 MeV. Based on the documented uncertainties and additional information from the authors, he generated a covariance matrix for each experiment, and used these values in the data fitting process performed with the least squares

methods.

The ^{252}Cf spontaneous fission neutron spectrum evaluated by Mannhart[45] was illustrated relative to a Maxwellian distribution[46] with T=1.42 MeV in **Fig. 3.2.1**. The uncertainties were obtained from the diagonal elements of the resultant covariance matrix. The relative uncertainty is 2 % between 0.25 and 8 MeV, more than 5 % in the lower range, and more than 10 % in the higher energy range.

^{235}U Thermal Fission Neutron Field

This fission spectrum was recommended as a reference neutron field[42]. A large number of experimental works have been carried out to obtain the ^{235}U fission neutron spectrum[47], and the results have been tried to fit with semi-empirical formulas such as a Maxwellian or a Watt-type spectrum[46,48]. Theoretical works have been also performed to predict the ^{235}U fission neutron spectrum[49-52]. Kimura and Kobayashi presented the characteristics of the fission neutron spectrum with a large fission plate, and measured some fission spectrum-averaged cross sections[53,54]. Kobayashi et al. also obtained the ^{235}U fission neutron spectrum by the neutron spectrum adjustment method using multi-foil activation data[41,54].

In recent years, much attention has been paid to the covariance matrix in the neutron spectrum which is required to give the uncertainties to the calculated spectrum-averaged cross sections. However, few papers report the neutron spectrum with the covariance matrix, except for the Kobayashi's and Petilli's works[41,55], while some of recent cross section libraries contain the covariance matrix.

In ENDF/B-IV and JENDL-2, the Maxwellian distribution with E_{av} =1.98 MeV was adopted. A Watt-type spectrum was employed in ENDF/B-V. In the JENDL-3 General Purpose File[3], the Madland-Nix model description[49] was taken as the ^{235}U fission neutron spectrum. Very recently, Ohsawa[52] proposed a modified description of the Madland-Nix model and the result was taken in the JENDL-3.2. The fission spectrum in JENDL-3.2 seems to be rather underestimated than the Watt-type in the higher energy region. Works by Johansson[48], Kobayashi[41] and Nakazawa[4] support the Watt-type spectrum as the ^{235}U fission neutron spectrum, and show that the Maxwellian spectrum gives overestimation compared with the Watt-type spectrum, especially in the higher energy region above 10 MeV. The Watt-type spectrum gave general agreement between the measurement and the calculation of the spectrum-averaged cross sections using the JENDL/D-91[4].

3.2.2. Measured Average Cross Sections

^{252}Cf Spontaneous Fission Spectrum-Averaged Cross Sections

Spectrum-averaged cross sections measured with the ^{252}Cf spontaneous fission neutron field are available for about 40 neutron reactions of importance in the reactor dosimetry[56]. There are two groups of experiments for the average cross sections: those with a complete uncertainty description and those to which the detailed information for uncertainty treatment is not always given. The former group of experiments is of particular importance, owing to their high accuracy and suitability for the evaluation of energy dependent cross sections.

In the present work, the data summarized by Mannhart[56] are practically used for the comparison with the calculated average cross sections. He included the experimental data with the covariance matrices measured by himself, Kobayashi and other seven groups, and he gave the

covariance matrices to the summarized and evaluated 31 kinds of reactions. Additionally, the average cross section data[56], which were incomplete with experimental uncertainty and were not given in the best set of the above 31 least squares evaluation data, were also employed as supplemental data for the comparison with the calculated average cross sections.

^{235}U Thermal Fission Spectrum-Averaged Cross Sections

Many groups have prepared and established the ^{235}U fission neutron field and measured spectrum-averaged cross sections which are often used for the integral assessment of energy dependant cross sections[41,53-55,57-61]. A review of all available data is given in the IAEA Technical Reports Series No.156[57]. Unfortunately, a detailed list of uncertainty contribution which makes it possible to generate covariance matrices is not given in Ref. 57. Then, it may be difficult to estimate the quality of these data, and this fact hampers trustworthy evaluation of the experimental data.

Some of the experimental data of the ^{235}U fission spectrum-averaged cross sections have been carefully measured with detailed experimental uncertainties. Mannhart[59] measured the average cross sections of 17 reactions of importance in reactor dosimetry by making use of the ^{235}U fission neutron field of the BR1 at Mol. A cylinder type of the ^{235}U fission neutron source and sample foils were set at the center of a spherical cavity of 1 m in diameter inside the vertical graphite thermal column. He gave a complete covariance matrix to his results. The uncertainties in his experiment were 4 to 6 %. Gilliam et al.[58] observed fission rates by means of NBS (now NIST) fission ionization chambers inserted into the central cavity of the Mol reactor BR1. The experimental uncertainties obtained were about 2 to 3 %. Petilli and Gilliam[55] analyzed these measured data and generated the covariance matrix.

Recently, Kobayashi et al. measured 12 kinds of threshold reactions for the ^{235}U fission neutron spectrum-averaged cross sections[41,53,54]. They used a big fission plate of 31.3 cm in diameter and 1.1 cm thick, which was installed in an irradiation room ($2.4 \times 2.4 \times 2.4$ m^3) of the heavy water thermal neutron facility at the Kyoto University Reactor, KUR. They also gave a complete set of the correlation matrix to their results with the resultant uncertainties of several percent.

In this report, the experimental data obtained by Mannhart and Kobayashi et al. have been practically employed for the comparison of the calculated average cross sections. The measured average cross sections for the (n,f) reactions on ^{235}U, ^{238}U, ^{237}Np and ^{239}Pu have been adopted from the Gilliam's work[58].

Very recently, Mannhart presented a best set of average cross section measurements for 30 dosimetry reactions in the ^{235}U fission neutron spectrum field[61]. The systematic evaluation is based on 38 experiments and has been performed by comparing the data between the ^{252}Cf and the ^{235}U fission neutron spectrum fields.

3.2.3 Comparison of Average Cross Section Data

Spectrum-averaged cross sections and the error of calculated average cross sections have been derived by using Eqs. (1) and (2) given in the former Section 3.1.2. As standard neutron fields, the ^{252}Cf spontaneous fission neutron spectrum evaluated by Mannhart[45] and two kinds of ^{235}U fission neutron spectra were used as shown below. The calculated average cross sections were compared with experimental data. Since the covariance matrix was not always given in the neutron spectrum, the following covariance matrix was assumed for the present calculations, as seen in the former section: all of the diagonal elements have 5 % uncertainties, and all of the off-diagonal elements

2 %.

^{252}Cf Spontaneous Fission Spectrum-Averaged Cross Sections

For the comparison of the calculated and measured spectrum-averaged cross sections, the ^{252}Cf spontaneous fission neutron spectrum evaluated by Mannhart[45] was employed. The experimental data were taken from the Mannhart's recommended values and/or compilation data[56]. The measured and the calculated ^{252}Cf spectrum-averaged cross sections are given in **Table 3.2.1**.

From the comparison of the calculated data with the measured ones as shown in Table 3.2.1, it can be found that most of the spectrum-averaged cross sections calculated with JENDL/D-99 are in agreement within 5 to 10% with the measured ones. However, the calculated cross section for the ^{55}Mn(n,2n)^{54}Mn reaction is larger by more than 20 % than the measured, while the cross section calculated with the ^{59}Co(n,γ)^{60}Co reaction is smaller by almost 20 % than the measured one. These tendencies were commonly seen in both of the Maxwellian and the Mannhart spectra in the previous report[4]. There was much improvement in the cross sections of ^{60}Ni(n,p)^{60}Co and ^{63}Cu(n,γ)^{64}Cu reactions, as seen in Table 3.2.1.

For the validation test of the dosimetry cross section, we have made the following calculation using the JENDL/D-91 and the JENDL/D-99:

$$Diff = \sum_i \frac{\{Exp(i) - Calc(i)\}^2}{\{Exp(i)\}^2} \qquad (5)$$

where Exp(i) stands for the measurements, Calc(i) the calculations, and " i " the number of the reactions used. Each value of *Diff* for the JENDL/D-91 and the JENDL/D-99 was 0.474 and 0.159, respectively. It can be said that the agreement between the measurement and the calculation using the JENDL/D-99 has been improved compared to that using the JENDL/D-91.

It can be seen that most of the averaged cross sections for the (n,2n) reactions with the Mannhart spectrum are rather in agreement with the measured ones, except for the ^{55}Mn(n,2n)^{54}Mn reaction, compared to the averaged cross sections with the ^{235}U fission neutron spectra, as mentioned below.

^{235}U Thermal Fission Spectrum-Averaged Cross Sections

Neutron spectrum used for the present calculation of the spectrum-averaged cross sections is the Watt-type spectrum:

$$X(E) \propto \exp(-E / 0.988) \sinh(\sqrt{2.249E})$$ [46],

where E is an emitted neutron energy in MeV.

For the supplementary comparison, we have also employed the neutron spectrum by the modified Madland-Nix model, which was proposed by Ohsawa[52] and adopted in JENDL-3.2.

The experimental data appearing in **Table 3.2.2** were practically taken for the comparison of the calculated data. These data are close in principle to the recent data evaluated by Mannhart[61] within the uncertainty. Most of the calculated average cross sections are close to the measured ones. We have had following findings by the detailed comparison between the calculation and the measurement with each fission neutron spectrum. The results of the integral comparison using the Eq.(5), the values of *Diff* for the sets of Watt-type/JENDL/D-91, Watt-type/JENDL/D-99 and Madland-Nix/JENDL/D-99 are 0.248, 0.239 and 0.359, respectively. From the results and those in Table 3.2.2, it may be said that the use of the Madland-Nix spectrum leads to smaller cross sections

than that of the Watt type. There was a marked improvement, as seen in Table 3.2.2, for the $^{64}Zn(n,p)^{64}Cu$ reaction in JENDL/D- 99 compared to that in JENDL/D-91. In cases of the (n,2n) reactions on ^{59}Co, ^{58}Ni, ^{90}Zr and ^{93}Nb, all of the C/E ratios are lower than unity, although the ratios for the Maxwellian fission spectrum, which were not indicated in Table 3.2.2, gave higher values than unity. For the $^{90}Zr(n, 2n)^{89}Zr$ reaction, Kobayashi et al. measured the value of 0.0860 ± 0.0065 mb[54], which was in better agreement with the calculations.

The C/E ratios observed in the calculated and the measured average cross sections listed in Tables 3.2.1 and 3.2.2 show the same tendency between the data for both ^{252}Cf and ^{235}U Watt-type fission neutron spectra, although the results by the ^{252}Cf spectrum are generally closer to the measurements than those by the ^{235}U spectrum.

3.3 Integral Test with Reactor Neutron Fields

3.3.1 Reactor Neutron Fields

For the integral tests of JENDL/D-99, four kinds of reactor neutron fields were selected: ISNF, CFRMF, ΣΣ and YAYOI as used in the previous integral tests of JENDL/D-91. The report of the JENDL/D-91 file[4] includes the numerical data of their well characterized neutron spectrum fields and abundant experimental data available for the integral tests. Neutron spectrum data for the JOYO and the JMTR were newly added to the present integral tests. By using these neutron spectra which are illustrated in Figs. 3.1.1(a),(b),(c) and (d), averaged cross sections have been calculated from JENDL/D-99, -91 and IRDF-90V2, and compared with the corresponding experimental data, respectively. In cases of the spectrum fields of BIG-TEN, ORR and NEACRP, however, the calculated results have not been used for the integral tests, because the spectrum shape of ORR is in general agreement with that of JMTR, and the spectrum shapes of BIG-TEN and NEACRP are close to those of YAYOI and ISNF/CFRMF, respectively, as seen in Figs. 3.1.1(b), 3.1.1(c) and 3.1.1(d).

Here are presented the results of the integral tests with brief descriptions of the neutron spectrum fields and available data for testing the dosimetry reactions.

3.3.2 ISNF

The Intermediate-Energy Standard Neutron Field (ISNF) is an irradiation facility designed to produce neutron spectrum components in the energy range of interest for fast reactors[4,31,61,62], as seen in Fig. 3.1.1(b). The neutron spectrum shape in this system can be calculated with comparatively good accuracy because of the spherical symmetry of the system and the use of materials whose nuclear cross sections are among the best known. The simplicity of one dimensional calculation permits detailed investigation of the spectrum and cross section sensitivity to uncertainties in physical and nuclear parameters of the system and spectrum perturbation due to extraneous materials required for fabrication. The mean energy of the spectrum is about 0.58 MeV, with 98% of the neutron fluence between 1.2 keV and 5.6 MeV. The low energy tail below 10 keV is calculable with an accuracy better than 5%.

For the present integral test of the JENDL/D-99, the following spectrum-averaged cross sections measured in the ISNF were used as seen in **Table 3.3.1**: $^{23}Na(n,\gamma)^{24}Na$, $^{45}Sc(n,\gamma)^{46}Sc$, $^{59}Co(n,\gamma)^{60}Co$, $^{115}In(n,n')^{115m}In$ and $^{197}Au(n,\gamma)^{198}Au$, of which uncertainties are from 2.6% to 6.4% and consist of those from their neutron fluence and the activation measurement. Since, except the $^{115}In(n,n')^{115m}In$ reaction, they are resonant reactions, the dominant uncertainties are caused by some

corrections of self-absorption effects and energy-dependent fluence gradient.

3.3.3 CFRMF

The Coupled Fast Reactivity Measurements Facility (CFRMF) located at the Idaho National Engineering Laboratory (INEL) is a zone-core critical assembly with a fast neutron spectrum zone in the center[4,32,64-67]. As shown in Fig. 3.1.1(b), the neutron spectrum of the central zone is spanned over the intermediate neutron energy range, where 95% of the neutrons are between 4 keV and 4 MeV and the mean neutron energy is about 370 keV. The characterization of the central spectrum shape is established by means of an extensive program of spectrum measurements and neutronics calculations using transport, Monte Carlo and resonance theory codes. The measurement by the proton-recoil spectrometry defined the differential spectrum to $\pm 5\%$ over the energy region from 10 keV to 1.0 MeV. The agreement among the calculated neutron spectra is reasonably good under the difficulty of a suitable calculation model for the complex assembly.

The spectrum-averaged cross sections of 22 reactions in **Table 3.3.2** are available for the present integral tests. Some of them were obtained from the intercomparison study on the reaction rate measurements among several U.S. laboratories, demonstrating that reaction rate would be able to be determined with an accuracy of $\sim \pm 2\% (1\sigma)$.

3.3.4 ΣΣ

The ΣΣ facility at Mol is a thermal-fast coupled spherical source assembly located within a conventional graphite thermal column[4,34,68], which features a one-dimensional geometry composed of homogeneous material zones of known size and composition with reasonably well-known cross sections. The recommended neutron spectrum at the center of ΣΣ, as seen in Fig. 3.1.1(b), was evaluated from the inter-laboratory neutron spectrometry measurements combined with a discrete-ordinate transport calculation. A $\pm 5\%$ agreement is generally found from 0.02 up to 4 MeV between the various experimental spectra.

The discrepancies between the spectrometry measurements and the calculations never exceed $\pm 15\%$ above 3 keV and are interpretable in terms of nuclear data inaccuracy of the ΣΣ structural materials, while the tremendous deviations between the various calculations below 3 keV can be explained due to differences in the self-shielding prescriptions and the ^{238}U nuclear data.

The spectrum-averaged cross sections of 15 reactions are available from the recommended ΣΣ central reaction rate data, as seen in **Table 3.3.3**. They were measured relatively to a specific ΣΣ thermal neutron flux, which was based on the activation reactions of $^{115}In(n,n')^{115m}In$ and $^{197}Au(n,\gamma)^{198}Au$ and corrected by the transport calculation.

3.3.5 YAYOI

The YAYOI at Nuclear Engineering Research Laboratory, the University of Tokyo, is a 2 kW air-cooled fast neutron source reactor with 93% enriched uranium metal fuel[4,36,69-71], which can provide a variety of standard neutron fields by moving the core assembly in different surroundings such as heavy-concrete shields, a lead octagonal pile and bare of shield. The core-center neutron spectrum can be expressed by a linear combination of two spectrum modes from a fission neutron source and a spectrum with neutron inelastic scattering, as shown in Fig. 3.1.1(c). Experimental data were employed to determine the spectrum parameters by using the least squares method. The uncertainty of the neutron spectrum is roughly estimated as $\pm 10\% (1\sigma)$ between 0.1 and 10 MeV,

and ±30%(1σ) outside of this energy region.

The spectrum-averaged cross sections for 22 reactions in **Table 3.3.4**, which were derived from the reaction rate data or the relative ratio data to the ^{58}Ni(n,p)^{58}Co reaction measured in the YAYOI core center field, were used for the present integral test. Some of these spectrum-averaged cross sections and their uncertainties were justified through the intercomparison studies on reaction rate measurements in Japan.

3.3.6 JOYO

The experimental fast reactor JOYO at Oarai Engineering Center of Japan Nuclear Cycle Development Institute is a sodium-cooled fast reactor[38,72]. The present Mark-II core uses high enriched plutonium and uranium mixed oxide fuel. The core is small and surrounded by stainless steel reflectors, therefore it has a relatively hard neutron spectrum as seen in Fig. 3.1.1(c) and the mean neutron energy in the core center is about 200 keV. The reactor has been operated as an irradiation test facility for testing fuels and materials for future fast reactors and for fusion materials. The accuracy of neutron fluence evaluation had been confirmed within 3% through the integral tests in a fast reactor neutron field in YAYOI and the reactor dosimetry intercomparison study between JOYO and EBR-II.

In order to evaluate the applicability of the JENDL/D-99 file, the integral tests have been performed with the fast neutron spectrum field at the center of the JOYO Mark-II core. A set of dosimeter foils consisting of eight reactions of ^{46}Ti(n,p)^{46}Sc, ^{54}Fe(n,p)^{54}Mn, ^{58}Fe(n,γ)^{59}Fe, ^{58}Ni(n,p)^{58}Co, ^{59}Co(n,γ)^{60}Co, ^{63}Cu(n,α)^{60}Co, ^{238}U fission and ^{237}Np fission was irradiated there for approximately 30 days. The neutron spectrum at the dosimeter position is shown in **Fig. 3.3.1**.

The neutron spectrum at the dosimeter foils was calculated using the two dimensional discrete ordinate transport code DORT[73]. The core configuration was modeled in XY geometry, and the 100 group cross section set of JSD-J2/JFT-J2, which was processed from JENDL-2 library[74], was utilized. The 103 group cross section data were processed by the NJOY code[75] for nuclides to be used in the JOYO dosimetry. The absolute value of neutron flux was normalized so that the ^{235}U fission rate using the calculated neutron spectrum agreed with the measured reaction rate. The adjusted neutron spectrum is shown in Fig. 3.3.1 or Fig.3.1.1(c), and the fluxes are estimated to be 3.8×10^{15} n/cm^2/s (total) and 2.6×10^{15} n/cm^2/s (E_n>0.1MeV).

Table 3.3.5 shows the calculated results for JENDL/D-99 and JENDL/D-91. At the core center position of JOYO, all calculated values of the averaged cross sections based on JENDL/D-99 agreed well with the experimental values. The C/E ratios ranges from 0.96 to 1.23. By comparing the results between JENDL/D-99 and JENDL/D-91, small differences exist, except for the ^{58}Fe(n,γ)^{59}Fe reaction whose data were improved significantly in JENDL/D-99.

3.3.7 JMTR

The Japan Materials Testing Reactor (JMTR) at O-arai Research Establishment of JAERI is a light water moderated and cooled 50 MW tank-type reactor with fuels of 19.75%-^{235}U enriched U_3Si_2 dispersion alloy. It has been utilized[39] for wide range irradiation of reactor materials and for isotope production since 1968.

The integral tests have been performed with eight reactions of ^{46}Ti(n,p)^{46}Sc, ^{55}Mn(n,2n)^{54}Mn, ^{54}Fe(n,p)^{54}Mn, ^{58}Fe(n,γ)^{59}Fe, ^{59}Co(n,γ)^{60}Co, ^{58}Ni(n,p)^{58}Co, ^{63}Cu(n,α)^{60}Co, and ^{109}Ag(n,γ)^{110m}Ag. The dosimeter set for the reactions was irradiated for 25 days.

Figure 3.3.2 or Fig. 3.1.1(d) shows the neutron spectrum of 137 energy groups at the irradiation position near the core center (H-9) of the JMTR. The neutron fluxes there were estimated to be 7.4×10^{14} n/cm^2/s (1.3×10^{14} n/cm^2/s for E_n>1.0 MeV, and 1.5×10^{14} n/cm^2/s for E_n<0.68eV) and the neutron fluence was 1.6×10^{21} n/cm^2, respectively. The neutron spectrum was calculated using the ANISN code[76] and normalized to the measured reaction rates of three gradient monitors placed near the dosimeter set. The neutron cross sections and their covariance matrices based on JENDL/D-99, JENDL/D-91 and IRDF-90V2 were processed into 137 energy groups by the NJOY code[77]. The calculated results of the spectrum-averaged cross sections were compared with the experimental data, and the uncertainty analysis was carried out using the NEUPAC code[78].

Table 3.3.6 shows the results of the integral tests using JENDL/D-99, JENDL/D-91 and IRDF-90V2 at the H-9 position of the JMTR irradiation field[79]. All of the calculated spectrum-averaged cross sections based on JENDL/D-99 are in good agreement with the experimental values within about ± 15%. Especially, the C/E values of the ^{54}Fe(n,p)^{54}Mn, ^{59}Co(n,γ)^{60}Co, ^{58}Ni(n,p)^{58}Co and ^{63}Cu(n,α)^{60}Co reactions show good agreement within ± 5%. Comparing with the average cross sections from IRDF-90V2, it is found that the calculated values of the ^{46}Ti(n,p)^{46}Sc, ^{55}Mn(n,2n)^{54}Mn, ^{58}Fe(n,γ)^{59}Fe and ^{63}Cu(n, α)^{60}Co reactions in JENDL/D-99 show slightly improvement in the C/E ratios. In case of the ^{109}Ag(n,γ)^{110m}Ag reaction, the average cross section calculated from JENDL/D-99 is somewhat larger than the experimental value.

3.3.8 Results and Discussion

Tables 3.3.1 to 3.3.6 summarize the comparison of the measured average cross sections and those calculated with JENDL/D-99, -91 and IRDF-90V2 using the neutron fields in ISNF, CFRMF, ΣΣ, YAYOI, JOYO and JMTR, respectively.

In the ISNF results, the C/E ratio of the ^{45}Sc(n,γ) cross section in JENDL/D-99 has been fairly improved from that in JENDL/D-91. Except for the ^{197}Au(n,γ) reaction, the JENDL/D-99 data would be reasonable, since some systematic discrepancies in the C/E ratios between threshold and non-threshold reactions might be due to insufficient correction of self-shielding effects for the experimental data.

For the CFRMF results, the trend of the C/E ratios for the ^{45}Sc(n,γ) and ^{59}Co(n,γ) reactions in JENDL/D-99 resembles that for the ISNF results. The C/E ratios for the ^{46,47,48}Ti(n,p) cross sections in JENDL/D-99 have been greatly improved within the estimated uncertainties as compared to those in JENDL/D-91 and IRDF-90V2. The C/E ratio for the ^{58}Fe(n,γ) reaction in JENDL/D-99 has been drastically improved.

In the ΣΣ results, it is found that the C/E ratio for the ^{63}Cu(n,γ) reaction in JENDL/D-99 has been fairly improved from that in JENDL/D-91 as that for the CFRMF result. Concerning the (n,f) reactions of ^{232}Th, ^{235}U, ^{238}U, ^{237}Np and ^{239}Pu, the JENDL/D-99 data give reasonable C/E ratios. However, the C/E ratios for the threshold reactions are found to be underestimated systematically.

The YAYOI results show that the C/E ratio have trends of systematic over-estimation for the high threshold energy reactions and underestimation for the (n,γ) reactions although the C/E ratios of JENDL/D-99 seem generally better than those of the other two files.

These systematic discrepancies in the Σ Σ and YAYOI results are considered mainly due to larger uncertainties of the neutron spectrum data used for the calculation than those assumed in the higher energy region about several MeV and also in the thermal/epithermal energy region.

From the results of eight reactions using the JOYO Mark-II core spectrum, reasonable C/E ratios

with the data in JENDL/D-99 were obtained from 0.96 to 1.23. It is said that the data in JENDL/D-99 were much improved, especially with the $^{58}Fe(n,\gamma)^{59}Fe$ reaction.

With the JMTR spectrum, the average cross sections by JENDL/D-99 are generally closer to the experimental values than those by JENDL/D-91. The calculated results based on the JENDL/D-99 yield a small difference from those based on JENDL/D-91 and IRDF-90V2, and show better agreement, in general, with experimental data for all of the selected reactions. The C/E ratios range from 0.86 to 1.08 and the averaged C/E ratio is 0.959 ± 6.7%. It was concluded that a good evaluation was made for JENDL/D-99 in the high flux neutron field of fission reactors.

4. Integral Tests for Fusion Reactors

4. 1 Integral Test in D-T Fusion Neutron Environment

Several important reaction-cross-sections in the updated JENDL Dosimetry File (JENDL/D-99) for the fusion applications were tested by using experimental data of reaction rates in D-T neutron fields. The test was carried out by comparing the reaction rates calculated from the neutron spectra and cross sections in the JENDL/D-99 with experimental values. Also the test for the old version JENDL Dosimetry File (JENDL/D-91) was performed for comparison. In this section, results of the test are described in detail.

4.1.1 Neutron Fields Used in the Tests

Two neutron spectra, which are shown in **Fig. 4.1.1**, were used for the integral test. They are the same ones as those used in the test for JENDL/D-91[4,80-82]. In the spectrum A denoted as Position #1, the fractions of neutron flux integrated above 10 MeV to those above 1.0 MeV and 5.0 MeV were 36 % and 77 %, respectively. Thus, this spectrum was considered appropriate for the test of cross sections around 14 MeV for the reactions with threshold energies around 5 MeV. In the spectrum B denoted as Position #2, the fractions were 22 % and 58 %, respectively. This indicated that the weight of low energy component below 10 MeV increased in comparison with that of the spectrum A at the position #1. In particular, the spectrum B at the position #2 had an important role in the test for the low threshold reactions because the contribution of 14 MeV flux to the total reaction rate was reasonably expected to be lower than 10 %. The numerical data of the spectra with a 125 neutron group structure are given in **Table 4.1.1**.

4.1.2 Criteria of the Test

Class A: When calculated reaction rates agree with experiments within ± 5 %, they are assigned Class A which indicates that the cross sections are good. This criterion is considered reasonable because almost all experimental errors are within ± 5 % .

Class B: If the discrepancy between the calculated and measured reaction rates is in the range from ± 5 % to ± 10 % , we assign the cross sections Class B which indicates that the cross sections are almost adequate. However, there is a necessity of further examination of the cross sections.

Class C: When the difference of the calculated reaction rate from the experiment is larger than ± 10% , the cross sections are assigned Class C which clearly indicates unreasonable evaluation of the cross sections. The cross sections in Class C should be reevaluated with high priority.

4.1.3 Results of the Integral Test

The results of the integral test are summarized in **Tables 4.1.2** and **4.1.3** for the Spectra A and B, respectively. In the tables, the results for JENDL/D-91 are given for comparison. The tables show types of reactions, measured reaction rates with experimental errors, reaction rates with JENDL/D-99 and JENDL/D-91, difference in % and criteria status of the test between the measurements and JENDL/D-99 calculations. The criterion of the discrepancy in (C-E)/E is given as follows: without * mark (Class A) for $<5\%$, * (Class B) for $>5\%$, ** (Class C) for $>10\%$.

Ratios of the calculated to the measured reaction rates are giving in parentheses. The test was based on the deviation and examined in accordance with the criterion as specified.

Comparison of JENDL/D-99 with JENDL/D-91

As a whole, the standard deviations of C/E values for the entire reaction rates in Spectrum A from the experiments for JENDL/D-99 and JENDL/D-91 are 4.7 % and 6.1 %, respectively, whereas in Spectrum B they are 3.3 % and 7.1 %, respectively. This result shows JENDL/D-99 gives a better agreement with experiments than JENDL/D-91. The difference between JENDL/D-99 and JENDL/D-91 for each reaction rate is not so large except for the $^{64}Zn(n,p)^{64}Cu$ reactions. Note that the production cross sections of ^{46}Sc, ^{47}Sc and ^{48}Sc for natural titanium were prepared by adding two contributing reaction cross section in the isotopes, i.e., $^{46}Ti(n,p)^{46}Sc + {}^{47}Ti(n,np)^{46}Sc$, $^{47}Ti(n,p)^{47}Sc + {}^{48}Ti(n,np)^{47}Sc$, and $^{48}Ti(n,p)^{48}Sc + {}^{49}Ti(n,np)^{48}Sc$.

Discussion on Individual Reactions

$^{27}Al(n,\alpha)^{24}Na$

As seen in Tables 4.1.2 and 4.1.3, the reaction rate ratio calculated with JENDL/D-99 clearly differs from the one with JENDL/D-91 in the Spectrum A, while the reaction rates of both JENDL/D-99 and JENDL/D-91 for the Spectrum B agree with each other. Thus, it suggests that the cross sections around 14 MeV in JENDL/D-99 is lower than that in JENDL/D-91. The range of the discrepancies between the calculated and measured reaction rates, however, seems reasonably small by taking both errors in the experiment and spectra used. As long as the present test is concerned, JENDL/D-99 gives a satisfactory result by referring the criterion of the test.

$^{N}Ti(n, x)^{46}Sc$

The agreement of JENDL/D-99 with the experiment is better than that of JENDL/D-91 for both spectra. Although the experimental error of the reaction rate for the Spectrum B is large, it is concluded that the cross section of JENDL/D-99 is adequate, being in Class A.

$^{N}Ti(n,x)^{47}Sc$

The agreement of JENDL/D-99 with the experiment is in a reasonable range for both Spectra. However, it is noted that the agreement is improved for the Spectrum B in comparison with JENDL/D-91. For Spectrum A, the calculations rather underestimate the experiments. This is explained by the fact that the evaluated cross section for the $^{48}Ti(n,np)^{47}Sc$ reaction is lower than the 14 MeV experiments[83] done at FNS. In the Spectrum B, the contribution from this reaction decreases because the high energy neutron flux decreases. On the other hand, it is concluded that the cross section for the $^{47}Ti(n,p)^{47}Sc$ reaction is properly evaluated.

$^{N}Ti(n,x)^{48}Sc$

JENDL/D-99 and JENDL/D-91 give almost same results and they are in good agreement with the experiment. They are in Class A.

$^{54}Fe(n,p)^{54}Mn$

JENDL/D-99 and JENDL/D-91 give the same result and they overestimate and underestimate

the experiments of Spectra A and B by 9 % and 6 %, respectively. Considering that Spectrum A has much weight in the 14 MeV region, the overestimation may be attributed to too large cross-section values around 14 MeV. Nevertheless, verification of data over the whole energy range is recommended because this reaction has a low threshold energy around 1 MeV. In particular, it has been pointed out that a large uncertainty exists in the cross section around several-MeV region. The problem that was pointed out in the previous report [4] still remains.

^{56}Fe(n,p)^{56}Mn

The reaction rate ratios of JENDL/D-99 to JENDL/D-91 for both Spectra A and B are slightly larger than 1.0. This indicates that the cross section of JENDL/D-99 is higher than that of JENDL/D-91. Both JENDL/D-99 and JENDL/D-91 calculations, however, adequately reproduce the measurements and are regarded as Class A.

^{58}Ni(n,2n)^{57}Ni

JENDL/D-99 and JENDL/D-91 give reasonably good agreement with the experiment. Both of the data are in Class A. There must be an improvement in the cross section around the 14 MeV region because the better C/E value of JENDL/D-99 for the Spectrum A than that of JENDL/D-91 was obtained.

^{58}Ni(n,p)$^{58m+g}$Co

JENDL/D-99 tends to give larger C/E values for both Spectra A and B than JENDL/D-91. The overestimation, however, is in the range of Class B and Class A for the Spectra A and B, respectively.

^{59}Co(n,2n)$^{58m+g}$Co

Both JENDL/D-99 and JENDL/D-91 are in good agreement with the experiments for Spectra A and B. This result suggests that the JENDL/D-99 data are adequate and in Class A.

^{59}Co(n,α)^{56}Mn

Both JENDL/D-99 and JENDL/D-91 give almost same results and they agree with experiments within 5 %. Thus, it is concluded that the cross section is adequate.

^{64}Zn(n,p)^{64}Cu

The ^{64}Zn(n,p)^{64}Cu reaction cross section of JENDL/D-99 seems adequate. The new evaluation is based on the latest experimental data done by CIAE group[84], which gives data points in a wide energy range. Taking the FNS data[85] into consideration, the cross section curve should be much lower than that of JENDL/D-91.

^{90}Zr(n,2n)$^{89m+g}$Zr

Both JENDL/D-99 and JENDL/D-91 are in reasonable agreement with the experiments. The cross sections are in Class A

^{93}Nb(n,2n)^{92m}Nb

The JENDL/D-99 and JENDL/D-91 calculations are consistent with the measurements for both

Spectra A and B. The presently evaluated data are in Class A.

$^{115}In(n,n')^{115m}In$

Slight overestimation of JENDL/D-99 is observed for the spectra A and B. The agreement of JENDL/D-99 and JENDL/D-91 with the experiments, however, is within 5% and it can be concluded that the cross sections of JENDL/D-99 and JENDL/D-91 are adequate.

4.1.4 Summary

In summary, JENDL/D-99 gives reasonable results as a whole. In particular, good agreement between the calculations based on JENDL/D-99 and the measurements is observed for the $^{64}Zn(n,p)^{64}Cu$ reaction with the Spectra A and B as compared with those based on JENDL/D-91. As a whole, modest improvements were made in JENDL/D-99 because JENDL/D-91 has already shown high quality. These results assure an improvement over the previous version and good reliability of the JENDL/D-99 in the D-T fusion dosimetry applications.

4.2 Integral Test using Thick Li(d,n) Neutron Field

In this section, we describe the cross section validation using the thick Li(d,n) neutron field. This neutron field is characterized by a rather flat spectrum with relatively high intensity up to above 10 MeV because of the large Q-value of this reaction; therefore, the neutron field is available in the facility of a small accelerator. It has been pointed out that the neutron field is advantageous to the test of cross sections for both low and high threshold reactions.

The average cross sections for several dosimetry reactions in the thick Li(d,n) neutron field, which was provided by the 4.5 MeV Dynamitron accelerator of Fast Neutron Laboratory at Tohoku University, were measured[86]. Those average cross sections are the same ones that have been used for the validation of JENDL/D-91 as reported previously[4]. The new dosimetry file JENDL/D-99 is validated through the comparison of the ratios of the calculated values to experimental ones; more exactly, we assess the file by the degree of discrepancy of the above two values, (C-E)/E in percent with the following 5 classes (C-E)/E: without * mark for $<5\%$, * for $>5\%$, ** for $>10\%$, *** for $>20\%$, and **** for $>40\%$. The cross sections with the discrepancies within 20% would be adequate.

Detailed description of the measurements and neutron field characterization was already given elsewhere[4,86], and thus we describe them briefly here.

4.2.1 Characteristics of Neutron Field

A disk of metal lithium of natural element (8 mm in diameter and 1 mm in thickness) on a Cu metal disk was used as a neutron producing target. The thickness of the target was enough to stop the deuterium beam of a few MeV. The target was mounted on a low mass copper chamber with a forced air cooling system, and was bombarded by a DC deuterium beam of 10 μ A with the energy of 2 MeV from the Dynamitron accelerator. Since the $^{7}Li(d,n)$ reaction has a high Q-value of 15.02 MeV, neutrons of the energy up to about 17 MeV can be produced, as illustrated in **Fig. 4.2.1**. In order to correct the anisotropy effect of the source on the irradiated samples, the angular spectra of the neutron source were measured with a time-of-flight spectrometer consisting of a shielded NE-213 detector (5.08cm in diameter and 5.08cm thick) and a goniometer in the angular range from

0 to 90 deg. by 5 or 10 deg. step. In the spectrum measurement, a pulsed deuterium beam with a nanosecond width was used at the repetition rate of 0.25 MHz.

The detection efficiency of the neutron spectrometer was carefully determined from the measurement of the time-of-flight spectrum of ^{252}Cf neutrons relative to its evaluated standard spectrum[87]. The higher energy part of the efficiency curve was also estimated with the Monte Carlo simulation calculation using the O5S code[88].

The measured neutron spectrum at 0 deg. is shown in Fig.4.2.1. Because of the energy degradation of the deuterons in the thick target, the shape of peaks corresponding to each excited state of ^{8}Be are fully broadened. The covariance of the neutron energy distribution was evaluated considering the correlation in the detector efficiency values due to the ^{252}Cf standard spectrum[87]. The variances of the neutron energy distribution were mainly due to the statistical fluctuations in the Monte Carlo calculation of the efficiency values and of the data of the time-of-flight spectrum of ^{252}Cf because of relatively low counting statistics due to the weakness of the ^{252}Cf source used.

4.2.2 Benchmark Experiment

Two packets of activation samples were prepared. Foils of each packet are arranged in a sandwich geometry in an order from the neutron source side as shown in **Table 4.2.1**. In the packets, several foils were placed between two or three monitor foils of aluminum. The #1 packet was fixed by the plastic tape on the hollow stainless steel disk at the position (P1) 50 mm apart from the target in the 0-deg. direction; the #2 was attached on the end surface of the chamber at 7 mm (P2) from the target considering small cross sections and/or long half-lives of induced activities for some reactions. Both packets were simultaneously irradiated for 48 hours. Measurements of gamma-rays from the irradiated samples were performed with a calibrated high purity germanium detector in order to obtain the reaction rates. Most of the associated decay data of the tested dosimetry reactions are given in Refs. 4 and 10.

At the position P1, the degree of the anisotropy of the source neutrons was not appreciable. However, because of the large angle spanning of the sample #2 from zero to 20 deg., the anisotropic distribution of the source neutrons on the sample was not negligible and has been exactly corrected using the data on the measured angular distribution.

4.2.3 Average Cross Sections

The measured cross section E^i of the reaction i averaged over the spectrum is obtained by the formula[4],

$$E^i = (R^i/R^{Al}) < \sigma^{Al} >_{Calc.} F^i \quad ,$$

where R^i is the reaction rate for i, R^{Al} is the reaction rate of the ^{27}Al(n,α) reaction and F^i the correction factor of the flux difference between the foil positions for i and Al, which can be estimated from the reaction rates of a pair of aluminum foils. The symbol $< \sigma^{Al} >_{Calc.}$ is the average cross section of the ^{27}Al(n,α) reaction calculated from JENDL-3[3,86]. In the estimation of errors of the E^i values, the correlation between the R^i and R^{Al} were considered. Major experimental error sources were due to the gamma counting statistics, detector efficiency calibration, and flux corrections.

These data for E^i were compared with the corresponding calculated values C^i from the

following formula:

$$C^i = <\sigma^i>_{Calc.} = (\Sigma_g \phi_g \sigma^i_g \Delta E_g)/(\Sigma_g \phi_g \Delta E_g),$$

where ϕ_g is the relative group flux of the Li(d,n) neutrons, ΔE_g the energy bin width of the group g, and σ^i_g the group cross section taken from the dosimetry file. In the error estimation of the calculated average cross sections and their ratios to experimental ones, both covariances between group cross sections and those between the data of each bin of the neutron flux were taken into account. The former covariance data were from JENDL/D-99. The latter ones were estimated from the analysis of the spectrum data. Main part of the flux variances originated from the measured ^{252}Cf standard spectrum and Monte Carlo calculations used for the estimation of the detector efficiency as mentioned before. The correlations between ϕ_g and σ^i_g were neglected even if they might exist.

4.2.4 Results of the Integral Test

Numerical data of the results for the E^i values of JENDL/D-91, -99, as well as IRDF-90V2 are given in **Table 4.2.2.** The table also shows the values of discrepancies $(C^i-E^i)/E^i$ between the JENDL/D-99 and the experiments, and the criteria status.

Discussion on Individual Reactions

$^{23}Na(n,2n)^{22}Na$

A large discrepancy of about 10% was found for this reaction in JENDL/D-91, while the discrepancy was drastically resolved with the new evaluation.

$^{24}Mg(n,p)^{24}Na$

No large change is found in the performance of JENDL/D-91 and JENDL/D-99; both give quite satisfactory results with the discrepancy less than 1%.

$^{27}Al(n,\alpha)^{24}Na$

This reference cross section was taken from the evaluated cross sections of IRDF-90V2. Agreement between the measurements[4,86] and the calculations with the JENDL/D-99 data is satisfactory.

$^{N}Ti(n,x)^{46}Sc$

No significant change is found in the performance of JENDL/D-91 and JENDL/D-99.

$^{N}Ti(n,x)^{48}Sc$

No significant change is found between JENDL/D-91 and JENDL/D-99. The cross section calculated from JENDL/D-99 is in good agreement with the experimental data.

$^{55}Mn(n,2n)^{54}Mn$

A large discrepancy of JENDL/D-91 could not be resolved by using JENDL/D-99.

$^{54}Fe(n,p)^{54}Mn$

There is no significant improvement in the (C-E)/E value. Considering the significance of this reaction, the 12% deviation is not so good, but may be tolerable as the typical low threshold reaction.

$^{59}Co(n,2n)^{58}Co$

This reaction showed a large C/E value of JENDL/D-91, and no significant improvement was attained in the C/E value of JENDL/D-99.

$^{58}Ni(n,2n)^{57}Ni$

The JENDL/D-91 calculation deviates from the experimental data by a few %. The new version JENDL/D-99 yields a value consistent with the measurements within 1 %.

$^{58}Ni(n,p)^{58}Co$

Much improvement was made on this reaction. The deviation from the measurements was reduced.

$^{60}Ni(n,p)^{60}Co$

The deviation of this reaction becomes larger from 6% to 12%; not a small discrepancy still exists for this reaction in JENDL/D-99.

$^{63}Cu(n,\alpha)^{60}Co$

No significant change in (C-E)/E value is found, but the status of this reaction is quite satisfactory.

$^{93}Nb(n,2n)^{92m}Nb$

There is a slight improvement in discrepancy from 8% to 6% due to the new evaluation.

$^{197}Au(n,2n)^{198}Au$

The discrepancy of JENDL/D-99 is about 5%, which becomes twice larger than that of JENDL/D-91 (2.5%), although both libraries are satisfactory.

4.2.5 Summary

Summarizing this section, JENDL/D-99 shows generally good performance in the Li(d,n) neutron field, and the quality of the evaluation is similar with the previous one concerning the tested 14 threshold reactions.

As for the $^{55}Mn(n,2n)^{54}Mn$ reaction, the cross section calculated from JENDL/D-99 shows a relatively large deviation more than 20%, while that from IRDF-90V2 also shows a deviation of over 10%. The presently evaluated cross-section curve follows existing individual differential data as seen in Ref. 7. A further study is needed for this reaction from the point of view of the average cross section measurement in the same field.

As a whole, the cross sections in JENDL/D-99 agree with the measured cross sections satisfactorily; most of the cross sections deviate from the measurements by 1σ of the experimental uncertainties of about 8 – 9% and the rest of them lie within at most 2σ, with the exception of the $^{55}Mn(n,2n)^{54}Mn$ reaction.

5. Summary Discussion on the Integral Tests

5.1 Integral Tests of the Dosimetry Cross Sections for Fission Reactors

Integral tests of group-wise cross sections of the JENDL/D-99 file have been carried out by applying the standard, reference and controlled neutron spectrum fields, as shown in Figs. 3.1.1(a), (b), (c) and (d), with respect to fission reactors such as light water reactors and fast breeder reactors. As described in the Section 3.2, the calculated cross sections averaged with the ^{252}Cf spontaneous fission neutron spectrum evaluated by Mannhart[45] give better agreement[4] with the measured ones[56] than those with the Maxwellian distribution spectrum of ^{252}Cf. Concerning the ^{235}U fission neutron spectrum, in general, agreement between the measured average cross sections[41,58,59,61] and the calculated ones using the Watt-type spectrum[46] are better than those obtained by using the Maxwellian[48] and the Madland-Nix- type[52] spectra. Average cross sections by the Maxwellian spectrum gave larger values[4] than those by the Watt-type spectrum especially for higher energy threshold reactions. On the other hand, the Madland-Nix-type spectrum gave lower values. Therefore, in the present report for the integral tests, we have selected the results by the Mannhart and the Watt-type spectra for the ^{252}Cf and the ^{235}U fission neutron spectra, respectively. The C/E ratio values, which show the criterion of data consistency between the calculated and the measured average cross sections, are shown in Tables 3.2.1 and 3.2.2. The quoted uncertainty comprises the uncertainties of measured and calculated cross sections which are uncorrelated with each other.

The data used for the present comparison between the calculated and the measured average cross sections are taken from Tables 3.2.1 and 3.2.2 and Tables 3.3.1～3.3.6, and these results are summarized in **Figs. 5.1.1～5.1.8**. In general, most of the average cross sections calculated by the JENDL/D-99 file for each standard and reference neutron field show good agreement with those measured, except for several reactions. Especially, good agreement was obtained for the ^{252}Cf and ^{235}U fission neutron spectra, except for the reactions of ^{55}Mn(n,2n)^{54}Mn and ^{59}Co(n,γ)^{60}Co for the ^{252}Cf spectrum and except for ^{58}Ni(n,2n)^{57}Ni, ^{90}Zr(n,2n)^{89}Zr and ^{93}Nb(n,2n)^{92m}Nb for the ^{235}U spectrum, respectively. This means, in principle, that the data evaluated in JENDL/D-99 is adequate. There was no reaction that showed common disagreement in both of the ^{252}Cf and the ^{235}U spectra. Comparing with the cross section data in JENDL/D-91, there was much improvement in the JENDL/D-99 cross sections of ^{19}F(n,2n)^{18}F, ^{60}Ni(n,p)^{60}Co, ^{63}Cu(n,γ)^{64}Cu and ^{64}Zn(n,p)^{64}Cu for the ^{252}Cf spectrum and in the JENDL/D-99 cross sections of ^{47}Ti(n,p)^{47}Sc and ^{64}Zn(n,p)^{64}Cu for the ^{235}U spectrum, as seen in Figs. 5.1.1 and 5.1.2. Concerning the integral tests with four neutron spectra of ISNF, CFRMF, ΣΣ and YAYOI spectra, as shown in Figs. 5.1.3～5.1.6, relatively large deviation (that corresponds to the criterion **** more than 40 % in *Diff*=(C-E)/E) can be seen between the calculated average cross sections and the measured ones for the ^{58}Ni(n,2n)^{57}Ni, ^{63}Cu(n,2n)^{62}Cu and ^{93}Nb(n,2n)^{92m}Nb reactions. With the neutron spectrum near the core center of JOYO, general agreement has been seen in Fig. 5.1.7, except for the ^{63}Cu(n,α)^{60}Co reaction. The ^{58}Fe(n,γ)^{59}Fe cross section data have been markedly improved in the JENDL/D-99 file. For the JMTR spectrum, good agreement is observed between the calculated and the measured average cross sections, as shown in Fig. 5.1.8. The ^{109}Ag(n,γ)^{110m}Ag reaction has been newly introduced to the JENDL/D-99 file. The calculations of the ^{46}Ti(n,p)^{46}Sc and ^{55}Mn(n,2n)^{54}Mn reactions seem to be lower than the measurements, and the same tendency can be found in the IRDF-90V2 data.

In this report, we have compared the average cross sections calculated from JENDL/D-99 with

those from IRDF-90V2, using twelve standard or reference neutron fields, as shown in Section 3.1.2. The data given in Tables 3.1.2 to 3.1.13 are plotted in **Fig. 5.1.9** to make a comparison of the data with the both files. One can see large differences in the spectrum-averaged cross sections for the $^{23}Na(n,\gamma)^{24}Na$, $^{47}Ti(n,np)^{46}Sc$, $^{58}Fe(n,\gamma)^{59}Fe$, and $^{109}Ag(n,\gamma)^{110m}Ag$ reactions between JENDL/D-99 and IRDF-90V2. However, the $^{109}Ag(n,\gamma)^{110m}Ag$ cross sections calculated from JENDL/D-99 are consistent with those from IRDF-90V2 in the thermal reactor spectrum. In the case of the $^{23}Na(n,\gamma)^{24}Na$ reaction, the quality of the JENDL/D-99 calculations depends on the neutron spectrum used: JENDL/D-99 is better than IRDF-90V2 in the ISNF spectrum, but worse than IRDF-90V2 in the YAYOI spectrum. The cross sections for the $^{58}Fe(n,\gamma)^{59}Fe$ reaction calculated from JENDL/D-99 have a tendency to show a better agreement with measurements than those from IRDF-90V2 in the reactor spectra, as seen in Tables 3.3.2, 3.3.5 and 3.3.6.

5.2 Integral Tests of the Threshold Reaction Cross Sections for Fusion Reactors

The integral tests for the JENDL/D-99 file have been conducted in the two accelerator-based neutron fields. The cross sections for twenty threshold reactions in total were tested, i.e., the fourteen reactions in the DT fusion simulated field at FNS, JAERI, and the common eight and the six reactions in the Li(d,n) neutron source at FNL, Tohoku University, as described in Sections 4.1 and 4.2, respectively.

In order to clarify the trend of agreement between the calculation and both integral experiments, we have rearranged the C/E values of Tables 4.1.2 and 4.1.3 into **Figs. 5.2.1** and **5.2.2**, respectively. Comparing the JENDL/D-99 data with the JENDL/D-91 ones, the ratio results are illustrated in **Fig. 5.2.3**. The data in Table 4.2.2 are shown in **Fig. 5.2.4**.

First, for the JENDL/D-99 file we check the consistency of the two tests using the DT and the Li(d,n) neutron fields. Among the eight commonly tested reactions for the neutron fields, both tests assigned Class A (*Diff*: <5%) to three reactions $^{27}Al(n,\alpha)^{24}Na$, $^{N}Ti(n,x)^{48}Sc$ and $^{58}Ni(n,2n)^{57}Ni$. Class A or B (*Diff*: 5% to 10%) was assigned to three reactions $^{N}Ti(n,x)^{46}Sc$, $^{58}Ni(n,p)^{58}Co$ and $^{93}Nb(n,2n)^{92m}Nb$. In case of the $^{59}Co(n,2n)^{58}Co$ reaction, the test assigned Class A for the DT neutron field and Class C (*Diff*: >10%) for the Li(d,n) neutron field. The $^{54}Fe(n,p)^{54}Mn$ reaction was assigned to be Classes B and C for the DT and the Li(d,n) neutron fields, respectively. Thus, the consistency between the tests has been verified.

It is recommended that further differential and integral measurements and evaluation should be performed for the following reactions assigned as Classes B and C; four reactions assigned Class B from the test in the DT field: $^{N}Ti(n,x)^{47}Sc$, $^{54}Fe(n,p)^{54}Mn$, $^{58}Ni(n,p)^{58}Co$, and $^{115}In(n,n')^{115m}In$; six reactions assigned Class B or C from the test in the Li(d,n): $^{N}Ti(n,x)^{46}Sc$, $^{55}Mn(n,2n)^{54}Mn$, $^{54}Fe(n,p)^{54}Mn$, $^{59}Co(n,2n)^{58}Co$, $^{60}Ni(n,p)^{60}Co$ and $^{93}Nb(n,2n)^{92m}Nb$. For the $^{55}Mn(n,2n)^{54}Mn$ reaction, one can see a deviation of about 23 % between the measurement and the calculation with the Li(d,n) field, as shown in Table 4.2.2. In contrast to this, the C/E ratio by the JMTR spectrum is 0.87, as seen in Table 3.3.6. Such an inconsistency between the integral tests may be caused by the different responses in the reactor spectrum (sensitive to lower energies) and the Li(d,n) neutron field (sensitive to higher energies). It may be necessary to review all of the data not only for the evaluated cross section but also for the experimental benchmark ones.

6. Conclusion

The latest version of the dosimetry file, JENDL Dosimetry File 99 (JENDL/D-99), has been released, and here are summarized all the documentations for 67 reactions with 47 nuclides in this JENDL/D-99 file including the comparison studies with the previous JENDL Dosimetry File (JENDL/D-91) and the IRDF-90V2 file by the integral tests with benchmark neutron fields. In this JENDL/D-99 file, major dosimetry cross sections for 34 reactions and their covariance data were simultaneously generated, and the covariances for other reactions were adopted from the JENDL/D-91 file.

Good agreement has been generally obtained in these comparison studies between the evaluated and the measured data and there has been a marked improvement on some dosimetry cross sections. It can be expected that many people will use JENDL/D-99 for their dosimetry work.

Finally, we welcome any comments, questions and suggestions to this dosimetry file, which we would like to consider for the future evaluation work.

Acknowledgments

The authors especially wish to write here the name of the late Dr. Yasuyuki Kikuchi. He was very interested in the application of nuclear data and he encouraged this work. They are truly glad to have had an opportunity to dedicate this JENDL Dosimetry File 99 to him.

References

1) Cullen D.E., Kocherov N., and McLaughlin P.M.: "The International Reactor Dosimetry File (IRDF-82)", IAEA-NDS-41/R, rev.0 (1982). IRDF-85 is a modified version with additional cross section data.
2) BNL/National Nuclear Data Center: ENDF/B-V.
3) Shibata K., Nakagawa T., Asami T., Fukahori T., Narita T., Chiba S., Mizumoto M., Hasegawa A., Kikuchi Y., Nakajima Y., and Igarasi S.: "Japanese Evaluated Nuclear Data Library, Version-3", JAERI 1319 (1990).
4) Nakazawa M., Kobayashi K., Iwasaki S., Iguchi T., Sakurai K., Ikeda Y., and Nakagawa T.: "JENDL Dosimetry File", JAERI 1325 (1992).
5) Kocherov N.P. and McLaughlin P.K.: "The International Reactor Dosimetry File (IRDF-90 Version 2)", IAEA-NDS-141 Rev.3 (1996).
6) Peonitz W. P.: Proc. Conf. on Nucl. Data Evaluation Methods and Procedures, BNL-NCS-51363, p.249 (1981).
7) Iwasaki S.: Proc. Int. Conf. Nuclear Data for Science and Technology, Gatlinburg, Tennessee, May 9-13, 1994. Proceedings, Vol 2, p.614, ANS, Inc., (1994).
8) Nuclear Data Center Network: "EXFOR Systems Manual: Nuclear Reaction Data Exchange Format", BNL-NCS-63330 (1996), compiled and edited by V. McLane, NNDC, BNL.
9) Nakagawa T., Shibata K., Chiba S., Fukahori T., Nakajima Y., Kikuchi Y., Kawano T., Kanda Y. Ohsawa T., Matsunobu H., Kawai M., Zukeran A., Watanabe T., Igarasi S., Kosako K., and Asami T.: "Japanese Evaluated Nuclear Data Library Version 3 Revision 2: JENDL-3.2", J. Nucl. Sci. Technol., **32**, 1259 (1995), and Shibata K. and Narita T.: "Descriptive Data of JENDL- 3.2", JAERI-Data/Code 98-006 (1998).
10) Kobayashi K., Iwasaki S., Odano N., Iguchi T., Uno Y., Ikeda Y., Nakagawa T., Shibata K., Sakurai K., Aoyama T., Shimakawa S., and Nakazawa M.: Proc. 9-th Int'l Symp. on Reactor Dosimetry, World Scientific, Singapore, p.457 (1998).
11) Firestone R.B., Baglin C.M. and Frank Chu S.Y. (Eds.): "Table of Isotopes Eighth Edition 1998 Upgrade", John Wiley and Sons, New York (1998).
12) Kawano T. and Shibata K.: "Covariance Evaluation System", JAERI-Data/Code 97-037 (1997) [in Japanese].
13) Kawai M., Iijima S., Nakagawa T., Nakajima Y., Sugi T., Watanabe T., Matsunobu H., Sasaki M. and Zukeran A.: "JENDL-3 Fission Product Nuclear Data Library", J. Nucl. Sci. Technol., **29**, 195 (1992).
14) Cross Section Evaluation Working Group: "ENDF/B-VI Summary Documentation", Report BNL-NCS-17541 (ENDF-201) (1991), edited by P.F. Rose, National Nuclear Data Center, BNL.
15) Sublet J.-Ch., Kopecky J., and Forrest R.A.: "The European Activation File: EAF-99 Cross Section Library", UKAEA FUS 408 (1998).
16) Kocherov N.P.: "International Reactor Dosimetry File IRDF-90, Status and Testing", Proc. of 7-th ASTM-Euratom Symposium on Reactor Dosimetry, Strasbourg 1990, p.357 (1992).
17) Smith A. B., Chiba S., Smith D.L., Meadows J.W., Guenther P.T., Lawason R.D. and Howerton R.J.: "Evaluated Neutronic File for Indium", ANL/NDM-115 (1990).
18) Yamamuro N.: "A Nuclear Cross Section Calculation System with Simplified Input Format

Version II (SINCROS-II)", JAERI-M 90-006 (1990).
19) The Cross Section Evaluation Working Group: "Data Formats and Procedures for the Evaluated Nuclear Data File ENDF-6", BNL-NCS-44945, National Nuclear Data Center, Brookhaven National Laboratory (1997).
20) Nakagawa T.: "Program RESENDD (version 84-07): A Program for Reconstruction of Resonance Cross Sections from Evaluated Nuclear Data in the ENDF/B Format", JAERI-M 84-192 (1984).
21) Berg S. and McElroy W.N.: "A Computer-Automated Interactive Method for Neutron Flux Spectra Determination by Foil Activation", AFWL-TR-67-41, Vol. II: "SAND II (Spectrum Analysis by Neutron Detectors II) and Associated Codes" (1967).
22) Nakagawa T.: "CRECTJ: A Computer Program for Computation of Evaluated Nuclear Data", JAERI-Data/Code 99-041 (1999).
23) Nakagawa T.: Private communication.
24) Adamski L., Herman M. and Marcinkowski A.: Ann. Nucl. Energy, **7**, 397 (1980).
25) Strohmaier B. et al.: Physik Daten, 13-2 (1980).
26) Sakurai K.: J. At. Energy Soc. Jpn., **39**, 231 (1997) [in Japanese].
27) Mughabghab S.F., Divadeenam M., and Holden N.E.: "Neutron Cross Sections, Vol. 1, Part A", Academic Press (1981), and Mughabghab S.F.: "Neutron Cross Sections, Vol. 1, Part B", Academic Press (1984).
28) Kobayashi K., Kimura I., Yamamoto S., Miki R., and Itoh T.: Proc. Conf. on Neutron Physics, Sept. 1987, Kiev, Vol.4, p.238 (1988).
29) Heaton H.T.II, Gilliam D.M., Spiegel V., Eisenhauer C., and Grundl J.A.: Proc. NEANDC /NEACRP Specialists Meeting on Fast Neutron Fission Cross Sections of U-233, U-235, U-238, and Pu-239, Argonne, USA, Jun. 28 - 30, 1976, ANL-76-90, p. 333 (1976).
30) Grundl J.A., and Eisenhauer C.M.: Proc. Conf. on Nuclear Cross Sections and Technology, Washington, USA, Mar. 3-7, 1975, Vol. I, p. 250 (1975).
31) Eisenhauer C.M., Grundl J.A., and Fabry A.: Proc. Int. Specialists Symposium on Neutron Standards and Applications, Gaithersburg, USA, Mar. 28-3 1, 1977, p. 329 (1977).
32) Rogers J.W., Harker Y.D., and Millsap D.A.: Proc. Consultants' Meeting on Integral Cross-section Measurements in Standard Neutron Fields for Reactor Dosimetry, IAEA Vienna, Austria, Nov. 15 -19, 1976, IAEA-208, vol. II, p. 117 (1978).
33) Dowdy E.J., Lozito E.J., and Plassman E.A.: Nucl. Tech., **25**, 381 (1975).
34) Grundl J., and Eisenhauer C.: Proc. Consultants' Meeting on Integral Cross-section Measurements in Standard Neutron Fields for Reactor Dosimetry, IAEA Vienna, Austria, Nov. 15-19, 1976, IAEA -208, Vol.I, p. 53 (1978).
35) Greenwood L.: Oak Ridge Research Reactor (ORR), private communication to IAEA(1981).
36) Kobayashi K., Kimura I., Nakazawa M., and Akiyama M.: J. Nucl. Sci. Technol., **13**, 531 (1976), and Greenwood L.: private communication to IAEA.
37) Goel B.: private communication to IAEA (1981).
38) Aoyama T., Ito C. and Suzuki S.: "Current Status and Upgrading Activity of Reactor Material Dosimetry in the Experimental Fast Reactor JOYO," Proc. of the 9th International Symposium on Reactor Dosimetry, World Scientific, Singapore, p.302 (1998).
39) Shimakawa S., Nagao Y., Komori Y., Iguchi T., Ooka N. and Kondo I.: Proc. of the 9th International Symposium on Reactor Dosimetry, World Scientific, Singapore, p.857 (1998).

40) Mannhart W.: "Handbook on Nuclear Activation Data", IAEA Technical Report Series No.273, IAEA, p.163 (1987).
41) Kobayashi K., Kimura I., Li ZhaoHuan and Wang YongQing: Proc. 7-th ASTM-EURATOM Symp. on Reactor Dosimetry, Strasbourg, France, Aug. 27-31, 1990, Kluwer Academic Publications, p.263 (1992).
42) Vlasov M.F.(Ed.): Proc. IAEA Consultants' Meeting on Integral Cross-section Measurements in Standard Fields, IAEA Vienna, Nov. 15-19, 1976, INDC (NDS)-81/L+M (1977).
43) Okamoto K.(Ed.): Proc. IAEA Advisory Group Meeting on Properties of Neutron Source, Leningrad, USSR, Jun. 9-13, 1986, IAEA-TECDOC-410 (1987).
44) Lemmel H.D.(Ed.): Proc. IAEA Consultants' Meeting on Physics of Neutron Emission in Fission, Mito, Japan, May 24-27, 1988, INDC (NDS)-220/L (1989).
45) Mannhart W.: Proc. 6-th ASTM-EURATOM Symposium on Reactor Dosimetry, Jackson Hole, USA, May 31 - Jun. 5, 1987, p.340 (1989) and IAEA Consultants' Meeting on Physics of Neutron Emission in Fission, Mito, May 24-27, 1988, INDC(NDS)-220/L, p. 305 (1989).
46) Baard J.H., Zijp W.L., Nolthenius H.J.: "Nuclear Data Guide for Reactor Neutron Metrology", Kluwer Academic Publishers (1989).
47) Armitage B.H., and Sowerby M.G. (Ed.): Proc. Specialist Meeting on Inelastic Scattering and Fission Neutron Spectra, Harwell, UK, Apr. 14-16, 1975, AERE-R 8636 (1977).
48) Johansson P.1., and Holmqvist B.: Nucl. Sci. Eng., **62**, 695 (1977).
49) Madland D.G., and Nix J.R.: Nucl. Sci. Eng., **81**, 213 (1982).
50) Maerten H., and Seeliger D.: Proc. Advisory Group Meeting on Nuclear Standards Reference Data, Geel, Belgium, Nov. 12-16, 1984, IAEA-TECDOC-335, p. 255 (1985).
51) Browne J.C., and Dietrich F.S.: Phys. Rev., **C10**, 2545 (1974).
52) Ohsawa T.: Proc. of the 9-th Int'l Symp. on Reactor Dosimetry, Prague, Czech Republic, 2-6 Sept. 1996, World Scientific, Singapore, p.656 (1998).
53) Kimura I., and Kobayashi K.: Nucl. Sci. Eng., **106**, 332 (1990).
54) Kobayashi K., and Kobayashi T.: NEANDC(J)-155/U, p. 52 (1990).
55) Petilli M., and Gilliam D.M.: Proc. 5-th ASTM-EURATOM Symp. on Reactor Dosimetry, Geesthacht, Germany, Sep. 24-28, 1984, p.657 (1984).
56) Mannhart W.: "Handbook on Nuclear Activation Data", IAEA Technical Report Series No.273, IAEA, p. 413 (1987).
57) Calamand A.: "Handbook on Nuclear Activation Cross Sections", IAEA Technical Reports series No.156, IAEA, p. 273 (1974).
58) Gilliam D.M., Grundl J.A., Lamaze G.P., McGarry E.D., and Fabry A.: Proc. 5-th ASTM-EURATOM Symposium on Reactor Dosimetry, Geesthacht, Germany, Sep. 24-28, 1984, Vol. 2, p. 867 (1984).
59) Mannhart W.: ibid., Vol. 2, p. 813 (1985).
60) Cullen D.E., Kocherov N.P., and McLaughlin P.M.: Nucl. Sci. Eng., **83**, 497 (1983).
61) Mannhart, W.: "Evaluation of a 'Best Set' of Average Cross Section Measurements in the 235U(nth,f) Neutron Field", NEA/NSC/DC (99)10, p.40(1999), INDC(Ger)-045 Jul. 3660 (1999).
62) Lamaze G.P., Eisenhauer C.M., Grundl J.A., McGarry E.D., Schima F.J., and Spiegel V.: Proc. Int. Conf. on Nuclear Data for Sci. Technol., Mito, Japan, May 30 - Jun. 3, 1988, p. 1033 (1988).

63) Broadhead B.L., et al.: Trans. Am. Nucl. Soc., **30**, 590 (1978).
64) Greenwood R.G., Helmer R.G., Rogers J.W., Dudey N.D., Popek R.J., Kellogg L.S., and Zimmer W. H.: Nucl. Technol., **25**, 274 (1975).
65) Rogers J.W., Millsap D.A., and Harker Y.D.: Nucl. Technol., **25**, 330 (1975).
66) Ryskamp J.M., Andrel R.A., Broadhead B.L., Ford W.E., Lucius J.L., Marable J.H., and Wagschal J.J.: Nucl. Technol., **57**, 20 (1982).
67) Anderl R.A., Millsap D.A., Rogers J.W., and Harker Y.D.: "INEL Integral Data Testing Report for ENDF/B-V Dosimetry Cross Sections", USDOE Report EGG-PHYS-5608 (1981).
68) Fabry A., De Leeuw G., and De Leeuw S.: Nucl. Technol., **25**, 349 (1975).
69) Nakazawa M., and Sekiguchi A.: "Dosimetry Data Collection in the Fast Neutron Source Reactor YAYOI", UTNL-R 0037 (1976).
70) Nakazawa M., Taniguchi T., Kato M., Sekiguchi A., Kobayashi K., Sakurai K., and Suzuki S.: "The YAYOI Blind Intercomparison on Multi-Foil Reaction Rate Measurements", UTNL-R 0099 (1981).
71) Zijp W.L., Nolthenius H.J., Zsolnay E.M., Szondi E.J., Verhaag G.C.H.M., Cullen D.E., and Ertek C.: "Interim Report on the REAL-80 Exercise", ECN-82-65 (1982).
72) Aoyama T. and Sekine T.: "Integral Test of JENDL Dosimetry File Using Fast Neutron Field in the Experimental Fast Reactor JOYO," JNC TN9400 99-068 (1999) [in Japanese].
73) Rhoades W. A. and Childs R. L.: "The DORT Two-Dimensional Discrete Ordinates Transport Code System," CCC-484 (1989).
74) Nakagawa T.: "Summary of JENDL-2 General Purpose File," JAERI-M 84-103 (1984).
75) MacFarlane R. E. et al.: LA-9303-M Vol. I and II (1982).
76) Koyama K. et al.: " ANISN-JR, A One Dimentional Dicreat Ordinates Code for Neutron and Gamma-ray Transport Calculations ", JAERI- M6954 (1977).
77) MacFarlane R. E. et al.: LA-9303-M: Vol. I and II (1982).
78) Taniguchi T. et al.: "Systematic Study on Spectral Effects in the Adjustment Calculation using the NEUPAC-83 Code", Proc. 9th ASTM-EURATOM Symp. (1984).
79) Shimakawa S.: JAERI-Code/Data 99-043 (1999).
80) Nakamura T., and Abdou M.A.: Proc. First Int. Symposium on Fusion Nucl. Technol., Tokyo, Japan, Apr. 11-15, 1988, Fusion Eng. Design, 9, 303 (1989).
81) Oyama Y.: ibid., 9, 309 (1989).
82) Nakamura T., Maekawa H., Kusano J., Oyama Y., Ikeda Y., Kutsukake C., Tanaka S., and Tanaka Shu.: Proc. 4th Symp. on Accelerator Sci. Technol., RIKEN, Saitama, Japan, Nov. 24-26, 1982, p. 155 (1982).
83) Ikeda Y., Konno C., Oishi K., Nakamura T., Miyade H., Kawade K., Yamamoto H. and Katoh T.: " Activation Cross Section Measurements for Fusion Reactor Structural Materials at Neutron Energy from 13.3 o 15.0 MeV Using FNS Facility ", JAERI 1312 (1988).
84) Huang X., Yu W., Han X., Zhao W., Lu H., Chen J., Shi Z., Tang G., and Zhang G.: Nucl. Sci.Eng., **131**, 267 (1999).
85) Konno C., Ikeda Y., Oishi K., Kawade K., Yamamoto H., and Maekawa H.: "Activation Cross Section Measurement at Neutron Energy from 13.3 to 14.9 MeV Using the FNS Facility", JAERI 1329 (1993).
86) Dumais J.R., Iwasaki S., Tanaka S., Odano N., and Sugiyama K.: Proc. 7-th ASTM Euratom Symp. on Reactor Dosimetry, Strasbourg, Kluwer Academic Publ., London, p.421 (1992).

87) Mannhart W.: Proc. IAEA Advisory Group Meeting on Properties of Neutron Source, Leningrad, USSR, Jun. 9-13, 1986, IAEA-TECDOC-410, p. 158 (1987).
88) Textor R.E., and Verbinski V.V.: "O5S Monte Carlo Code", ORNL-4160 (1968).

Table 2.2.1 List of reactions in the JENDL Dosimetry File 99 (JENDL/D-99)

Nuclide	MAT	Reaction	Threshold energy (MeV)[+]	Half-life of product[++]	Data source[+++] sigma	cov.
^{6}Li	325	(n, t) α	10^{-5} eV		J3.2	I
		α production	10^{-5} eV		J3.2	I
^{7}Li	328	t production	2.822		J3.2	I
^{10}B	525	(n, α) ^{7}Li	10^{-5} eV		J3.2	I
		α production	10^{-5} eV		J3.2	I
^{19}F	925	(n, 2n) ^{18}F	10.9854	109.77 m	G	G
^{23}Na	1125	(n, 2n) ^{22}Na	12.9633	2.6019 y	S	S
		(n, γ) ^{24}Na	10^{-5} eV	14.9590 h	J3.2	I
^{24}Mg	1225	(n, p) ^{24}Na	4.9306	14.9590 h	G	G
^{27}Al	1325	(n, p) ^{27}Mg	1.8227	9.458 m	G	G
		(n, α) ^{24}Na	3.2467	14.9590 h	I90.2	I90.2
^{31}P	1525	(n, p) ^{31}Si	0.730746	157.3 m	G	G
^{32}S	1625	(n, p) ^{32}P	0.958	14.262 d	J3.2	I
^{45}Sc	2125	(n, γ) ^{46}Sc	10^{-5} eV	83.79 d	J3.2	I
^{N}Ti*	2200	(n, x) ^{46}Sc	1.6184	83.79 d	A	A
		(n, x) ^{47}Sc	10^{-5} eV	3.3492 d	A	A
		(n, x) ^{48}Sc	3.2792	43.67 h	A	A
^{46}Ti	2225	(n, 2n) ^{45}Ti	13.4865	184.8 m	G	G
		(n, p) ^{46}Sc	1.6184	83.79 d	G	G
^{47}Ti	2228	(n, np) ^{46}Sc	10.6858	83.79 d	A	K
		(n, p) ^{47}Sc	10^{-5} eV	3.3492 d	A	K
^{48}Ti	2231	(n, np) ^{47}Sc	11.6858	3.3492 d	K	K
		(n, p) ^{48}Sc	3.2792	43.67 h	G	G
^{49}Ti	2234	(n, np) ^{48}Sc	11.588	43.67 h	G	G
^{50}Cr	2425	(n, γ) ^{51}Cr	10^{-5} eV	27.702 d	J3.2	B6
^{52}Cr	2431	(n, 2n) ^{51}Cr	12.2721	27.702 d	G	G
^{55}Mn	2525	(n, 2n) ^{54}Mn	10.4141	312.3 d	S	S
		(n, γ) ^{56}Mn	10^{-5} eV	2.5785 h	J3.2	J3.2
^{54}Fe	2625	(n, p) ^{54}Mn	10^{-5} eV	312.3 d	G	G
^{56}Fe	2631	(n, p) ^{56}Mn	2.9662	2.5785 h	J3.2	I
^{57}Fe	2634	(n, np) ^{56}Mn	10.7461	2.5785 h	J3.2	B6
^{58}Fe	2637	(n, γ) ^{59}Fe	10^{-5} eV	44.503 d	J3.2	A
^{59}Co	2725	(n, 2n) ^{58}Co	10.6323	70.82 d	S	S
		(n, γ) ^{60}Co	10^{-5} eV	5.2714 y	J3.2	I
		(n, α) ^{56}Mn	10^{-5} eV	2.5785 h	J3.2	I
^{58}Ni	2825	(n, 2n) ^{57}Ni	12.4321	35.60 h	G	G
		(n, p) ^{58}Co	10^{-5} eV	70.82 d	G	G
^{60}Ni	2831	(n, p) ^{60}Co	2.075	5.2714 y	S	S
^{63}Cu	2925	(n, 2n) ^{62}Cu	11.0263	9.74 m	G	G
		(n, γ) ^{64}Cu	10^{-5} eV	12.700 h	J3.2	I
		(n, α) ^{60}Co	10^{-5} eV	5.2714 y	G	G
^{65}Cu	2931	(n, 2n) ^{64}Cu	10.0633	12.700 h	G	G
^{64}Zn	3025	(n, p) ^{64}Cu	10^{-5} eV	12.700 h	G	G
^{89}Y	3925	(n, 2n) ^{88}Y	11.6096	106.65 d	G	G
^{90}Zr	4025	(n, 2n) ^{89}Zr	12.1057	78.41 h	G	G

Table 2.2.1 (Continued)

Nuclide	MAT	Reaction	Threshold energy (MeV)+	Half-life of product++	Data source +++ sigma	cov.
^{93}Nb	4125	(n, n') ^{93m}Nb	0.03073	16.13 y	A	A
		(n, 2n) ^{92m}Nb	9.0522	10.15 d	S	S
^{103}Rh	4525	(n, n') ^{103m}Rh	0.04	56.12 m	I	I
^{109}Ag	4731	(n, γ) ^{110m}Ag	10^{-5} eV	249.79 d	E	I90.2
^{115}In	4931	(n, n') ^{115m}In	0.32	4.486 h	C	C
		(n, γ) ^{116m}In	10^{-5} eV	54.29 m	J3F	I
^{127}I	5325	(n,2n) ^{126}I	9.21779	13.11 d	G	G
^{151}Eu	6325	(n, γ) ^{152}Eu	10^{-5} eV	13.537 y	J3.2	JD91
^{169}Tm	6925	(n,2n) ^{168}Tm	8.08036	93.1 d	G	G
^{181}Ta	7328	(n, γ) ^{182}Ta	10^{-5} eV	114.43 d	J3.2	JD91
^{186}W	7443	(n, γ) ^{187}W	10^{-5} eV	23.72 h	A	JD91
^{197}Au	7925	(n, 2n) ^{196}Au	8.11273	6.183 d	G	G
		(n, γ) ^{198}Au	10^{-5} eV	2.69517 d	Y	I
^{199}Hg	8034	(n, n') ^{199m}Hg	0.5337	42.6 m	JD91	JD91
^{232}Th	9040	fission	10^{-5} eV		J3.2	I
		(n, γ) ^{233}Th	10^{-5} eV	22.3 m	J3.2	I
^{235}U	9228	fission	10^{-5} eV		J3.2	I
^{238}U	9237	fission	10^{-5} eV		J3.2	I
		(n, γ) ^{239}U	10^{-5} eV	23.45 m	J3.2	I
^{237}Np	9346	fission	10^{-5} eV		G,J3.2	G
^{239}Pu	9437	fission	10^{-5} eV		J3.2	I
^{241}Am	9543	fission	10^{-5} eV		J3.2	B6

For the nuclide with capture and/or fission cross sections, the total cross sections, which were taken from JENDL-3.2 [9], are also given in the library.

+: The energy of 10^{-5} eV is the lowest energy of the data in the cases of reactions with a positive Q-value.

++ : Table of Isotopes Eighth Edition 1998 Upgrade [11]

+++: Data source

*: The symbol ^{N}Ti stands for natural Ti.

G: evaluated in the present work by using GMA code [6]

K: evaluated in the present work by using KALMAN code [12]

S: evaluated in the present work by using spline fitting method [7]

A: evaluated in the present work by methods described in the text

J3.2 : JENDL-3.2 General Purpose File [9]

J3F : JENDL-3 Fission Product Nuclear Data File [13]

JD91 : JENDL Dosimetry File 91 [4]

B6 : ENDF/B-VI [14]

E : EAF-99 [15]

I : IRDF-85 [1]

I90 : IRDF-90 [16]

I90.2 : IRDF-90V2 [5]

C : evaluated by A.B. Smith et al.[17]

Y : evaluated by N. Yamamuro [18]

Table 2.2.2 SAND-II type energy intervals

No.	Energy (eV)		No.	Energy (eV)		No.	Energy (eV)	
	lower	upper		lower	upper		lower	upper
1	1.0000E-5	1.0000E-4	46	9.6000E-4	1.0000E-3	91	9.6000E-3	1.0000E-2
2	1.0000E-4	1.0500E-4	47	1.0000E-3	1.0500E-3	92	1.0000E-2	1.0500E-2
3	1.0500E-4	1.1000E-4	48	1.0500E-3	1.1000E-3	93	1.0500E-2	1.1000E-2
4	1.1000E-4	1.1500E-4	49	1.1000E-3	1.1500E-3	94	1.1000E-2	1.1500E-2
5	1.1500E-4	1.2000E-4	50	1.1500E-3	1.2000E-3	95	1.1500E-2	1.2000E-2
6	1.2000E-4	1.2750E-4	51	1.2000E-3	1.2750E-3	96	1.2000E-2	1.2750E-2
7	1.2750E-4	1.3500E-4	52	1.2750E-3	1.3500E-3	97	1.2750E-2	1.3500E-2
8	1.3500E-4	1.4250E-4	53	1.3500E-3	1.4250E-3	98	1.3500E-2	1.4250E-2
9	1.4250E-4	1.5000E-4	54	1.4250E-3	1.5000E-3	99	1.4250E-2	1.5000E-2
10	1.5000E-4	1.6000E-4	55	1.5000E-3	1.6000E-3	100	1.5000E-2	1.6000E-2
11	1.6000E-4	1.7000E-4	56	1.6000E-3	1.7000E-3	101	1.6000E-2	1.7000E-2
12	1.7000E-4	1.8000E-4	57	1.7000E-3	1.8000E-3	102	1.7000E-2	1.8000E-2
13	1.8000E-4	1.9000E-4	58	1.8000E-3	1.9000E-3	103	1.8000E-2	1.9000E-2
14	1.9000E-4	2.0000E-4	59	1.9000E-3	2.0000E-3	104	1.9000E-2	2.0000E-2
15	2.0000E-4	2.1000E-4	60	2.0000E-3	2.1000E-3	105	2.0000E-2	2.1000E-2
16	2.1000E-4	2.2000E-4	61	2.1000E-3	2.2000E-3	106	2.1000E-2	2.2000E-2
17	2.2000E-4	2.3000E-4	62	2.2000E-3	2.3000E-3	107	2.2000E-2	2.3000E-2
18	2.3000E-4	2.4000E-4	63	2.3000E-3	2.4000E-3	108	2.3000E-2	2.4000E-2
19	2.4000E-4	2.5500E-4	64	2.4000E-3	2.5500E-3	109	2.4000E-2	2.5500E-2
20	2.5500E-4	2.7000E-4	65	2.5500E-3	2.7000E-3	110	2.5500E-2	2.7000E-2
21	2.7000E-4	2.8000E-4	66	2.7000E-3	2.8000E-3	111	2.7000E-2	2.8000E-2
22	2.8000E-4	3.0000E-4	67	2.8000E-3	3.0000E-3	112	2.8000E-2	3.0000E-2
23	3.0000E-4	3.2000E-4	68	3.0000E-3	3.2000E-3	113	3.0000E-2	3.2000E-2
24	3.2000E-4	3.4000E-4	69	3.2000E-3	3.4000E-3	114	3.2000E-2	3.4000E-2
25	3.4000E-4	3.6000E-4	70	3.4000E-3	3.6000E-3	115	3.4000E-2	3.6000E-2
26	3.6000E-4	3.8000E-4	71	3.6000E-3	3.8000E-3	116	3.6000E-2	3.8000E-2
27	3.8000E-4	4.0000E-4	72	3.8000E-3	4.0000E-3	117	3.8000E-2	4.0000E-2
28	4.0000E-4	4.2500E-4	73	4.0000E-3	4.2500E-3	118	4.0000E-2	4.2500E-2
29	4.2500E-4	4.5000E-4	74	4.2500E-3	4.5000E-3	119	4.2500E-2	4.5000E-2
30	4.5000E-4	4.7500E-4	75	4.5000E-3	4.7500E-3	120	4.5000E-2	4.7500E-2
31	4.7500E-4	5.0000E-4	76	4.7500E-3	5.0000E-3	121	4.7500E-2	5.0000E-2
32	5.0000E-4	5.2500E-4	77	5.0000E-3	5.2500E-3	122	5.0000E-2	5.2500E-2
33	5.2500E-4	5.5000E-4	78	5.2500E-3	5.5000E-3	123	5.2500E-2	5.5000E-2
34	5.5000E-4	5.7500E-4	79	5.5000E-3	5.7500E-3	124	5.5000E-2	5.7500E-2
35	5.7500E-4	6.0000E-4	80	5.7500E-3	6.0000E-3	125	5.7500E-2	6.0000E-2
36	6.0000E-4	6.3000E-4	81	6.0000E-3	6.3000E-3	126	6.0000E-2	6.3000E-2
37	6.3000E-4	6.6000E-4	82	6.3000E-3	6.6000E-3	127	6.3000E-2	6.6000E-2
38	6.6000E-4	6.9000E-4	83	6.6000E-3	6.9000E-3	128	6.6000E-2	6.9000E-2
39	6.9000E-4	7.2000E-4	84	6.9000E-3	7.2000E-3	129	6.9000E-2	7.2000E-2
40	7.2000E-4	7.6000E-4	85	7.2000E-3	7.6000E-3	130	7.2000E-2	7.6000E-2
41	7.6000E-4	8.0000E-4	86	7.6000E-3	8.0000E-3	131	7.6000E-2	8.0000E-2
42	8.0000E-4	8.4000E-4	87	8.0000E-3	8.4000E-3	132	8.0000E-2	8.4000E-2
43	8.4000E-4	8.8000E-4	88	8.4000E-3	8.8000E-3	133	8.4000E-2	8.8000E-2
44	8.8000E-4	9.2000E-4	89	8.8000E-3	9.2000E-3	134	8.8000E-2	9.2000E-2
45	9.2000E-4	9.6000E-4	90	9.2000E-3	9.6000E-3	135	9.2000E-2	9.6000E-2

Table 2.2.2 (continued)

No.	Energy (eV)		No.	Energy (eV)		No.	Energy (eV)	
	lower	upper		lower	upper		lower	upper
136	9.6000E-2	1.0000E-1	181	9.6000E-1	1.0000E+0	226	9.6000E+0	1.0000E+1
137	1.0000E-1	1.0500E-1	182	1.0000E+0	1.0500E+0	227	1.0000E+1	1.0500E+1
138	1.0500E-1	1.1000E-1	183	1.0500E+0	1.1000E+0	228	1.0500E+1	1.1000E+1
139	1.1000E-1	1.1500E-1	184	1.1000E+0	1.1500E+0	229	1.1000E+1	1.1500E+1
140	1.1500E-1	1.2000E-1	185	1.1500E+0	1.2000E+0	230	1.1500E+1	1.2000E+1
141	1.2000E-1	1.2750E-1	186	1.2000E+0	1.2750E+0	231	1.2000E+1	1.2750E+1
142	1.2750E-1	1.3500E-1	187	1.2750E+0	1.3500E+0	232	1.2750E+1	1.3500E+1
143	1.3500E-1	1.4250E-1	188	1.3500E+0	1.4250E+0	233	1.3500E+1	1.4250E+1
144	1.4250E-1	1.5000E-1	189	1.4250E+0	1.5000E+0	234	1.4250E+1	1.5000E+1
145	1.5000E-1	1.6000E-1	190	1.5000E+0	1.6000E+0	235	1.5000E+1	1.6000E+1
146	1.6000E-1	1.7000E-1	191	1.6000E+0	1.7000E+0	236	1.6000E+1	1.7000E+1
147	1.7000E-1	1.8000E-1	192	1.7000E+0	1.8000E+0	237	1.7000E+1	1.8000E+1
148	1.8000E-1	1.9000E-1	193	1.8000E+0	1.9000E+0	238	1.8000E+1	1.9000E+1
149	1.9000E-1	2.0000E-1	194	1.9000E+0	2.0000E+0	239	1.9000E+1	2.0000E+1
150	2.0000E-1	2.1000E-1	195	2.0000E+0	2.1000E+0	240	2.0000E+1	2.1000E+1
151	2.1000E-1	2.2000E-1	196	2.1000E+0	2.2000E+0	241	2.1000E+1	2.2000E+1
152	2.2000E-1	2.3000E-1	197	2.2000E+0	2.3000E+0	242	2.2000E+1	2.3000E+1
153	2.3000E-1	2.4000E-1	198	2.3000E+0	2.4000E+0	243	2.3000E+1	2.4000E+1
154	2.4000E-1	2.5500E-1	199	2.4000E+0	2.5500E+0	244	2.4000E+1	2.5500E+1
155	2.5500E-1	2.7000E-1	200	2.5500E+0	2.7000E+0	245	2.5500E+1	2.7000E+1
156	2.7000E-1	2.8000E-1	201	2.7000E+0	2.8000E+0	246	2.7000E+1	2.8000E+1
157	2.8000E-1	3.0000E-1	202	2.8000E+0	3.0000E+0	247	2.8000E+1	3.0000E+1
158	3.0000E-1	3.2000E-1	203	3.0000E+0	3.2000E+0	248	3.0000E+1	3.2000E+1
159	3.2000E-1	3.4000E-1	204	3.2000E+0	3.4000E+0	249	3.2000E+1	3.4000E+1
160	3.4000E-1	3.6000E-1	205	3.4000E+0	3.6000E+0	250	3.4000E+1	3.6000E+1
161	3.6000E-1	3.8000E-1	206	3.6000E+0	3.8000E+0	251	3.6000E+1	3.8000E+1
162	3.8000E-1	4.0000E-1	207	3.8000E+0	4.0000E+0	252	3.8000E+1	4.0000E+1
163	4.0000E-1	4.2500E-1	208	4.0000E+0	4.2500E+0	253	4.0000E+1	4.2500E+1
164	4.2500E-1	4.5000E-1	209	4.2500E+0	4.5000E+0	254	4.2500E+1	4.5000E+1
165	4.5000E-1	4.7500E-1	210	4.5000E+0	4.7500E+0	255	4.5000E+1	4.7500E+1
166	4.7500E-1	5.0000E-1	211	4.7500E+0	5.0000E+0	256	4.7500E+1	5.0000E+1
167	5.0000E-1	5.2500E-1	212	5.0000E+0	5.2500E+0	257	5.0000E+1	5.2500E+1
168	5.2500E-1	5.5000E-1	213	5.2500E+0	5.5000E+0	258	5.2500E+1	5.5000E+1
169	5.5000E-1	5.7500E-1	214	5.5000E+0	5.7500E+0	259	5.5000E+1	5.7500E+1
170	5.7500E-1	6.0000E-1	215	5.7500E+0	6.0000E+0	260	5.7500E+1	6.0000E+1
171	6.0000E-1	6.3000E-1	216	6.0000E+0	6.3000E+0	261	6.0000E+1	6.3000E+1
172	6.3000E-1	6.6000E-1	217	6.3000E+0	6.6000E+0	262	6.3000E+1	6.6000E+1
173	6.6000E-1	6.9000E-1	218	6.6000E+0	6.9000E+0	263	6.6000E+1	6.9000E+1
174	6.9000E-1	7.2000E-1	219	6.9000E+0	7.2000E+0	264	6.9000E+1	7.2000E+1
175	7.2000E-1	7.6000E-1	220	7.2000E+0	7.6000E+0	265	7.2000E+1	7.6000E+1
176	7.6000E-1	8.0000E-1	221	7.6000E+0	8.0000E+0	266	7.6000E+1	8.0000E+1
177	8.0000E-1	8.4000E-1	222	8.0000E+0	8.4000E+0	267	8.0000E+1	8.4000E+1
178	8.4000E-1	8.8000E-1	223	8.4000E+0	8.8000E+0	268	8.4000E+1	8.8000E+1
179	8.8000E-1	9.2000E-1	224	8.8000E+0	9.2000E+0	269	8.8000E+1	9.2000E+1
180	9.2000E-1	9.6000E-1	225	9.2000E+0	9.6000E+0	270	9.2000E+1	9.6000E+1

Table 2.2.2 (continued)

No.	Energy (eV) lower	upper	No.	Energy (eV) lower	upper	No.	Energy (eV) lower	upper
271	9.6000E+1	1.0000E+2	316	9.6000E+2	1.0000E+3	361	9.6000E+3	1.0000E+4
272	1.0000E+2	1.0500E+2	317	1.0000E+3	1.0500E+3	362	1.0000E+4	1.0500E+4
273	1.0500E+2	1.1000E+2	318	1.0500E+3	1.1000E+3	363	1.0500E+4	1.1000E+4
274	1.1000E+2	1.1500E+2	319	1.1000E+3	1.1500E+3	364	1.1000E+4	1.1500E+4
275	1.1500E+2	1.2000E+2	320	1.1500E+3	1.2000E+3	365	1.1500E+4	1.2000E+4
276	1.2000E+2	1.2750E+2	321	1.2000E+3	1.2750E+3	366	1.2000E+4	1.2750E+4
277	1.2750E+2	1.3500E+2	322	1.2750E+3	1.3500E+3	367	1.2750E+4	1.3500E+4
278	1.3500E+2	1.4250E+2	323	1.3500E+3	1.4250E+3	368	1.3500E+4	1.4250E+4
279	1.4250E+2	1.5000E+2	324	1.4250E+3	1.5000E+3	369	1.4250E+4	1.5000E+4
280	1.5000E+2	1.6000E+2	325	1.5000E+3	1.6000E+3	370	1.5000E+4	1.6000E+4
281	1.6000E+2	1.7000E+2	326	1.6000E+3	1.7000E+3	371	1.6000E+4	1.7000E+4
282	1.7000E+2	1.8000E+2	327	1.7000E+3	1.8000E+3	372	1.7000E+4	1.8000E+4
283	1.8000E+2	1.9000E+2	328	1.8000E+3	1.9000E+3	373	1.8000E+4	1.9000E+4
284	1.9000E+2	2.0000E+2	329	1.9000E+3	2.0000E+3	374	1.9000E+4	2.0000E+4
285	2.0000E+2	2.1000E+2	330	2.0000E+3	2.1000E+3	375	2.0000E+4	2.1000E+4
286	2.1000E+2	2.2000E+2	331	2.1000E+3	2.2000E+3	376	2.1000E+4	2.2000E+4
287	2.2000E+2	2.3000E+2	332	2.2000E+3	2.3000E+3	377	2.2000E+4	2.3000E+4
288	2.3000E+2	2.4000E+2	333	2.3000E+3	2.4000E+3	378	2.3000E+4	2.4000E+4
289	2.4000E+2	2.5500E+2	334	2.4000E+3	2.5500E+3	379	2.4000E+4	2.5500E+4
290	2.5500E+2	2.7000E+2	335	2.5500E+3	2.7000E+3	380	2.5500E+4	2.7000E+4
291	2.7000E+2	2.8000E+2	336	2.7000E+3	2.8000E+3	381	2.7000E+4	2.8000E+4
292	2.8000E+2	3.0000E+2	337	2.8000E+3	3.0000E+3	382	2.8000E+4	3.0000E+4
293	3.0000E+2	3.2000E+2	338	3.0000E+3	3.2000E+3	383	3.0000E+4	3.2000E+4
294	3.2000E+2	3.4000E+2	339	3.2000E+3	3.4000E+3	384	3.2000E+4	3.4000E+4
295	3.4000E+2	3.6000E+2	340	3.4000E+3	3.6000E+3	385	3.4000E+4	3.6000E+4
296	3.6000E+2	3.8000E+2	341	3.6000E+3	3.8000E+3	386	3.6000E+4	3.8000E+4
297	3.8000E+2	4.0000E+2	342	3.8000E+3	4.0000E+3	387	3.8000E+4	4.0000E+4
298	4.0000E+2	4.2500E+2	343	4.0000E+3	4.2500E+3	388	4.0000E+4	4.2500E+4
299	4.2500E+2	4.5000E+2	344	4.2500E+3	4.5000E+3	389	4.2500E+4	4.5000E+4
300	4.5000E+2	4.7500E+2	345	4.5000E+3	4.7500E+3	390	4.5000E+4	4.7500E+4
301	4.7500E+2	5.0000E+2	346	4.7500E+3	5.0000E+3	391	4.7500E+4	5.0000E+4
302	5.0000E+2	5.2500E+2	347	5.0000E+3	5.2500E+3	392	5.0000E+4	5.2500E+4
303	5.2500E+2	5.5000E+2	348	5.2500E+3	5.5000E+3	393	5.2500E+4	5.5000E+4
304	5.5000E+2	5.7500E+2	349	5.5000E+3	5.7500E+3	394	5.5000E+4	5.7500E+4
305	5.7500E+2	6.0000E+2	350	5.7500E+3	6.0000E+3	395	5.7500E+4	6.0000E+4
306	6.0000E+2	6.3000E+2	351	6.0000E+3	6.3000E+3	396	6.0000E+4	6.3000E+4
307	6.3000E+2	6.6000E+2	352	6.3000E+3	6.6000E+3	397	6.3000E+4	6.6000E+4
308	6.6000E+2	6.9000E+2	353	6.6000E+3	6.9000E+3	398	6.6000E+4	6.9000E+4
309	6.9000E+2	7.2000E+2	354	6.9000E+3	7.2000E+3	399	6.9000E+4	7.2000E+4
310	7.2000E+2	7.6000E+2	355	7.2000E+3	7.6000E+3	400	7.2000E+4	7.6000E+4
311	7.6000E+2	8.0000E+2	356	7.6000E+3	8.0000E+3	401	7.6000E+4	8.0000E+4
312	8.0000E+2	8.4000E+2	357	8.0000E+3	8.4000E+3	402	8.0000E+4	8.4000E+4
313	8.4000E+2	8.8000E+2	358	8.4000E+3	8.8000E+3	403	8.4000E+4	8.8000E+4
314	8.8000E+2	9.2000E+2	359	8.8000E+3	9.2000E+3	404	8.8000E+4	9.2000E+4
315	9.2000E+2	9.6000E+2	360	9.2000E+3	9.6000E+3	405	9.2000E+4	9.6000E+4

Table 2.2.2 (continued)

No.	Energy (eV)		No.	Energy (eV)		No.	Energy (eV)	
	lower	upper		lower	upper		lower	upper
406	9.6000E+4	1.0000E+5	451	9.6000E+5	1.0000E+6	496	5.4000E+6	5.5000E+6
407	1.0000E+5	1.0500E+5	452	1.0000E+6	1.1000E+6	497	5.5000E+6	5.6000E+6
408	1.0500E+5	1.1000E+5	453	1.1000E+6	1.2000E+6	498	5.6000E+6	5.7000E+6
409	1.1000E+5	1.1500E+5	454	1.2000E+6	1.3000E+6	499	5.7000E+6	5.8000E+6
410	1.1500E+5	1.2000E+5	455	1.3000E+6	1.4000E+6	500	5.8000E+6	5.9000E+6
411	1.2000E+5	1.2750E+5	456	1.4000E+6	1.5000E+6	501	5.9000E+6	6.0000E+6
412	1.2750E+5	1.3500E+5	457	1.5000E+6	1.6000E+6	502	6.0000E+6	6.1000E+6
413	1.3500E+5	1.4250E+5	458	1.6000E+6	1.7000E+6	503	6.1000E+6	6.2000E+6
414	1.4250E+5	1.5000E+5	459	1.7000E+6	1.8000E+6	504	6.2000E+6	6.3000E+6
415	1.5000E+5	1.6000E+5	460	1.8000E+6	1.9000E+6	505	6.3000E+6	6.4000E+6
416	1.6000E+5	1.7000E+5	461	1.9000E+6	2.0000E+6	506	6.4000E+6	6.5000E+6
417	1.7000E+5	1.8000E+5	462	2.0000E+6	2.1000E+6	507	6.5000E+6	6.6000E+6
418	1.8000E+5	1.9000E+5	463	2.1000E+6	2.2000E+6	508	6.6000E+6	6.7000E+6
419	1.9000E+5	2.0000E+5	464	2.2000E+6	2.3000E+6	509	6.7000E+6	6.8000E+6
420	2.0000E+5	2.1000E+5	465	2.3000E+6	2.4000E+6	510	6.8000E+6	6.9000E+6
421	2.1000E+5	2.2000E+5	466	2.4000E+6	2.5000E+6	511	6.9000E+6	7.0000E+6
422	2.2000E+5	2.3000E+5	467	2.5000E+6	2.6000E+6	512	7.0000E+6	7.1000E+6
423	2.3000E+5	2.4000E+5	468	2.6000E+6	2.7000E+6	513	7.1000E+6	7.2000E+6
424	2.4000E+5	2.5500E+5	469	2.7000E+6	2.8000E+6	514	7.2000E+6	7.3000E+6
425	2.5500E+5	2.7000E+5	470	2.8000E+6	2.9000E+6	515	7.3000E+6	7.4000E+6
426	2.7000E+5	2.8000E+5	471	2.9000E+6	3.0000E+6	516	7.4000E+6	7.5000E+6
427	2.8000E+5	3.0000E+5	472	3.0000E+6	3.1000E+6	517	7.5000E+6	7.6000E+6
428	3.0000E+5	3.2000E+5	473	3.1000E+6	3.2000E+6	518	7.6000E+6	7.7000E+6
429	3.2000E+5	3.4000E+5	474	3.2000E+6	3.3000E+6	519	7.7000E+6	7.8000E+6
430	3.4000E+5	3.6000E+5	475	3.3000E+6	3.4000E+6	520	7.8000E+6	7.9000E+6
431	3.6000E+5	3.8000E+5	476	3.4000E+6	3.5000E+6	521	7.9000E+6	8.0000E+6
432	3.8000E+5	4.0000E+5	477	3.5000E+6	3.6000E+6	522	8.0000E+6	8.1000E+6
433	4.0000E+5	4.2500E+5	478	3.6000E+6	3.7000E+6	523	8.1000E+6	8.2000E+6
434	4.2500E+5	4.5000E+5	479	3.7000E+6	3.8000E+6	524	8.2000E+6	8.3000E+6
435	4.5000E+5	4.7500E+5	480	3.8000E+6	3.9000E+6	525	8.3000E+6	8.4000E+6
436	4.7500E+5	5.0000E+5	481	3.9000E+6	4.0000E+6	526	8.4000E+6	8.5000E+6
437	5.0000E+5	5.2500E+5	482	4.0000E+6	4.1000E+6	527	8.5000E+6	8.6000E+6
438	5.2500E+5	5.5000E+5	483	4.1000E+6	4.2000E+6	528	8.6000E+6	8.7000E+6
439	5.5000E+5	5.7500E+5	484	4.2000E+6	4.3000E+6	529	8.7000E+6	8.8000E+6
440	5.7500E+5	6.0000E+5	485	4.3000E+6	4.4000E+6	530	8.8000E+6	8.9000E+6
441	6.0000E+5	6.3000E+5	486	4.4000E+6	4.5000E+6	531	8.9000E+6	9.0000E+6
442	6.3000E+5	6.6000E+5	487	4.5000E+6	4.6000E+6	532	9.0000E+6	9.1000E+6
443	6.6000E+5	6.9000E+5	488	4.6000E+6	4.7000E+6	533	9.1000E+6	9.2000E+6
444	6.9000E+5	7.2000E+5	489	4.7000E+6	4.8000E+6	534	9.2000E+6	9.3000E+6
445	7.2000E+5	7.6000E+5	490	4.8000E+6	4.9000E+6	535	9.3000E+6	9.4000E+6
446	7.6000E+5	8.0000E+5	491	4.9000E+6	5.0000E+6	536	9.4000E+6	9.5000E+6
447	8.0000E+5	8.4000E+5	492	5.0000E+6	5.1000E+6	537	9.5000E+6	9.6000E+6
448	8.4000E+5	8.8000E+5	493	5.1000E+6	5.2000E+6	538	9.6000E+6	9.7000E+6
449	8.8000E+5	9.2000E+5	494	5.2000E+6	5.3000E+6	539	9.7000E+6	9.8000E+6
450	9.2000E+5	9.6000E+5	495	5.3000E+6	5.4000E+6	540	9.8000E+6	9.9000E+6

Table 2.2.2 (continued)

No.	Energy (eV) lower	upper	No.	Energy (eV) lower	upper	No.	Energy (eV) lower	upper
541	9.9000E+6	1.0000E+7	586	1.4400E+7	1.4500E+7	631	1.8900E+7	1.9000E+7
542	1.0000E+7	1.0100E+7	587	1.4500E+7	1.4600E+7	632	1.9000E+7	1.9100E+7
543	1.0100E+7	1.0200E+7	588	1.4600E+7	1.4700E+7	633	1.9100E+7	1.9200E+7
544	1.0200E+7	1.0300E+7	589	1.4700E+7	1.4800E+7	634	1.9200E+7	1.9300E+7
545	1.0300E+7	1.0400E+7	590	1.4800E+7	1.4900E+7	635	1.9300E+7	1.9400E+7
546	1.0400E+7	1.0500E+7	591	1.4900E+7	1.5000E+7	636	1.9400E+7	1.9500E+7
547	1.0500E+7	1.0600E+7	592	1.5000E+7	1.5100E+7	637	1.9500E+7	1.9600E+7
548	1.0600E+7	1.0700E+7	593	1.5100E+7	1.5200E+7	638	1.9600E+7	1.9700E+7
549	1.0700E+7	1.0800E+7	594	1.5200E+7	1.5300E+7	639	1.9700E+7	1.9800E+7
550	1.0800E+7	1.0900E+7	595	1.5300E+7	1.5400E+7	640	1.9800E+7	1.9900E+7
551	1.0900E+7	1.1000E+7	596	1.5400E+7	1.5500E+7	641	1.9900E+7	2.0000E+7
552	1.1000E+7	1.1100E+7	597	1.5500E+7	1.5600E+7			
553	1.1100E+7	1.1200E+7	598	1.5600E+7	1.5700E+7			
554	1.1200E+7	1.1300E+7	599	1.5700E+7	1.5800E+7			
555	1.1300E+7	1.1400E+7	600	1.5800E+7	1.5900E+7			
556	1.1400E+7	1.1500E+7	601	1.5900E+7	1.6000E+7			
557	1.1500E+7	1.1600E+7	602	1.6000E+7	1.6100E+7			
558	1.1600E+7	1.1700E+7	603	1.6100E+7	1.6200E+7			
559	1.1700E+7	1.1800E+7	604	1.6200E+7	1.6300E+7			
560	1.1800E+7	1.1900E+7	605	1.6300E+7	1.6400E+7			
561	1.1900E+7	1.2000E+7	606	1.6400E+7	1.6500E+7			
562	1.2000E+7	1.2100E+7	607	1.6500E+7	1.6600E+7			
563	1.2100E+7	1.2200E+7	608	1.6600E+7	1.6700E+7			
564	1.2200E+7	1.2300E+7	609	1.6700E+7	1.6800E+7			
565	1.2300E+7	1.2400E+7	610	1.6800E+7	1.6900E+7			
566	1.2400E+7	1.2500E+7	611	1.6900E+7	1.7000E+7			
567	1.2500E+7	1.2600E+7	612	1.7000E+7	1.7100E+7			
568	1.2600E+7	1.2700E+7	613	1.7100E+7	1.7200E+7			
569	1.2700E+7	1.2800E+7	614	1.7200E+7	1.7300E+7			
570	1.2800E+7	1.2900E+7	615	1.7300E+7	1.7400E+7			
571	1.2900E+7	1.3000E+7	616	1.7400E+7	1.7500E+7			
572	1.3000E+7	1.3100E+7	617	1.7500E+7	1.7600E+7			
573	1.3100E+7	1.3200E+7	618	1.7600E+7	1.7700E+7			
574	1.3200E+7	1.3300E+7	619	1.7700E+7	1.7800E+7			
575	1.3300E+7	1.3400E+7	620	1.7800E+7	1.7900E+7			
576	1.3400E+7	1.3500E+7	621	1.7900E+7	1.8000E+7			
577	1.3500E+7	1.3600E+7	622	1.8000E+7	1.8100E+7			
578	1.3600E+7	1.3700E+7	623	1.8100E+7	1.8200E+7			
579	1.3700E+7	1.3800E+7	624	1.8200E+7	1.8300E+7			
580	1.3800E+7	1.3900E+7	625	1.8300E+7	1.8400E+7			
581	1.3900E+7	1.4000E+7	626	1.8400E+7	1.8500E+7			
582	1.4000E+7	1.4100E+7	627	1.8500E+7	1.8600E+7			
583	1.4100E+7	1.4200E+7	628	1.8600E+7	1.8700E+7			
584	1.4200E+7	1.4300E+7	629	1.8700E+7	1.8800E+7			
585	1.4300E+7	1.4400E+7	630	1.8800E+7	1.8900E+7			

Table 3.1.1 Comparison of resonance integrals (unit: barn)

Reaction	JENDL/D-99	JENDL/D-91[4]	IRDF-90V2[5]	Kobayashi et al.[28]	Mughabghab et al.[27]
$^{6}Li(n,t)^{4}He$	424.7	424.7	425.0	-	-
$^{10}B(n,\alpha)^{11}B$	1718.6	1718.6	1723.8	-	1722±5
$^{23}Na(n,\gamma)^{24}Na$	0.312	0.312	0.316	0.3197±0.0132	0.311±0.010
$^{45}Sc(n,\gamma)^{46}Sc$	11.87	11.89	11.88	-	12.0±0.5
$^{50}Cr(n,\gamma)^{51}Cr$	7.405	-	-	-	7.8±0.4
$^{55}Mn(n,\gamma)^{56}Mn$	11.79	11.79	11.79	13.90±0.41	14.0±0.3
$^{58}Fe(n,\gamma)^{59}Fe$	1.371	1.586	1.513	-	1.7±0.1
$^{59}Co(n,\gamma)^{60}Co$	75.58	75.68	74.52	73.34±3.60	74±2
$^{63}Cu(n,\gamma)^{64}Cu$	4.984	4.948	4.972	-	4.97±0.08 ($^{64}Cu^{g}$)
$^{109}Ag(n,\gamma)^{110m}Ag$	67.86	-	-	56.89±2.83	72.3±4.0
$^{115}In(n,\gamma)^{116m}In$	2577.5	2577.5	-	2695±155	2650±100
$^{151}Eu(n,\gamma)^{152}Eu$	3070.7	3070.7	-	-	3300±300
$^{181}Ta(n,\gamma)^{182}Ta$	658.7	658.7	-	655.4±27.8	660±23
$^{186}W(n,\gamma)^{187}W$	478.9	349.2	-	510.7±24.3	485±15
$^{197}Au(n,\gamma)^{198}Au$	1563.7	1563.7	1566.2	1550±28	1550±28
$^{232}Th(n,\gamma)^{233}Th$	84.20	84.20	85.85	85.71±2.94	85±3
$^{235}U(n,f)$	278.3	274.8	278.8	-	275±5
$^{238}U(n,\gamma)^{239}U$	277.8	278.5	277.6	274.8±11.2	277±3
$^{237}Np(n,f)$	7.070	6.360	6.870	-	6.9±1.0
$^{239}Pu(n,f)$	302.8	299.4	298.9	-	301±10
$^{241}Am(n,f)$	13.87	13.87	-	-	14.4±1.0

Table 3.1.2 Average cross sections calculated with the ^{252}Cf spontaneous fission spectrum (NBS evaluation)

Reaction	JENDL/D-99 (mb)	Error (%)	IRDF-90V2 (mb)	Diff.*1 (%)
$^{6}Li(n,t)\alpha$	3.295E+02	3.44	3.176E+02	−3.6
^{6}Li α-production	4.780E+02	3.84		
^{7}Li t-production	2.446E+01	4.55		
$^{10}B(n,\alpha)^{7}Li$	4.262E+02	6.44	4.427E+02	3.9
^{10}B α-production	5.405E+02	6.91		
$^{19}F(n,2n)^{18}F$	1.692E−02	3.49	1.562E−02	−7.7 *
$^{23}Na(n,2n)^{22}Na$	7.206E−03	2.45		
$^{23}Na(n,\gamma)^{24}Na$	2.233E−01	12.98	2.675E−01	19.8 **
$^{24}Mg(n,p)^{24}Na$	2.236E+00	2.43	2.215E+00	−0.9
$^{27}Al(n,p)^{27}Mg$	5.276E+00	2.21	4.769E+00	−9.6 *
$^{27}Al(n,\alpha)^{24}Na$	1.060E+00	2.49	1.060E+00	0.0
$^{31}P(n,p)^{31}Si$	3.218E+01	2.53	3.065E+01	−4.7
$^{32}S(n,p)^{32}P$	7.498E+01	8.13	7.025E+01	−6.3 *
$^{45}Sc(n,\gamma)^{46}Sc$	5.997E+00	3.97	4.804E+00	−19.9 **
$^{N}Ti(n,X)^{46}Sc$	1.145E+00	3.12		
$^{N}Ti(n,X)^{47}Sc$	1.381E+00	2.43		
$^{N}Ti(n,X)^{48}Sc$	2.977E−01	2.98		
$^{46}Ti(n,2n)^{45}Ti$	1.039E−02	2.85		
$^{46}Ti(n,p)^{46}Sc$	1.387E+01	3.11	1.259E+01	−9.2 *
$^{47}Ti(n,np)^{46}Sc$	1.423E−02	3.34	2.063E−02	45.0 ****
$^{47}Ti(n,p)^{47}Sc$	1.852E+01	2.43	1.937E+01	4.6
$^{48}Ti(n,np)^{47}Sc$	3.272E−03	2.82	3.437E−03	5.0 *
$^{48}Ti(n,p)^{48}Sc$	4.037E−01	2.77	3.951E−01	−2.1
$^{49}Ti(n,np)^{48}Sc$	2.121E−03	11.25		
$^{50}Cr(n,\gamma)^{51}Cr$	6.222E+00	10.87		
$^{52}Cr(n,2n)^{51}Cr$	8.491E−02	2.50	8.603E−02	1.3
$^{55}Mn(n,2n)^{54}Mn$	4.796E−01	8.61	4.574E−01	−4.6
$^{55}Mn(n,\gamma)^{56}Mn$	2.812E+00	12.50	2.813E+00	0.0
$^{54}Fe(n,p)^{54}Mn$	8.957E+01	2.30	8.841E+01	−1.3
$^{56}Fe(n,p)^{56}Mn$	1.449E+00	4.90	1.408E+00	−2.9
$^{57}Fe(n,np)^{56}Mn$	1.592E−03	17.38		
$^{58}Fe(n,\gamma)^{59}Fe$	1.790E+00	3.59	2.450E+00	36.9 ***
$^{59}Co(n,2n)^{58}Co$	3.939E−01	2.52	3.995E−01	1.4
$^{59}Co(n,\gamma)^{60}Co$	5.564E+00	4.97	6.028E+00	8.3 *

Reaction	JENDL/D-99 (mb)	Error (%)	IRDF-90V2 (mb)	Diff. (%)
$^{59}Co(n,\alpha)^{56}Mn$	2.360E−01	4.68	2.211E−01	−6.3 *
$^{58}Ni(n,2n)^{57}Ni$	7.815E−03	2.30	8.045E−03	2.9
$^{58}Ni(n,p)^{58}Co$	1.150E+02	2.17	1.155E+02	0.5
$^{60}Ni(n,p)^{60}Co$	2.347E+00	18.93	2.561E+00	9.1 *
$^{63}Cu(n,2n)^{62}Cu$	1.943E−01	2.49	1.924E−01	−1.0
$^{63}Cu(n,\gamma)^{64}Cu$	1.047E+01	19.43	1.038E+01	−0.8
$^{63}Cu(n,\alpha)^{60}Co$	7.455E−01	2.55	6.961E−01	−6.6 *
$^{65}Cu(n,2n)^{64}Cu$	6.689E−01	2.28	6.471E−01	−3.3
$^{64}Zn(n,p)^{64}Cu$	3.838E+01	2.63	4.214E+01	9.8 *
$^{89}Y(n,2n)^{88}Y$	3.167E−01	2.55	3.170E−01	0.1
$^{90}Zr(n,2n)^{89}Zr$	1.943E−01	2.19	1.989E−01	2.3
$^{93}Nb(n,2n)^{92m}Nb$	7.444E−01	4.64	7.663E−01	2.9
$^{93}Nb(n,n')^{93m}Nb$	1.485E+02	3.86	1.415E+02	−4.7
$^{103}Rh(n,n')^{103m}Rh$	7.122E+02	3.72	7.103E+02	−0.3
$^{109}Ag(n,\gamma)^{110m}Ag$	6.636E+00	9.99	9.376E+00	41.3 ****
$^{115}In(n,n')^{115m}In$	1.881E+02	3.02	1.881E+02	0.0
$^{115}In(n,\gamma)^{116m}In$	1.258E+02	4.60	1.535E+02	22.0 ***
$^{127}I(n,2n)^{126}I$	2.217E+00	3.68	2.144E+00	−3.3
$^{151}Eu(n,\gamma)^{152}Eu$	3.597E+02	3.38		
$^{169}Tm(n,2n)^{168}Tm$	6.237E+00	3.11		
$^{181}Ta(n,\gamma)^{182}Ta$	8.291E+01	5.91		
$^{186}W(n,\gamma)^{187}W$	3.459E+01	5.07		
$^{197}Au(n,2n)^{196}Au$	5.762E+00	2.41	5.727E+00	−0.6
$^{197}Au(n,\gamma)^{198}Au$	7.493E+01	8.85	7.418E+01	−1.0
$^{199}Hg(n,n')^{199m}Hg$	2.471E+02	8.07		
$^{232}Th(n,f)$	8.164E+01	5.50	7.807E+01	−4.4
$^{232}Th(n,\gamma)^{233}Th$	8.341E+01	12.04	8.969E+01	7.5 *
$^{235}U(n,f)$	1.235E+03	2.87	1.217E+03	−1.5
$^{238}U(n,f)$	3.166E+02	2.91	3.130E+02	−1.1
$^{238}U(n,\gamma)^{239}U$	6.467E+01	6.07	6.790E+01	5.0
$^{237}Np(n,f)$	1.330E+03	2.12	1.352E+03	1.6
$^{239}Pu(n,f)$	1.801E+03	2.92	1.773E+03	−1.6
$^{241}Am(n,f)$	1.386E+03	3.51		

*1) Judgment from deviations: * for >5%; ** for >10%; *** for >20%; **** for >40%.

Table 3.1.3 Average cross sections calculated with the ^{235}U thermal fission spectrum (NBS evaluation)

Reaction	JENDL/D-99 (mb)	Error (%)	IRDF-90V2 (mb)	Diff.*1 (%)
$^{6}Li(n,t)\alpha$	3.476E+02	3.39	3.346E+02	−3.7
^{6}Li α-production	4.791E+02	3.68		
^{7}Li t-production	1.951E+01	4.88		
$^{10}B(n,\alpha)^{7}Li$	4.476E+02	6.15	4.626E+02	3.4
^{10}B α-production	5.530E+02	6.68		
$^{19}F(n,2n)^{18}F$	7.193E−03	3.86	6.597E−03	−8.3 *
$^{23}Na(n,2n)^{22}Na$	2.727E−03	2.47		
$^{23}Na(n,\gamma)^{24}Na$	2.305E−01	12.73	2.783E−01	20.8 ***
$^{24}Mg(n,p)^{24}Na$	1.507E+00	2.46	1.492E+00	−1.0
$^{27}Al(n,p)^{27}Mg$	4.253E+00	2.21	3.846E+00	−9.6 *
$^{27}Al(n,\alpha)^{24}Na$	6.949E−01	2.52	6.949E−01	0.0
$^{31}P(n,p)^{31}Si$	2.892E+01	2.52	2.742E+01	−5.2 *
$^{32}S(n,p)^{32}P$	6.676E+01	8.42	6.250E+01	−6.4 *
$^{45}Sc(n,\gamma)^{46}Sc$	6.405E+00	3.84	5.161E+00	−19.4 **
$^{N}Ti(n,X)^{46}Sc$	9.183E−01	3.11		
$^{N}Ti(n,X)^{47}Sc$	1.234E+00	2.48		
$^{N}Ti(n,X)^{48}Sc$	2.001E−01	2.93		
$^{46}Ti(n,2n)^{45}Ti$	3.778E−03	2.83		
$^{46}Ti(n,p)^{46}Sc$	1.113E+01	3.10	1.008E+01	−9.4 *
$^{47}Ti(n,np)^{46}Sc$	5.527E−03	3.40	8.472E−03	53.3 ****
$^{47}Ti(n,p)^{47}Sc$	1.658E+01	2.48	1.735E+01	4.7
$^{48}Ti(n,np)^{47}Sc$	1.252E−03	2.69	1.364E−03	8.9 *
$^{48}Ti(n,p)^{48}Sc$	2.714E−01	2.82	2.637E−01	−2.8
$^{49}Ti(n,np)^{48}Sc$	7.792E−04	10.59		
$^{50}Cr(n,\gamma)^{51}Cr$	6.488E+00	10.69		
$^{52}Cr(n,2n)^{51}Cr$	3.386E−02	2.51	3.429E−02	1.3
$^{55}Mn(n,2n)^{54}Mn$	2.216E−01	9.23	2.109E−01	−4.8
$^{55}Mn(n,\gamma)^{56}Mn$	2.968E+00	13.64	2.968E+00	0.0
$^{54}Fe(n,p)^{54}Mn$	7.869E+01	2.31	7.790E+01	−1.0
$^{56}Fe(n,p)^{56}Mn$	1.026E+00	5.01	1.003E+00	−2.3
$^{57}Fe(n,np)^{56}Mn$	5.846E−04	17.30		
$^{58}Fe(n,\gamma)^{59}Fe$	1.879E+00	3.53	2.563E+00	36.4 ***
$^{59}Co(n,2n)^{58}Co$	1.783E−01	2.59	1.812E−01	1.6
$^{59}Co(n,\gamma)^{60}Co$	5.812E+00	4.80	6.279E+00	8.0 *

Reaction	JENDL/D-99 (mb)	Error (%)	IRDF-90V2 (mb)	Diff. (%)
$^{59}Co(n,\alpha)^{56}Mn$	1.599E−01	4.78	1.489E−01	−6.9 *
$^{58}Ni(n,2n)^{57}Ni$	3.054E−03	2.33	3.153E−03	3.2
$^{58}Ni(n,p)^{58}Co$	1.017E+02	2.18	1.025E+02	0.8
$^{60}Ni(n,p)^{60}Co$	1.692E+00	21.34	1.895E+00	12.0 **
$^{63}Cu(n,2n)^{62}Cu$	8.375E−02	2.53	8.231E−02	−1.7
$^{63}Cu(n,\gamma)^{64}Cu$	1.101E+01	19.32	1.083E+01	−1.6
$^{63}Cu(n,\alpha)^{60}Co$	5.623E−01	2.55	5.086E−01	−9.6 *
$^{65}Cu(n,2n)^{64}Cu$	3.163E−01	2.32	3.032E−01	−4.1
$^{64}Zn(n,p)^{64}Cu$	3.367E+01	2.66	3.724E+01	10.6 **
$^{89}Y(n,2n)^{88}Y$	1.341E−01	2.60	1.339E−01	−0.2
$^{90}Zr(n,2n)^{89}Zr$	7.890E−02	2.19	8.086E−02	2.5
$^{93}Nb(n,2n)^{92m}Nb$	3.852E−01	5.12	3.987E−01	3.5
^{93}Nb $n,n')^{93m}Nb$	1.420E+02	3.93	1.352E+02	−4.8
$^{103}Rh(n,n')^{103m}Rh$	6.890E+02	3.75	6.871E+02	−0.3
$^{109}Ag(n,\gamma)^{110m}Ag$	6.913E+00	9.56	9.961E+00	44.1 ****
$^{115}In(n,n')^{115m}In$	1.793E+02	3.03	1.793E+02	0.0
$^{115}In(n,\gamma)^{116m}In$	1.321E+02	4.55	1.603E+02	21.3 ***
$^{127}I(n,2n)^{126}I$	1.126E+00	3.82	1.080E+00	−4.1
$^{151}Eu(n,\gamma)^{152}Eu$	3.855E+02	3.42		
$^{169}Tm(n,2n)^{168}Tm$	3.518E+00	3.18		
$^{181}Ta(n,\gamma)^{182}Ta$	8.817E+01	5.90		
$^{186}W(n,\gamma)^{187}W$	3.621E+01	5.07		
$^{197}Au(n,2n)^{196}Au$	3.200E+00	2.43	3.172E+00	−0.9
$^{197}Au(n,\gamma)^{198}Au$	7.955E+01	8.46	7.889E+01	−0.8
$^{199}Hg(n,n')^{199m}Hg$	2.312E+02	8.15		
$^{232}Th(n,f)$	7.575E+01	5.51	7.240E+01	−4.4
$^{232}Th(n,\gamma)^{233}Th$	8.770E+01	11.84	9.424E+01	7.5 *
$^{235}U(n,f)$	1.234E+03	2.86	1.217E+03	−1.5
$^{238}U(n,f)$	2.976E+02	2.94	2.940E+02	−1.2
$^{238}U(n,\gamma)^{239}U$	6.831E+01	5.97	7.160E+01	4.8
$^{237}Np(n,f)$	1.301E+03	2.13	1.322E+03	1.6
$^{239}Pu(n,f)$	1.794E+03	2.92	1.766E+03	−1.5
$^{241}Am(n,f)$	1.344E+03	3.50		

*1) Judgment from deviations: * for >5%; ** for >10%; *** for >20%; **** for >40%.

Table 3.1.4 Average cross sections calculated with the ^{235}U thermal fission spectrum (ENDF/B-V)

Reaction	JENDL/D-99 (mb)	Error (%)	IRDF-90V2 (mb)	Diff.*1 (%)
$^{6}Li(n,t)\alpha$	3.307E+02	3.46	3.184E+02	−3.7
^{6}Li α-production	4.679E+02	3.78		
^{7}Li t-production	2.006E+01	4.92		
$^{10}B(n,\alpha)^{7}Li$	4.355E+02	6.45	4.512E+02	3.6
^{10}B α-production	5.437E+02	6.95		
$^{19}F(n,2n)^{18}F$	7.019E−03	3.98	6.425E−03	−8.5 *
$^{23}Na(n,2n)^{22}Na$	2.554E−03	2.49		
$^{23}Na(n,\gamma)^{24}Na$	2.258E−01	13.03	2.715E−01	20.2 ***
$^{24}Mg(n,p)^{24}Na$	1.563E+00	2.46	1.547E+00	−1.0
$^{27}Al(n,p)^{27}Mg$	4.391E+00	2.21	3.975E+00	−9.5 *
$^{27}Al(n,\alpha)^{24}Na$	7.211E−01	2.52	7.211E−01	0.0
$^{31}P(n,p)^{31}Si$	3.014E+01	2.52	2.856E+01	−5.2 *
$^{32}S(n,p)^{32}P$	6.959E+01	8.46	6.521E+01	−6.3 *
$^{45}Sc(n,\gamma)^{46}Sc$	6.183E+00	3.95	4.974E+00	−19.6 **
$^{N}Ti(n,X)^{46}Sc$	9.482E−01	3.10		
$^{N}Ti(n,X)^{47}Sc$	1.283E+00	2.49		
$^{N}Ti(n,X)^{48}Sc$	2.068E−01	2.93		
$^{46}Ti(n,2n)^{45}Ti$	3.480E−03	2.83		
$^{46}Ti(n,p)^{46}Sc$	1.149E+01	3.10	1.042E+01	−9.3 *
$^{47}Ti(n,np)^{46}Sc$	5.227E−03	3.44	8.168E−03	56.3 ****
$^{47}Ti(n,p)^{47}Sc$	1.723E+01	2.49	1.804E+01	4.7
$^{48}Ti(n,np)^{47}Sc$	1.178E−03	2.66	1.301E−03	10.4 **
$^{48}Ti(n,p)^{48}Sc$	2.805E−01	2.82	2.725E−01	−2.8
$^{49}Ti(n,np)^{48}Sc$	7.208E−04	10.33		
$^{50}Cr(n,\gamma)^{51}Cr$	6.357E+00	10.77		
$^{52}Cr(n,2n)^{51}Cr$	3.233E−02	2.51	3.275E−02	1.3
$^{55}Mn(n,2n)^{54}Mn$	2.216E−01	9.41	2.107E−01	−4.9
$^{55}Mn(n,\gamma)^{56}Mn$	2.897E+00	13.94	2.898E+00	0.0
$^{54}Fe(n,p)^{54}Mn$	8.189E+01	2.31	8.108E+01	−1.0
$^{56}Fe(n,p)^{56}Mn$	1.058E+00	5.00	1.033E+00	−2.4
$^{57}Fe(n,np)^{56}Mn$	5.407E−04	17.27		
$^{58}Fe(n,\gamma)^{59}Fe$	1.829E+00	3.60	2.521E+00	37.8 ***
$^{59}Co(n,2n)^{58}Co$	1.773E−01	2.61	1.803E−01	1.7
$^{59}Co(n,\gamma)^{60}Co$	5.703E+00	4.94	6.174E+00	8.3 *

Reaction	JENDL/D-99 (mb)	Error (%)	IRDF-90V2 (mb)	Diff. (%)
$^{59}Co(n,\alpha)^{56}Mn$	1.653E−01	4.77	1.540E−01	−6.8 *
$^{58}Ni(n,2n)^{57}Ni$	2.895E−03	2.34	2.992E−03	3.4
$^{58}Ni(n,p)^{58}Co$	1.058E+02	2.18	1.067E+02	0.9
$^{60}Ni(n,p)^{60}Co$	1.742E+00	21.13	1.952E+00	12.1 **
$^{63}Cu(n,2n)^{62}Cu$	8.210E−02	2.54	8.048E−02	−2.0
$^{63}Cu(n,\gamma)^{64}Cu$	1.073E+01	19.28	1.059E+01	−1.3
$^{63}Cu(n,\alpha)^{60}Co$	5.812E−01	2.55	5.247E−01	−9.7 *
$^{65}Cu(n,2n)^{64}Cu$	3.180E−01	2.32	3.041E−01	−4.4
$^{64}Zn(n,p)^{64}Cu$	3.503E+01	2.66	3.882E+01	10.8 **
$^{89}Y(n,2n)^{88}Y$	1.307E−01	2.62	1.304E−01	−0.3
$^{90}Zr(n,2n)^{89}Zr$	7.585E−02	2.19	7.776E−02	2.5
$^{93}Nb(n,2n)^{92m}Nb$	3.948E−01	5.20	4.090E−01	3.6
$^{93}Nb(n,n')^{93m}Nb$	1.464E+02	3.89	1.394E+02	−4.7
$^{103}Rh(n,n')^{103m}Rh$	7.051E+02	3.74	7.031E+02	−0.3
$^{109}Ag(n,\gamma)^{110m}Ag$	6.783E+00	9.85	9.602E+00	41.6 ****
$^{115}In(n,n')^{115m}In$	1.854E+02	3.03	1.854E+02	0.0
$^{115}In(n,\gamma)^{116m}In$	1.292E+02	4.59	1.578E+02	22.1 ***
$^{127}I(n,2n)^{126}I$	1.149E+00	3.85	1.101E+00	−4.2
$^{151}Eu(n,\gamma)^{152}Eu$	3.703E+02	3.35		
$^{169}Tm(n,2n)^{168}Tm$	3.647E+00	3.19		
$^{181}Ta(n,\gamma)^{182}Ta$	8.562E+01	5.82		
$^{186}W(n,\gamma)^{187}W$	3.549E+01	5.07		
$^{197}Au(n,2n)^{196}Au$	3.311E+00	2.43	3.282E+00	−0.9
$^{197}Au(n,\gamma)^{198}Au$	7.698E+01	8.84	7.616E+01	−1.1
$^{199}Hg(n,n')^{199m}Hg$	2.395E+02	8.15		
$^{232}Th(n,f)$	7.850E+01	5.50	7.504E+01	−4.4
$^{232}Th(n,\gamma)^{233}Th$	8.566E+01	12.04	9.197E+01	7.4 *
$^{235}U(n,f)$	1.235E+03	2.87	1.217E+03	−1.5
$^{238}U(n,f)$	3.083E+02	2.94	3.045E+02	−1.2
$^{238}U(n,\gamma)^{239}U$	6.643E+01	6.07	6.981E+01	5.1 *
$^{237}Np(n,f)$	1.326E+03	2.13	1.347E+03	1.6
$^{239}Pu(n,f)$	1.800E+03	2.92	1.772E+03	−1.6
$^{241}Am(n,f)$	1.378E+03	3.50		

*1) Judgment from deviations: * for >5%; ** for >10%; *** for >20%; **** for >40%.

Table 3.1.5 Average cross sections calculated with the ISNF spectrum

Reaction	JENDL/D-99 (mb)	Error (%)	IRDF-90V2 (mb)	Diff.*1 (%)
^{6}Li(n,t)α	7.736E+02	2.42	7.548E+02	−2.4
^{6}Li α-production	8.183E+02	2.44		
^{7}Li t-production	5.770E+00	5.16		
^{10}B(n,α)^{7}Li	1.698E+03	2.24	1.719E+03	1.2
^{10}B α-production	1.749E+03	2.34		
^{19}F(n,2n)^{18}F	1.970E−03	3.87	1.806E−03	−8.3 *
^{23}Na(n,2n)^{22}Na	7.418E−04	2.48		
^{23}Na(n,γ)^{24}Na	1.756E+00	9.67	1.917E+00	9.2 *
^{24}Mg(n,p)^{24}Na	4.224E−01	2.46	4.182E−01	−1.0
^{27}Al(n,p)^{27}Mg	1.281E+00	2.21	1.163E+00	−9.2 *
^{27}Al(n,α)^{24}Na	1.944E−01	2.52	1.944E−01	0.0
^{31}P(n,p)^{31}Si	1.084E+01	2.50	1.017E+01	−6.3 *
^{32}S(n,p)^{32}P	2.409E+01	8.92	2.227E+01	−7.6 *
^{45}Sc(n,γ)^{46}Sc	2.786E+01	2.69	2.746E+01	−1.5
^{N}Ti(n,X)^{46}Sc	2.747E−01	3.09		
^{N}Ti(n,X)^{47}Sc	4.837E−01	2.61		
^{N}Ti(n,X)^{48}Sc	5.640E−02	2.92		
^{46}Ti(n,2n)^{45}Ti	1.023E−03	2.83		
^{46}Ti(n,p)^{46}Sc	3.328E+00	3.09	3.020E+00	−9.2 *
^{47}Ti(n,np)^{46}Sc	1.506E−03	3.41	2.315E−03	53.8 ****
^{47}Ti(n,p)^{47}Sc	6.497E+00	2.61	6.781E+00	4.4
^{48}Ti(n,np)^{47}Sc	3.397E−04	2.67	3.715E−04	9.4 *
^{48}Ti(n,p)^{48}Sc	7.649E−02	2.82	7.413E−02	−3.1
^{49}Ti(n,np)^{48}Sc	2.107E−04	10.63		
^{50}Cr(n,γ)^{51}Cr	2.346E+01	7.12		
^{52}Cr(n,2n)^{51}Cr	9.252E−03	2.51	9.370E−03	1.3
^{55}Mn(n,2n)^{54}Mn	6.087E−02	9.25	5.791E−02	−4.9
^{55}Mn(n,γ)^{56}Mn	3.271E+01	25.00	3.270E+01	0.0
^{54}Fe(n,p)^{54}Mn	2.746E+01	2.33	2.738E+01	−0.3
^{56}Fe(n,p)^{56}Mn	2.913E−01	5.02	2.848E−01	−2.2
^{57}Fe(n,np)^{56}Mn	1.579E−04	17.30		
^{58}Fe(n,γ)^{59}Fe	7.499E+00	11.80	9.531E+00	27.1 ***
^{59}Co(n,2n)^{58}Co	4.895E−02	2.59	4.974E−02	1.6
^{59}Co(n,γ)^{60}Co	4.217E+01	2.77	4.297E+01	1.9

Reaction	JENDL/D-99 (mb)	Error (%)	IRDF-90V2 (mb)	Diff. (%)
^{59}Co(n,α)^{56}Mn	4.506E−02	4.78	4.194E−02	−6.9 *
^{58}Ni(n,2n)^{57}Ni	8.331E−04	2.33	8.604E−04	3.3
^{58}Ni(n,p)^{58}Co	3.680E+01	2.18	3.755E+01	2.0
^{60}Ni(n,p)^{60}Co	4.815E−01	21.86	5.461E−01	13.4 **
^{63}Cu(n,2n)^{62}Cu	2.296E−02	2.53	2.255E−02	−1.8
^{63}Cu(n,γ)^{64}Cu	4.999E+01	6.36	4.882E+01	−2.3
^{63}Cu(n,α)^{60}Co	1.709E−01	2.52	1.465E−01	−14.3 **
^{65}Cu(n,2n)^{64}Cu	8.689E−02	2.32	8.328E−02	−4.2
^{64}Zn(n,p)^{64}Cu	1.181E+01	2.67	1.305E+01	10.5 **
^{89}Y(n,2n)^{88}Y	3.674E−02	2.60	3.667E−02	−0.2
^{90}Zr(n,2n)^{89}Zr	2.158E−02	2.19	2.212E−02	2.5
^{93}Nb(n,2n)^{92m}Nb	1.059E−01	5.12	1.096E−01	3.5
^{93}Nb(n,n')^{93m}Nb	7.135E+01	4.79	6.773E+01	−5.1 *
^{103}Rh(n,n')^{103m}Rh	3.876E+02	4.13	3.857E+02	−0.5
^{109}Ag(n,γ)^{110m}Ag	2.002E+01	7.26	2.785E+01	39.1 ***
^{115}In(n,n')^{115m}In	8.725E+01	3.05	8.725E+01	0.0
^{115}In(n,γ)^{116m}In	3.383E+02	5.30	3.603E+02	6.5 *
^{127}I(n,2n)^{126}I	3.094E−01	3.82	2.969E−01	−4.0
^{151}Eu(n,γ)^{152}Eu	2.054E+03	4.04		
^{169}Tm(n,2n)^{168}Tm	9.676E−01	3.18		
^{181}Ta(n,γ)^{182}Ta	4.928E+02	4.12		
^{186}W(n,γ)^{187}W	1.163E+02	3.89		
^{197}Au(n,2n)^{196}Au	8.801E−01	2.43	8.725E−01	−0.9
^{197}Au(n,γ)^{198}Au	3.853E+02	5.30	4.050E+02	5.1 *
^{199}Hg(n,n')^{199m}Hg	1.047E+02	8.48		
^{232}Th(n,f)	3.419E+01	5.68	3.258E+01	−4.7
^{232}Th(n,γ)^{233}Th	2.468E+02	10.69	2.638E+02	6.9 *
^{235}U(n,f)	1.607E+03	2.82	1.606E+03	−0.1
^{238}U(n,f)	1.386E+02	3.10	1.368E+02	−1.3
^{238}U(n,γ)^{239}U	2.190E+02	4.29	2.213E+02	1.1
^{237}Np(n,f)	7.824E+02	2.14	7.928E+02	1.3
^{239}Pu(n,f)	1.818E+03	3.15	1.796E+03	−1.2
^{241}Am(n,f)	7.416E+02	3.37		

*1) Judgment from deviations: * for >5%; ** for >10%; *** for >20%; **** for >40%.

Table 3.1.6 Average cross sections calculated with the CFRMF spectrum

Reaction	JENDL/D-99 (mb)	Error (%)	IRDF-90V2 (mb)	Diff.*1 (%)
$^{6}Li(n,t)\alpha$	9.102E+02	2.50	8.882E+02	−2.4
^{6}Li α-production	9.397E+02	2.49		
^{7}Li t-production	4.449E+00	4.72		
$^{10}B(n,\alpha)^{7}Li$	1.681E+03	2.14	1.701E+03	1.2
^{10}B α-production	1.717E+03	2.18		
$^{19}F(n,2n)^{18}F$	2.229E−03	3.45	2.061E−03	−7.6 *
$^{23}Na(n,2n)^{22}Na$	1.102E−03	2.49		
$^{23}Na(n,\gamma)^{24}Na$	1.339E+00	9.49	1.508E+00	12.7 **
$^{24}Mg(n,p)^{24}Na$	3.796E−01	2.45	3.762E−01	−0.9
$^{27}Al(n,p)^{27}Mg$	9.670E−01	2.21	8.757E−01	−9.4 *
$^{27}Al(n,\alpha)^{24}Na$	1.768E−01	2.51	1.768E−01	0.0
$^{31}P(n,p)^{31}Si$	6.733E+00	2.51	6.363E+00	−5.5 *
$^{32}S(n,p)^{32}P$	1.533E+01	8.45	1.427E+01	−6.9 *
$^{45}Sc(n,\gamma)^{46}Sc$	2.476E+01	2.69	2.402E+01	−3.0
$^{N}Ti(n,X)^{46}Sc$	2.088E−01	3.12		
$^{N}Ti(n,X)^{47}Sc$	2.982E−01	2.50		
$^{N}Ti(n,X)^{48}Sc$	4.994E−02	2.91		
$^{46}Ti(n,2n)^{45}Ti$	1.603E−03	2.99		
$^{46}Ti(n,p)^{46}Sc$	2.529E+00	3.12	2.295E+00	−9.2 *
$^{47}Ti(n,np)^{46}Sc$	2.083E−03	3.37	2.895E−03	39.0 ***
$^{47}Ti(n,p)^{47}Sc$	4.003E+00	2.50	4.216E+00	5.3 *
$^{48}Ti(n,np)^{47}Sc$	5.025E−04	3.66	4.919E−04	−2.1
$^{48}Ti(n,p)^{48}Sc$	6.771E−02	2.81	6.601E−02	−2.5
$^{49}Ti(n,np)^{48}Sc$	3.388E−04	11.74		
$^{50}Cr(n,\gamma)^{51}Cr$	1.873E+01	7.32		
$^{52}Cr(n,2n)^{51}Cr$	1.208E−02	2.50	1.219E−02	1.0
$^{55}Mn(n,2n)^{54}Mn$	6.192E−02	9.09	5.893E−02	−4.8
$^{55}Mn(n,\gamma)^{56}Mn$	3.201E+01	19.18	3.201E+01	0.0
$^{54}Fe(n,p)^{54}Mn$	1.796E+01	2.31	1.782E+01	−0.8
$^{56}Fe(n,p)^{56}Mn$	2.499E−01	4.96	2.432E−01	−2.7
$^{57}Fe(n,np)^{56}Mn$	2.574E−04	17.41		
$^{58}Fe(n,\gamma)^{59}Fe$	7.385E+00	7.80	9.300E+00	25.9 ***
$^{59}Co(n,2n)^{58}Co$	5.039E−02	2.53	5.063E−02	0.5
$^{59}Co(n,\gamma)^{60}Co$	8.786E+01	3.22	8.732E+01	−0.6

Reaction	JENDL/D-99 (mb)	Error (%)	IRDF-90V2 (mb)	Diff. (%)
$^{59}Co(n,\alpha)^{56}Mn$	3.983E−02	4.74	3.721E−02	−6.6 *
$^{58}Ni(n,2n)^{57}Ni$	1.134E−03	2.31	1.165E−03	2.7
$^{58}Ni(n,p)^{58}Co$	2.365E+01	2.17	2.401E+01	1.5
$^{60}Ni(n,p)^{60}Co$	4.084E−01	19.89	4.496E−01	10.1 **
$^{63}Cu(n,2n)^{62}Cu$	2.489E−02	2.46	2.468E−02	−0.8
$^{63}Cu(n,\gamma)^{64}Cu$	4.491E+01	8.40	4.330E+01	−3.6
$^{63}Cu(n,\alpha)^{60}Co$	1.343E−01	2.54	1.217E−01	−9.4 *
$^{65}Cu(n,2n)^{64}Cu$	8.799E−02	2.30	8.445E−02	−4.0
$^{64}Zn(n,p)^{64}Cu$	7.729E+00	2.64	8.496E+00	9.9 *
$^{89}Y(n,2n)^{88}Y$	4.079E−02	2.50	4.083E−02	0.1
$^{90}Zr(n,2n)^{89}Zr$	2.678E−02	2.21	2.733E−02	2.0
$^{93}Nb(n,2n)^{92m}Nb$	1.039E−01	4.96	1.077E−01	3.6
$^{93}Nb(n,n')^{93m}Nb$	4.559E+01	6.29	4.330E+01	−5.0 *
$^{103}Rh(n,n')^{103m}Rh$	2.797E+02	4.61	2.792E+02	−0.2
$^{109}Ag(n,\gamma)^{110m}Ag$	2.034E+01	6.72	3.033E+01	49.1 ****
$^{115}In(n,n')^{115m}In$	5.154E+01	3.03	5.154E+01	0.0
$^{115}In(n,\gamma)^{116m}In$	3.237E+02	4.49	3.489E+02	7.8 *
$^{127}I(n,2n)^{126}I$	3.056E−01	3.84	2.957E−01	−3.2
$^{151}Eu(n,\gamma)^{152}Eu$	2.044E+03	3.80		
$^{169}Tm(n,2n)^{168}Tm$	9.348E−01	3.16		
$^{181}Ta(n,\gamma)^{182}Ta$	5.014E+02	4.35		
$^{186}W(n,\gamma)^{187}W$	1.289E+02	3.92		
$^{197}Au(n,2n)^{196}Au$	8.555E−01	2.44	8.465E−01	−1.0
$^{197}Au(n,\gamma)^{198}Au$	3.882E+02	4.45	4.041E+02	4.1
$^{199}Hg(n,n')^{199m}Hg$	6.327E+01	8.34		
$^{232}Th(n,f)$	1.956E+01	5.52	1.862E+01	−4.8
$^{232}Th(n,\gamma)^{233}Th$	2.503E+02	10.92	2.695E+02	7.7 *
$^{235}U(n,f)$	1.569E+03	2.83	1.569E+03	0.0
$^{238}U(n,f)$	7.801E+01	3.04	7.707E+01	−1.2
$^{238}U(n,\gamma)^{239}U$	2.276E+02	4.14	2.283E+02	0.3
$^{237}Np(n,f)$	5.786E+02	2.13	5.857E+02	1.2
$^{239}Pu(n,f)$	1.768E+03	3.17	1.757E+03	−0.7
$^{241}Am(n,f)$	4.791E+02	3.16		

*1) Judgment from deviations: * for >5%; ** for >10%; *** for >20%; **** for >40%.

Table 3.1.7 Average cross sections calculated with the BIG-TEN spectrum

Reaction	JENDL/D-99 (mb)	Error (%)	IRDF-90V2 (mb)	Diff.*1 (%)
^{6}Li(n,t)α	8.933E+02	2.68	8.698E+02	−2.6
^{6}Li α-production	9.135E+02	2.67		
^{7}Li t-production	3.033E+00	4.75		
^{10}B(n,α)^{7}Li	1.205E+03	2.24	1.223E+03	1.5
^{10}B α-production	1.233E+03	2.27		
^{19}F(n,2n)^{18}F	1.951E−03	3.59	1.799E−03	−7.8 *
^{23}Na(n,2n)^{22}Na	8.118E−04	2.46		
^{23}Na(n,γ)^{24}Na	5.190E−01	9.36	6.466E−01	24.6 ***
^{24}Mg(n,p)^{24}Na	2.696E−01	2.44	2.672E−01	−0.9
^{27}Al(n,p)^{27}Mg	6.634E−01	2.21	6.016E−01	−9.3 *
^{27}Al(n,α)^{24}Na	1.276E−01	2.49	1.276E−01	0.0
^{31}P(n,p)^{31}Si	4.574E+00	2.51	4.320E+00	−5.5 *
^{32}S(n,p)^{32}P	1.044E+01	8.42	9.747E+00	−6.6 *
^{45}Sc(n,γ)^{46}Sc	1.940E+01	3.06	1.843E+01	−5.0 *
^{N}Ti(n,X)^{46}Sc	1.435E−01	3.11		
^{N}Ti(n,X)^{47}Sc	2.035E−01	2.49		
^{N}Ti(n,X)^{48}Sc	3.594E−02	2.98		
^{46}Ti(n,2n)^{45}Ti	1.162E−03	2.85		
^{46}Ti(n,p)^{46}Sc	1.738E+00	3.10	1.579E+00	−9.2 *
^{47}Ti(n,np)^{46}Sc	1.611E−03	3.34	2.359E−03	46.4 ****
^{47}Ti(n,p)^{47}Sc	2.731E+00	2.49	2.883E+00	5.6 *
^{48}Ti(n,np)^{47}Sc	3.709E−04	2.83	3.915E−04	5.6 *
^{48}Ti(n,p)^{48}Sc	4.873E−02	2.77	4.763E−02	−2.3
^{49}Ti(n,np)^{48}Sc	2.387E−04	10.86		
^{50}Cr(n,γ)^{51}Cr	1.212E+01	9.26		
^{52}Cr(n,2n)^{51}Cr	9.676E−03	2.52	9.796E−03	1.2
^{55}Mn(n,2n)^{54}Mn	5.604E−02	8.73	5.344E−02	−4.6
^{55}Mn(n,γ)^{56}Mn	8.196E+00	55.05	8.195E+00	0.0
^{54}Fe(n,p)^{54}Mn	1.225E+01	2.31	1.216E+01	−0.8
^{56}Fe(n,p)^{56}Mn	1.756E−01	4.91	1.706E-01	−2.8
^{57}Fe(n,np)^{56}Mn	1.793E−04	17.31		
^{58}Fe(n,γ)^{59}Fe	4.624E+00	4.49	6.093E+00	31.8 ***
^{59}Co(n,2n)^{58}Co	4.589E−02	2.53	4.654E−02	1.4
^{59}Co(n,γ)^{60}Co	1.206E+01	2.87	1.250E+01	3.7

Reaction	JENDL/D-99 (mb)	Error (%)	IRDF-90V2 (mb)	Diff. (%)
^{59}Co(n,α)^{56}Mn	2.848E−02	4.69	2.668E−02	−6.3 *
^{58}Ni(n,2n)^{57}Ni	8.858E−04	2.31	9.125E−04	3.0
^{58}Ni(n,p)^{58}Co	1.614E+01	2.17	1.640E+01	1.6
^{60}Ni(n,p)^{60}Co	2.847E−01	19.16	3.128E−01	9.9 *
^{63}Cu(n,2n)^{62}Cu	2.244E−02	2.50	2.221E−02	−1.0
^{63}Cu(n,γ)^{64}Cu	2.544E+01	16.79	2.333E+01	−8.3 *
^{63}Cu(n,α)^{60}Co	9.329E−02	2.54	8.504E−02	−8.8 *
^{65}Cu(n,2n)^{64}Cu	7.846E−02	2.29	7.576E−02	−3.4
^{64}Zn(n,p)^{64}Cu	5.278E+00	2.64	5.807E+00	10.0 **
^{89}Y(n,2n)^{88}Y	3.649E−02	2.56	3.648E−02	0.0
^{90}Zr(n,2n)^{89}Zr	2.221E−02	2.19	2.274E−02	2.4
^{93}Nb(n,2n)^{92m}Nb	8.820E−02	4.68	9.083E−02	3.0
^{93}Nb(n,n')^{93m}Nb	3.363E+01	7.50	3.185E+01	−5.3 *
^{103}Rh(n,n')^{103m}Rh	2.232E+02	5.24	2.231E+02	−0.1
^{109}Ag(n,γ)^{110m}Ag	1.472E+01	7.17	2.564E+01	74.1 ****
^{115}In(n,n')^{115m}In	3.594E+01	3.02	3.594E+01	0.0
^{115}In(n,γ)^{116m}In	2.542E+02	4.71	2.768E+02	8.9 *
^{127}I(n,2n)^{126}I	2.622E−01	3.69	2.534E−01	−3.4
^{151}Eu(n,γ)^{152}Eu	1.168E+03	5.25		
^{169}Tm(n,2n)^{168}Tm	7.442E−01	3.12		
^{181}Ta(n,γ)^{182}Ta	2.340E+02	6.43		
^{186}W(n,γ)^{187}W	7.657E+01	6.15		
^{197}Au(n,2n)^{196}Au	6.869E−01	2.41	6.827E−01	−0.6
^{197}Au(n,γ)^{198}Au	2.129E+02	4.69	2.142E+02	0.6
^{199}Hg(n,n')^{199m}Hg	4.395E+01	8.40		
^{232}Th(n,f)	1.330E+01	5.50	1.265E+01	−4.9
^{232}Th(n,γ)^{233}Th	1.697E+02	10.91	1.819E+02	7.2 *
^{235}U(n,f)	1.355E+03	2.94	1.350E+03	−0.3
^{238}U(n,f)	5.310E+01	3.04	5.246E+01	−1.2
^{238}U(n,γ)^{239}U	1.454E+02	5.00	1.454E+02	0.0
^{237}Np(n,f)	4.607E+02	2.12	4.674E+02	1.5
^{239}Pu(n,f)	1.591E+03	3.33	1.586E+03	−0.3
^{241}Am(n,f)	3.525E+02	3.06		

*1) Judgment from deviations: * for >5%; ** for >10%; *** for >20%; **** for >40%.

Table 3.1.8 Average cross sections calculated with the ΣΣ spectrum

Reaction	JENDL/D-99 (mb)	Error (%)	IRDF-90V2 (mb)	Diff.*1 (%)
^{6}Li(n,t)α	8.617E+02	2.55	8.394E+02	−2.6
^{6}Li α-production	8.906E+02	2.53		
^{7}Li t-production	4.095E+00	4.86		
^{10}B(n,α)^{7}Li	1.488E+03	2.19	1.506E+03	1.2
^{10}B α-production	1.525E+03	2.23		
^{19}F(n,2n)^{18}F	1.209E−03	4.63	1.098E−03	−9.2 *
^{23}Na(n,2n)^{22}Na	2.499E−04	3.00		
^{23}Na(n,γ)^{24}Na	9.814E−01	9.31	1.119E+00	14.1 **
^{24}Mg(n,p)^{24}Na	3.339E−01	2.46	3.308E−01	−0.9
^{27}Al(n,p)^{27}Mg	8.899E−01	2.22	8.095E−01	−9.0 *
^{27}Al(n,α)^{24}Na	1.542E−01	2.52	1.542E−01	0.0
^{31}P(n,p)^{31}Si	6.757E+00	2.51	6.339E+00	−6.2 *
^{32}S(n,p)^{32}P	1.517E+01	8.70	1.404E+01	−7.5 *
^{45}Sc(n,γ)^{46}Sc	2.317E+01	2.74	2.227E+01	−3.9
^{N}Ti(n,X)^{46}Sc	1.913E−01	3.20		
^{N}Ti(n,X)^{47}Sc	3.014E−01	2.55		
^{N}Ti(n,X)^{48}Sc	4.397E−02	2.93		
^{46}Ti(n,2n)^{45}Ti	1.936E−04	2.82		
^{46}Ti(n,p)^{46}Sc	2.318E+00	3.19	2.094E+00	−9.7 *
^{47}Ti(n,np)^{46}Sc	6.222E−04	4.54	1.201E−03	93.1 ****
^{47}Ti(n,p)^{47}Sc	4.050E+00	2.55	4.254E+00	5.1 *
^{48}Ti(n,np)^{47}Sc	1.233E−04	4.06	1.673E−04	35.7 ***
^{48}Ti(n,p)^{48}Sc	5.965E−02	2.83	5.806E−02	−2.7
^{49}Ti(n,np)^{48}Sc	5.348E−05	5.52		
^{50}Cr(n,γ)^{51}Cr	1.719E+01	7.55		
^{52}Cr(n,2n)^{51}Cr	4.606E−03	2.63	4.642E−03	0.8
^{55}Mn(n,2n)^{54}Mn	4.380E−02	10.21	4.165E−02	−4.9
^{55}Mn(n,γ)^{56}Mn	2.518E+01	23.52	2.517E+01	0.0
^{54}Fe(n,p)^{54}Mn	1.756E+01	2.32	1.747E+01	−0.6
^{56}Fe(n,p)^{56}Mn	2.248E−01	5.00	2.194E−01	−2.4
^{57}Fe(n,np)^{56}Mn	3.838E−05	18.33		
^{58}Fe(n,γ)^{59}Fe	6.960E+00	8.03	8.789E+00	26.3 ***
^{59}Co(n,2n)^{58}Co	3.438E−02	2.71	3.523E−02	2.5
^{59}Co(n,γ)^{60}Co	4.182E+01	2.82	4.212E+01	0.7

Reaction	JENDL/D-99 (mb)	Error (%)	IRDF-90V2 (mb)	Diff. (%)
^{59}Co(n,α)^{56}Mn	3.515E−02	4.81	3.273E−02	−6.9 *
^{58}Ni(n,2n)^{57}Ni	3.626E−04	2.67	3.839E−04	5.9 *
^{58}Ni(n,p)^{58}Co	2.335E+01	2.18	2.382E+01	2.0
^{60}Ni(n,p)^{60}Co	3.694E−01	20.43	4.047E−01	9.6 *
^{63}Cu(n,2n)^{62}Cu	1.486E−02	2.62	1.423E−02	−4.3
^{63}Cu(n,γ)^{64}Cu	3.716E+01	9.95	3.558E+01	−4.2
^{63}Cu(n,α)^{60}Co	1.231E−01	2.54	1.095E−01	−11.0 **
^{65}Cu(n,2n)^{64}Cu	6.395E−02	2.36	6.079E−02	−4.9
^{64}Zn(n,p)^{64}Cu	7.550E+00	2.65	8.348E+00	10.6 **
^{89}Y(n,2n)^{88}Y	2.299E−02	2.78	2.274E−02	−1.1
^{90}Zr(n,2n)^{89}Zr	1.179E−02	2.29	1.216E−02	3.1
^{93}Nb(n,2n)^{92m}Nb	8.282E−02	5.30	8.587E−02	3.7
^{93}Nb(n,n')^{93m}Nb	4.794E+01	6.20	4.558E+01	−4.9
^{103}Rh(n,n')^{103m}Rh	2.923E+02	4.57	2.919E+02	−0.1
^{109}Ag(n,γ)^{110m}Ag	1.836E+01	6.69	2.813E+01	53.2 ****
^{115}In(n,n')^{115m}In	5.466E+01	3.04	5.466E+01	0.0
^{115}In(n,γ)^{116m}In	3.014E+02	4.38	3.262E+02	8.2 *
^{127}I(n,2n)^{126}I	2.393E−01	3.91	2.291E−01	−4.3
^{151}Eu(n,γ)^{152}Eu	1.731E+03	3.81		
^{169}Tm(n,2n)^{168}Tm	7.756E−01	3.21		
^{181}Ta(n,γ)^{182}Ta	4.092E+02	4.19		
^{186}W(n,γ)^{187}W	1.099E+02	4.04		
^{197}Au(n,2n)^{196}Au	7.026E−01	2.44	6.962E−01	−0.9
^{197}Au(n,γ)^{198}Au	3.245E+02	4.20	3.369E+02	3.8
^{199}Hg(n,n')^{199m}Hg	6.608E+01	8.43		
^{232}Th(n,f)	2.060E+01	5.58	1.961E+01	−4.8
^{232}Th(n,γ)^{233}Th	2.238E+02	10.85	2.390E+02	6.8 *
^{235}U(n,f)	1.494E+03	2.81	1.492E+03	−0.1
^{238}U(n,f)	8.298E+01	3.07	8.195E+01	−1.2
^{238}U(n,γ)^{239}U	2.033E+02	4.25	2.043E+02	0.5
^{237}Np(n,f)	6.060E+02	2.13	6.136E+02	1.2
^{239}Pu(n,f)	1.734E+03	3.14	1.722E+03	−0.7
^{241}Am(n,f)	5.072E+02	3.17		

*1) Judgment from deviations: * for >5%; ** for >10%; *** for >20%; **** for >40%.

Table 3.1.9 Average cross sections calculated with the ORR spectrum

Reaction	JENDL/D-99 (mb)	Error (%)	IRDF-90V2 (mb)	Diff.*1 (%)
$^{6}Li(n,t)\alpha$	2.123E+05	2.11	2.125E+05	0.1
^{6}Li α-production	2.123E+05	2.11		
^{7}Li t-production	4.978E+00	4.80		
$^{10}B(n,\alpha)^{7}Li$	8.652E+05	2.08	8.662E+05	0.1
^{10}B α-production	8.652E+05	2.08		
$^{19}F(n,2n)^{18}F$	4.813E-03	2.66	4.501E-03	-6.5 *
$^{23}Na(n,2n)^{22}Na$	3.075E-03	2.37		
$^{23}Na(n,\gamma)^{24}Na$	1.215E+02	2.86	1.206E+02	-0.8
$^{24}Mg(n,p)^{24}Na$	3.838E-01	2.45	3.804E-01	-0.9
$^{27}Al(n,p)^{27}Mg$	1.077E+00	2.22	9.749E-01	-9.5 *
$^{27}Al(n,\alpha)^{24}Na$	1.766E-01	2.49	1.766E-01	0.0
$^{31}P(n,p)^{31}Si$	7.570E+00	2.52	7.147E+00	-5.6 *
$^{32}S(n,p)^{32}P$	1.728E+01	8.49	1.609E+01	-6.8 *
$^{45}Sc(n,\gamma)^{46}Sc$	6.134E+03	2.23	6.127E+03	-0.1
$^{N}Ti(n,X)^{46}Sc$	2.327E-01	3.16		
$^{N}Ti(n,X)^{47}Sc$	3.290E-01	2.51		
$^{N}Ti(n,X)^{48}Sc$	5.227E-02	2.93		
$^{46}Ti(n,2n)^{45}Ti$	5.262E-03	2.84		
$^{46}Ti(n,p)^{46}Sc$	2.816E+00	3.16	2.547E+00	-9.6 *
$^{47}Ti(n,np)^{46}Sc$	5.634E-03	3.50	6.782E-03	20.4 ***
$^{47}Ti(n,p)^{47}Sc$	4.406E+00	2.51	4.604E+00	4.5
$^{48}Ti(n,np)^{47}Sc$	1.597E-03	5.14	1.350E-03	-15.5 **
$^{48}Ti(n,p)^{48}Sc$	7.082E-02	2.75	6.882E-02	-2.8
$^{49}Ti(n,np)^{48}Sc$	1.130E-03	11.86		
$^{50}Cr(n,\gamma)^{51}Cr$	3.609E+03	4.97		
$^{52}Cr(n,2n)^{51}Cr$	2.875E-02	2.44	2.936E-02	2.1
$^{55}Mn(n,2n)^{54}Mn$	1.023E-01	6.45	9.810E-02	-4.1
$^{55}Mn(n,\gamma)^{56}Mn$	3.133E+03	4.72	3.134E+03	0.0
$^{54}Fe(n,p)^{54}Mn$	2.027E+01	2.31	2.009E+01	-0.9
$^{56}Fe(n,p)^{56}Mn$	2.632E-01	4.96	2.582E-01	-1.9
$^{57}Fe(n,np)^{56}Mn$	8.811E-04	16.80		
$^{58}Fe(n,\gamma)^{59}Fe$	3.079E+02	12.33	2.791E+02	-9.4 *
$^{59}Co(n,2n)^{58}Co$	8.905E-02	2.34	8.936E-02	0.3
$^{59}Co(n,\gamma)^{60}Co$	9.854E+03	2.20	9.866E+03	0.1

Reaction	JENDL/D-99 (mb)	Error (%)	IRDF-90V2 (mb)	Diff. (%)
$^{59}Co(n,\alpha)^{56}Mn$	4.142E-02	4.72	3.844E-02	-7.2 *
$^{58}Ni(n,2n)^{57}Ni$	2.904E-03	2.22	2.971E-03	2.3
$^{58}Ni(n,p)^{58}Co$	2.642E+01	2.18	2.672E+01	1.2
$^{60}Ni(n,p)^{60}Co$	4.334E-01	21.72	4.841E-01	11.7 **
$^{63}Cu(n,2n)^{62}Cu$	5.130E-02	2.47	5.238E-02	2.1
$^{63}Cu(n,\gamma)^{64}Cu$	1.066E+03	2.77	1.061E+03	-0.5
$^{63}Cu(n,\alpha)^{60}Co$	1.440E-01	2.55	1.298E-01	-9.9 *
$^{65}Cu(n,2n)^{64}Cu$	1.352E-01	2.20	1.337E-01	-1.1
$^{64}Zn(n,p)^{64}Cu$	8.674E+00	2.65	9.591E+00	10.6 **
$^{89}Y(n,2n)^{88}Y$	8.696E-02	2.43	8.769E-02	0.8
$^{90}Zr(n,2n)^{89}Zr$	6.199E-02	2.17	6.303E-02	1.7
$^{93}Nb(n,2n)^{92m}Nb$	1.232E-01	4.00	1.258E-01	2.1
$^{93}Nb(n,n')^{93m}Nb$	4.118E+01	4.32	3.915E+01	-4.9
$^{103}Rh(n,n')^{103m}Rh$	2.128E+02	4.09	2.122E+02	-0.3
$^{109}Ag(n,\gamma)^{110m}Ag$	2.818E+03	6.58	3.044E+03	8.0 *
$^{115}In(n,n')^{115m}In$	5.092E+01	3.03	5.092E+01	0.0
$^{115}In(n,\gamma)^{116m}In$	1.019E+05	6.50	1.308E+05	28.3 ***
$^{127}I(n,2n)^{126}I$	3.808E-01	3.36	3.709E-01	-2.6
$^{151}Eu(n,\gamma)^{152}Eu$	2.029E+06	2.83		
$^{169}Tm(n,2n)^{168}Tm$	9.524E-01	2.96		
$^{181}Ta(n,\gamma)^{182}Ta$	2.305E+04	4.06		
$^{186}W(n,\gamma)^{187}W$	2.878E+04	5.21		
$^{197}Au(n,2n)^{196}Au$	8.866E-01	2.36	8.840E-01	-0.3
$^{197}Au(n,\gamma)^{198}Au$	6.345E+04	3.49	6.352E+04	0.1
$^{199}Hg(n,n')^{199m}Hg$	6.411E+01	8.21		
$^{232}Th(n,f)$	2.104E+01	5.54	2.009E+01	-4.5
$^{232}Th(n,\gamma)^{233}Th$	4.101E+03	7.34	4.125E+03	0.6
$^{235}U(n,f)$	1.309E+05	2.10	1.311E+05	0.2
$^{238}U(n,f)$	8.337E+01	2.99	8.237E+01	-1.2
$^{238}U(n,\gamma)^{239}U$	1.035E+04	4.40	1.034E+04	-0.1
$^{237}Np(n,f)$	4.402E+02	2.12	4.293E+02	-2.5
$^{239}Pu(n,f)$	2.087E+05	2.17	2.088E+05	0.1
$^{241}Am(n,f)$	1.456E+03	2.62		

*1) Judgment from deviations: * for >5%; ** for >10%; *** for >20%; **** for >40%.

Table 3.1.10 Average cross sections calculated with the YAYOI spectrum

Reaction	JENDL/D-99 (mb)	Error (%)	IRDF-90V2 (mb)	Diff.*1 (%)
^{6}Li(n,t)α	5.441E+02	2.94	5.252E+02	−3.5
^{6}Li α-production	6.191E+02	2.96		
^{7}Li t-production	1.103E+01	4.76		
^{10}B(n,α)^{7}Li	6.554E+02	3.53	6.676E+02	1.9
^{10}B α-production	7.278E+02	3.97		
^{19}F(n,2n)^{18}F	1.023E−02	2.92	9.524E−03	−6.9 *
^{23}Na(n,2n)^{22}Na	5.530E−03	2.38		
^{23}Na(n,γ)^{24}Na	3.064E−01	9.9	3.850E−01	25.7 ***
^{24}Mg(n,p)^{24}Na	1.012E+00	2.43	1.003E+00	−0.9
^{27}Al(n,p)^{27}Mg	2.433E+00	2.21	2.208E+00	−9.3 *
^{27}Al(n,α)^{24}Na	4.838E−01	2.47	4.838E−01	0.0
^{31}P(n,p)^{31}Si	1.691E+01	2.50	1.597E+01	−5.5 *
^{32}S(n,p)^{32}P	3.864E+01	8.48	3.611E+01	−6.5 *
^{45}Sc(n,γ)^{46}Sc	1.005E+01	3.01	8.636E+00	−14.1 **
^{N}Ti(n,X)^{46}Sc	5.270E−01	3.11		
^{N}Ti(n,X)^{47}Sc	7.421E−01	2.50		
^{N}Ti(n,X)^{48}Sc	1.355E−01	2.95		
^{46}Ti(n,2n)^{45}Ti	8.817E−03	2.82		
^{46}Ti(n,p)^{46}Sc	6.378E+00	3.10	5.800E+00	−9.1 *
^{47}Ti(n,np)^{46}Sc	1.042E−02	3.35	1.352E−02	29.7 ***
^{47}Ti(n,p)^{47}Sc	9.947E+00	2.50	1.041E+01	4.6
^{48}Ti(n,np)^{47}Sc	2.703E−03	4.12	2.490E−03	−7.9 *
^{48}Ti(n,p)^{48}Sc	1.837E−01	2.75	1.795E−01	−2.3
^{49}Ti(n,np)^{48}Sc	1.858E−03	11.36		
^{50}Cr(n,γ)^{51}Cr	8.290E+00	10.10		
^{52}Cr(n,2n)^{51}Cr	5.717E−02	2.45	5.808E−02	1.6
^{55}Mn(n,2n)^{54}Mn	2.479E−01	7.36	2.370E−01	−4.4
^{55}Mn(n,γ)^{56}Mn	4.312E+00	23.14	4.312E+00	0.0
^{54}Fe(n,p)^{54}Mn	4.524E+01	2.31	4.488E+01	−0.8
^{56}Fe(n,p)^{56}Mn	6.501E−01	4.88	6.299E−01	−3.1
^{57}Fe(n,np)^{56}Mn	1.426E−03	16.75		
^{58}Fe(n,γ)^{59}Fe	2.686E+00	3.37	3.463E+00	28.9 ***
^{59}Co(n,2n)^{58}Co	2.097E−01	2.40	2.112E−01	0.7
^{59}Co(n,γ)^{60}Co	7.544E+00	3.42	7.966E+00	5.6 *

Reaction	JENDL/D-99 (mb)	Error (%)	IRDF-90V2 (mb)	Diff. (%)
^{59}Co(n,α)^{56}Mn	1.071E−01	4.69	1.006E−01	−6.1 *
^{58}Ni(n,2n)^{57}Ni	5.537E−03	2.24	5.677E−03	2.5
^{58}Ni(n,p)^{58}Co	5.919E+01	2.17	5.993E+01	1.3
^{60}Ni(n,p)^{60}Co	1.048E+00	18.70	1.153E+00	10.1 **
^{63}Cu(n,2n)^{62}Cu	1.129E−01	2.45	1.137E−01	0.7
^{63}Cu(n,γ)^{64}Cu	1.532E+01	18.84	1.453E+01	−5.2 *
^{63}Cu(n,α)^{60}Co	3.448E−01	2.53	3.144E−01	−8.8 *
^{65}Cu(n,2n)^{64}Cu	3.369E−01	2.23	3.290E−01	−2.4
^{64}Zn(n,p)^{64}Cu	1.945E+01	2.64	2.147E+01	10.4 **
^{89}Y(n,2n)^{88}Y	1.889E−01	2.47	1.898E−01	0.5
^{90}Zr(n,2n)^{89}Zr	1.264E−01	2.17	1.289E−01	2.0
^{93}Nb(n,2n)^{92m}Nb	3.522E−01	4.67	3.624E−01	2.9
^{93}Nb(n,n')^{93m}Nb	9.605E+01	4.61	9.123E+01	−5.0 *
^{103}Rh(n,n')^{103m}Rh	5.087E+02	3.97	5.075E+02	−0.2
^{109}Ag(n,γ)^{110m}Ag	9.095E+00	7.64	1.493E+01	64.2 ****
^{115}In(n,n')^{115m}In	1.174E+02	3.03	1.174E+02	0.0
^{115}In(n,γ)^{116m}In	1.715E+02	4.26	1.960E+02	14.3 **
^{127}I(n,2n)^{126}I	1.055E+00	3.55	1.017E+00	−3.7
^{151}Eu(n,γ)^{152}Eu	6.161E+02	4.28		
^{169}Tm(n,2n)^{168}Tm	2.980E+00	3.10		
^{181}Ta(n,γ)^{182}Ta	1.295E+02	6.34		
^{186}W(n,γ)^{187}W	4.787E+01	5.15		
^{197}Au(n,2n)^{196}Au	2.735E+00	2.39	2.719E+00	−0.6
^{197}Au(n,γ)^{198}Au	1.188E+02	5.27	1.193E+02	0.4
^{199}Hg(n,n')^{199m}Hg	1.469E+02	8.23		
^{232}Th(n,f)	4.771E+01	5.52	4.553E+01	−4.6
^{232}Th(n,γ)^{233}Th	1.144E+02	10.54	1.234E+02	7.9 *
^{235}U(n,f)	1.254E+03	2.83	1.241E+03	−1.1
^{238}U(n,f)	1.890E+02	3.00	1.868E+02	−1.2
^{238}U(n,γ)^{239}U	9.323E+01	5.25	9.534E+01	2.3
^{237}Np(n,f)	1.005E+03	2.13	1.021E+03	1.6
^{239}Pu(n,f)	1.716E+03	2.95	1.699E+03	−1.0
^{241}Am(n,f)	9.616E+02	3.39		

*1) Judgment from deviations: * for >5%; ** for >10%; *** for >20%; **** for >40%.

Table 3.1.11 Average cross sections calculated with the NEACRP benchmark spectrum

Reaction	JENDL/D-99 (mb)	Error (%)	IRDF-90V2 (mb)	Diff.*1 (%)
$^{6}Li(n,t)\alpha$	1.085E+03	2.32	1.066E+03	−1.8
^{6}Li α-production	1.100E+03	2.31		
^{7}Li t-production	1.918E+00	5.06		
$^{10}B(n,\alpha)^{7}Li$	2.681E+03	2.08	2.713E+03	1.2
^{10}B α-production	2.700E+03	2.09		
$^{19}F(n,2n)^{18}F$	0.000E+00		0.000E+00	
$^{23}Na(n,2n)^{22}Na$	0.000E+00			
$^{23}Na(n,\gamma)^{24}Na$	1.451E+00	9.83	1.607E+00	10.7 **
$^{24}Mg(n,p)^{24}Na$	1.214E−01	2.51	1.201E−01	−1.1
$^{27}Al(n,p)^{27}Mg$	4.198E−01	2.22	3.787E−01	−9.8 *
$^{27}Al(n,\alpha)^{24}Na$	5.312E−02	2.58	5.312E−02	0.0
$^{31}P(n,p)^{31}Si$	3.520E+00	2.51	3.314E+00	−5.8 *
$^{32}S(n,p)^{32}P$	7.828E+00	9.02	7.215E+00	−7.8 *
$^{45}Sc(n,\gamma)^{46}Sc$	4.260E+01	2.95	4.295E+01	0.8
$^{N}Ti(n,X)^{46}Sc$	8.957E−02	3.12		
$^{N}Ti(n,X)^{47}Sc$	1.550E−01	2.60		
$^{N}Ti(n,X)^{48}Sc$	1.571E−02	2.99		
$^{46}Ti(n,2n)^{45}Ti$	0.000E+00			
$^{46}Ti(n,p)^{46}Sc$	1.086E+00	3.12	9.826E−01	−9.5 *
$^{47}Ti(n,np)^{46}Sc$	0.000E+00		0.000E+00	
$^{47}Ti(n,p)^{47}Sc$	2.083E+00	2.60	2.188E+00	5.1 *
$^{48}Ti(n,np)^{47}Sc$	0.000E+00		0.000E+00	
^{48}Ti (n,p)^{48}Sc	2.131E−02	2.99	2.042E−02	−4.1
$^{49}Ti(n,np)^{48}Sc$	0.000E+00			
$^{50}Cr(n,\gamma)^{51}Cr$	3.506E+01	7.53		
$^{52}Cr(n,2n)^{51}Cr$	0.000E+00		0.000E+00	
$^{55}Mn(n,2n)^{54}Mn$	2.623E−05	214.81	2.090E−05	−20.3 ***
$^{55}Mn(n,\gamma)^{56}Mn$	5.113E+01	31.33	5.111E+01	0.0
$^{54}Fe(n,p)^{54}Mn$	8.947E+00	2.33	8.926E+00	−0.2
$^{56}Fe(n,p)^{56}Mn$	8.804E−02	5.21	8.657E−02	−1.7
$^{57}Fe(n,np)^{56}Mn$	0.000E+00			
$^{58}Fe(n,\gamma)^{59}Fe$	1.167E+01	15.21	1.478E+01	26.6 ***
$^{59}Co(n,2n)^{58}Co$	0.000E+00		0.000E+00	
$^{59}Co(n,\gamma)^{60}Co$	3.552E+01	2.53	3.697E+01	4.1

Reaction	JENDL/D-99 (mb)	Error (%)	IRDF-90V2 (mb)	Diff. (%)
$^{59}Co(n,\alpha)^{56}Mn$	1.282E−02	5.09	1.182E−02	−7.9 *
$^{58}Ni(n,2n)^{57}Ni$	0.000E+00		0.000E+00	
$^{58}Ni(n,p)^{58}Co$	1.194E+01	2.18	1.220E+01	2.2
$^{60}Ni(n,p)^{60}Co$	1.488E−01	24.45	1.714E−01	15.2 **
$^{63}Cu(n,2n)^{62}Cu$	0.000E+00		0.000E+00	
$^{63}Cu(n,\gamma)^{64}Cu$	6.772E+01	5.88	6.594E+01	−2.6
$^{63}Cu(n,\alpha)^{60}Co$	5.341E−02	2.55	4.525E−02	−15.3 **
$^{65}Cu(n,2n)^{64}Cu$	8.450E−04	3.13	3.161E−04	−62.6 ****
$^{64}Zn(n,p)^{64}Cu$	3.847E+00	2.68	4.255E+00	10.6 **
$^{89}Y(n,2n)^{88}Y$	0.000E+00		0.000E+00	
$^{90}Zr(n,2n)^{89}Zr$	0.000E+00		0.000E+00	
$^{93}Nb(n,2n)^{92m}Nb$	8.515E−03	13.65	9.452E−03	11.0 **
$^{93}Nb(n,n')^{93m}Nb$	2.541E+01	6.21	2.421E+01	−4.7
$^{103}Rh(n,n')^{103m}Rh$	1.594E+02	5.35	1.586E+02	−0.5
$^{109}Ag(n,\gamma)^{110m}Ag$	3.026E+01	7.65	4.199E+01	38.8 ***
$^{115}In(n,n')^{115m}In$	2.869E+01	3.04	2.869E+01	0.0
$^{115}In(n,\gamma)^{116m}In$	4.820E+02	6.07	5.116E+02	6.1 *
$^{127}I(n,2n)^{126}I$	1.909E−02	8.13	1.370E−02	−28.2 ***
$^{151}Eu(n,\gamma)^{152}Eu$	3.235E+03	4.72		
$^{169}Tm(n,2n)^{168}Tm$	1.785E−01	3.89		
$^{181}Ta(n,\gamma)^{182}Ta$	7.524E+02	4.62		
$^{186}W(n,\gamma)^{187}W$	1.628E+02	4.71		
$^{197}Au(n,2n)^{196}Au$	1.433E−01	2.73	1.403E−01	−2.1
$^{197}Au(n,\gamma)^{198}Au$	5.984E+02	5.93	6.300E+02	5.3 *
$^{199}Hg(n,n')^{199m}Hg$	3.449E+01	8.54		
$^{232}Th(n,f)$	1.078E+01	5.62	1.026E+01	−4.9
$^{232}Th(n,\gamma)^{233}Th$	3.571E+02	11.18	3.762E+02	5.3 *
$^{235}U(n,f)$	1.885E+03	3.24	1.896E+03	0.6
$^{238}U(n,f)$	4.367E+01	3.09	4.311E+01	−1.3
$^{238}U(n,\gamma)^{239}U$	3.236E+02	4.39	3.250E+02	0.4
$^{237}Np(n,f)$	3.317E+02	2.12	3.319E+02	0.1
$^{239}Pu(n,f)$	1.782E+03	3.76	1.765E+03	−1.0
$^{241}Am(n,f)$	2.716E+02	3.12		

*1) Judgment from deviations: * for >5%; ** for >10%; *** for >20%; **** for >40%.

Table 3.1.12 Average cross sections calculated with the JOYO spectrum

Reaction	JENDL/D-99 (mb)	Error (%)	IRDF-90V2 (mb)	Diff.*1 (%)
^{6}Li(n,t)α	9.445E+02	2.42	9.239E+02	−2.2
^{6}Li α-production	9.665E+02	2.41		
^{7}Li t-production	2.896E+00	5.06		
^{10}B(n,α)^{7}Li	1.957E+03	2.12	1.983E+03	1.3
^{10}B α-production	1.986E+03	2.14		
^{19}F(n,2n)^{18}F	9.637E−04	4.54	8.819E−04	−8.5 *
^{23}Na(n,2n)^{22}Na	3.236E−04	2.54		
^{23}Na(n,γ)^{24}Na	1.095E+00	9.65	1.255E+00	14.6 **
^{24}Mg(n,p)^{24}Na	2.214E−01	2.46	2.192E−01	−1.0
^{27}Al(n,p)^{27}Mg	6.435E−01	2.21	5.829E−01	−9.4 *
^{27}Al(n,α)^{24}Na	1.023E−01	2.51	1.023E−01	0.0
^{31}P(n,p)^{31}Si	5.300E+00	2.50	4.979E+00	−6.1 *
^{32}S(n,p)^{32}P	1.181E+01	8.92	1.093E+01	−7.5 *
^{45}Sc(n,γ)^{46}Sc	3.032E+01	2.91	3.007E+01	−0.9
^{N}Ti(n,X)^{46}Sc	1.380E−01	3.11		
^{N}Ti(n,X)^{47}Sc	2.364E−01	2.59		
^{N}Ti(n,X)^{48}Sc	2.939E−02	2.94		
^{46}Ti(n,2n)^{45}Ti	4.187E−04	2.79		
^{46}Ti(n,p)^{46}Sc	1.673E+00	3.11	1.518E+00	−9.2 *
^{47}Ti(n,np)^{46}Sc	6.765E−04	3.59	1.095E−03	61.9 ****
^{47}Ti(n,p)^{47}Sc	3.175E+00	2.59	3.328E+00	4.8
^{48}Ti(n,np)^{47}Sc	1.507E−04	2.68	1.701E−04	12.9 **
^{48}Ti(n,p)^{48}Sc	3.987E−02	2.82	3.872E−02	−2.9
^{49}Ti(n,np)^{48}Sc	8.852E−05	10.20		
^{50}Cr(n,γ)^{51}Cr	2.335E+01	7.40		
^{52}Cr(n,2n)^{51}Cr	4.334E−03	2.51	4.381E−03	1.1
^{55}Mn(n,2n)^{54}Mn	3.151E−02	9.53	2.995E−02	−4.9
^{55}Mn(n,γ)^{56}Mn	3.061E+01	34.41	3.060E+01	0.0
^{54}Fe(n,p)^{54}Mn	1.351E+01	2.33	1.348E+01	−0.2
^{56}Fe(n,p)^{56}Mn	1.503E−01	5.00	1.467E−01	−2.4
^{57}Fe(n,np)^{56}Mn	6.686E−05	17.08		
^{58}Fe(n,γ)^{59}Fe	8.067E+00	12.67	1.033E+01	28.1 ***
^{59}Co(n,2n)^{58}Co	2.500E−02	2.64	2.538E−02	1.5
^{59}Co(n,γ)^{60}Co	2.484E+01	2.55	2.553E+01	2.8

Reaction	JENDL/D-99 (mb)	Error (%)	IRDF-90V2 (mb)	Diff. (%)
^{59}Co (n,α)^{56}Mn	2.346E−02	4.77	2.187E−02	−6.8 *
^{58}Ni(n,2n)^{57}Ni	3.780E−04	2.45	3.934E−04	4.1
^{58}Ni(n,p)^{58}Co	1.809E+01	2.18	1.847E+01	2.1
^{60}Ni(n,p)^{60}Co	2.475E−01	21.49	2.793E−01	12.8 **
^{63}Cu(n,2n)^{62}Cu	1.130E−02	2.57	1.114E−02	−1.4
^{63}Cu(n,γ)^{64}Cu	5.166E+01	7.48	4.987E+01	−3.4
^{63}Cu(n,α)^{60}Co	8.670E−02	2.53	7.511E−02	−13.4 **
^{65}Cu(n,2n)^{64}Cu	4.549E−02	2.35	4.349E−02	−4.4
^{64}Zn(n,p)^{64}Cu	5.822E+00	2.67	6.437E+00	10.6 **
^{89}Y(n,2n)^{88}Y	1.803E−02	2.66	1.791E−02	−0.7
^{90}Zr(n,2n)^{89}Zr	1.021E−02	2.22	1.051E−02	2.9
^{93}Nb(n,2n)^{92m}Nb	5.732E−02	5.21	5.947E−02	3.7
^{93}Nb(n,n')^{93m}Nb	3.786E+01	5.84	3.590E+01	−5.2 *
^{103}Rh(n,n')^{103m}Rh	2.282E+02	4.87	2.274E+02	−0.4
^{109}Ag(n,γ)^{110m}Ag	2.262E+01	7.17	3.326E+01	47.0 ****
^{115}In(n,n')^{115m}In	4.359E+01	3.04	4.359E+01	0.0
^{115}In(n,γ)^{116m}In	3.715E+02	5.29	3.986E+02	7.3 *
^{127}I(n,2n)^{126}I	1.666E−01	3.85	1.597E−01	−4.2
^{151}Eu(n,γ)^{152}Eu	2.249E+03	4.41		
^{169}Tm(1,2n)^{168}Tm	5.275E−01	3.20		
^{181}Ta(n,γ)^{182}Ta	5.103E+02	4.45		
^{186}W(n,γ)^{187}W	1.220E+02	4.71		
^{197}Au(n,2n)^{196}Au	4.791E−01	2.45	4.745E−01	−1.0
^{197}Au(n,γ)^{198}Au	4.194E+02	5.43	4.381E+02	4.4
^{199}Hg(n,n')^{199m}Hg	5.225E+01	8.51		
^{232}Th(n,f)	1.658E+01	5.62	1.578E+01	−4.8
^{232}Th(n,γ)^{233}Th	2.667E+02	11.00	2.827E+02	6.0 *
^{235}U(n,f)	1.640E+03	2.96	1.643E+03	0.2
^{238}U(n,f)	6.712E+01	3.10	6.627E+01	−1.3
^{238}U(n,γ)^{239}U	2.382E+02	4.44	2.394E+02	0.5
^{237}Np(n,f)	4.697E+02	2.12	4.742E+02	1.0
^{239}Pu(n,f)	1.718E+03	3.43	1.704E+03	−0.8
^{241}Am(n,f)	3.994E+02	3.21		

*1) Judgment from deviations: * for >5%; ** for >10%; *** for >20%; **** for 40%.

Table 3.1.13 Average cross sections calculated with the JMTR spectrum

Reaction	JENDL/D-99 (mb)	Error (%)	IRDF-90V2 (mb)	Diff.*1 (%)
^{6}Li(n,t)α	1.457E+05	2.11	1.458E+05	0.1
^{6}Li α-production	1.457E+05	2.11		
^{7}Li t-production	3.711E+00	5.04		
^{10}B(n,α)^{7}Li	5.937E+05	2.08	5.942E+05	0.1
^{10}B α-production	5.937E+05	2.08		
^{19}F(n,2n)^{18}F	1.389E-03	3.67	1.280E-03	-7.9 *
^{23}Na(n,2n)^{22}Na	5.106E-04	2.51		
^{23}Na(n,γ)^{24}Na	8.496E+01	2.84	8.439E+01	-0.7
^{24}Mg(n,p)^{24}Na	2.867E-01	2.46	2.843E-01	-0.8
^{27}Al(n,p)^{27}Mg	8.177E-01	2.21	7.421E-01	-9.3 *
^{27}Al(n,α)^{24}Na	1.320E-01	2.51	1.320E-01	0.0
^{31}P(n,p)^{31}Si	6.275E+00	2.50	5.904E+00	-5.9 *
^{32}S(n,p)^{32}P	1.415E+01	8.67	1.318E+01	-6.9 *
^{45}Sc(n,γ)^{46}Sc	4.208E+03	2.26	4.202E+03	-0.1
^{N}Ti(n,X)^{46}Sc	1.760E-01	3.11		
^{N}Ti(n,X)^{47}Sc	2.759E-01	2.55		
^{N}Ti(n,X)^{48}Sc	3.798E-02	2.93		
^{46}Ti(n,2n)^{45}Ti	6.472E-04	2.96		
^{46}Ti(n,p)^{46}Sc	2.132E+00	3.10	1.932E+00	-9.4 *
^{47}Ti(n,np)^{46}Sc	1.035E-03	3.56	1.621E-03	56.6 ****
^{47}Ti(n,p)^{47}Sc	3.707E+00	2.55	3.876E+00	4.6
^{48}Ti(n,np)^{47}Sc	2.190E-04	2.68	2.498E-04	14.0 **
^{48}Ti(n,p)^{48}Sc	5.151E-02	2.81	5.001E-02	-2.9
^{49}Ti(n,np)^{48}Sc	1.306E-04	13.33		
^{50}Cr(n,γ)^{51}Cr	2.483E+03	5.04		
^{52}Cr(n,2n)^{51}Cr	6.526E-03	2.47	6.611E-03	1.3
^{55}Mn(n,2n)^{54}Mn	4.314E-02	8.63	4.096E-02	-5.0 *
^{55}Mn(n,γ)^{56}Mn	2.271E+03	4.72	2.270E+03	0.0
^{54}Fe(n,p)^{54}Mn	1.635E+01	2.32	1.627E+01	-0.5
^{56}Fe(n,p)^{56}Mn	1.942E-01	5.01	1.898E-01	-2.2
^{57}Fe(n,np)^{56}Mn	9.670E-05	17.70		
^{58}Fe(n,γ)^{59}Fe	2.276E+02	11.77	2.118E+02	-6.9 *
^{59}Co(n,2n)^{58}Co	3.474E-02	2.59	3.530E-02	1.6
^{59}Co(n,γ)^{60}Co	7.577E+03	2.26	7.568E+03	-0.1
^{59}Co(n,α)^{56}Mn	3.032E-02	4.79	2.826E-02	-6.8 *
^{58}Ni(n,2n)^{57}Ni	5.854E-04	2.33	6.040E-04	3.2
^{58}Ni(n,p)^{58}Co	2.162E+01	2.18	2.197E+01	1.6
^{60}Ni(n,p)^{60}Co	3.197E-01	21.05	3.593E-01	12.4 **
^{63}Cu(n,2n)^{62}Cu	1.637E-02	2.54	1.608E-02	-1.7
^{63}Cu(n,γ)^{64}Cu	71964E+02	2.67	7.923E+02	-0.5
^{63}Cu(n,α)^{60}Co	1.096E-01	2.54	9.657E-02	-11.9 **
^{65}Cu(n,2n)^{64}Cu	6.096E-02	2.32	5.890E-02	-3.4
^{64}Zn(n,p)^{64}Cu	7.024E+00	2.66	7.765E+00	10.6 **
^{89}Y(n,2n)^{88}Y	2.657E-02	2.62	2.652E-02	-0.2
^{90}Zr(n,2n)^{89}Zr	1.537E-02	2.22	1.571E-02	2.2
^{93}Nb(n,2n)^{92m}Nb	7.406E-02	5.21	7.661E-02	3.4
^{93}Nb(n,n')^{93m}Nb	3.809E+01	4.66	3.618E+01	-5.0
^{103}Rh(n,n')^{103m}Rh	2.037E+02	4.06	2.031E+02	-0.3
^{109}Ag(n,γ)^{110m}Ag	2.399E+03	6.75	2.477E+03	3.3
^{115}In(n,n')^{115m}In	4.665E+01	3.04	4.665E+01	0.0
^{115}In(n,γ)^{116m}In	9.968E+04	6.57	1.276E+05	28.0 ***
^{127}I(n,2n)^{126}I	2.153E-01	3.82	2.067E-01	-4.0
^{151}Eu(n,γ)^{152}Eu	1.344E+06	2.71		
^{169}Tm(n,2n)^{168}Tm	6.733E-01	3.18		
^{181}Ta(n,γ)^{182}Ta	2.164E+04	4.20		
^{186}W(n,γ)^{187}W	1.848E+04	4.97		
^{197}Au(n,2n)^{196}Au	6.127E-01	2.45	6.074E-01	-0.9
^{197}Au(n,γ)^{198}Au	5.991E+04	3.86	6.001E+04	0.2
^{199}Hg(n,n')^{199m}Hg	5.719E+01	8.35		
^{232}Th(n,f)	1.854E+01	5.59	1.768E+01	-4.7
^{232}Th(n,γ)^{233}Th	3.615E+03	8.27	3.671E+03	1.5
^{235}U(n,f)	8.835E+04	2.10	8.847E+04	0.1
^{238}U(n,f)	7.441E+01	3.04	7.346E+01	-1.3
^{238}U(n,γ)^{239}U	8.098E+03	4.38	8.091E+03	-0.1
^{237}Np(n,f)	4.347E+02	2.13	4.236E+02	-2.6
^{239}Pu(n,f)	1.619E+05	2.19	1.619E+05	0.0
^{241}Am(n,f)	1.270E+03	2.62		

*1) Judgment from deviations: * for >5%; ** for >10%; *** for 20%; **** for >40%.

Table 3.2.1 Comparison of ^{252}Cf spontaneous fission neutron spectrum-averaged cross sections. Values in parentheses are standard deviation in percent

Reaction	Measurement (mb)	Calculation and C/E ratio for Mannhart spectrum JENDL/D-91 mb (%)	JENDL/D-91 C/E ratio (%)	JENDL/D-99 mb (%)	JENDL/D-99 C/E ratio(%)
$^{19}F(n,2n)^{18}F$	0.01628±0.00054	0.02094 (3.94)	1.286(5.15)	0.01776 (3.43)	1.091(4.77)
$^{24}Mg(n,p)^{24}Na$	2.005±0.048	2.270 (4.64)	1.132(5.22)	2.176 (2.43)	1.085(3.41)
$^{27}Al(n,p)^{27}Mg$	4.892±0.106	5.073 (6.07)	1.037(6.45)	5.157 (2.21)	1.054(3.10)
$^{27}Al(n,\alpha)^{24}Na$	1.021±0.015	0.9910 (5.81)	0.9706(5.99)	1.035 (2.49)	1.014(2.89)
$^{32}S(n,p)^{32}P$	72.74±2.54	74.89 (8.20)	1.030(8.91)	74.89 (8.20)	1.030(8.91)
$^{46}Ti(n,p)^{46}Sc$	14.20±0.2	13.28 (12.7)	0.9352(12.8)	13.55 (3.10)	0.9542(3.41)
$^{47}Ti(n,p)^{47}Sc$	19.43±0.31	20.70 (11.4)	1.065(11.5)	18.52 (2.45)	0.9532(2.93)
$^{48}Ti(n,p)^{48}Sc$	0.4275±0.0078	0.3938 (10.5)	0.9212(10.7)	0.3945 (2.76)	0.9228(3.31)
$^{55}Mn(n,2n)^{54}Mn$	0.4079±0.0092	0.4731 (12.5)	1.160(12.7)	0.4959 (8.49)	1.216(8.79)
$^{54}Fe(n,p)^{54}Mn$	87.29±1.13	88.07 (4.04)	1.009(4.24)	89.13 (2.30)	1.021(2.64)
$^{56}Fe(n,p)^{56}Mn$	1.471±0.025	1.408 (4.89)	0.9572(5.18)	1.408 (4.89)	0.9572(5.18)
$^{59}Co(n,2n)^{58}Co$	0.4058±.0101	0.4128 (10.9)	1.017(11.2)	0.4088 (2.50)	1.007(3.53)
$^{59}Co(n,\gamma)^{60}Co$	6.97±0.34	5.255 (4.66)	0.7539(6.75)	5.677 (4.92)	0.8145(6.93)
$^{59}Co(n,\alpha)^{56}Mn$	0.2221±0.0039	0.2302 (4.67)	1.037(4.99)	0.2302 (4.67)	1.036(4.99)
$^{58}Ni(n,2n)^{57}Ni$	(8.965±0.279)×10^{-3}	8.295E-3 (11.1)	0.9212(11.5)	8.323E-3 (2.29)	0.9284(3.86)
$^{58}Ni(n,p)^{58}Co$	117.6±1.5	115.5 (6.78)	0.9821(6.90)	114.5 (2.17)	0.9736(2.52)
$^{60}Ni(n,p)^{60}Co$	2.39±.13	3.346 (7.76)	1.400(9.48)	2.278 (18.9)	0.9531(19.7)
$^{63}Cu(n,2n)^{62}Cu$	0.1866±0.0071	0.2135 (2.74)	1.144(4.68)	0.2034 (2.48)	1.090(4.54)
$^{63}Cu(n,\gamma)^{64}Cu$	10.55±0.32	8.565 (19.1)	0.8118(19.3)	10.53 (19.3)	0.9981(19.5)
$^{63}Cu(n,\alpha)^{60}Co$	0.6897±0.0130	0.7054 (5.80)	1.023(6.10)	0.7282 (2.54)	1.056(3.16)
$^{64}Zn(n,p)^{64}Cu$	40.47±0.75	46.89 (7.75)	1.159(7.97)	38.19 (2.63)	0.9437(3.22)
$^{90}Zr(n,2n)^{89}Zr$	0.2211±0.0061	0.2182 (3.12)	0.9869(4.17)	0.2056 (2.19)	0.9299(3.52)
$^{93}Nb(n,n')^{93m}Nb$	149±10	149.5 (6.82)	1.003(9.57)	149.6 (3.84)	1.004(7.73)
$^{103}Rh(n,n')^{103m}Rh$	757±53	716.1 (3.72)	0.9460(7.93)	716.1 (3.72)	0.9460(7.93)
$^{115}In(n,n')^{115m}In$	98.1±2.6	189.7 (3.02)	0.9576(3.29)	189.7 (3.02)	0.9576(3.29)
$^{197}Au(n,2n)^{196}Au$	5.531±.099	5.853 (4.77)	1.058(5.09)	5.757 (2.40)	1.041(2.99)
$^{197}Au(n,\gamma)^{198}Au$	77.11±1.19	75.24 (8.91)	0.9757(9.04)	75.24 (8.91)	0.9757(9.04)
$^{232}Th(n,fission)$	89.4±2.7	82.05 (5.50)	0.9178(6.27)	82.05 (5.50)	0.9178(6.27)
$^{232}Th(n,\gamma)^{233}Th$	87.8±4.0	83.59 (12.1)	0.9521(12.9)	83.59 (12.1)	0.9521(12.9)
$^{235}U(n,fission)$	1210±14	1236 (2.87)	1.022(3.10)	1236 (2.87)	1.022(3.10)
$^{238}U(n,fission)$	323.4±5.6	319.1 (2.91)	0.9867(3.39)	318.9 (2.91)	0.9861(3.39)
$^{237}Np(n,fission)$	1356±22	1346 (9.46)	0.9926(9.60)	1338 (2.12)	0.9867(2.67)
$^{239}Pu(n,fission)$	1811±25	1804 (2.92)	0.9961(3.23)	1804 (2.92)	0.9961(3.23)

Table 3.2.2 Comparison of ^{235}U thermal fission neutron spectrum-averaged cross sections.
Values in parentheses are standard deviation in percent.

Reaction	Measurement (mb)	Ref.	Calculation and C/E ratio (Uncertainty in %) Watt-type (JENDL/D-91) mb(%)	C/E ratio(%)	Watt-type (JENDL/D-99) mb(%)	C/E ratio(%)	Madland-Nix(JENDL/D-99) mb(%)	C/E ratio(%)
$^{24}Mg(n,p)^{24}Na$	1.50±0.06	59	1.640 (4.69)	1.093(6.16)	1.562 (2.46)	1.041(4,70)	1.411(2.46)	0.9407(4.70)
$^{27}Al(n,p)^{27}Mg$	3.95±0.20	59	4.286 (6.17)	1.085(7.97)	4.390 (2.21)	1.111(5.50)	4.042 (2.21)	1.023(5.50)
$^{27}Al(n,\alpha)^{24}Na$	0.706±.028	59	0.6880 (6.03)	0.9745(7.22)	0.720 (2.52)	1.020(4,70)	0.6513 (2.52)	0.9225(4.70)
$^{46}Ti(n,p)^{46}Sc$	11.6±0.4	59	11.25 (12.8)	0.9698(13.3)	11.48 (3.10)	0.9897(4.64)	10.56 (3.10)	0.9103(4.64)
$^{47}Ti(n,p)^{47}Sc$	17.7±0.6	59	19.28 (11.4)	1.089(11.9)	17.23 (2.49)	0.9734(4.20)	16.56 (2.51)	0.9356(4.22)
$^{48}Ti(n,p)^{48}Sc$	0.302±0.010	59	0.2781 (10.7)	0.9209(11.2)	0.2803 (2.82)	0.9281(4.35)	0.2542 (2.82)	0.8417(4.35)
$^{54}Fe(n,p)^{54}Mn$	80.5±2.3	59	80.73 (4.08)	1.003(4.98)	81.87 (2.31)	1.017(3.68)	77.56 (2.32)	0.9635(3.68)
$^{56}Fe(n,p)^{56}Mn$	1.09±0.04	59	1.057 (5.00)	0.9697(6.20)	1.057 (5.00)	0.9697(6.20)	0.9592 (5.00)	0.8800(6.20)
$^{59}Co(n,2n)^{58}Co$	0.202±0.006	59	0.1788 (12.2)	0.8851(12.6)	0.1771 (2.61)	0.8767(3.95)	0.1673 (2.59)	0.8282(3.94)
$^{59}Co(n,\alpha)^{56}Mn$	0.161±0.007	59	0.1652 (4.77)	1.026(6.46)	0.1652 (4.77)	1.026(6.46)	0.1497 (4.77)	0.9298(6.46)
$^{58}Ni(n,2n)^{57}Ni$	$(4.19\pm0.22)\times10^{-3}$	59	2.873E-3(11.1)	0.6857(12.3)	2.890E-3(2.34)	0.6897(5.75)	2.911E-3 (2.31)	0.6947(5.74)
$^{58}Ni(n,p)^{58}Co$	108.9±5.2	59	107.1 (6.90)	0.9835(8.39)	105.7 (2.18)	0.9706(5.25)	100.6 (2.18)	0.9238(5.25)
$^{64}Zn(n,p)^{64}Cu$	35.5±1.07	61	43.12 (7.71)	1.215(8.28)	35.02 (2.66)	0.9865(4.02)	33.18 (2.66)	0.9346(4.02)
$^{90}Zr(n,2n)^{89}Zr$	0.103±0.004	59	0.08123(3.30)	0.7886(5.09)	0.07573 (2.19)	0.7352(4.46)	0.07447 (2.19)	0.7230(4.46)
$^{93}Nb(n,2n)^{92m}Nb$	0.466±0.0117	61	0.4397 (4.55)	0.9435(5.20)	0.3943 (5.20)	0.8461(5.77)	0.3617 (5.13)	0.7762(5.71)
$^{103}Rh(n,n')^{103m}Rh$	673.5±52.2	54	705.0 (3.74)	1.047(8.60)	705.0 (3.74)	1.047(8.60)	699.9 (3.75)	1.039(8.61)
$^{115}In(n,n')^{115m}In$	190.3±7.3	59	185.4 (3.03)	0.9743(4.89)	185.4 (3.03)	0.9743(4.89)	180.5 (3.04)	0.9485(4.90)
$^{197}Au(n,2n)^{196}Au$	3.50±0.13	59	3.409 (5.00)	0.9740(6.23)	3.308 (2.43)	0.9451(4.43)	3.005 (2.43)	0.8586(4.43)
$^{232}Th(n,fission)$	83±2.57	58	78.49 (5.50)	0.9457(6.31)	78.49 (5.50)	0.9457(6.31)	76.92 (5.53)	0.9267(6.33)
$^{235}U(n,fission)$	1200±22.8	58	1235 (2.87)	1.029(3.44)	1235 (2.87)	1.029(3.44)	1234 (2.87)	1.028(3.44)
$^{238}U(n,fission)$	312±7.2	58	308.4 (2.94)	0.9885(3.74)	308.2 (2.94)	0.9878(3.74)	303.6 (2.96)	0.9731(3.75)
$^{237}Np(n,fission)$	1359±28.5	58	1334 (9.57)	0.9816(9.80)	1326 (2.13)	0.9757(2.99)	1324 (2.13)	0.9742(2.99)
$^{239}Pu(n,fission)$	1818±34.5	58	1800 (2.92)	0.9901(3.48)	1800 (2.92)	0.9901(3.48)	1801 (2.92)	0.9906(3.48)

Table 3.3.1 Comparison of spectrum-averaged cross sections in the ISNF spectrum

Reaction	Experiment (mb) (% error)	JENDL/D-99 Calc. (mb) (% error)	C/E	Deviation*1 (%)	JENDL/D-91 Calc. (mb)	Deviation*1 (%)	IRDF-90V2 Calc. (mb)	Deviation*1 (%)	Criterion*2 for JENDL/D-99
$^{23}Na(n,\gamma)^{24}Na$	1.57(6.4)	1.756(9.7)	1.118(11.62)	11.85	1.756	11.85	1.917	22.10	**
$^{45}Sc(n,\gamma)^{46}Sc$	24.4(3.3)	27.86(2.7)	1.142(4.26)	14.19	29.35	20.29	27.46	12.54	**
$^{59}Co(n,\gamma)^{60}Co$	36.3(4.1)	42.17(2.8)	1.162(4.96)	16.17	41.97	15.62	42.97	18.37	**
$^{115}In(n,n')^{115m}In$	97.0(2.6)	87.25(3.1)	0.899(4.05)	-10.05	87.25	-10.05	87.25	-10.05	**
$^{197}Au(n,\gamma)^{198}Au$	411(2.7)	385.3(5.3)	0.937(5.95)	-6.25	385.3	-6.25	405	-1.46	*

*1) $(C/E - 1.0)\times 100$.

*2) Judgment from deviations: * for > 5%; ** for > 10%.

Table 3.3.2 Comparison of spectrum-averaged cross sections in the CFRMF spectrum

Reaction	Experiment (mb) (% error)	JENDL/D-99 Calc. (mb) (% error)	C/E	Deviation*1 (%)	JENDL/D-91 Calc. (mb)	Deviation*1 (%)	IRDF-90V2 Calc. (mb)	Deviation*1 (%)	Criterion*2 for JENDL/D-99
^{6}Li α-production	954.5(2.7)	939.7(2.5)	0.984(3.68)	-1.55	939.7	-1.55	---	---	
^{10}B α-production	1876(2.8)	1717(2.2)	0.915(3.56)	-8.48	1717	-8.48	---	---	*
^{27}Al(n,p)^{27}Mg	0.863(3.4)	0.967(2.2)	1.121(4.05)	12.05	0.9486	9.92	0.8757	1.47	**
^{27}Al(n,α)^{24}Na	0.1596(3)	0.1768(2.5)	1.108(3.91)	10.78	0.1688	5.76	0.1768	10.78	**
^{45}Sc(n,γ)^{46}Sc	23.2(3.3)	24.76(2.7)	1.067(4.26)	6.72	26.61	14.70	24.02	3.53	*
^{46}Ti(n,p)^{46}Sc	2.58(3.4)	2.529(3.1)	0.980(4.60)	-1.98	2.474	-4.11	2.295	-11.05	
^{47}Ti(n,p)^{47}Sc	4.12(4.8)	4.003(2.5)	0.972(5.41)	-2.84	4.517	9.64	4.216	2.33	
^{48}Ti(n,p)^{48}Sc	0.068(4.1)	0.06771(2.8)	0.996(4.96)	-0.43	0.06739	-0.90	0.06601	-2.93	*
^{54}Fe(n,p)^{54}Mn	17.2(2.9)	17.96(2.3)	1.044(3.70)	4.42	17.71	2.97	17.82	3.60	
^{58}Fe(n,γ)^{59}Fe	6.04(3.1	7.385(7.8)	1.223(8.39)	22.27	10.67	76.66	9.3	53.97	***
^{59}Co(n,γ)^{60}Co	90.4(3.6)	87.86(3.2)	0.972(4.82)	-2.81	87.88	-2.79	87.32	-3.41	
^{58}Ni(n,p)^{58}Co	25.6(3.1)	23.65(2.2)	0.924(3.80)	-7.62	24.02	-6.17	24.01	-6.21	*
^{63}Cu(n,γ)^{64}Cu	43.3(6.2)	44.91(8.4)	1.037(10.44)	3.72	38.71	-10.60	43.3	-0.01	
^{115}In(n,n')^{115m}In	50.6(3.9)	51.54(3.0)	1.019(4.92)	1.86	51.54	1.86	51.54	1.86	
^{197}Au(n,γ)^{198}Au	419(2.9)	388.2(4.4)	0.926(5.27)	-7.35	388.2	-7.35	404.1	-3.56	*
^{232}Th(n,fission)	19.6(5.2)	19.56(5.5)	0.998(7.57)	-0.20	19.56	-0.20	18.62	-5.02	
^{232}Th(n,γ)^{233}Th	290(3.8)	250.3(10.9)	0.863(11.54)	-13.69	250.3	-13.69	269.5	-7.07	**
^{235}U(n,fission)	1537(3.1)	1569(2.8)	1.021(4.18)	2.08	1569	2.08	1569	2.08	
^{238}U(n.fission)	75.1(3.3)	78.01(3.0)	1.039(4.46)	3.87	78.05	3.93	77.07	2.62	
^{238}U(n,γ)^{239}U	217(3.7)	227.6(4.1)	1.049(5.52)	4.88	227.2	4.70	228.3	5.21	
^{237}Np(n,fission)	548(3.3)	578.6(2.1)	1.056(3.91)	5.58	572.1	4.40	585.7	6.88	*
^{239}Pu(n,fission)	1792(2.2)	1768(3.2)	0.987(3.88)	-1.34	1768	-1.34	1757	-1.95	

*1) (C/E – 1.0)×100.

*2) Judgment from deviations: * for > 5%; ** for > 10%; *** for > 20%.

Table 3.3.3 Comparison of spectrum-averaged cross sections in the ΣΣ spectrum

Reaction	Experiment (mb) (% error)	JENDL/D-99 Calc. (mb) (% error)	JENDL/D-99 C/E	JENDL/D-99 Deviation*1 (%)	JENDL/D-91 Calc. (mb)	JENDL/D-91 Deviation*1 (%)	IRDF-90V2 Calc. (mb)	IRDF-90V2 Deviation*1 (%)	Criterion*2 for JENDL/D-99
$^{27}Al(n,p)^{27}Mg$	1.033(10)	0.8899(2.2)	0.861(10.24)	-13.86	0.8708	-15.70	0.8095	-21.63	**
$^{27}Al(n,\alpha)^{24}Na$	0.182(3.0)	0.1542(2.5)	0.847(3.91)	-15.30	0.1472	-19.15	0.1542	-15.30	**
$^{55}Mn(n,\gamma)^{56}Mn$	39.70(3.0)	25.18(23.5)	0.634(23.7)	36.57	25.18	-36.57	25.17	-36.59	***
$^{56}Fe(n,p)^{56}Mn$	0.273(3.0)	0.2248(5.0)	0.823(5.83)	-17.66	0.2248	-17.66	0.2194	-19.64	**
$^{58}Ni(n,p)^{58}Co$	28.80(2.5)	23.35(2.2)	0.811(3.33)	-18.93	23.80	-17.38	23.82	-17.30	**
$^{63}Cu(n,\gamma)^{64}Cu$	40.00(5.0)	37.16(10.0)	0.923(11.2)	-7.11	31.13	-22.18	35.58	-11.05	*
$^{115}In(n,n')^{115m}In$	58.60(2.0)	54.66(3.0)	0.933(3.61)	-6.73	54.66	-6.73	54.66	-6.73	*
$^{115}In(n,\gamma)^{116m}In$	261.0(3.5)	301.4(4.4)	1.155(5.62)	15.49	301.4	15.49	326.2	24.98	**
$^{197}Au(n,\gamma)^{198}Au$	442.0(2.0)	324.5(4.2)	0.734(4.65)	-26.58	324.5	-26.58	336.9	-23.78	***
$^{232}Th(n,fission)$	21.60(6.0)	20.60(5.6)	0.954(8.21)	-4.62	20.60	-4.62	19.61	-9.24	
$^{235}U(n,fission)$	1589.0(3.5)	1494.0(2.8)	0.940(4.48)	-5.97	1493.0	-6.06	1492.0	-6.08	*
$^{238}U(n.fission)$	87.40(3.5)	82.98(3.1)	0.949(4.68)	-5.06	83.03	-5.00	81.95	-6.24	*
$^{238}U(n,\gamma)^{239}U$	194.0(4.0)	203.3(4.3)	1.048(5.87)	4.81	202.9	4.61	204.3	5.29	
$^{237}Np(n,fission)$	634.0(3.5)	606.0(2.1)	0.956(4.08)	-4.42	600.3	-5.32	613.6	-3.23	
$^{239}Pu(n,fission)$	1875.0(3.5)	1734.0(3.1)	0.925(4.68)	-7.51	1734.0	-7.55	1722.0	-8.18	*

*1) (C/E – 1.0)×100.

*2) Judgment from deviations: * for > 5%; ** for > 10%; *** for > 20%.

Table 3.3.4 Comparison of spectrum-averaged cross sections in the YAYOI spectrum

Reaction	Experiment (mb) (% error)	JENDL/D-99 Calc. (mb) (% error)	C/E	Deviation*1 (%)	JENDL/D-91 Calc. (mb)	Deviation*1 (%)	IRDF-90V2 Calc. (mb)	Deviation*1 (%)	Criterion*2 for JENDL/D-99
^{7}Li t-production	10.54(8.0)	11.03(4.8)	1.046(9.33)	4.61	11.03	4.61	---	---	
^{23}Na(n, γ)^{24}Na	0.419(7.8)	0.3064(10.)	0.731(12.7)	-26.88	0.3064	-26.88	0.3850	-8.12	***
^{24}Mg(n,p)^{24}Na	0.802(7.7)	1.1012(2.4)	1.262(8.07)	26.23	1.054	31.36	1.003	25.07	***
^{27}Al(n,p)^{27}Mg	2.140(11.)	2.433(2.2)	1.137(11.2)	13.70	2.394	11.86	2.208	3.17	**
^{27}Al(n, α)^{24}Na	0.376(7.7)	0.4838(2.5)	1.287(8.10)	28.66	0.463	23.14	0.4838	28.66	***
^{46}Ti(n,p)^{46}Sc	6.900(9.7)	6.378(3.1)	0.924(10.2)	-7.57	6.252	-9.39	5.800	-15.94	*
^{47}Ti(n,p)^{47}Sc	11.80(13.5)	9.947(2.5)	0.843(13.7)	-15.70	11.15	-5.54	10.41	-11.81	**
^{48}Ti(n,p)^{48}Sc	0.155(8.1)	0.1837(2.8)	1.185(8.57)	18.49	0.1832	18.17	0.1795	15.81	**
^{55}Mn(n, γ)^{56}Mn	4.610(7.6)	4.312(23.1)	0.935(24.3)	-6.47	4.312	-6.47	4.312	-6.46	*
^{56}Fe(n,p)^{56}Mn	0.579(7.6)	0.6501(4.9)	1.123(9.04)	12.27	0.6501	12.27	0.6299	8.80	**
^{59}Co(n, α)^{56}Mn	0.0813(7.9)	0.1071(4.7)	1.317(9.19)	31.67	0.1071	31.67	0.1006	23.69	***
^{58}Ni(n,2n)^{57}Ni	0.00303(4.7)	0.005537(2.2)	1.827(5.19)	82.73	0.005477	80.76	0.005677	87.35	****
^{58}Ni(n,p)^{58}Co	57.90(7.1)	59.19(2.2)	1.022(7.43)	2.23	60.05	3.72	59.93	3.51	
^{63}Cu(n,2n)^{62}Cu	0.0658(13.8)	0.1129(2.4)	1.716(14.0)	71.61	0.1185	80.12	0.1137	72.80	****
^{63}Cu(n, α)^{60}Co	0.275(7.0)	0.3448(2.5)	1.254(7.43)	25.36	0.3291	19.68	0.3144	14.33	***
^{90}Zr(n,2n)^{89}Zr	0.130(6.6)	0.1264(2.2)	0.972(6.96)	-2.79	0.1325	1.88	0.1289	-0.86	
^{93}Nb(n,2n)^{92m}Nb	0.244(6.5)	0.3522(4.7)	1.443(8.02)	44.36	0.3884	59.17	0.3624	48.52	****
^{115}In(n,n')^{115m}In	116.4(8.1)	117.4(3.0)	1.009(8.64)	0.86	117.4	0.86	117.4	0.86	
^{186}W(n, γ)^{187}W	62.80(8.6)	47.87(5.2)	0.762(10.1)	-23.78	47.85	-23.81	----	----	***
^{197}Au(n, γ)^{198}Au	155.9(8.1)	118.8(5.3)	0.762(9.68)	-23.78	118.8	-23.78	119.3	-23.48	***
^{232}Th(n,fission)	45.90(5.0)	47.71(5.5)	1.039(7.43)	3.94	47.71	3.94	45.53	-0.80	
^{238}U(n.fission)	172.7(5.1)	189.0(3.0)	1.094(5.92)	9.46	189.1	9.52	186.8	8.14	*

*1) (C/E – 1.0)×100.

*2) Judgment from deviations: * for > 5%; ** for > 10%; *** for > 20%; **** for > 40%.

Table 3.3.5 Comparison of spectrum-averaged cross sections in the JOYO spectrum

Reaction	Experiment (mb) (% error)	JENDL/D-99 Calc.(mb) (% error)	C/E	Deviation[*1] (%)	JENDL/D-91 Calc.(mb)	Deviation[*1] (%)	IRDF-90V2 Calc.(mb)	Deviation[*1] (%)	Criterion[*2] for JENDL/D-99
^{46}Ti(n,p)^{46}Sc	1.45E+00 (2.7)	1.66E+00 (3.1)	1.145 (4.11)	14.48	1.62E+00	11.72	1.52E+00	4.83	**
^{54}Fe(n,p)^{54}Mn	1.18E+01 (3.6)	1.34E+01 (2.3)	1.136 (4.27)	13.56	1.32E+01	11.86	1.35E+01	14.41	**
^{58}Fe(n,γ)^{59}Fe	7.53E+00 (0.4)	8.12E+00 (12.7)	1.078 (12.71)	7.84	1.34E+01	77.95	1.03E+01	36.79	*
^{59}Co(n,γ)^{60}Co	2.62E+01 (2.7)	2.51E+01 (2.6)	0.958 (3.75)	-4.20	2.54E+01	-3.05	2.55E+01	-2.67	
^{58}Ni(n,p)^{59}Co	1.67E+01 (3.1)	1.80E+01 (2.2)	1.078 (3.80)	7.78	1.84E+01	10.18	1.85E+01	10.78	*
^{63}Cu(n,α)^{60}Co	6.94E-02 (2.6)	8.55E-02 (2.5)	1.232 (3.61)	23.20	7.88E-02	13.54	7.51E-02	8.21	***
^{238}U(n,fission)	6.01E+01 (3.0)	6.70E+01 (3.1)	1.115 (4.31)	11.48	6.70E+01	11.48	6.63E+01	10.32	**
^{237}Np(n,fission)	4.44E+02 (3.4)	4.69E+02 (2.1)	1.056 (4.00)	5.63	4.63E+02	4.28	4.74E+02	6.76	*

*1) (C/E-1.0)×100.

*2) Judgment from deviations: * for >5%; ** for >10%; *** for >20%.

Table 3.3.6 Comparison of spectrum-averaged cross sections in the JMTR spectrum

Reaction	Experiment (mb) (% error)	JENDL/D-99 Calc.(mb) (% error)	C/E	Deviation[*1] (%)	JENDL/D-91 Calc.(mb)	Deviation[*1] (%)	IRDF-90V2 Calc.(mb)	Deviation[*1] (%)	Criterion[*2] for JENDL/D-99
$^{46}Ti(n,p)^{46}Sc$	2.37E+00 (6.8)	2.11E+00 (4.7)	0.890 (8.27)	-10.97	2.07E+00	-12.66	1.92E+00	-18.99	**
$^{55}Mn(n,2n)^{54}Mn$	4.75E-02 (4.9)	4.13E-02 (10.8)	0.869 (11.86)	-13.05	3.93E-02	-17.26	3.93E-02	-17.26	**
$^{54}Fe(n,p)^{54}Mn$	1.65E+01 (4.0)	1.63E+01 (3.6)	0.988 (5.38)	-1.21	1.60E+01	-3.03	1.62E+01	-1.82	
$^{58}Fe(n,\gamma)^{59}Fe$	2.65E+02 (10.7)	2.28E+02 (8.5)	0.860 (13.67)	-13.96	2.31E+02	-12.83	2.12E+02	-20.00	**
$^{59}Co(n,\gamma)^{60}Co$	7.39E+03 (3.4)	7.62E+03 (4.7)	1.031 (5.80)	3.11	7.66E+03	3.65	7.24E+03	-2.03	
$^{58}Ni(n,p)^{58}Co$	2.26E+01 (7.8)	2.15E+01 (3.3)	0.951 (8.47)	-4.87	2.19E+01	-3.10	2.19E+01	-3.10	
$^{63}Cu(n,\alpha)^{60}Co$	1.08E-01 (5.5)	1.08E-01 (4.0)	1.000 (6.80)	0.00	1.01E-01	-6.48	9.51E-02	-11.94	
$^{109}Ag(n,\gamma)^{110m}Ag$	2.29E+03 (7.0)	2.48E+03 (12.2)	1.083 (14.07)	8.30	--	--	2.37E+03	3.49	*

*1) (C/E-1.0)×100.

*2) Judgment from deviations: * for >5%; ** for >10%.

Table 4.1.1 Neutron Flux Spectra A (Position# 1) and B (Position# 2).

No.	Energy boundary		Flux(/Group)	
	E_{min}(MeV)	E_{max}(MeV)	Spectrum A(#1)	Spectrum B(#2)
1	1.00100E-11	3.22410E-07	7.19460E-06	3.22810E-18
2	3.22410E-07	5.31560E-07	1.54690E-06	1.19460E-16
3	5.31560E-07	8.76400E-07	1.76230E-06	1.93870E-15
4	8.76400E-07	1.44490E-06	1.98670E-06	2.62330E-14
5	1.44490E-06	2.38230E-06	2.22260E-06	2.84140E-13
6	2.38230E-06	3.92780E-06	2.46400E-06	2.52620E-12
7	3.92780E-06	6.47580E-06	2.71230E-06	1.80440E-11
8	6.47580E-06	1.06770E-05	2.96360E-06	1.04040E-10
9	1.06770E-05	1.76030E-05	3.21490E-06	4.86680E-10
10	1.76030E-05	2.90230E-05	3.46840E-06	1.88280E-09
11	2.90230E-05	4.78500E-05	3.71610E-06	6.11360E-09
12	4.78500E-05	7.88910E-05	3.96110E-06	1.65580E-08
13	7.88910E-05	1.30070E-04	4.19820E-06	3.84070E-08
14	1.30070E-04	2.14450E-04	4.42550E-06	7.77320E-08
15	2.14450E-04	3.53570E-04	4.63600E-06	1.39410E-07
16	3.53570E-04	5.82930E-04	4.85360E-06	2.24680E-07
17	5.82930E-04	9.61100E-04	5.06120E-06	3.31190E-07
18	9.61100E-04	1.23410E-03	2.58720E-06	2.20900E-07
19	1.23410E-03	1.58460E-03	2.74640E-06	2.56090E-07
20	1.58460E-03	2.03460E-03	2.79320E-06	2.89570E-07
21	2.03460E-03	2.61250E-03	2.88340E-06	3.23580E-07
22	2.61250E-03	3.35460E-03	2.97250E-06	3.56060E-07
23	3.35460E-03	4.30730E-03	3.01180E-06	3.85420E-07
24	4.30730E-03	5.53070E-03	3.00010E-06	4.12220E-07
25	5.53070E-03	7.10160E-03	2.97940E-06	4.35320E-07
26	7.10160E-03	9.11860E-03	2.90240E-06	4.56240E-07
27	9.11860E-03	1.17090E-02	3.13130E-06	4.86230E-07
28	1.17090E-02	1.50340E-02	3.28920E-06	5.06090E-07
29	1.50340E-02	1.93040E-02	2.97510E-06	5.09630E-07
30	1.93040E-02	2.18740E-02	1.56230E-06	2.66820E-07
31	2.18740E-02	2.47870E-02	1.67140E-06	2.68390E-07
32	2.47870E-02	2.80870E-02	2.26940E-06	2.85510E-07
33	2.80870E-02	3.18270E-02	1.16290E-06	2.39970E-07
34	3.18270E-02	3.60650E-02	1.61290E-06	2.68940E-07
35	3.60650E-02	4.08670E-02	1.67520E-06	2.71950E-07
36	4.08670E-02	4.63080E-02	1.75630E-06	2.73480E-07
37	4.63080E-02	5.24740E-02	1.83680E-06	2.73820E-07
38	5.24740E-02	5.94610E-02	1.77540E-06	2.70720E-07
39	5.94610E-02	6.73780E-02	1.83970E-06	2.71030E-07
40	6.73780E-02	7.63490E-02	1.84330E-06	2.68970E-07
41	7.63490E-02	8.65150E-02	1.97220E-06	2.67760E-07
42	8.65150E-02	9.80350E-02	1.93070E-06	2.63010E-07
43	9.80350E-02	1.11090E-01	1.83300E-06	2.57310E-07
44	1.11090E-01	1.25880E-01	1.98350E-06	2.54210E-07
45	1.25880E-01	1.42640E-01	2.21530E-06	2.47400E-07
46	1.42640E-01	1.61630E-01	1.91380E-06	2.33080E-07
47	1.61630E-01	1.83150E-01	2.17750E-06	2.12580E-07
48	1.83150E-01	2.07540E-01	2.08510E-06	1.58900E-07
49	2.07540E-01	2.35170E-01	2.24440E-06	9.75540E-08

Table 4.1.1 (continued)

No.	Energy boundary		Flux(/Group)	
	E_{min}(MeV)	E_{max}(MeV)	Spectrum A(#1)	Spectrum B(#2)
50	2.35170E-01	2.66490E-01	2.27550E-06	4.28480E-08
51	2.66490E-01	3.01970E-01	2.33880E-06	5.94520E-08
52	3.01970E-01	3.42170E-01	2.46760E-06	1.28500E-07
53	3.42170E-01	3.87740E-01	2.57050E-06	1.45650E-07
54	3.87740E-01	4.39360E-01	2.60880E-06	1.18210E-07
55	4.39360E-01	4.97860E-01	2.58070E-06	1.23830E-07
56	4.97860E-01	5.64150E-01	2.38840E-06	2.16890E-07
57	5.64150E-01	6.39270E-01	1.91510E-06	2.18110E-07
58	6.39270E-01	7.24380E-01	2.48450E-06	2.06510E-07
59	7.24380E-01	8.20840E-01	2.52060E-06	2.02150E-07
60	8.20840E-01	9.30130E-01	2.34690E-06	1.47310E-07
61	9.30130E-01	1.05400E+00	2.19070E-06	9.02450E-08
62	1.05400E+00	1.19430E+00	2.19480E-06	1.13160E-07
63	1.19430E+00	1.35330E+00	2.23870E-06	1.20420E-07
64	1.35330E+00	1.53350E+00	2.24540E-06	1.31440E-07
65	1.53350E+00	1.73770E+00	2.18460E-06	1.21370E-07
66	1.73770E+00	1.84980E+00	1.03490E-06	6.07020E-08
67	1.84980E+00	1.96910E+00	9.27680E-07	4.99850E-08
68	1.96910E+00	2.09610E+00	8.60080E-07	5.36270E-08
69	2.09610E+00	2.23130E+00	7.98680E-07	5.71740E-08
70	2.23130E+00	2.37520E+00	7.45510E-07	6.48950E-08
71	2.37520E+00	2.52840E+00	6.71060E-07	5.77250E-08
72	2.52840E+00	2.69140E+00	5.71320E-07	5.21270E-08
73	2.69140E+00	2.86500E+00	4.40750E-07	4.69680E-08
74	2.86500E+00	3.04980E+00	4.50560E-07	4.22020E-08
75	3.04980E+00	3.24650E+00	4.61650E-07	3.79810E-08
76	3.24650E+00	3.45590E+00	4.54360E-07	3.02560E-08
77	3.45590E+00	3.67870E+00	4.43270E-07	2.77870E-08
78	3.67870E+00	3.91600E+00	4.39380E-07	2.58620E-08
79	3.91600E+00	4.16860E+00	4.43480E-07	2.71280E-08
80	4.16860E+00	4.43740E+00	4.37830E-07	2.60200E-08
81	4.43740E+00	4.72360E+00	4.23830E-07	2.58580E-08
82	4.72360E+00	5.02820E+00	4.07910E-07	2.67830E-08
83	5.02820E+00	5.35250E+00	3.90960E-07	2.73140E-08
84	5.35250E+00	5.69780E+00	3.77290E-07	3.12150E-08
85	5.69780E+00	6.06520E+00	3.65330E-07	3.03060E-08
86	6.06520E+00	6.45640E+00	3.50550E-07	3.06620E-08
87	6.45640E+00	6.87280E+00	3.35560E-07	3.06120E-08
88	6.87280E+00	7.31610E+00	3.29990E-07	3.03150E-08
89	7.31610E+00	7.78790E+00	3.20620E-07	2.94310E-08
90	7.78790E+00	8.29020E+00	3.43690E-07	3.00610E-08
91	8.29020E+00	8.82490E+00	4.20070E-07	2.94980E-08
92	8.82490E+00	9.39400E+00	4.89120E-07	2.88380E-08
93	9.39400E+00	9.99990E+00	4.71780E-07	2.82200E-08
94	9.99990E+00	1.01570E+01	1.00600E-07	6.90220E-09
95	1.01570E+01	1.03170E+01	9.71870E-08	6.95150E-09
96	1.03170E+01	1.04800E+01	9.77980E-08	7.29170E-09
97	1.04800E+01	1.06450E+01	1.02160E-07	7.67170E-09
98	1.06450E+01	1.08120E+01	1.09060E-07	8.14220E-09

Table 4.1.1 (continued)

No.	Energy boundary		Flux(/Group)	
	E_{min}(MeV)	E_{max}(MeV)	Spectrum A(#1)	Spectrum B(#2)
99	1.08120E+01	1.09830E+01	1.18130E-07	8.46930E-09
100	1.09830E+01	1.11560E+01	1.25470E-07	8.38030E-09
101	1.11560E+01	1.13310E+01	1.29940E-07	8.63790E-09
102	1.13310E+01	1.15100E+01	1.29210E-07	9.29900E-09
103	1.15100E+01	1.16910E+01	1.18810E-07	9.75730E-09
104	1.16910E+01	1.18750E+01	1.01000E-07	1.05300E-08
105	1.18750E+01	1.20620E+01	8.05630E-08	1.15470E-08
106	1.20620E+01	1.22520E+01	6.85550E-08	1.29790E-08
107	1.22520E+01	1.24450E+01	6.03910E-08	1.41120E-08
108	1.24450E+01	1.26410E+01	5.56140E-08	1.55750E-08
109	1.26410E+01	1.28400E+01	4.80430E-08	1.73030E-08
110	1.28400E+01	1.30420E+01	3.99610E-08	1.89470E-08
111	1.30420E+01	1.32480E+01	3.64540E-08	2.14370E-08
112	1.32480E+01	1.34560E+01	5.02470E-08	2.34630E-08
113	1.34560E+01	1.36680E+01	6.99150E-08	2.55310E-08
114	1.36680E+01	1.38830E+01	9.44680E-08	2.72060E-08
115	1.38830E+01	1.41020E+01	6.85110E-08	2.97260E-08
116	1.41020E+01	1.43240E+01	7.36400E-08	3.22650E-08
117	1.43240E+01	1.45500E+01	3.60560E-07	3.56080E-08
118	1.45500E+01	1.47790E+01	2.79750E-06	3.74730E-08
119	1.47790E+01	1.50120E+01	4.86670E-06	2.92010E-08
120	1.50120E+01	1.52480E+01	2.67170E-06	1.39210E-08
121	1.52480E+01	1.54880E+01	1.70780E-06	6.02850E-09
122	1.54880E+01	1.57320E+01	0.00000E+00	0.00000E-00
123	1.57320E+01	1.59800E+01	0.00000E+00	0.00000E+00
124	1.59800E+01	1.62310E+01	0.00000E+00	0.00000E+00
125	1.62310E+01	1.64870E+01	0.00000E+00	0.00000E+00

Table 4.1.2 Comparison of reaction rates for Spectrum A

Reaction	Experiment Reaction rate(%)	Calc.(JENDL/D-99) Reaction rate(C/E)	Calc.(JENDL/D-91) Reaction rate(C/E)	Diff.[*2] between JENDL/D-99 and Exp. (%)	Criterion[*3]
$^{27}Al(n,\alpha)^{24}Na$	1.884E-30*[1](3)	1.79E-30 (0.95)	1.96E-30 (1.04)	-4.99	
$^{N}Ti(n,x)^{46}Sc$	2.781E-30(3)	2.85E-30 (1.03)	2.97E-30 (1.07)	2.48	
$^{N}Ti(n,x)^{47}Sc$	4.383E-31(4)	3.95E-31 (0.90)	4.19E-31 (0.96)	-9.88	*
$^{N}Ti(n,x)^{48}Sc$	9.003E-31(3)	8.88E-31 (0.99)	8.87E-31 (0.99)	-1.37	
$^{54}Fe(n,p)^{54}Mn$	7.417E-30(4)	8.07E-30 (1.09)	8.07E-30 (1.09)	8.80	*
$^{56}Fe(n,p)^{56}Mn$	1.641E-30(3)	1.69E-30 (1.03)	1.63E-30 (0.99)	2.99	
$^{59}Co(n,2n)^{58m+g}Co$	1.043E-29(3)	1.08E-29 (1.03)	1.06E-29 (1.02)	3.55	
$^{59}Co(n,\alpha)^{56}Mn$	4.7273E-31(3)	4.76E-31 (1.01)	4.68E-31 (0.99)	0.70	
$^{58}Ni(n,2n)^{57}Ni$	5.540E-31(3)	5.44E-31 (0.98)	5.30E-31 (0.96)	-1.81	
$^{58}Ni(n,p)^{58m+g}Co$	8.693E-30(3)	9.18E-30 (1.06)	8.74E-30 (1.00)	5.60	*
$^{64}Zn(n,p)^{64}Cu$	3.582E-30(3)	3.57E-30 (1.00)	4.26E-30 (1.19)	-0.34	
$^{90}Zr(n,2n)^{89m+g}Zn$	1.117E-29(3)	1.09E-29 (0.98)	1.12E-29 (1.00)	-2.42	
$^{93}Nb(n,2n)^{92m}Nb$	6.688E-30(3)	6.56E-30 (0.98)	6.57E-30 (0.98)	-1.91	
$^{115}In(n,n')^{115m}In$	6.757E-30(3)	7.12E-30 (1.05)	7.04E-30 (1.04)	5.37	*

*1) Read as 1.884×10^{-30}.

*2) Diff. is given as (C-E)/E in percent.

*3) Judgment from deviations: * for >5%.

Table 4.1.3 Comparison of reaction rates for Spectrum B

Reaction	Experiment	Calc.(JENDL/D-99)		Calc.(JENDL/D-91)		Diff.[*2] between JENDL/D-99 and Exp.	
	Reaction rate(%)	Reaction rate(C/E)		Reaction rate(C/E)		(%)	Criterion[*3]
$^{27}Al(n,\alpha)^{24}Na$	7.025E-32*[1](4)	6.85E-32	(0.97)	6.79E-32	(0.97)	-2.49	
$^{N}Ti(n,x)^{46}Sc$	1.120E-31(12)	1.11E-31	(0.99)	1.16E-31	(1.03)	-0.89	
$^{N}Ti(n,x)^{47}Sc$	1.316E-32(4)	1.33E-32	(1.01)	1.47E-32	(1.12)	1.06	
$^{N}Ti(n,x)^{48}Sc$	2.990E-32(5)	2.86E-32	(0.96)	2.98E-32	(1.00)	-4.35	
$^{54}Fe(n,p)^{54}Mn$	5.080E-31(10)	4.74E-31	(0.93)	4.75E-31	(0.93)	-6.69	*
$^{56}Fe(n,p)^{56}Mn$	6.531E-32(3)	6.43E-32	(0.98)	6.27E-32	(0.96)	-1.55	
$^{59}Co(n,2n)^{58m+g}Co$	2.454E-31(3)	2.55E-31	(1.04)	2.59E-31	(1.06)	3.91	
$^{59}Co(n,\alpha)^{56}Mn$	1.550E-32(4)	1.59E-32	(1.03)	1.60E-32	(1.03)	2.58	
$^{58}Ni(n,2n)^{57}Ni$	8.000E-33(5)	7.71E-33	(0.96)	7.92E-33	(0.99)	-3.63	
$^{58}Ni(n,p)^{58m+g}Co$	5.465E-31(3)	5.71E-31	(1.04)	5.43E-31	(0.99)	4.48	
$^{64}Zn(n,p)^{64}Cu$	2.088E-31(4)	2.11E-31	(1.01)	2.50E-31	(1.20)	1.05	
$^{90}Zr(n,2n)^{89m+g}Zn$	1.975E-31(4)	1.91E-31	(0.97)	1.88E-31	(0.95)	-3.29	
$^{93}Nb(n,2n)^{92m}Nb$	2.104E-31(3)	2.09E-31	(0.99)	2.14E-31	(1.02)	-0.67	
$^{115}In(n,n')^{115m}In$	4.942E-31(3)	5.06E-31	(1.02)	4.85E-31	(0.98)	2.39	

*1) Read as 7.025×10^{-32}.

*2) Diff. is given as (C-E)/E in percent.

*3) Judgment from deviations: * for >5%.

Table 4.2.1 List of samples contained in the foil packets

Packet No./position	Foils (ordered from the source side)
#1/P1	Al, Nb, Ni, Ti, Zr, Fe, Mg, Al, Au, Nb, Al, Mn*
#2/P2	Al, Nb, Cu, Ni, Fe, Nb, Al, NaCl*

*: Two powder samples of NaCl and Mn are contained in thin plastic bags in size of about 15 mm in diameter × 1.5mm in thickness; the rest ones are metal disks of 15 mm in diameter × 0.1-0.2 mm in thickness except for Cu (15mm in diameter × 1mm in thickness).

Table 4.2.2 Comparison of average cross sections in the Li(d,n) neutron field

Reaction	Experiment	JENDL/D-99		JENDL/D-91		IRDF-90V2		Diff.[*1] between JENDL/D-99 and Exp.	
		Calc.	C/E	Calc.	C/E	Calc.	C/E		
	(mb) (% error)	(mb) (% error)		(mb)		(mb)		(%)	Criterion[*2]
$^{23}Na(n,2n)^{22}Na$	6.960E+00(9.90)	6.807E+00(2.5)	0.978	6.236E+00	0.896	-	-	-2.19	
$^{24}Mg(n,p)^{24}Na$	6.980E+01(9.70)	6.964E+01(2.3)	0.998	7.042E+01	1.009	6.971E+01	0.999	-0.22	
$^{27}Al(n,\alpha)^{24}Na$	4.300E+01(8.60)	4.294E+01(2.2)	0.999	4.281E+01	0.996	4.294E+01	0.999	-0.13	
$^{N}Ti(n,x)^{46}Sc$	1.150E+01(9.10)	1.221E+01(13.2)	1.154	1.243E+01	1.081	-	-	6.17	*
$^{N}Ti(n,x)^{48}Sc$	2.010E+01(8.80)	1.990E+01(13.0)	0.990	2.078E+01	1.034	-	-	-0.10	
$^{55}Mn(n,2n)^{54}Mn$	1.600E+02(8.50)	1.971E+02(5.4)	1.232	1.898E+02	1.186	1.898E+02	1.186	23.16	***
$^{54}Fe(n,p)^{54}Mn$	2.950E+02(8.60)	2.580E+02(2.2)	0.875	2.604E+02	0.883	2.448E+02	0.830	-12.55	**
$^{59}Co(n,2n)^{58}Co$	1.620E+02(8.60)	1.809E+02(2.3)	1.117	1.821E+02	1.124	1.799E+02	1.110	11.68	**
$^{58}Ni(n,2n)^{57}Ni$	6.770E+00(9.80)	6.712E+00(2.3)	0.991	6.623E+00	0.978	6.835E+00	1.010	-0.86	
$^{58}Ni(n,p)^{58}Co$	3.190E+02(8.40)	3.043E+02(2.1)	0.954	2.885E+02	0.904	2.943E+02	0.923	-4.62	
$^{60}Ni(n,p)^{60}Co$	5.710E+01(8.90)	4.992E+01(3.2)	0.874	5.367E+01	0.940	5.141E+01	0.900	-12.57	**
$^{63}Cu(n,\alpha)^{60}Co$	1.380E+01(8.70)	1.341E+01(2.5)	0.972	1.347E+01	0.976	1.543E+01	1.118	-2.81	
$^{93}Nb(n,2n)^{92m}Nb$	1.380E+02(8.50)	1.470E+02(2.2)	1.065	1.488E+02	1.078	1.443E+02	1.046	6.49	*
$^{197}Au(n,2n)^{198}Au$	6.680E+02(8.50)	6.992E+02(2.3)	1.047	6.846E+02	1.025	7.125E+02	1.067	4.67	

*1) (C-E)/E in percent.
*2) Judgment from deviations: * for >5%; ** for >10%; *** for >20%.

```
 9.01900+ 3 1.88352+ 1          0          0          0          1 925 1451    1
 0.00000+ 0 0.00000+ 0          0          0          0          6 925 1451    2
 1.00000+ 0 0.00000+ 0          0          0         10          3 925 1451    3
 0.00000+ 0 0.00000+ 0          0          0         55          4 925 1451    4
  9-F - 19 NAG        EVAL-JUL96  T.IGUCHI                                925 1451    5
                      DIST-JUL98                                          925 1451    6
----JENDL/D-99        MATERIAL  925                                       925 1451    7
-----INCIDENT NEUTRON DATA                                              925 1451    8
------ENDF-6 FORMAT                                                      925 1451    9
HISTORY                                                                 925 1451   10
96-07   EVALUATION WAS PERFORMED FOR JENDL DOSIMETRY FILE BY            925 1451   11
        T.IGUCHI(NAGOYA UNIV.)                                          925 1451   12
                                                                        925 1451   13
            ===== GROUP-WISE DATA FILE =====                            925 1451   14
                                                                        925 1451   15
   CROSS SECTIONS WERE AVERAGED IN THE SAND-II TYPE 640 ENERGY          925 1451   16
   INTERVALS.                                                           925 1451   17
                                                                        925 1451   18
 <DOSIMETRY CROSS SECTION>                                              925 1451   19
     F-19 (N,2N) F-18  (HALF-LIFE = 109.77 M)                           925 1451   20
                                                                        925 1451   21
                                                                        925 1451   22
MF=1  GENERAL INFORMATION                                               925 1451   23
 MT=451  DESCRIPTIVE DATA AND DICTIONARY                                925 1451   24
                                                                        925 1451   25
MF=2  RESONANCE PARAMETERS                                              925 1451   26
 MT=151  PARAMETERS                                                     925 1451   27
     ONLY SPIN AND SCATTERING RADIUS ARE GIVEN.                         925 1451   28
                                                                        925 1451   29
MF=3    NEUTRON CROSS SECTIONS                                          925 1451   30
 MT=16  (N,2N) CROSS SECTION                                            925 1451   31
     - EXPERIMENTAL DATA/1-16/ IN NESTOR-2/17/ WERE TAKEN FOR           925 1451   32
       THE EVALUATION USING GMA CODE/18/.                               925 1451   33
                                                                        925 1451   34
MF=33   COVARIANCES OF NEUTRON CROSS SECTIONS                           925 1451   35
 MT=16  GENERATED USING THE GMA CODE.                                   925 1451   36
                                                                        925 1451   37
REFERENCES                                                              925 1451   38
 1) J.CSIKAI: EANDC-50S, 2, 102 (1965).                                 925 1451   39
 2) M.BORMANN+ : NUCLEAR PHYSICS,63,438 (1965).                         925 1451   40
 3) A.CHATTERJEE+ : BARC-305,30 (1967)                                  925 1451   41
 4) H.O.MENLOVE+ : PHYSICAL REVIEW, 163, 1308 (1967).                   925 1451   42
 5) A.PASQUARELLI : NUCLEAR PHYSICS/A, 93, 218 (1967).                  925 1451   43
 6) H.K.VONACH+ : NUCLEAR PHYSICS/A, 118, 9(1968)                       925 1451   44
 7) R.MOGHARRAB+ : AKE,19, 107 (1972).                                  925 1451   45
 8) J.ARAMINOWICZ+:INR-1464, 14 (1973).                                 925 1451   46
 9) J.C.ROBERTSON+ : JNE, 27, 531 (1973).                               925 1451   47
10) R.A.SIGG : DA/B, 37, 2237 (1976).                                   925 1451   48
11) T.B.RYVES+ : JP/G, 4(11), 1783  (1978).                             925 1451   49
12) Y.IKEDA+ : JAERI-1312 (1988).                                       925 1451   50
13) K.KOBAYASHI+:PROC. 88MITO, 261 (1988).                              925 1451   51
14) I.KIMURA+: NUCLEAR SCIENCE AND ENGINEERING, 106, 332 (1990)         925 1451   52
15) K.KOBAYASHI+ : PROC. 88MITO, 261 (1988).                            925 1451   53
16) C.L.HARTMANN+:NUCLEAR SCIENCE AND ENGINEERING, 109, 319 (1991)      925 1451   54
17) T.NAKAGAWA : THE JAERI NUCLEAR DATA CENTER, UNPUBLISHED.            925 1451   55
18) W.P.POENITZ : PROC. CONF. NUCLEAR DATA EVALUATION METHODS           925 1451   56
```

Fig. 2.3.1 An example of the group-wise data.

```
 AND PROCEDURES, BROOKHAVEN NATIONAL LAB. 1980, BNL-NCS-                925 1451   57
 51363, P.249 (1981).                                                   925 1451   58
                                                                        925 1451   59
                                  1          451           63          1 925 1451   60
                                  2          151            4          1 925 1451   61
                                  3           16           34          1 925 1451   62
                                 33           16           46          1 925 1451   63
                                                                        925 1  0   64
                                                                        925 0  0   65
 9.01900+ 3 1.88352+ 1            0            0            1          0 925 2151   66
 9.01900+ 3 1.00000+ 0            0            0            1          0 925 2151   67
 0.00000+ 0 0.00000+ 0            0            0            0          0 925 2151   68
 5.00000- 1 5.25000- 1            0            0            0          0 925 2151   69
                                                                        925 2  0   70
                                                                        925 0  0   71
 9.01900+ 3 1.88352+ 1            0            0            0          0 925 3 16   72
-1.04316+ 7-1.04316+ 7            0            0            1         92 925 3 16   73
        92          1              0            0            0          0 925 3 16   74
 1.09000+ 7 7.30000-12 1.10000+ 7 2.00000- 4 1.11000+ 7 6.00000- 4 925 3 16   75
 1.12000+ 7 1.00000- 3 1.13000+ 7 1.40000- 3 1.14000+ 7 1.80000- 3 925 3 16   76
 1.15000+ 7 2.40000- 3 1.16000+ 7 3.20000- 3 1.17000+ 7 4.00000- 3 925 3 16   77
 1.18000+ 7 4.80000- 3 1.19000+ 7 5.60000- 3 1.20000+ 7 6.58000- 3 925 3 16   78
 1.21000+ 7 7.74000- 3 1.22000+ 7 8.90000- 3 1.23000+ 7 1.00600- 2 925 3 16   79
 1.24000+ 7 1.12200- 2 1.25000+ 7 1.28240- 2 1.26000+ 7 1.48720- 2 925 3 16   80
 1.27000+ 7 1.69200- 2 1.28000+ 7 1.89680- 2 1.29000+ 7 2.10160- 2 925 3 16   81
 1.30000+ 7 2.28570- 2 1.31000+ 7 2.44910- 2 1.32000+ 7 2.61250- 2 925 3 16   82
 1.33000+ 7 2.77590- 2 1.34000+ 7 2.93930- 2 1.35000+ 7 3.11660- 2 925 3 16   83
 1.36000+ 7 3.30780- 2 1.37000+ 7 3.49900- 2 1.38000+ 7 3.69020- 2 925 3 16   84
 1.39000+ 7 3.88140- 2 1.40000+ 7 4.04790- 2 1.41000+ 7 4.18970- 2 925 3 16   85
 1.42000+ 7 4.33150- 2 1.43000+ 7 4.47330- 2 1.44000+ 7 4.61510- 2 925 3 16   86
 1.45000+ 7 4.77000- 2 1.46000+ 7 4.93800- 2 1.47000+ 7 5.10600- 2 925 3 16   87
 1.48000+ 7 5.27400- 2 1.49000+ 7 5.44200- 2 1.50000+ 7 5.59340- 2 925 3 16   88
 1.51000+ 7 5.72820- 2 1.52000+ 7 5.86300- 2 1.53000+ 7 5.99780- 2 925 3 16   89
 1.54000+ 7 6.13260- 2 1.55000+ 7 6.24760- 2 1.56000+ 7 6.34280- 2 925 3 16   90
 1.57000+ 7 6.43800- 2 1.58000+ 7 6.53320- 2 1.59000+ 7 6.62840- 2 925 3 16   91
 1.60000+ 7 6.72710- 2 1.61000+ 7 6.82930- 2 1.62000+ 7 6.93150- 2 925 3 16   92
 1.63000+ 7 7.03370- 2 1.64000+ 7 7.13590- 2 1.65000+ 7 7.24020- 2 925 3 16   93
 1.66000+ 7 7.34660- 2 1.67000+ 7 7.45300- 2 1.68000+ 7 7.55940- 2 925 3 16   94
 1.69000+ 7 7.66580- 2 1.70000+ 7 7.75030- 2 1.71000+ 7 7.81290- 2 925 3 16   95
 1.72000+ 7 7.87550- 2 1.73000+ 7 7.93810- 2 1.74000+ 7 8.00070- 2 925 3 16   96
 1.75000+ 7 8.06680- 2 1.76000+ 7 8.13640- 2 1.77000+ 7 8.20600- 2 925 3 16   97
 1.78000+ 7 8.27560- 2 1.79000+ 7 8.34520- 2 1.80000+ 7 8.45480- 2 925 3 16   98
 1.81000+ 7 8.60440- 2 1.82000+ 7 8.75400- 2 1.83000+ 7 8.90360- 2 925 3 16   99
 1.84000+ 7 9.05320- 2 1.85000+ 7 9.10040- 2 1.86000+ 7 9.04520- 2 925 3 16  100
 1.87000+ 7 8.99000- 2 1.88000+ 7 8.93480- 2 1.89000+ 7 8.87960- 2 925 3 16  101
 1.90000+ 7 8.84890- 2 1.91000+ 7 8.84270- 2 1.92000+ 7 8.83650- 2 925 3 16  102
 1.93000+ 7 8.83030- 2 1.94000+ 7 8.82410- 2 1.95000+ 7 8.83890- 2 925 3 16  103
 1.96000+ 7 8.87470- 2 1.97000+ 7 8.91050- 2 1.98000+ 7 8.94630- 2 925 3 16  104
 1.99000+ 7 8.98210- 2 2.00000+ 7 8.98210- 2                        925 3 16  105
                                                                    925 3  0  106
                                                                    925 0  0  107
 9.01900+ 3 1.88352+ 1            0            0            0          1 92533 16  108
 0.00000+ 0 0.00000+ 0            0           16            0          1 92533 16  109
 0.00000+ 0 0.00000+ 0            1            5          253         22 92533 16  110
 1.00000- 5 1.09854+ 7 1.09927+ 7 1.12500+ 7 1.17500+ 7 1.22500+ 7 92533 16  111
 1.27500+ 7 1.32500+ 7 1.37500+ 7 1.42500+ 7 1.47500+ 7 1.52500+ 7 92533 16  112
```

Fig. 2.3.1 (continued)

```
1.57500+ 7 1.62500+ 7 1.67500+ 7 1.72500+ 7 1.77500+ 7 1.82500+ 7 92533 16  113
1.87500+ 7 1.92500+ 7 1.97500+ 7 2.00000+ 7 0.00000+ 0 0.00000+ 0 92533 16  114
0.00000+ 0 0.00000+ 0 0.00000+ 0 0.00000+ 0 0.00000+ 0 0.00000+ 0 92533 16  115
0.00000+ 0 0.00000+ 0 0.00000+ 0 0.00000+ 0 0.00000+ 0 0.00000+ 0 92533 16  116
0.00000+ 0 0.00000+ 0 0.00000+ 0 0.00000+ 0 0.00000+ 0 0.00000+ 0 92533 16  117
0.00000+ 0 0.00000+ 0 0.00000+ 0 0.00000+ 0 0.00000+ 0 0.00000+ 0 92533 16  118
0.00000+ 0 0.00000+ 0 0.00000+ 0 0.00000+ 0 0.00000+ 0 0.00000+ 0 92533 16  119
0.00000+ 0 0.00000+ 0 0.00000+ 0 0.00000+ 0 0.00000+ 0 0.00000+ 0 92533 16  120
0.00000+ 0 0.00000+ 0 0.00000+ 0 9.00000- 2 0.00000+ 0 0.00000+ 0 92533 16  121
0.00000+ 0 0.00000+ 0 0.00000+ 0 0.00000+ 0 0.00000+ 0 0.00000+ 0 92533 16  122
0.00000+ 0 0.00000+ 0 0.00000+ 0 0.00000+ 0 0.00000+ 0 0.00000+ 0 92533 16  123
0.00000+ 0 0.00000+ 0 0.00000+ 0 0.00000+ 0 9.00000- 2 0.00000+ 0 92533 16  124
0.00000+ 0 0.00000+ 0 0.00000+ 0 0.00000+ 0 0.00000+ 0 0.00000+ 0 92533 16  125
0.00000+ 0 0.00000+ 0 0.00000+ 0 0.00000+ 0 0.00000+ 0 0.00000+ 0 92533 16  126
0.00000+ 0 0.00000+ 0 0.00000+ 0 0.00000+ 0 9.00000- 2 0.00000+ 0 92533 16  127
0.00000+ 0 0.00000+ 0 0.00000+ 0 0.00000+ 0 0.00000+ 0 0.00000+ 0 92533 16  128
0.00000+ 0 0.00000+ 0 0.00000+ 0 0.00000+ 0 0.00000+ 0 0.00000+ 0 92533 16  129
0.00000+ 0 0.00000+ 0 0.00000+ 0 3.59520- 3 2.07912- 4 6.13691- 5 92533 16  130
9.81569- 5 0.00000+ 0 5.83351- 5 0.00000+ 0 5.97597- 5 4.61452- 5 92533 16  131
1.97642- 4 4.48441- 5 4.03561- 5 1.96693- 4 8.07541- 5 2.12596- 4 92533 16  132
0.00000+ 0 2.93547- 3 5.66587- 5 9.49190- 5 0.00000+ 0 5.50035- 5 92533 16  133
0.00000+ 0 5.52847- 5 4.16969- 5 1.93168- 4 4.05212- 5 3.75077- 5 92533 16  134
1.83375- 4 7.88861- 5 1.98201- 4 0.00000+ 0 4.95062- 4 8.40311- 5 92533 16  135
6.83742- 8 9.27057- 5 0.00000+ 0 1.68958- 5 1.23076- 5 5.68768- 5 92533 16  136
1.22032- 5 1.11246- 5 5.44522- 5 2.34871- 5 5.88548- 5 0.00000+ 0 92533 16  137
2.06209- 4 4.41283- 8 6.71208- 5 0.00000+ 0 2.69202- 5 1.72679- 5 92533 16  138
1.24613- 4 1.68257- 5 1.98823- 5 8.97270- 5 4.65206- 5 9.61735- 5 92533 16  139
0.00000+ 0 9.44333- 6 6.49939- 8 0.00000+ 0 7.29223- 8 7.39056- 8 92533 16  140
0.00000+ 0 0.00000+ 0 5.90938- 8 0.00000+ 0 0.00000+ 0 0.00000+ 0 92533 16  141
0.00000+ 0 4.47322- 4 0.00000+ 0 1.60604- 5 1.11905- 5 5.97559- 5 92533 16  142
1.10727- 5 1.09813- 5 5.17601- 5 2.38656- 5 5.59451- 5 0.00000+ 0 92533 16  143
6.25000- 4 0.00000+ 0 0.00000+ 0 0.00000+ 0 0.00000+ 0 0.00000+ 0 92533 16  144
0.00000+ 0 0.00000+ 0 0.00000+ 0 0.00000+ 0 5.63113- 4 1.87192- 4 92533 16  145
5.42747- 5 1.83392- 4 1.51044- 4 5.31317- 5 1.50296- 4 5.74275- 5 92533 16  146
0.00000+ 0 5.78402- 4 3.39747- 5 1.96658- 4 1.61406- 4 4.00731- 5 92533 16  147
1.54949- 4 4.33131- 5 0.00000+ 0 4.52524- 3 3.35408- 5 4.01016- 5 92533 16  148
1.82143- 4 9.54965- 5 1.93084- 4 0.00000+ 0 6.21505- 4 1.58203- 4 92533 16  149
3.89431- 5 1.51544- 4 4.20918- 5 0.00000+ 0 3.69793- 4 3.60470- 5 92533 16  150
1.28795- 4 3.89615- 5 0.00000+ 0 2.71128- 3 7.39186- 5 1.87552- 4 92533 16  151
0.00000+ 0 1.32496- 3 7.98951- 5 0.00000+ 0 3.16744- 3 0.00000+ 0 92533 16  152
4.00000- 2                                                         92533 16  153
                                                                   92533  0  154
                                                                   925 0  0  155
                                                                     0 0  0  156
                                                                    -1 0  0    0
```

Fig. 2.3.1 (continued)

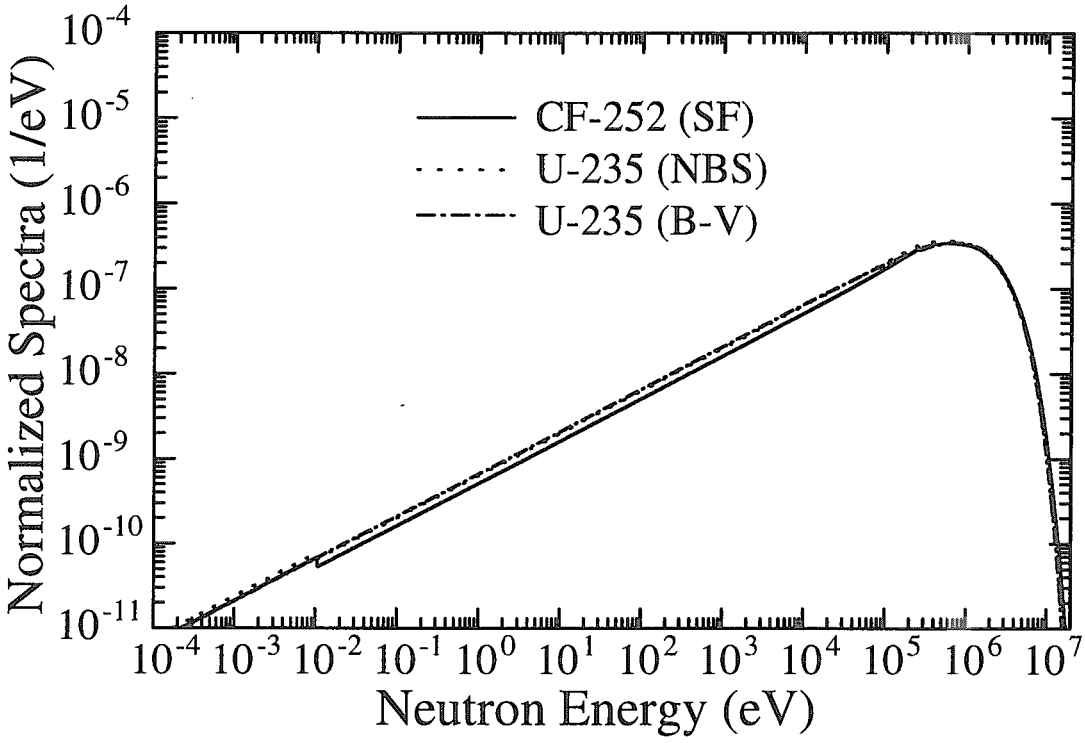

Fig. 3.1.1(a) Benchmark spectra.

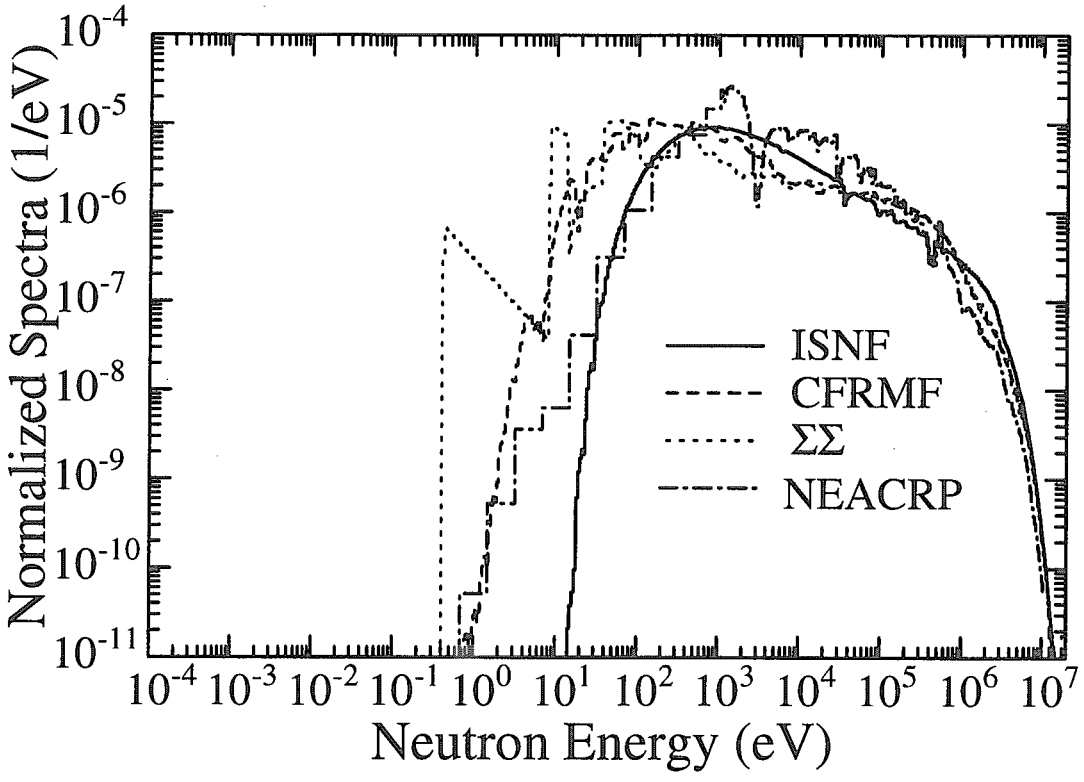

Fig. 3.1.1(b) Benchmark spectra.

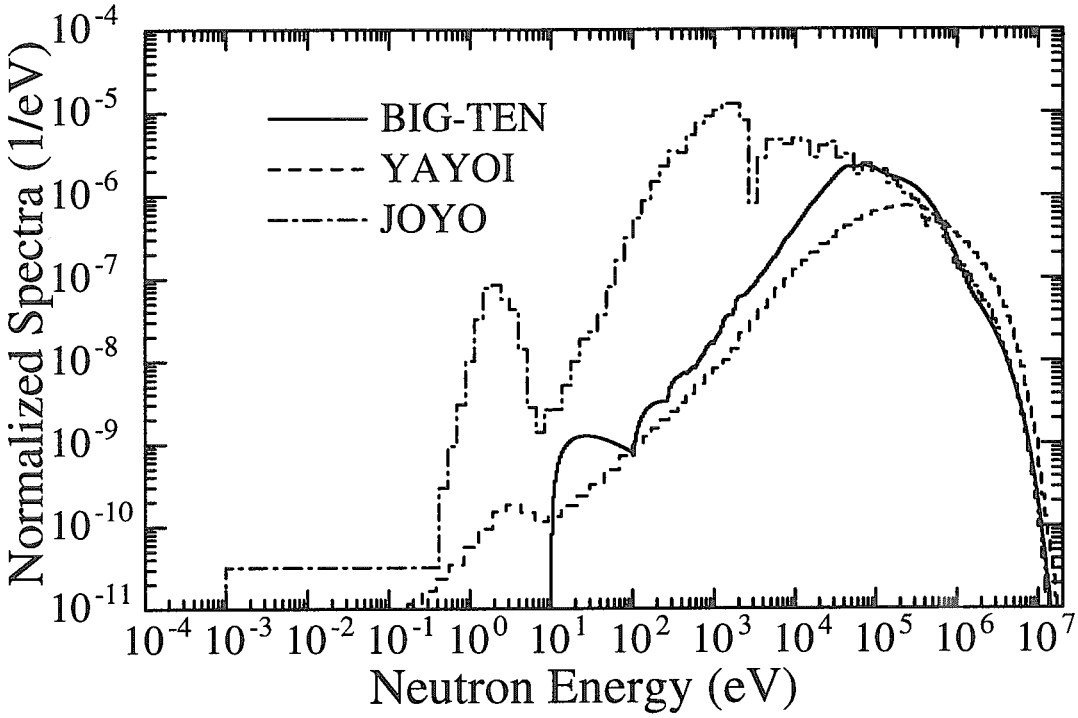

Fig. 3.1.1(c) Benchmark spectra.

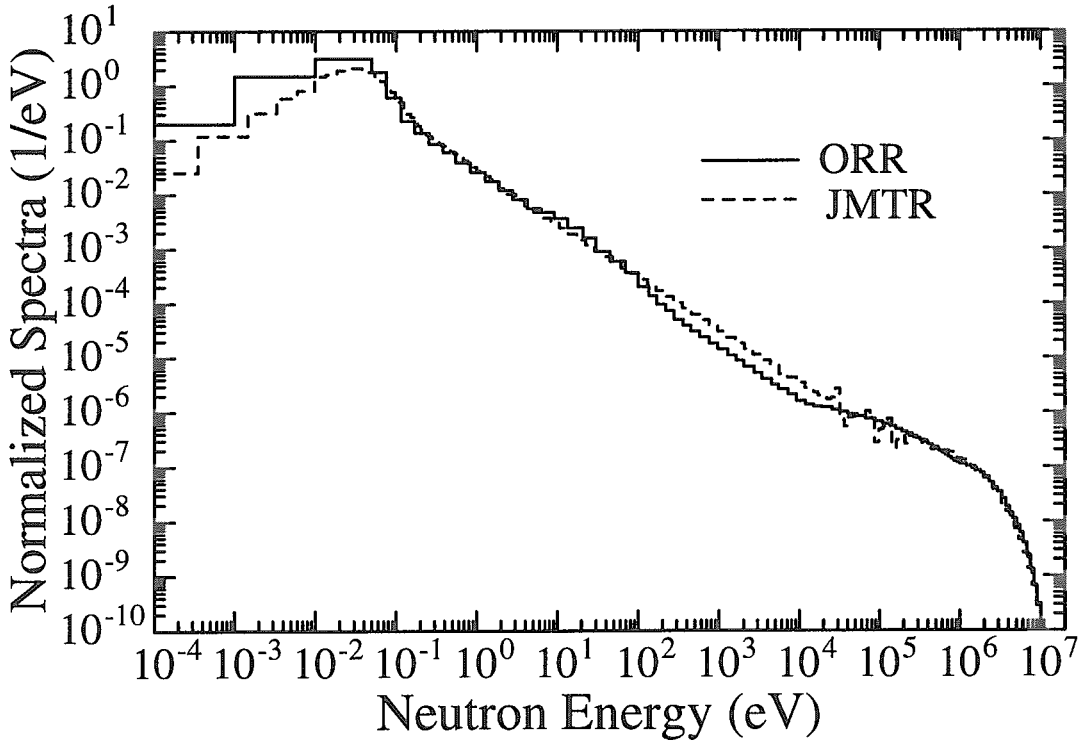

Fig. 3.1.1(d) Benchmark spectra.

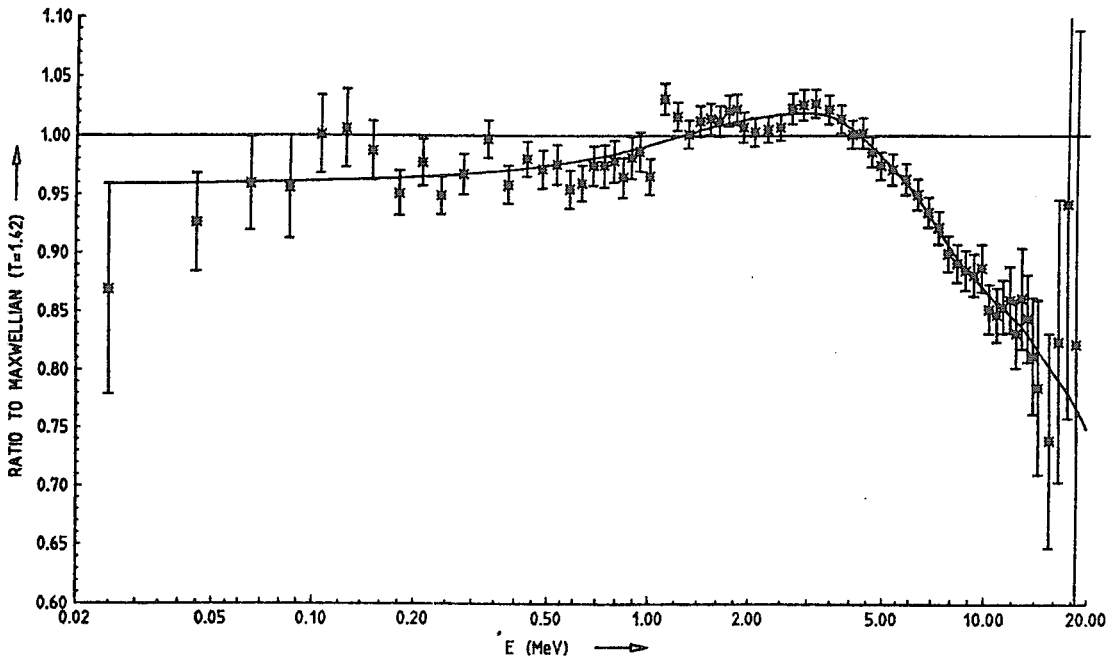

Fig. 3.2.1 Ratio of the evaluation of the spontaneous fission neutron spectrum of ^{252}Cf to the Maxwellian spectrum (T=1.42 MeV) given in Ref. 45. The data points represent the evaluation performed at discrete neutron energies. The solid curve is the continuous shape of the evaluated spectral distribution.

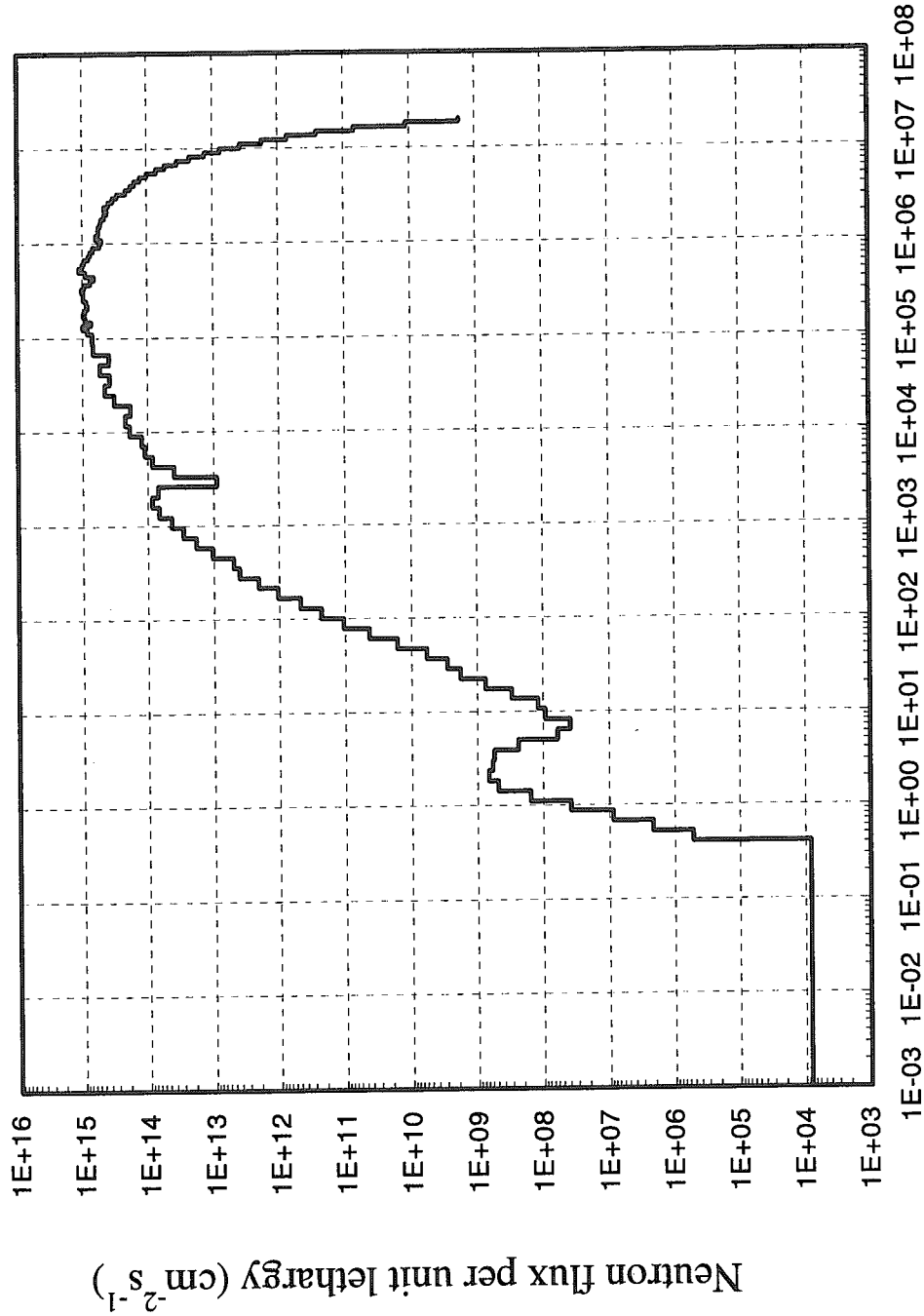

Fig. 3.3.1 Neutron spectrum near the center position of the JOYO Mk-II core.

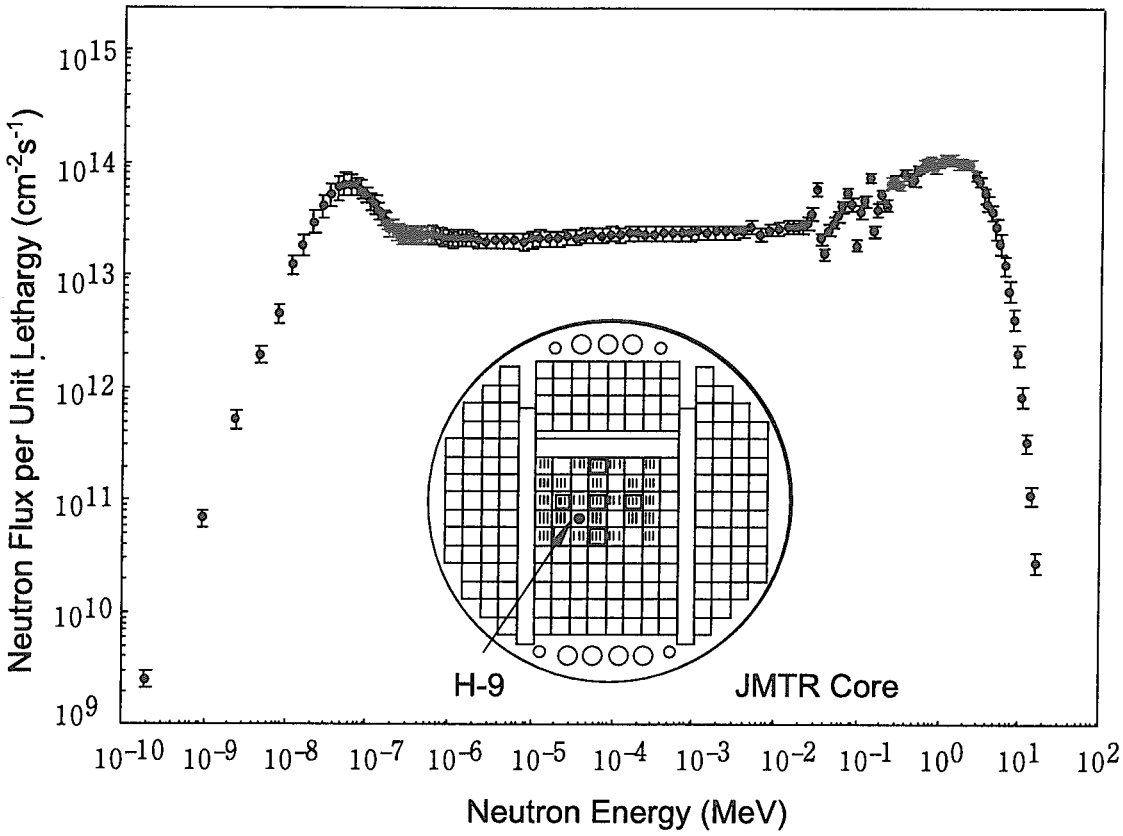

Fig. 3.3.2 Neutron Spectrum near the core center (H-9) of JMTR.

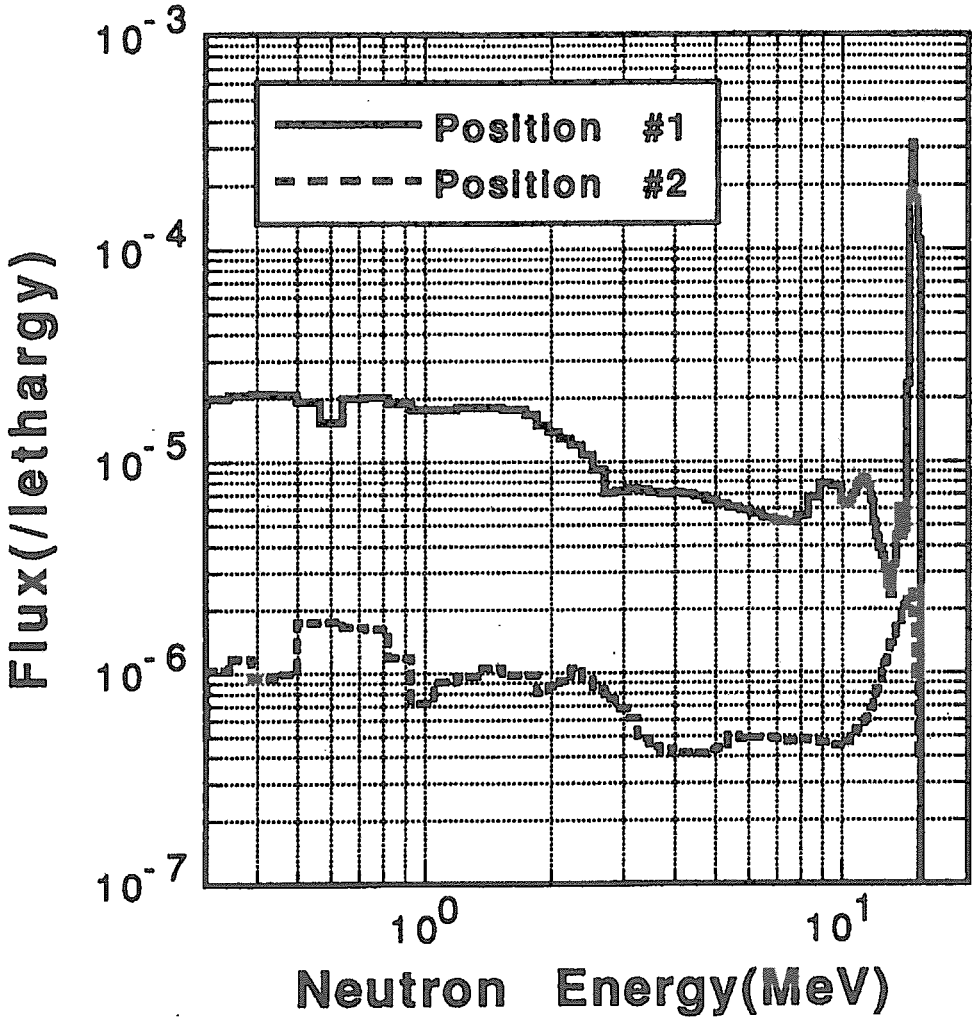

Fig. 4.1.1 Neutron spectra at positions #1 and #2.

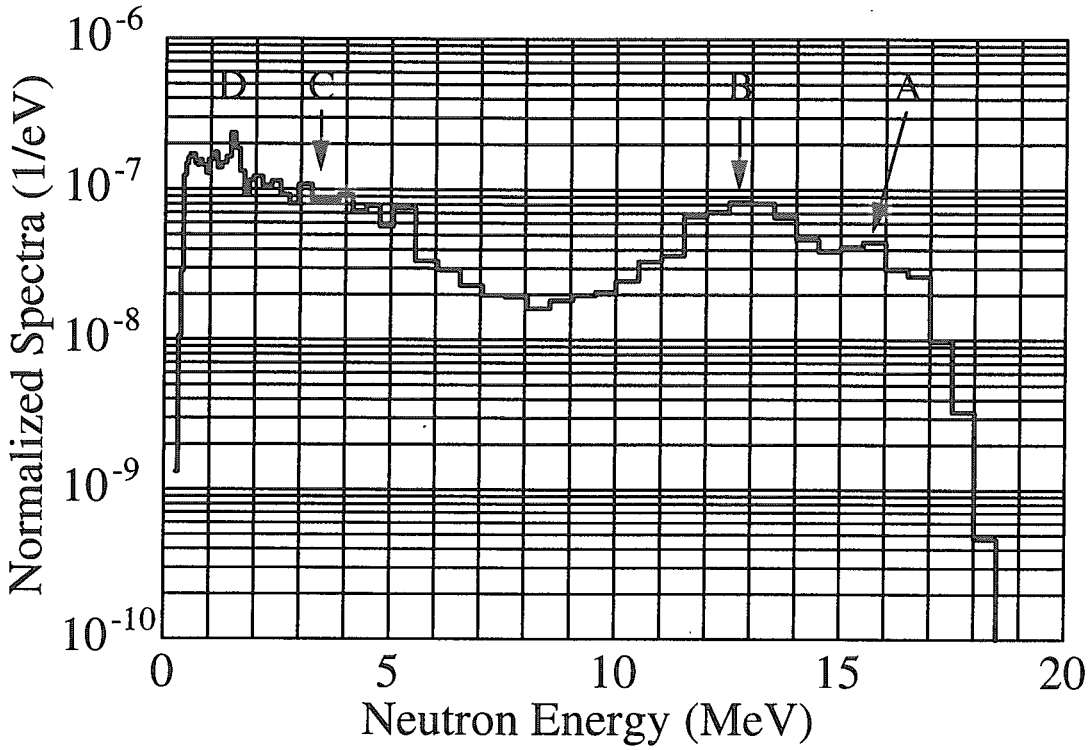

Fig. 4.2.1 Measured neutron spectrum of the thick Li(d,n) neutron source at 0-degree. Arrows in the figure indicate peaks corresponding to the ground state (A) and broad first (B) and fourth (C) excited states of residual nucleus of ^{8}Be, and a parasitic neutron group from ^{12}C(d,n) reactions (D).

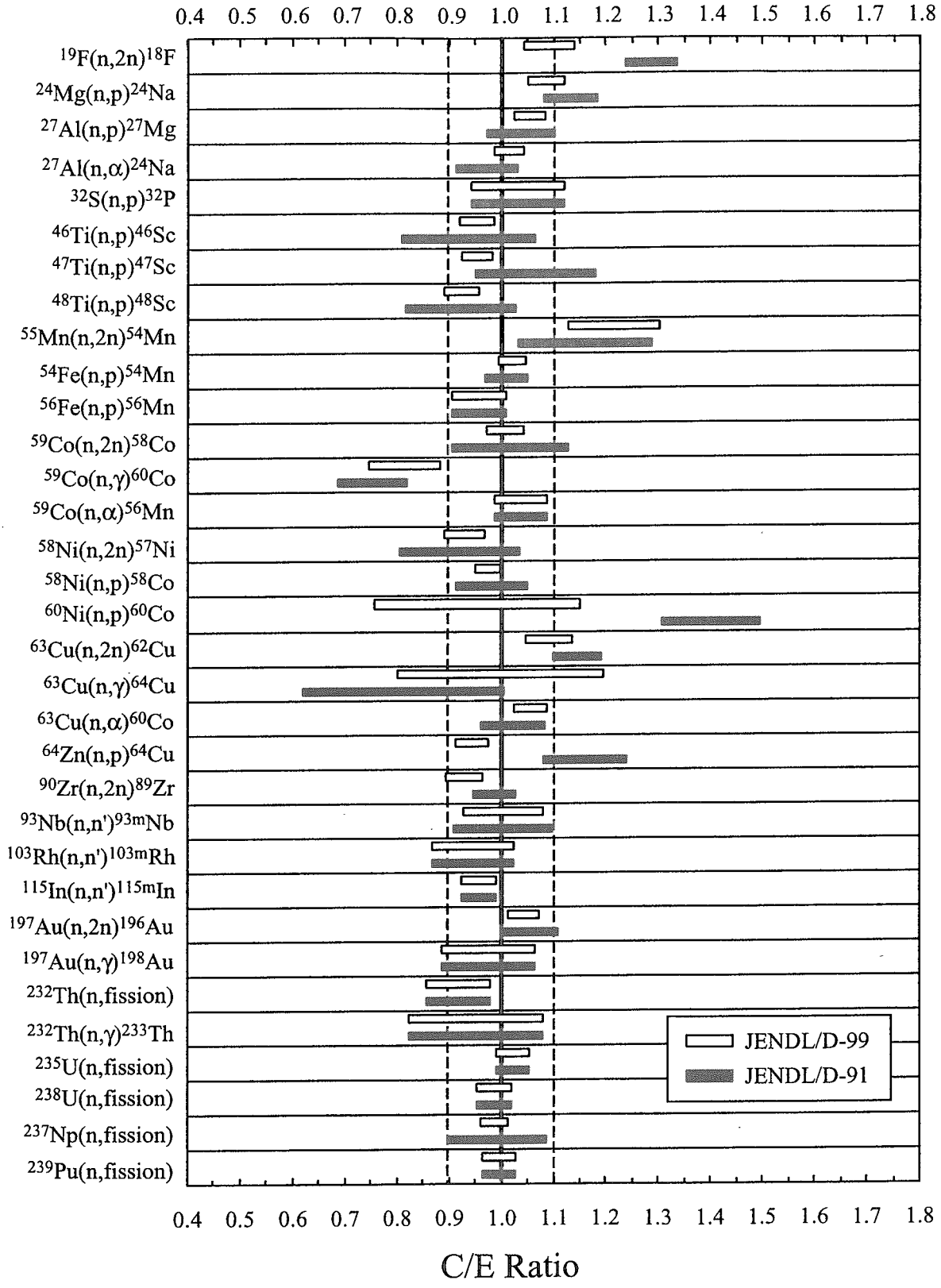

Fig. 5.1.1 C/E range of spectrum-averaged cross sections for ^{252}Cf spontaneous fission. Center and width of each rectangle show C/E and uncertainty, respectively.

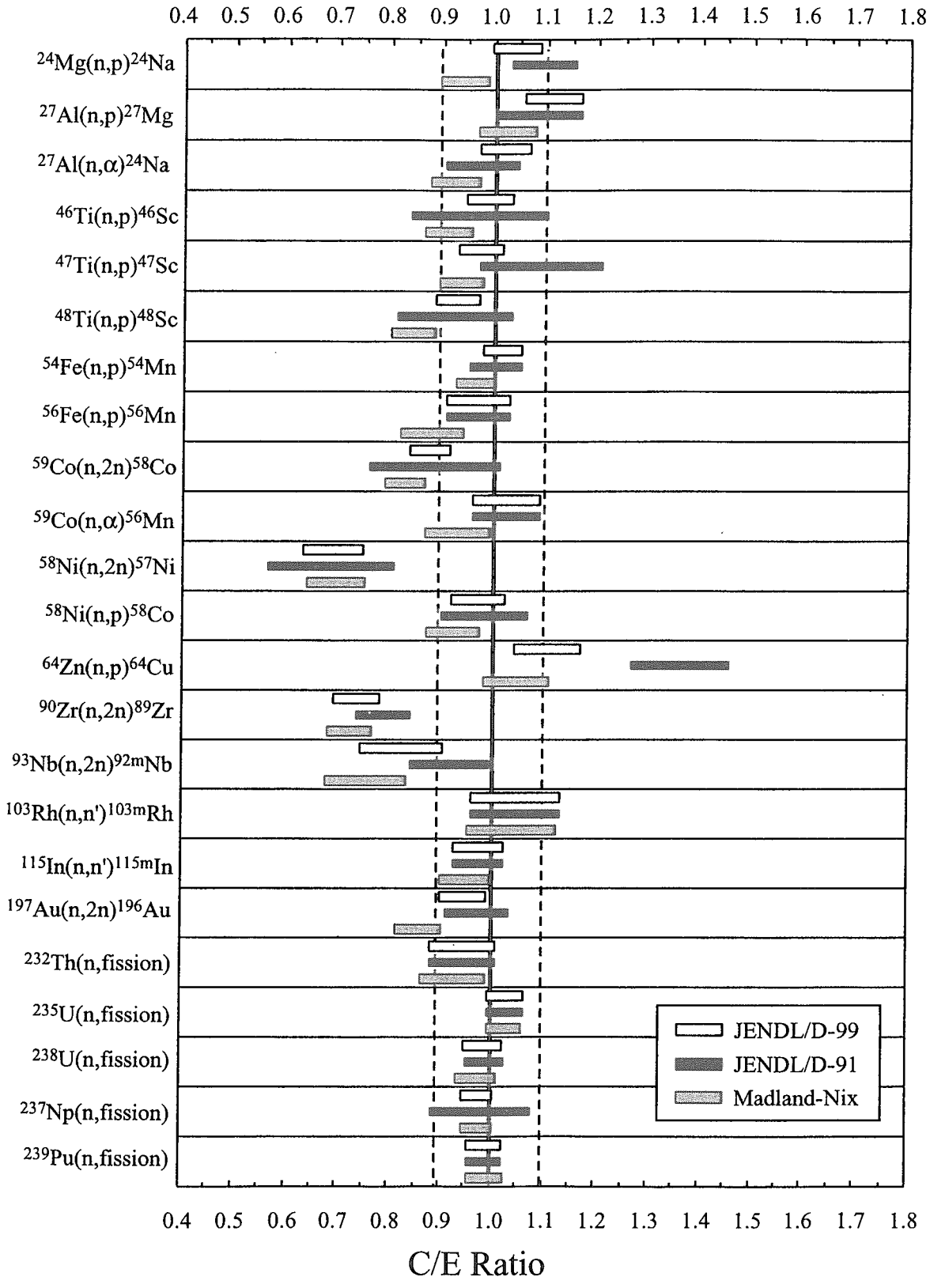

Fig. 5.1.2 C/E range of spectrum-averaged cross sections for ^{235}U thermal fission. Center and width of each rectangle show C/E and uncertainty, respectively.

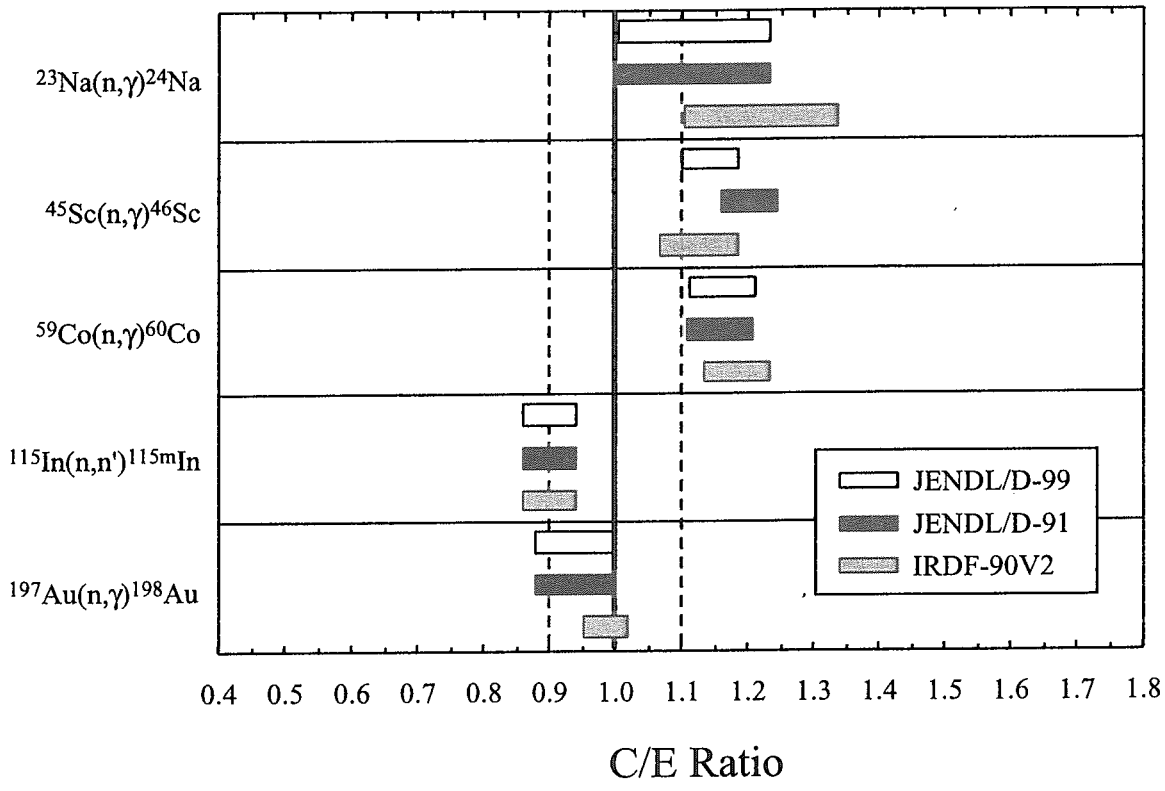

Fig. 5.1.3 C/E range of spectrum-averaged cross sections for ISNF spectrum. Center and width of each rectangle show C/E and uncertainty, respectively.

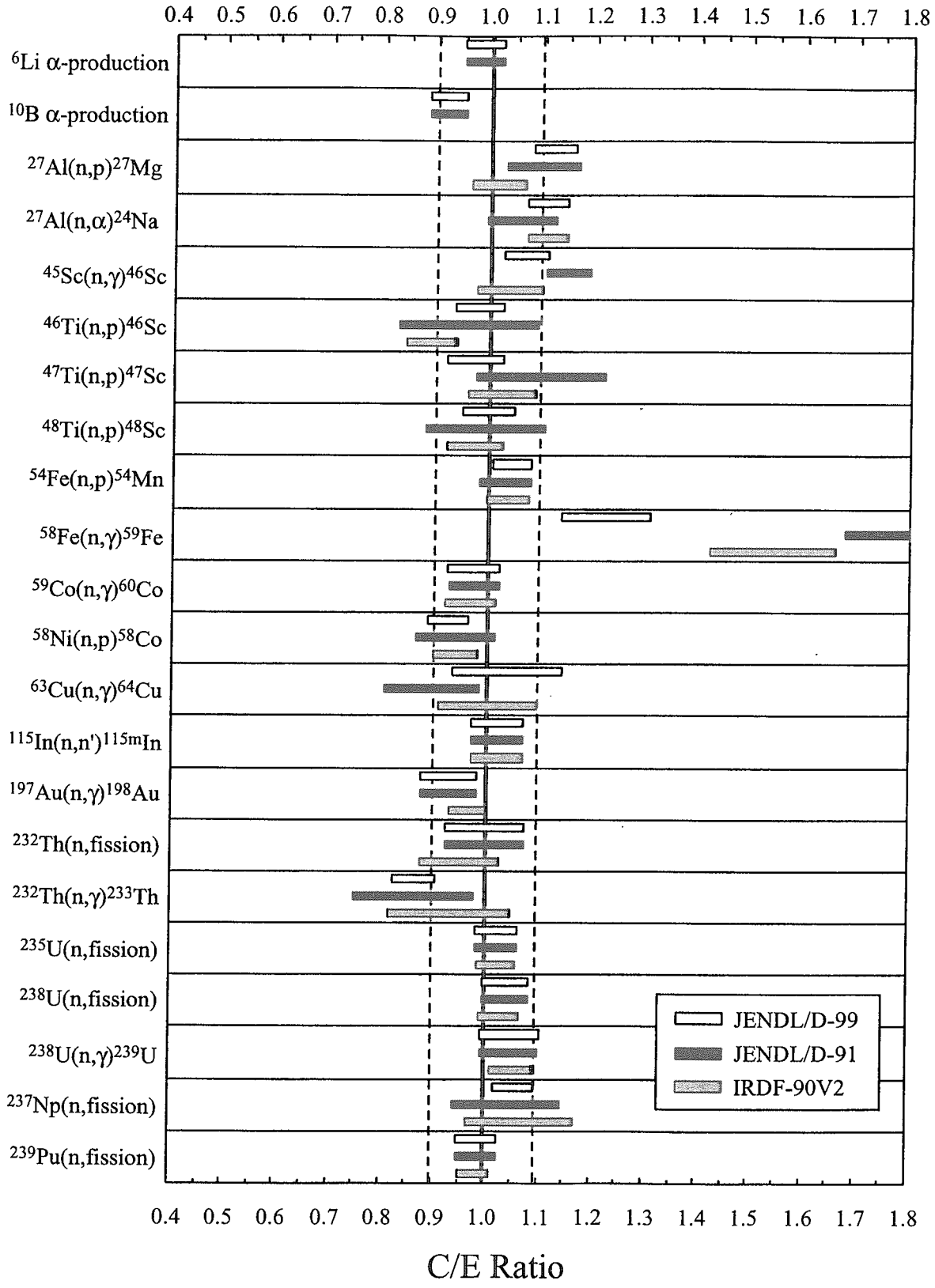

Fig. 5.1.4 C/E range of spectrum-averaged cross sections for CFRMF spectrum. Center and width of each rectangle show C/E and uncertainty, respectively.

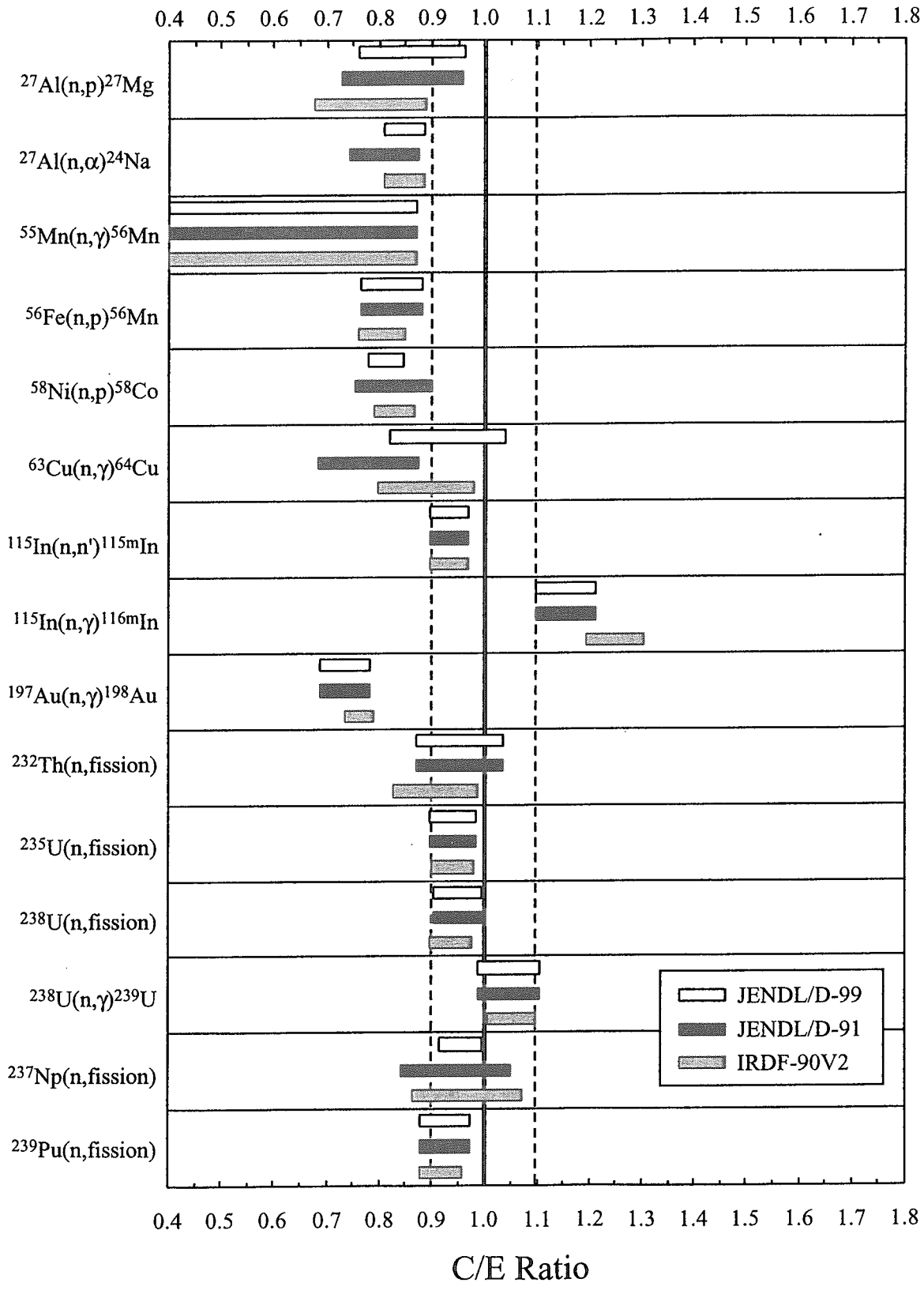

Fig. 5.1.5 C/E range of spectrum-averaged cross sections for ΣΣ spectrum.
Center and width of each rectangle show C/E and uncertainty, respectively

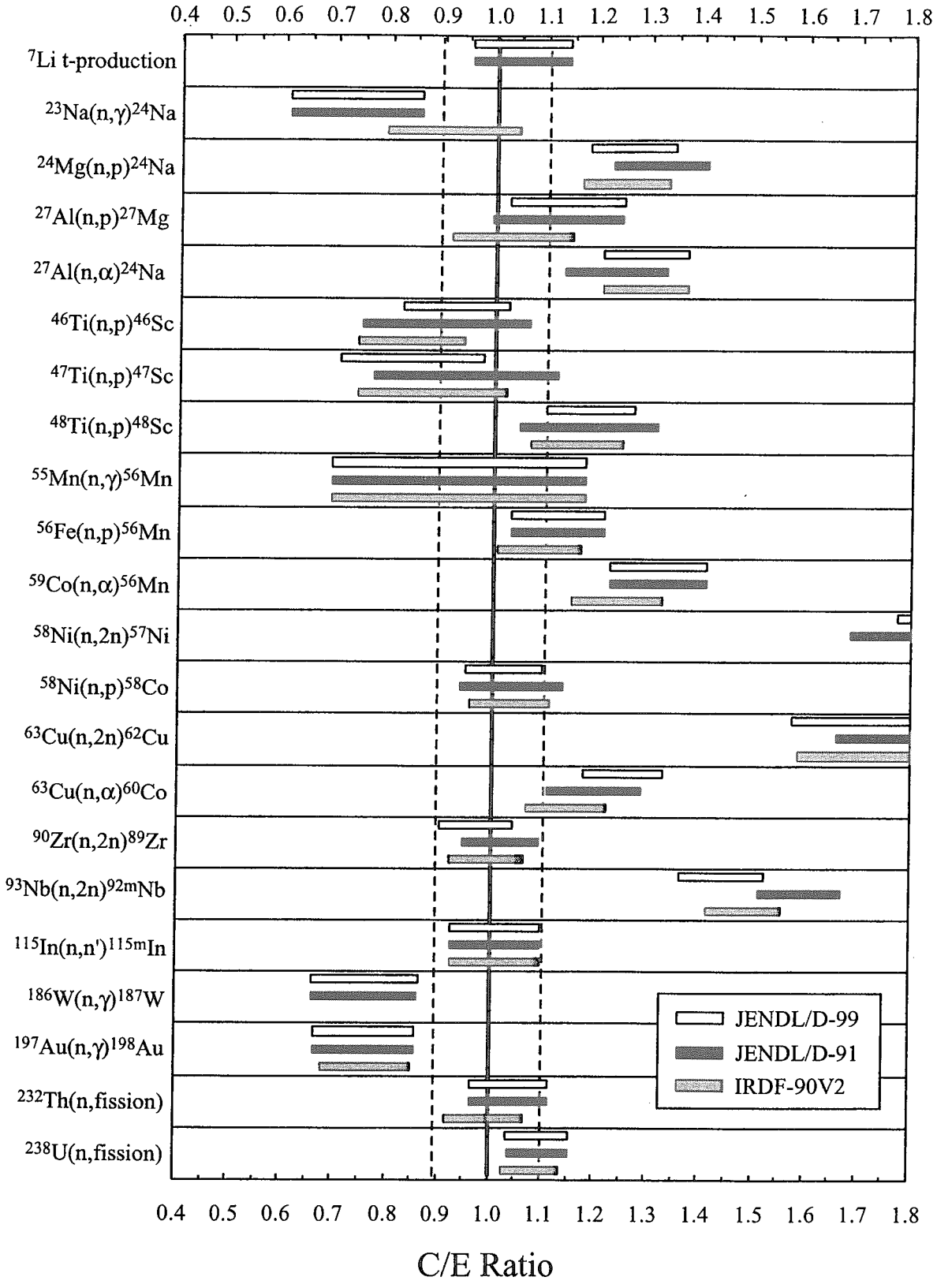

Fig. 5.1.6 C/E range of spectrum-averaged cross sections for YAYOI spectrum. Center and width of each rectangle show C/E and uncertainty, respectively.

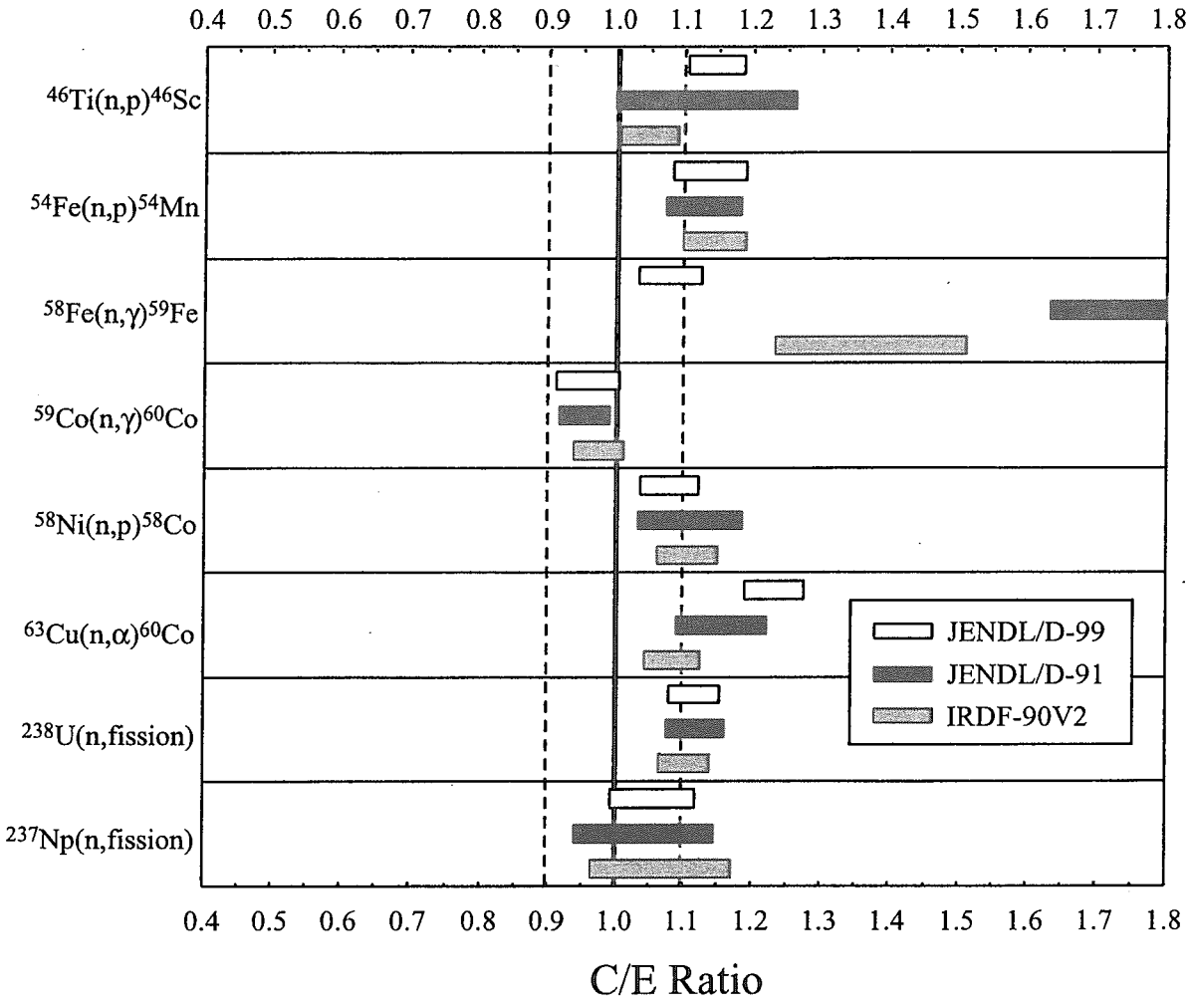

Fig. 5.1.7 C/E range of spectrum-averaged cross sections for JOYO integral test. Center and width of each rectangle show C/E and uncertainty, respectively.

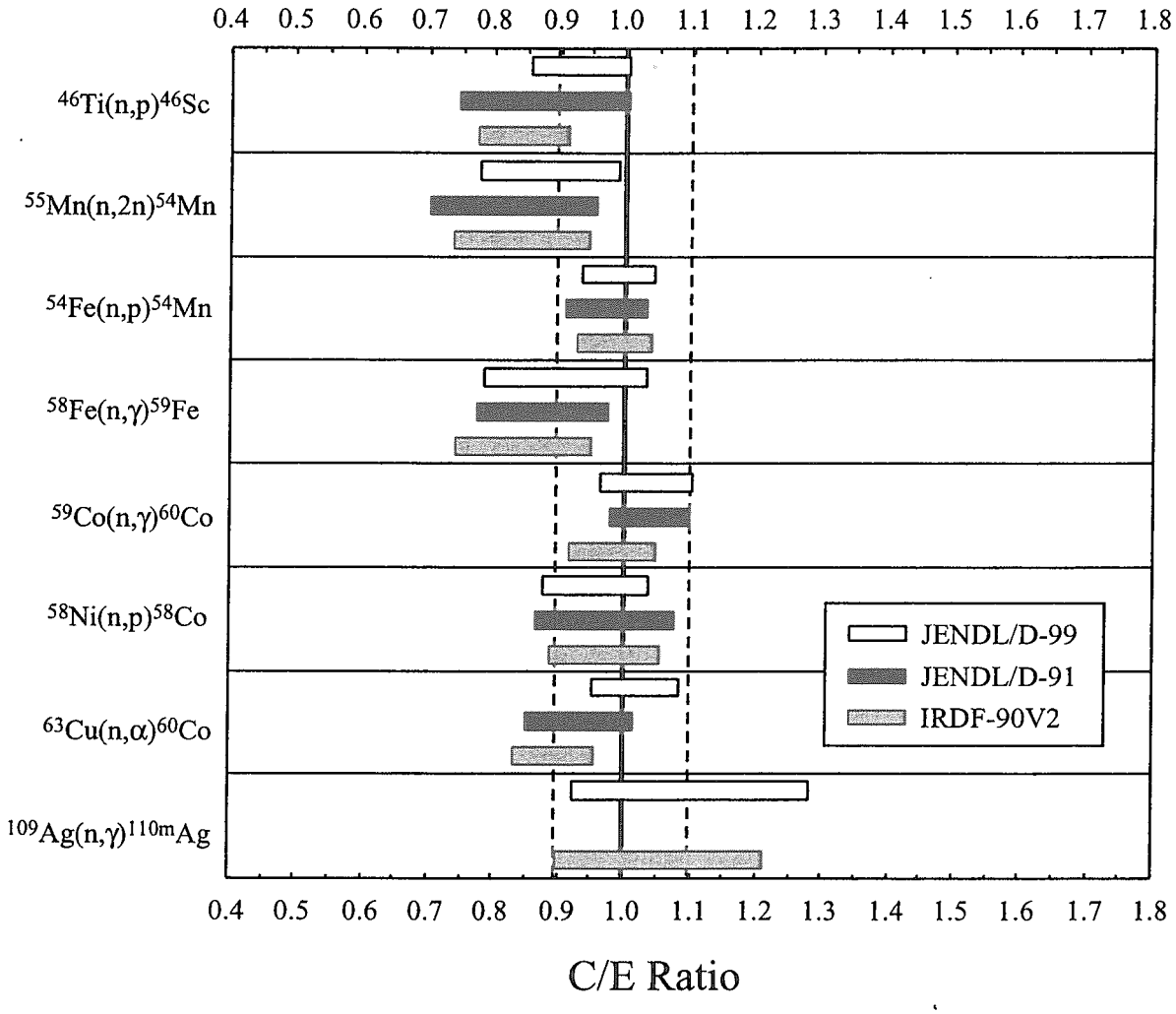

Fig. 5.1.8 C/E range of spectrum-averaged cross sections for JMTR integral test. Center and width of each rectangle show C/E and uncertainty, respectively.

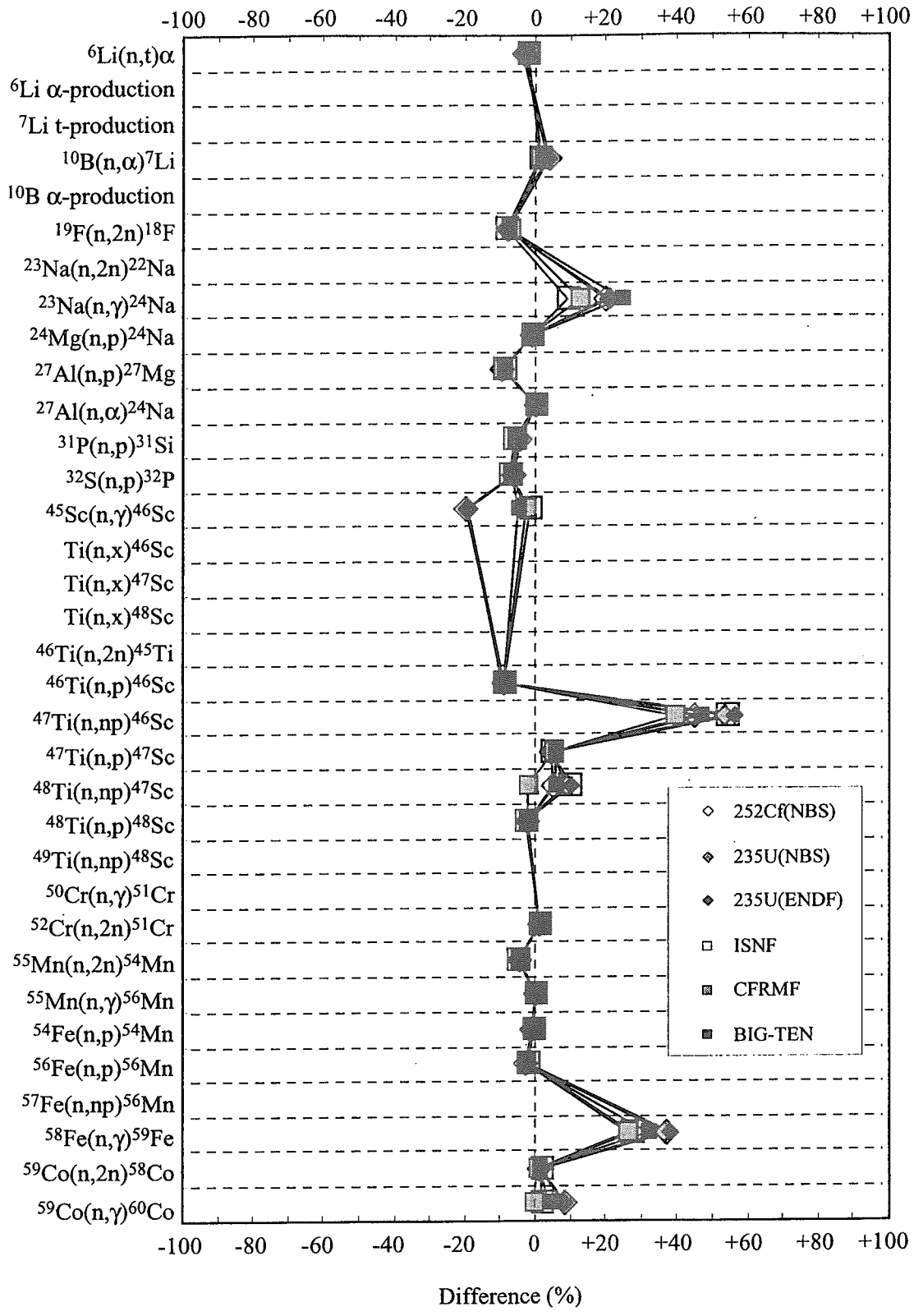

Fig. 5.1.9 Comparison of the spectrum-averaged cross sections by the relation of (IRDF-90V2 – JENDL/D-99)/JENDL/D-99.

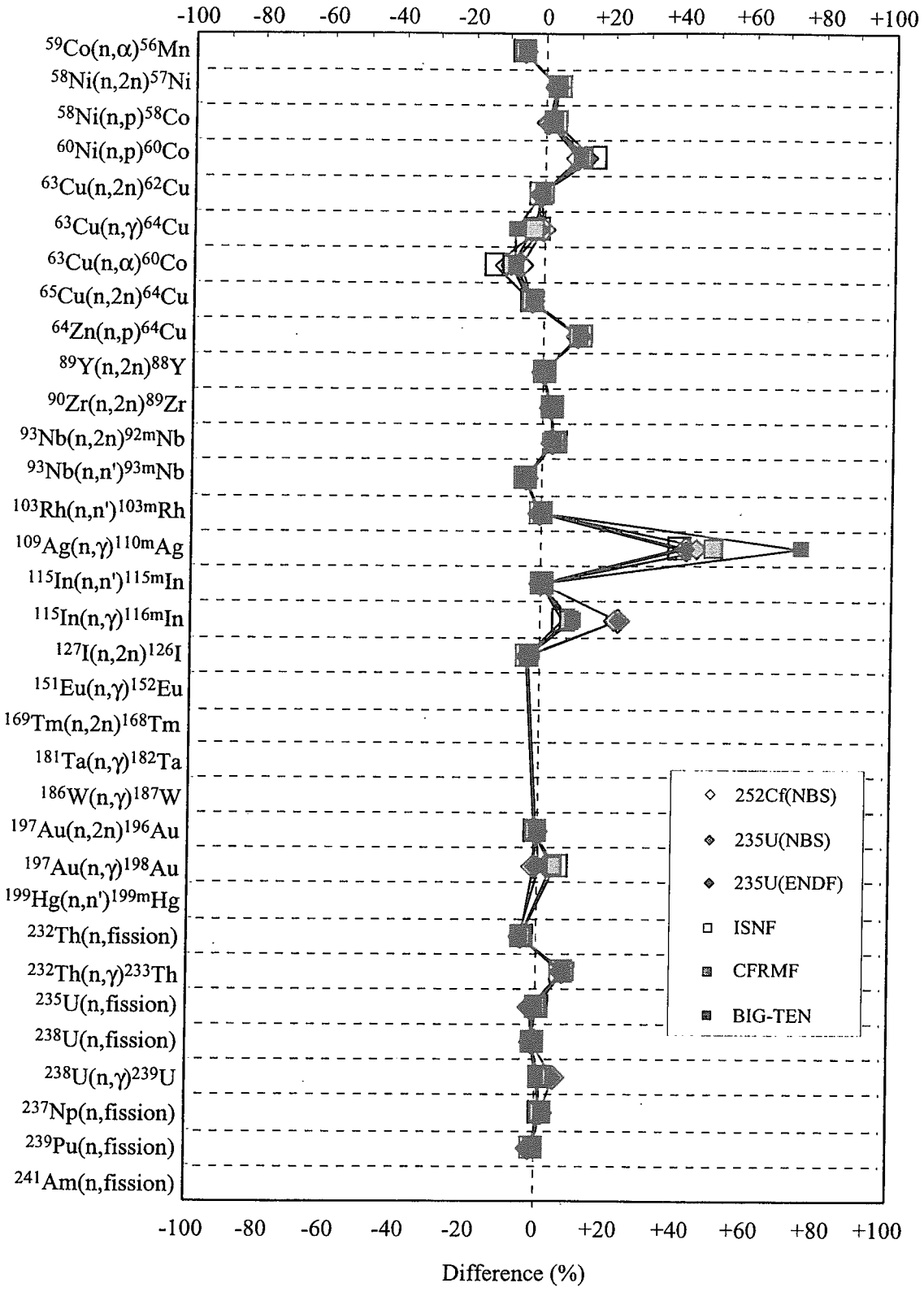

Fig. 5.1.9 (Continued)

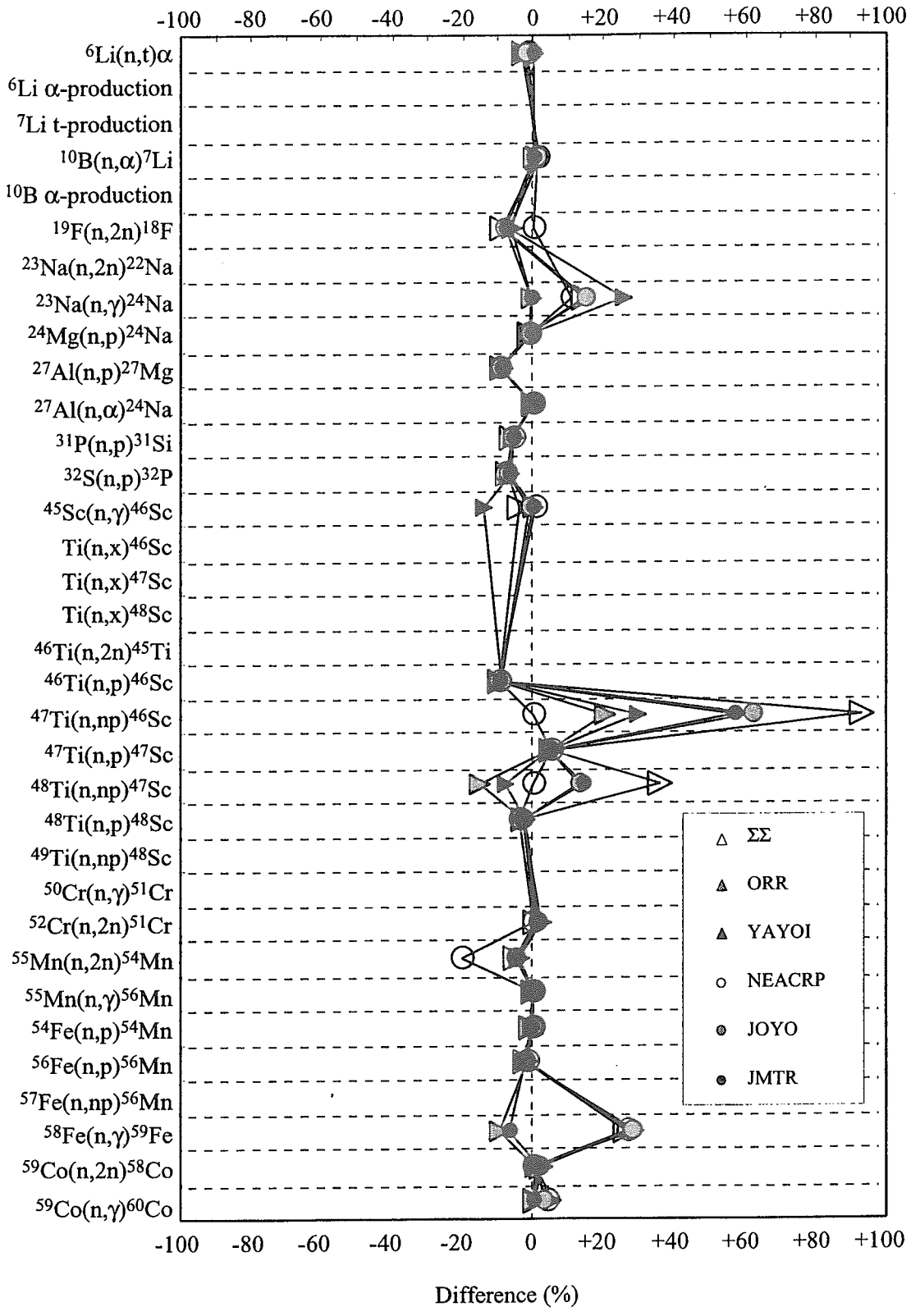

Fig. 5.1.9 (Continued)

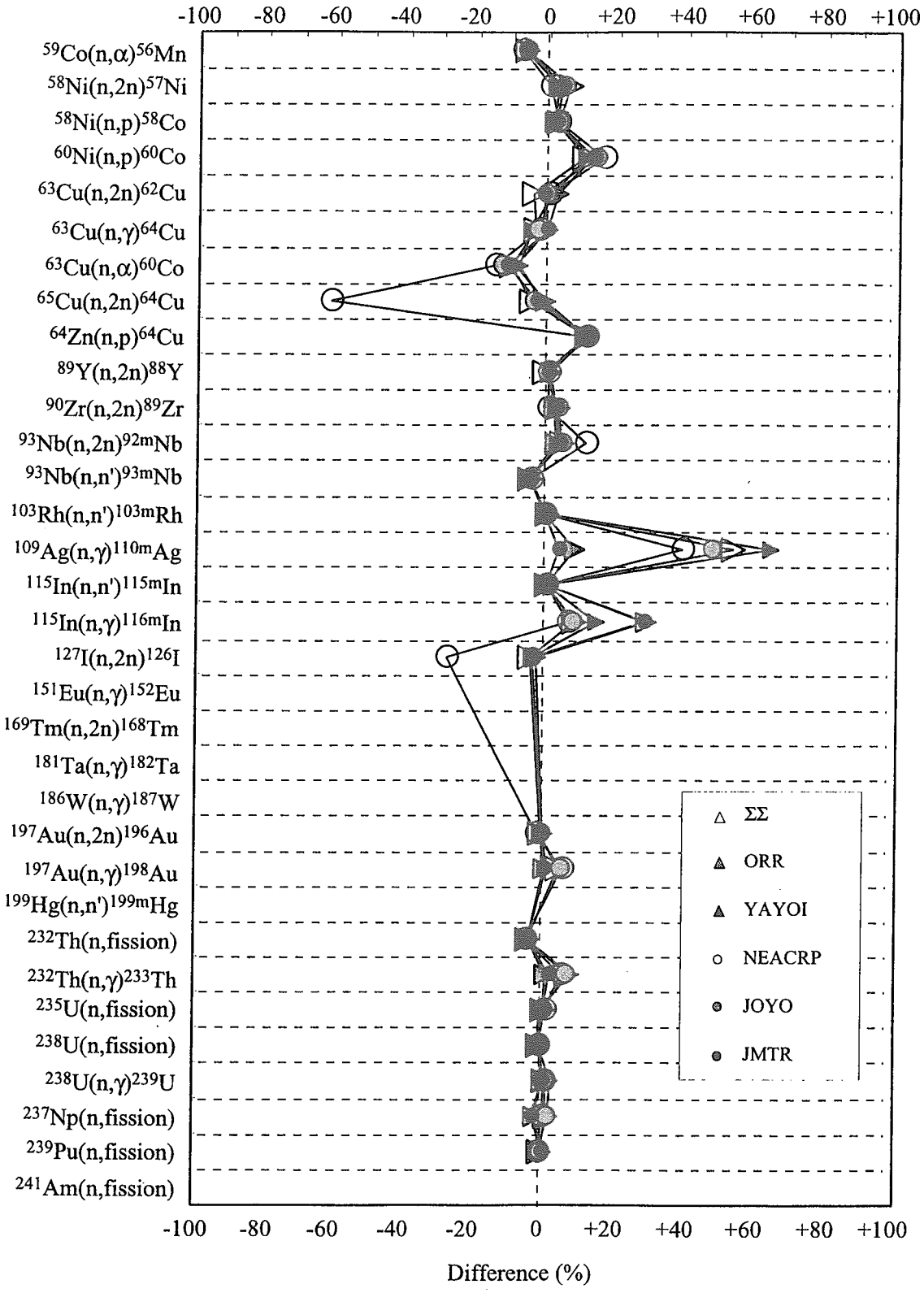

Fig. 5.1.9 (Continued)

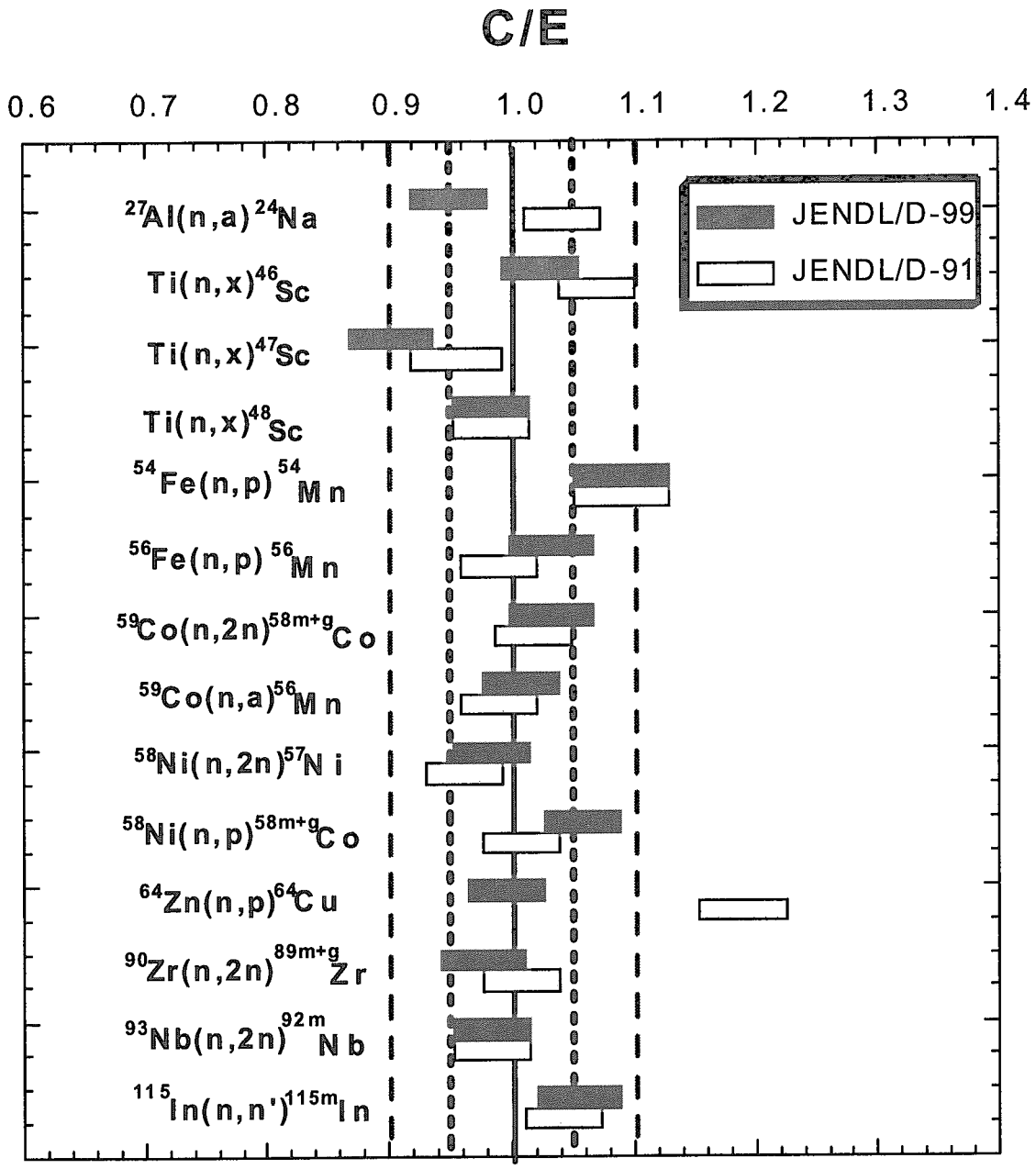

Fig. 5.2.1 C/E range of reaction rates for spectrum A.
Center and width of each rectangle show C/E and uncertainty, respectively.

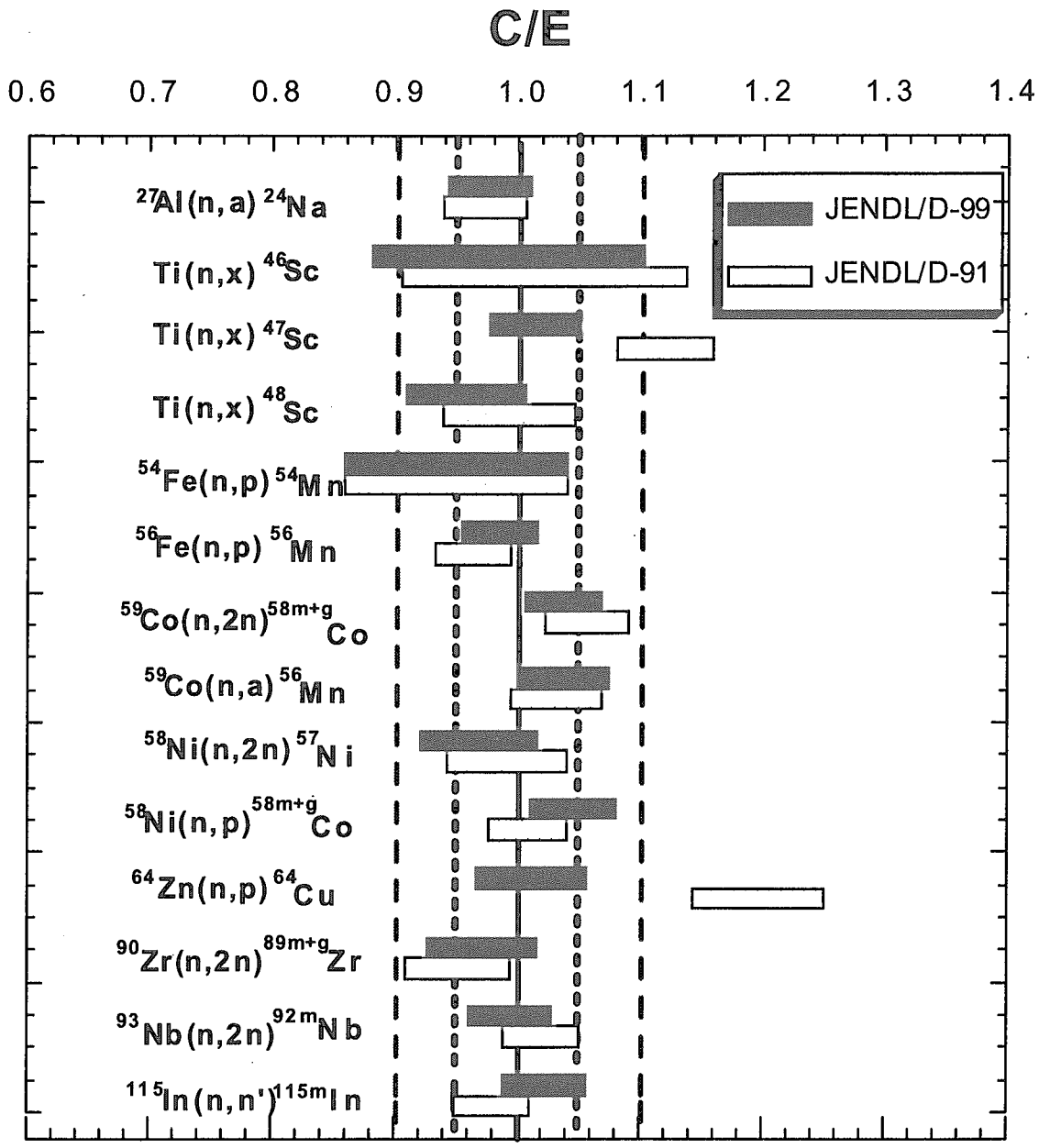

Fig. 5.2.2 C/E range of reaction rates for spectrum B.
Center and width of each rectangle show C/E and uncertainty, respectively.

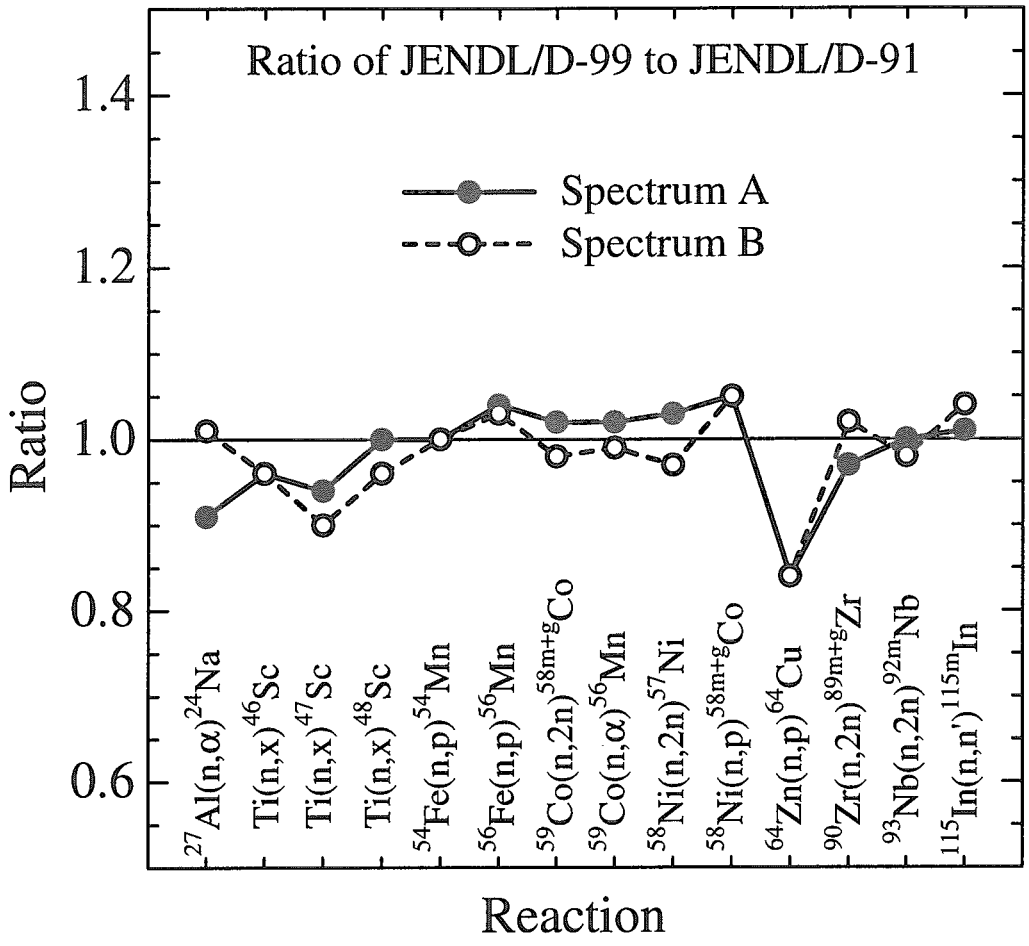

Fig. 5.2.3 Ratios of reaction rates of JENDL/D-99 to those of JENDL/D-91.

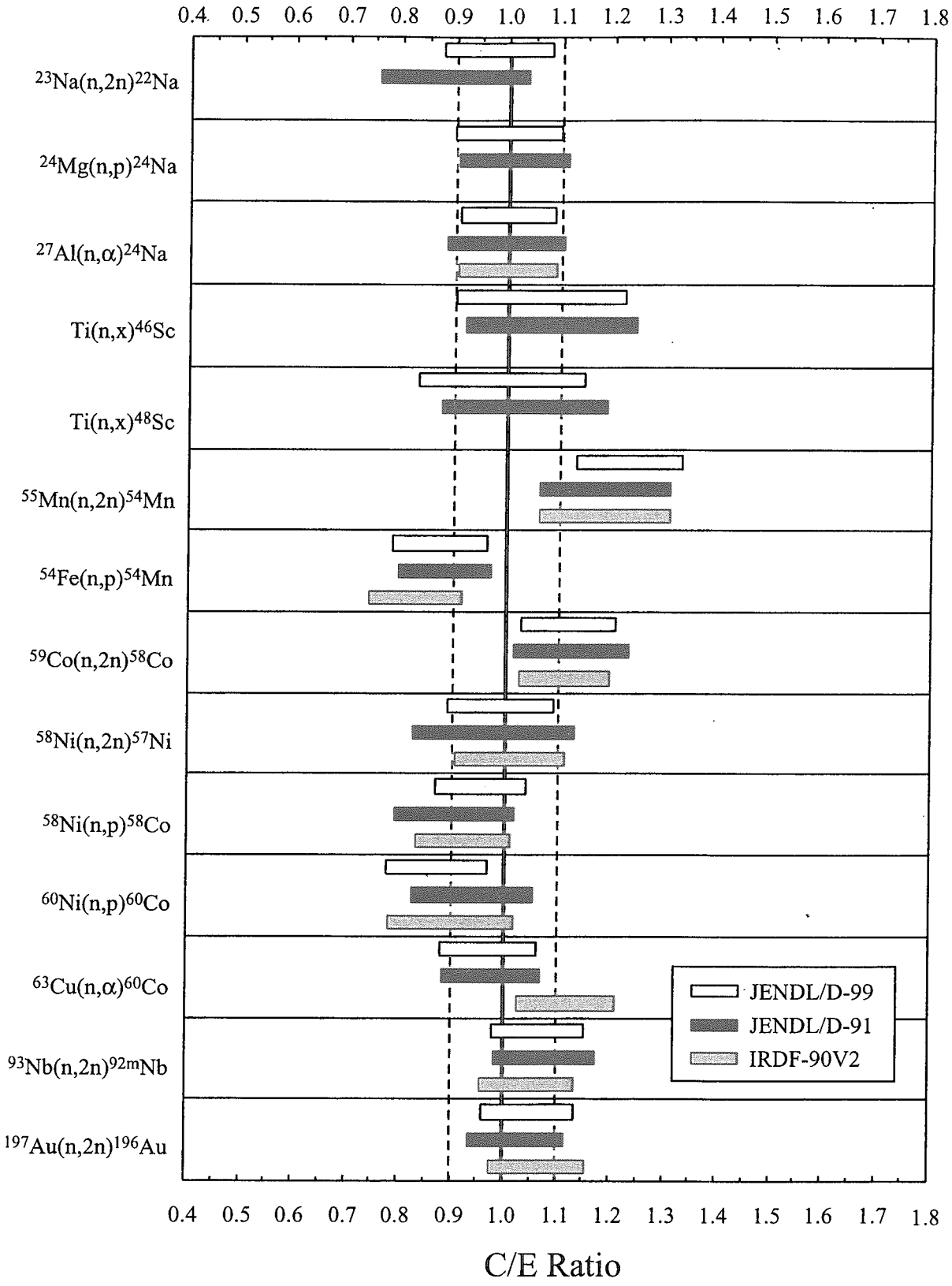

Fig. 5.2.4 C/E range of spectrum-averaged cross sections for Li(d,n) neutron field. Center and width of each rectangle show C/E and uncertainty, respectively.

Appendix Graphs of Dosimetry Cross Sections

In this Appendix, the cross sections stored in the JENDL Dosimetry File 99 are shown in a graphical form. As described in 2.3, there are two kinds of files: point-wise file and group-wise file. Here, only the group-wise data are shown together with their one standard deviation and data in IRDF-90V2. In the graphs, *thick red lines* represent the JENDL Dosimetry File 99, *thin red lines* their standard deviation and *blue dashed line* IRDF-90V2. The IRDF-90V2 curve is not illustrated if the data are either unavailable for a certain reaction or completely equivalent to the JENDL/D-99 data.

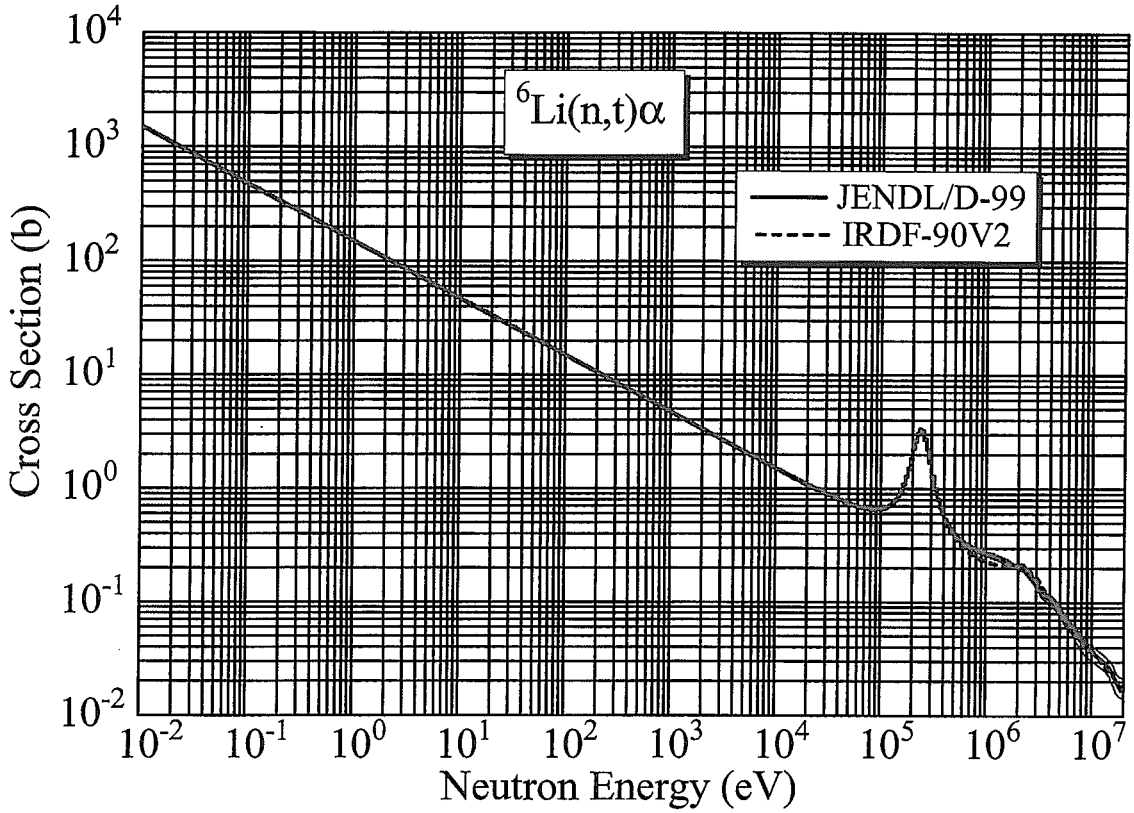

Fig. A.1 ^{6}Li(n, t)α cross section.

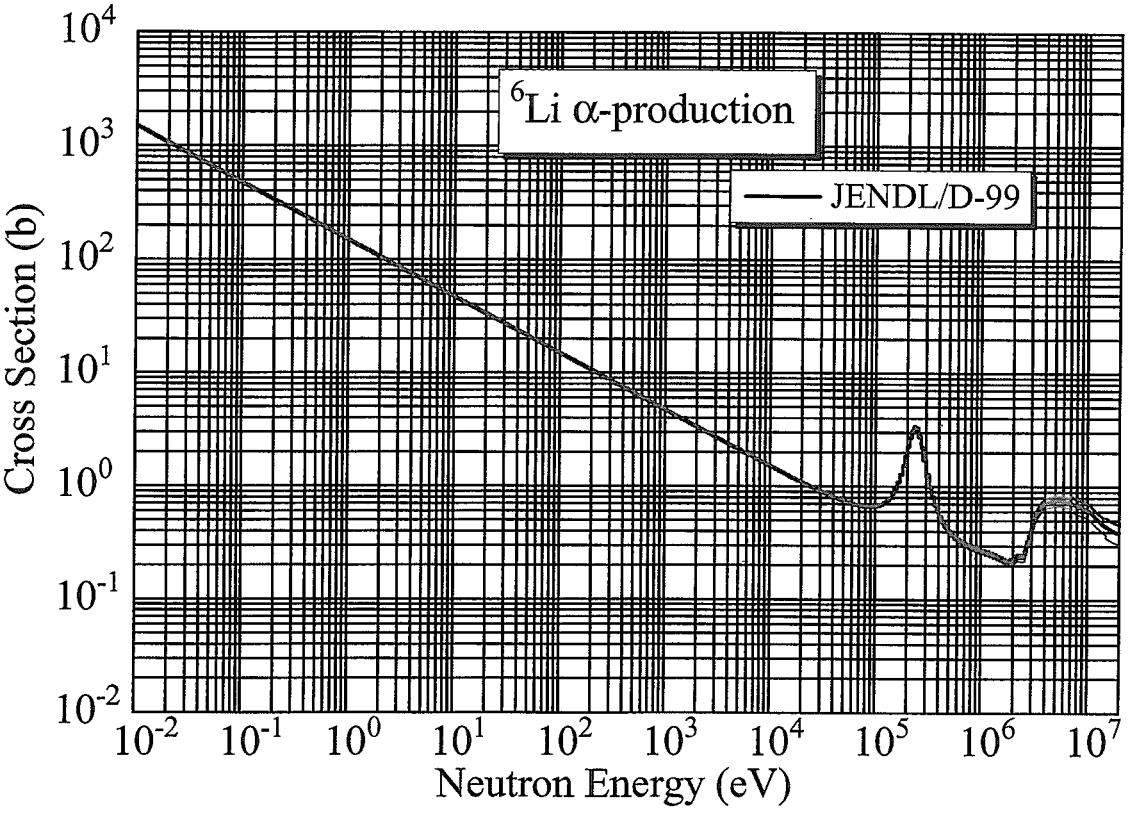

Fig. A.2 ^{6}Li α- production cross section.

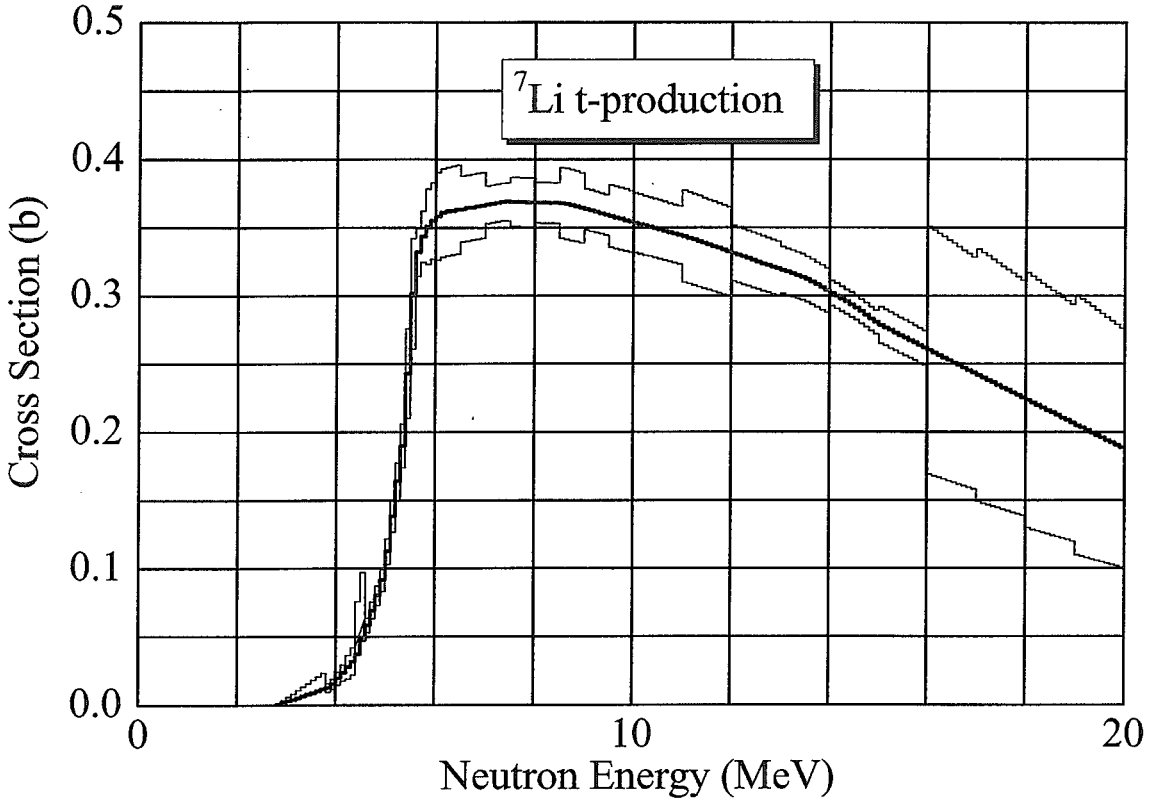

Fig. A.3 ^{7}Li t- production cross section.

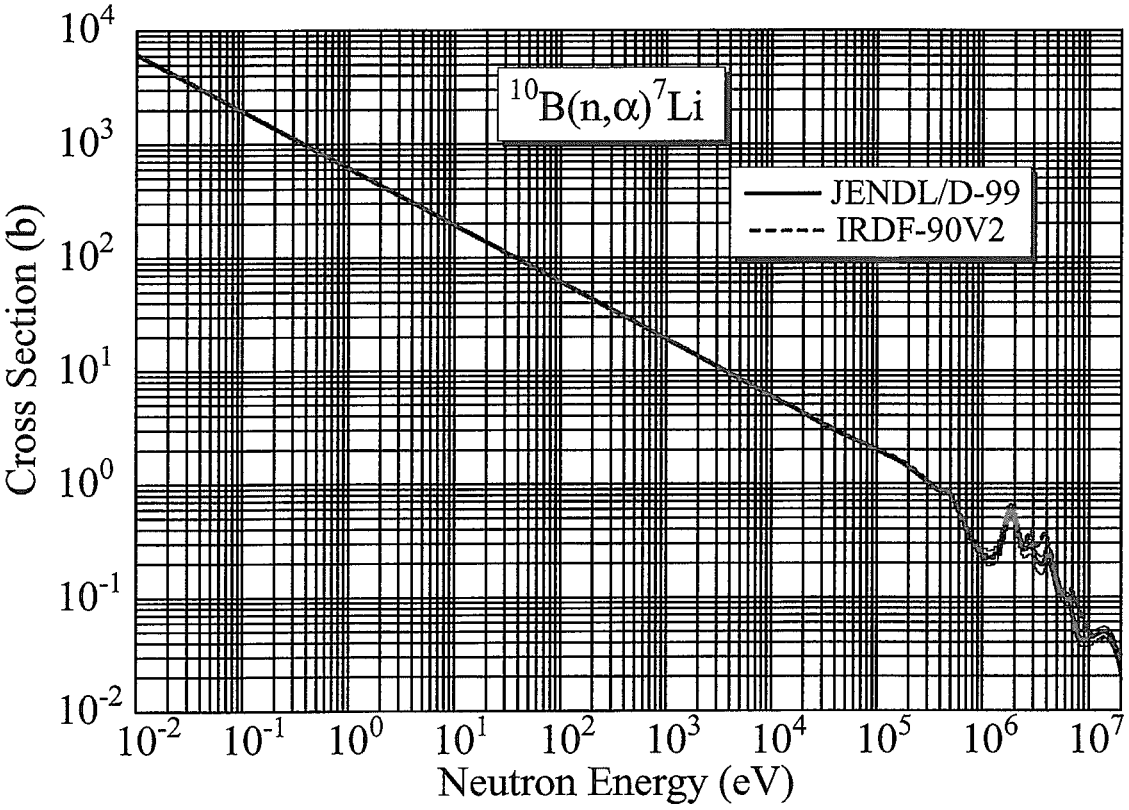

Fig. A.4 ^{10}B(n, α)^{7}Li cross section

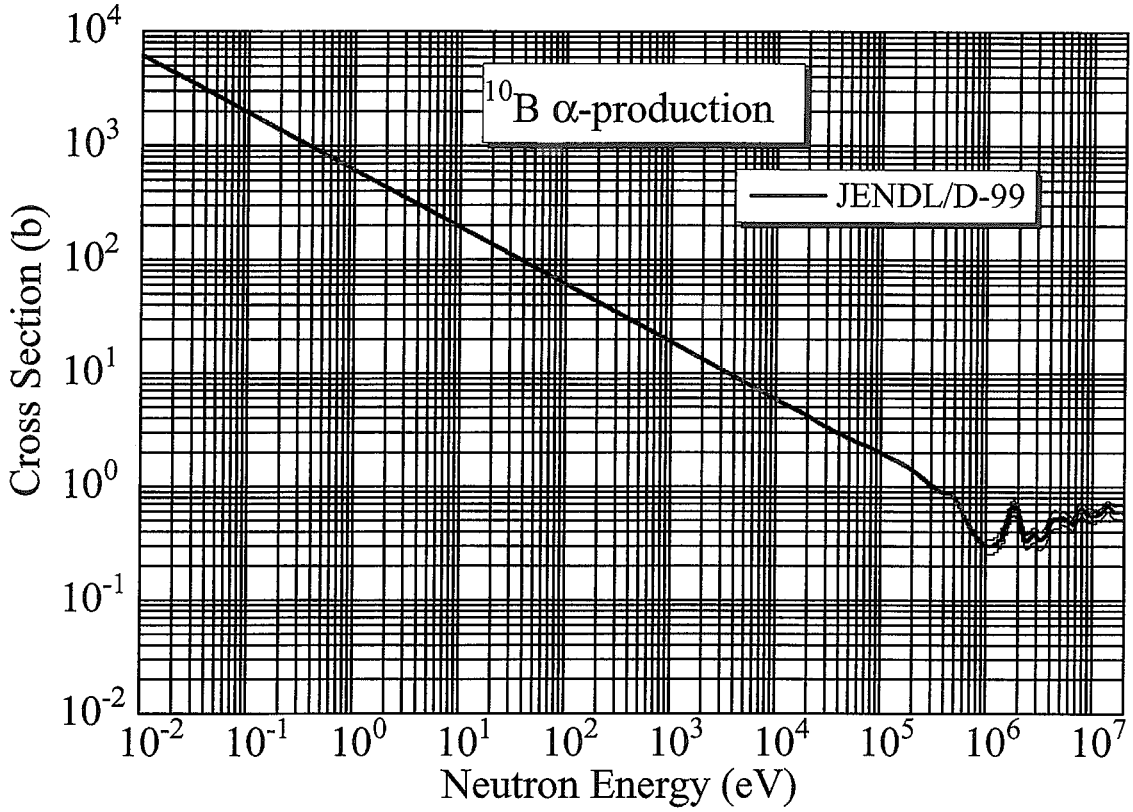

Fig. A.5 ^{10}B α-production cross section.

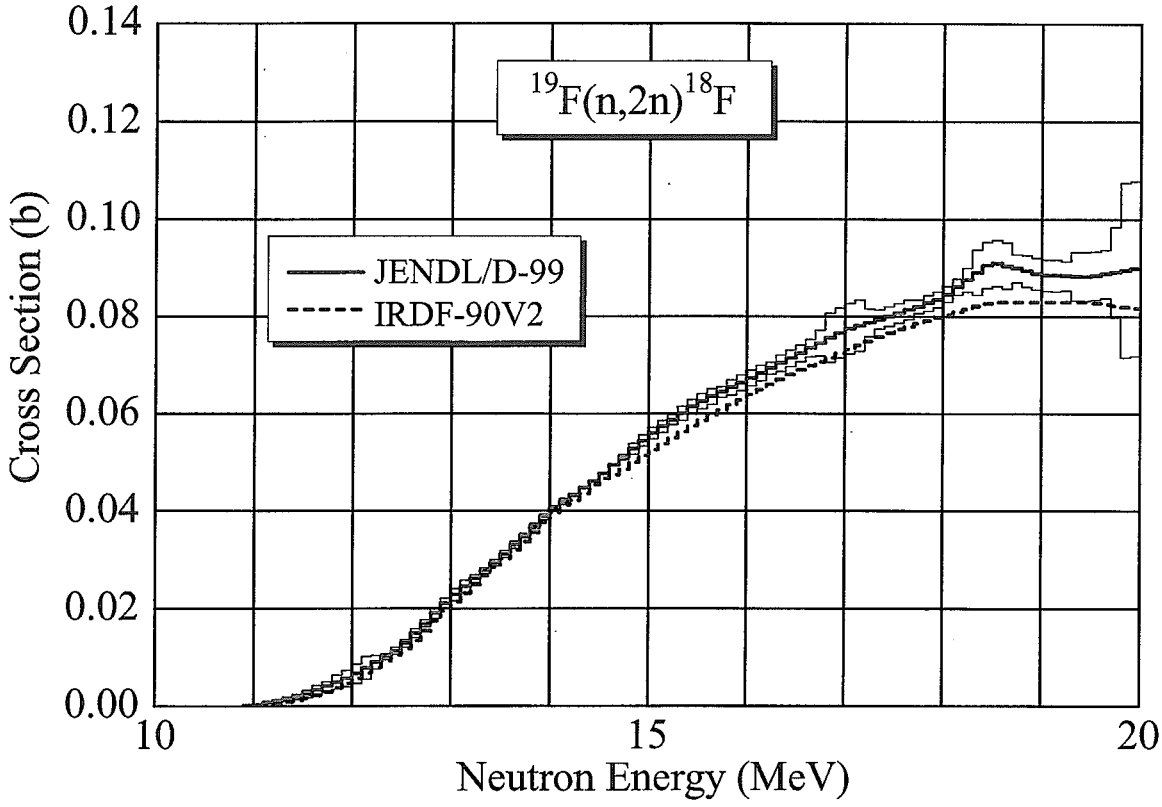

Fig. A.6 ^{19}F(n, 2n)^{18}F cross section.

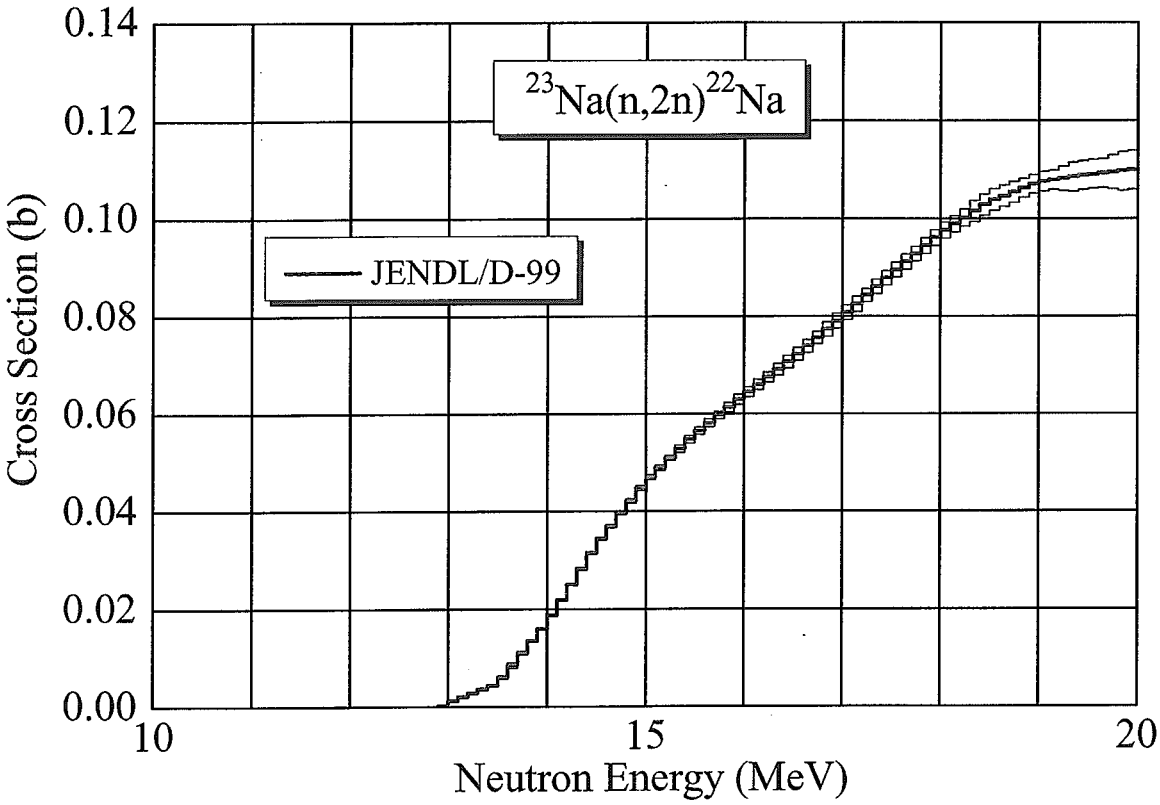

Fig. A.7 ^{23}Na(n, 2n)^{22}Na cross section.

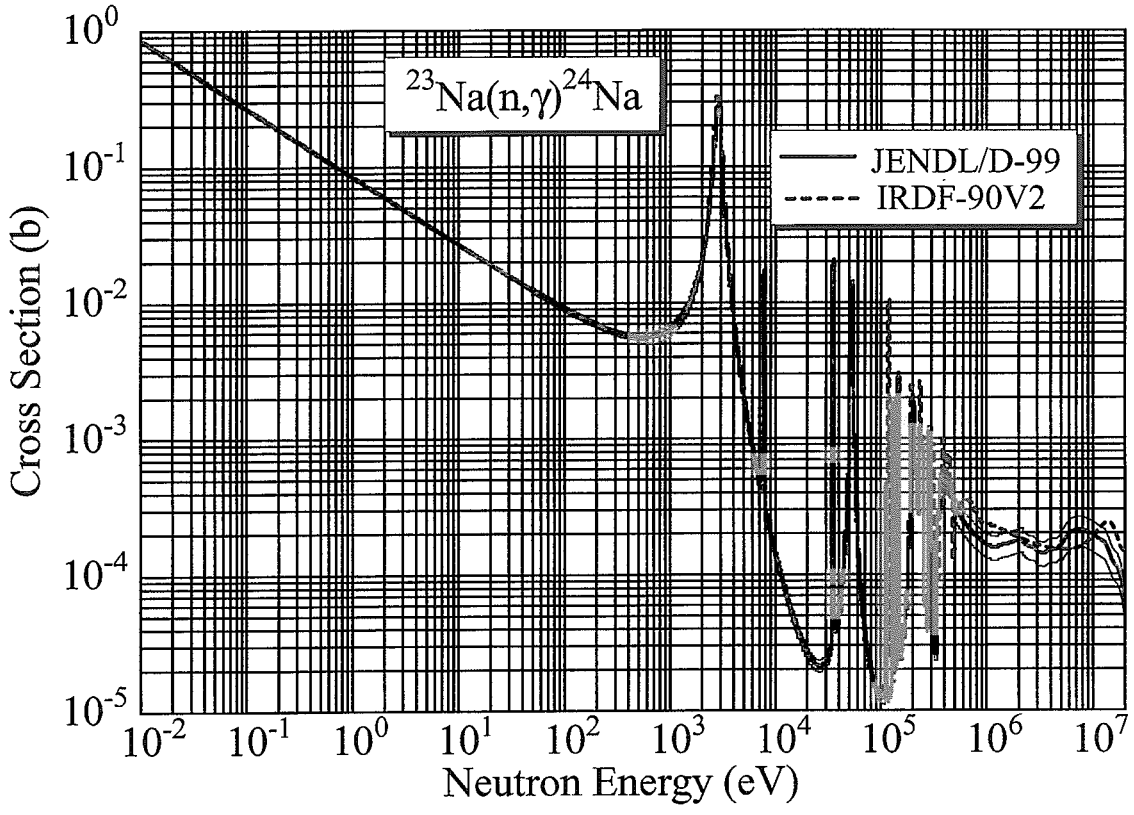

Fig. A.8 ^{23}Na(n, γ)^{24}Na cross section.

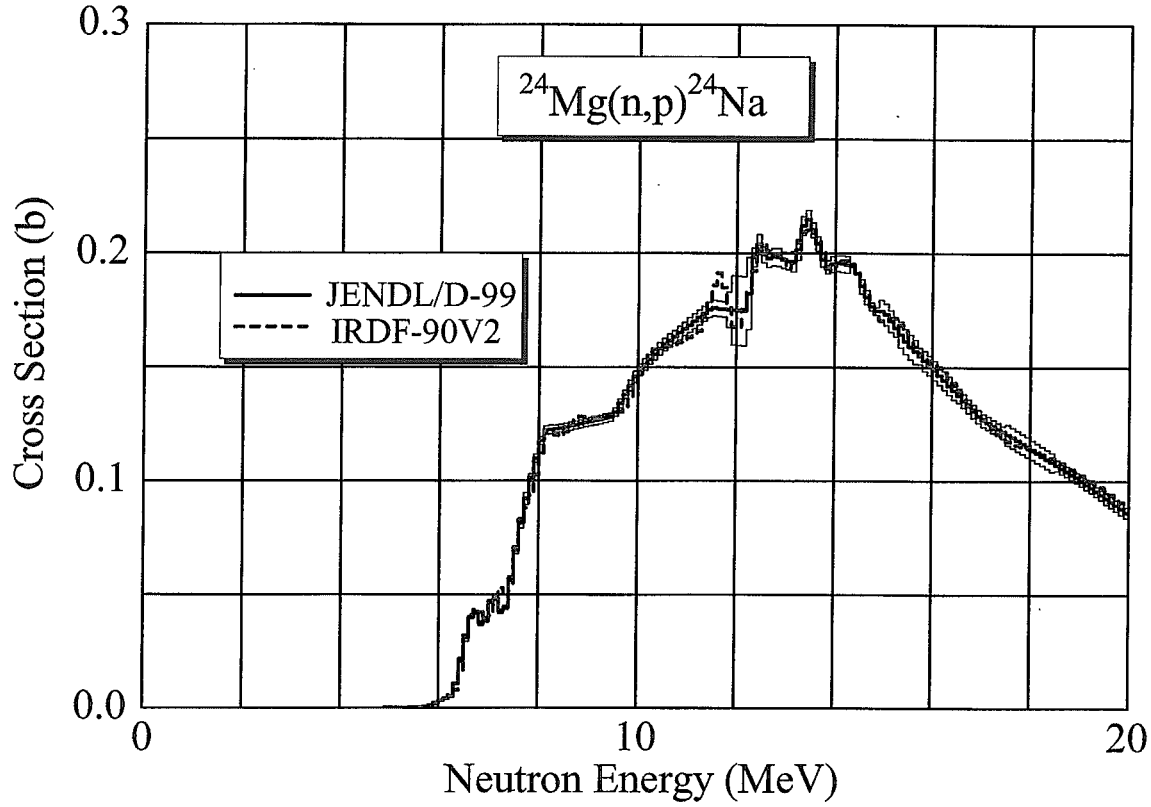

Fig. A.9 ^{24}Mg(n, p)^{24}Na cross section.

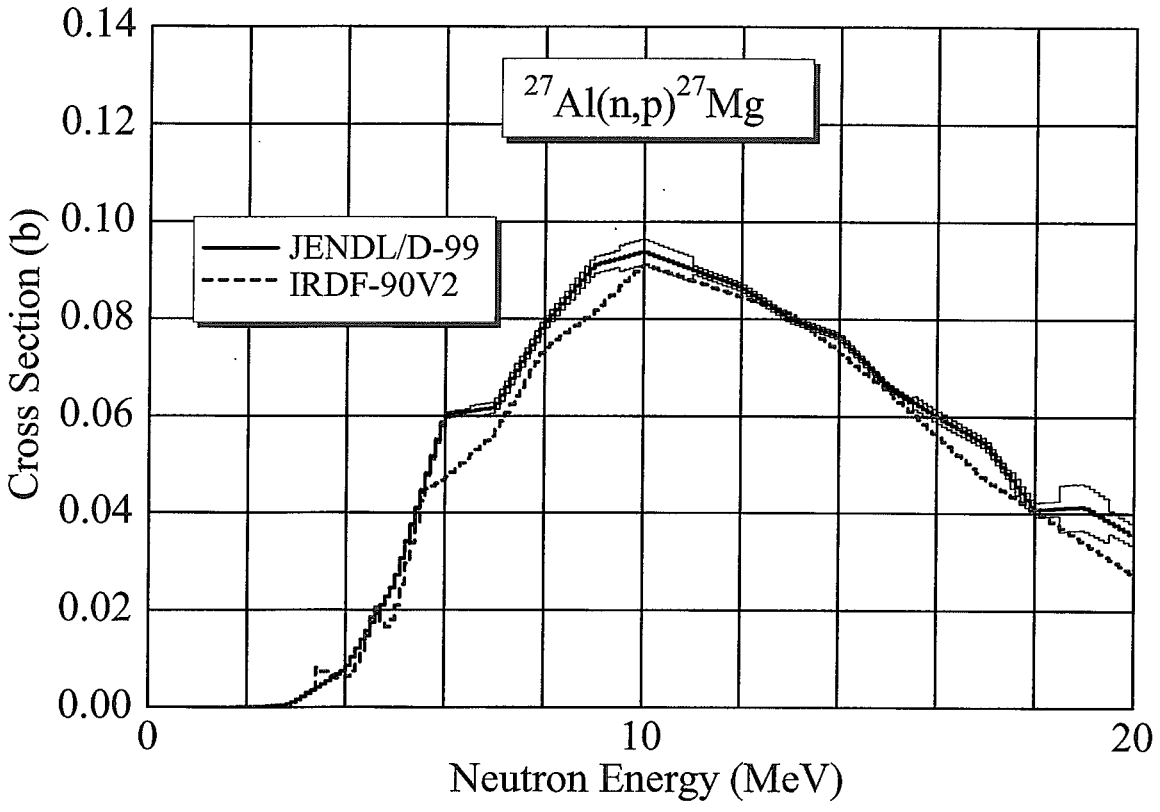

Fig. A.10 ^{27}Al(n, p)^{27}Mg cross section.

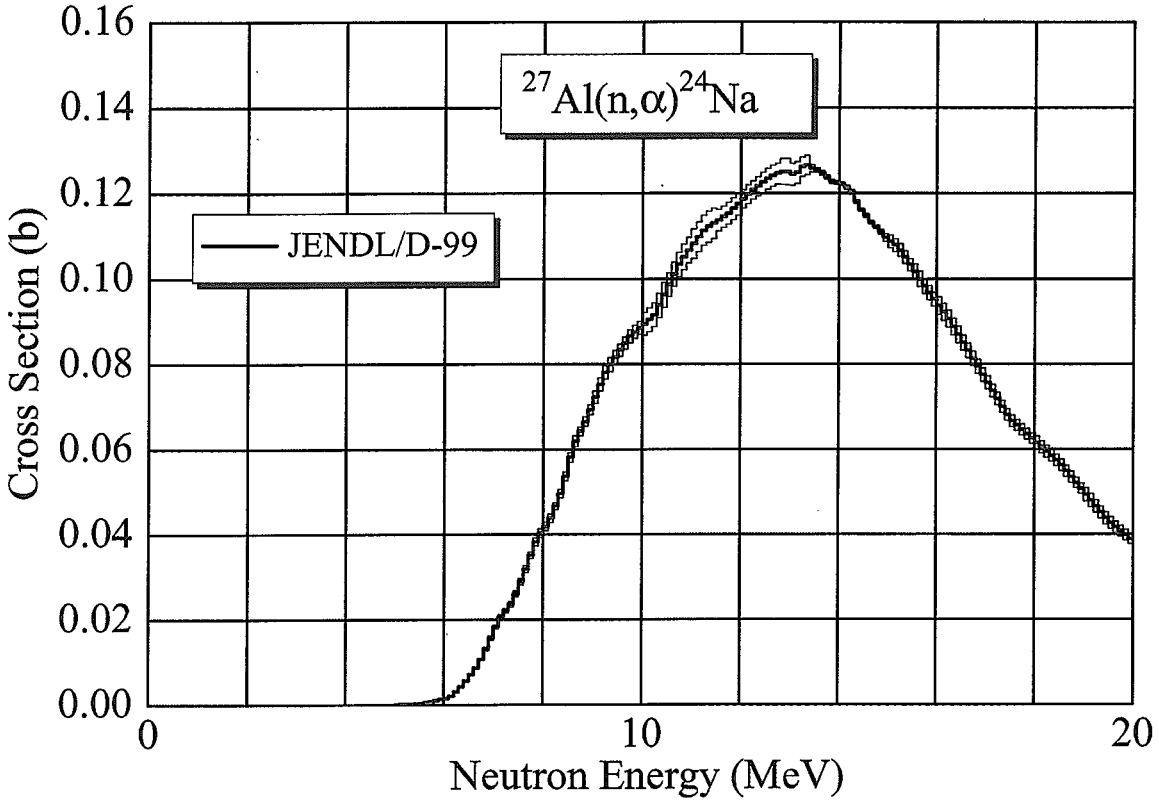

Fig. A.11 ^{27}Al(n, α)^{24}Na cross section.

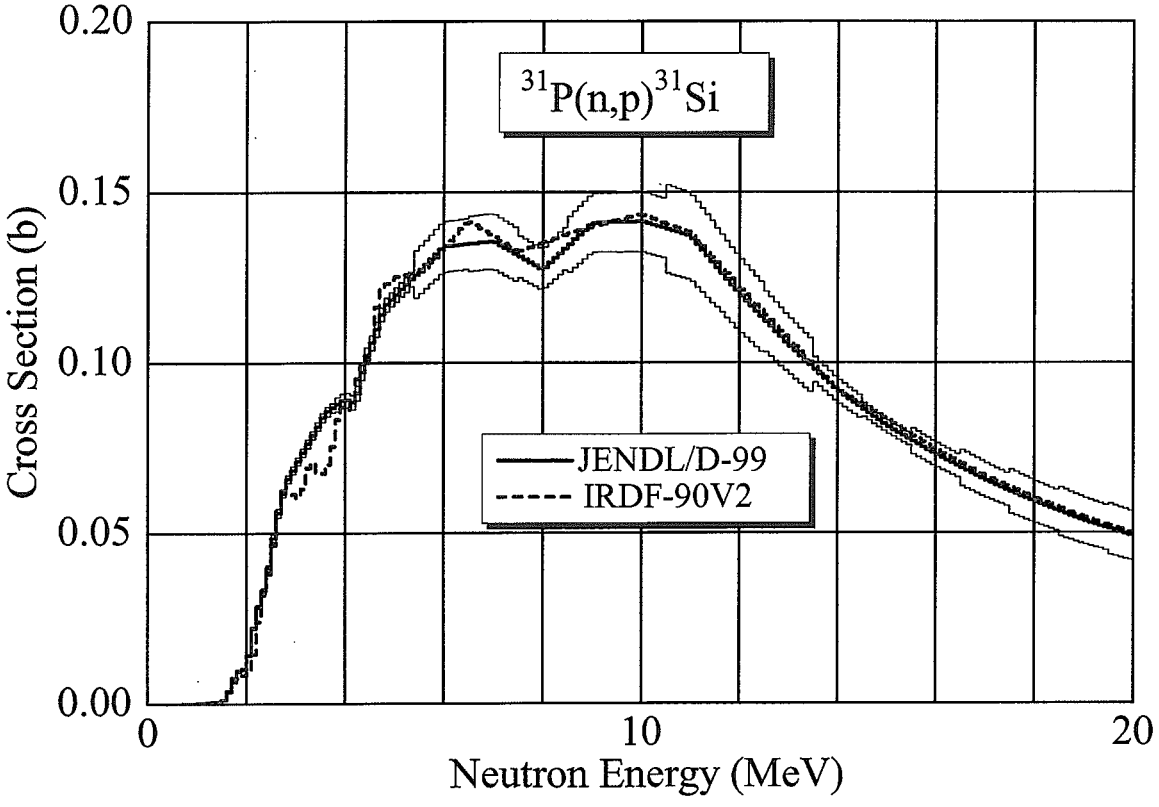

Fig. A.12 ^{31}P(n, p)^{31}Si cross section.

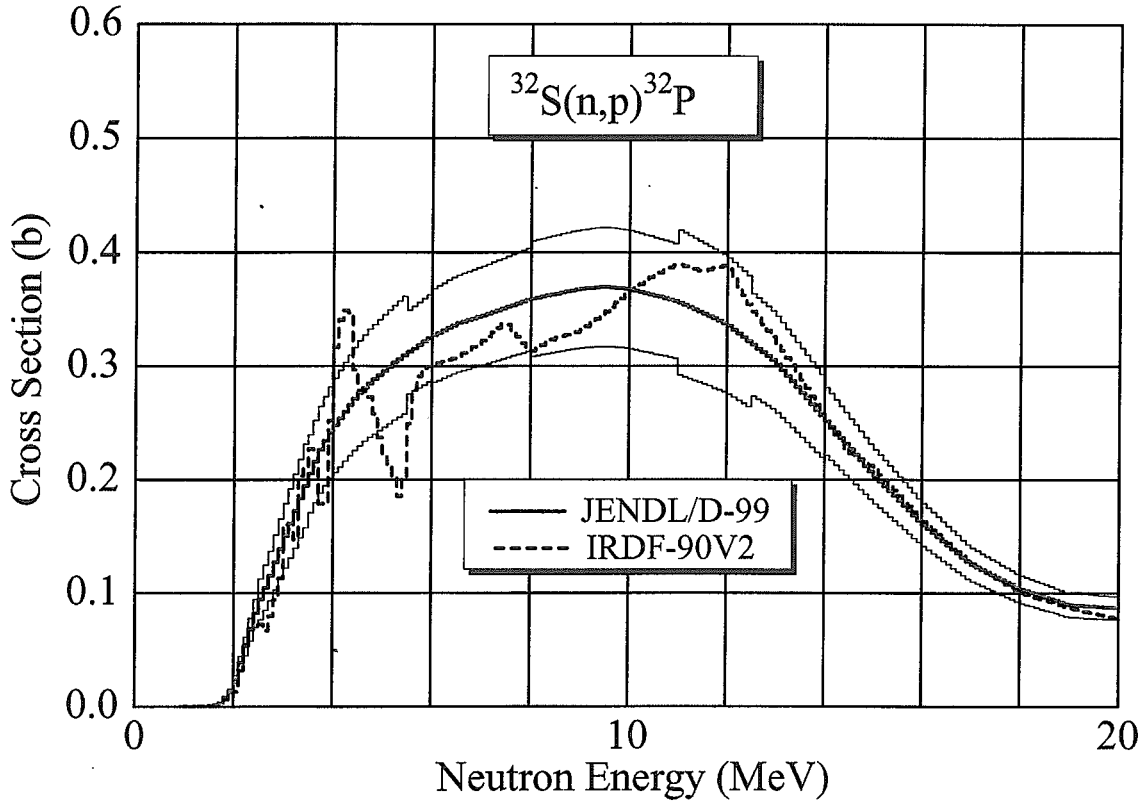

Fig. A.13 $^{32}S(n, p)^{32}P$ cross section.

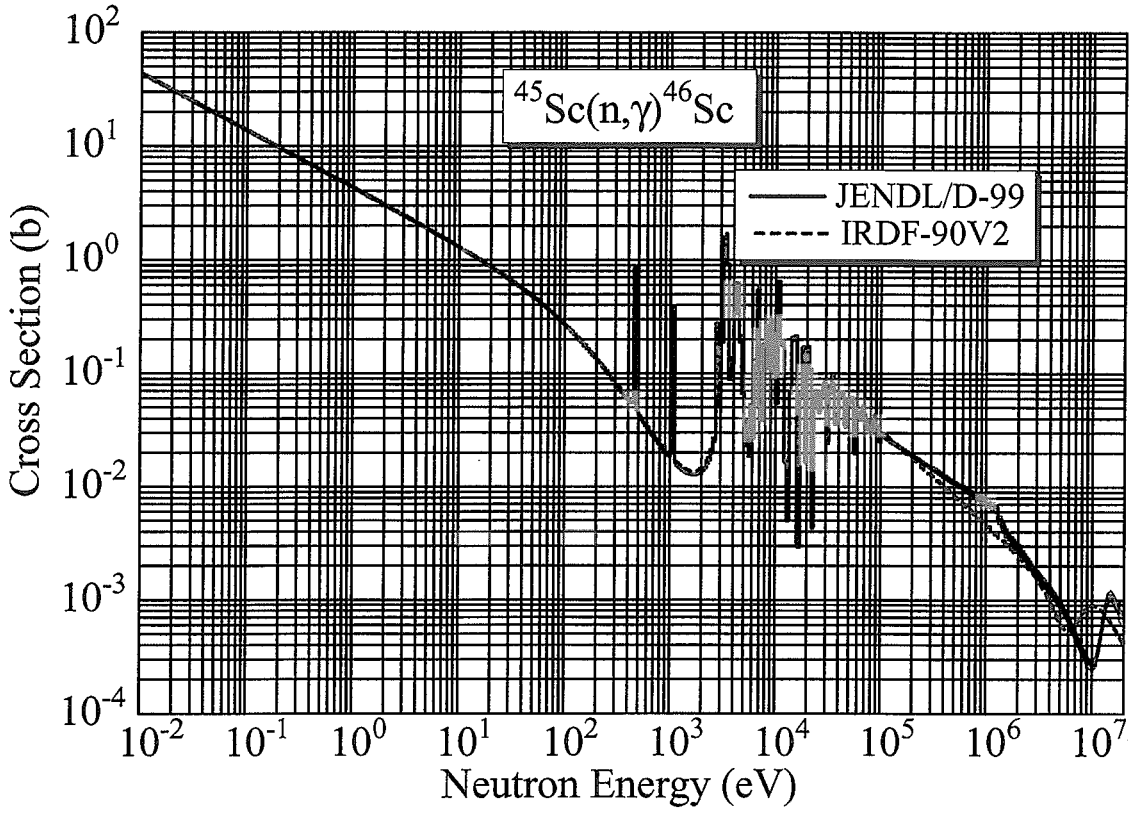

Fig. A.14 $^{45}Sc(n, \gamma)^{46}Sc$ cross section.

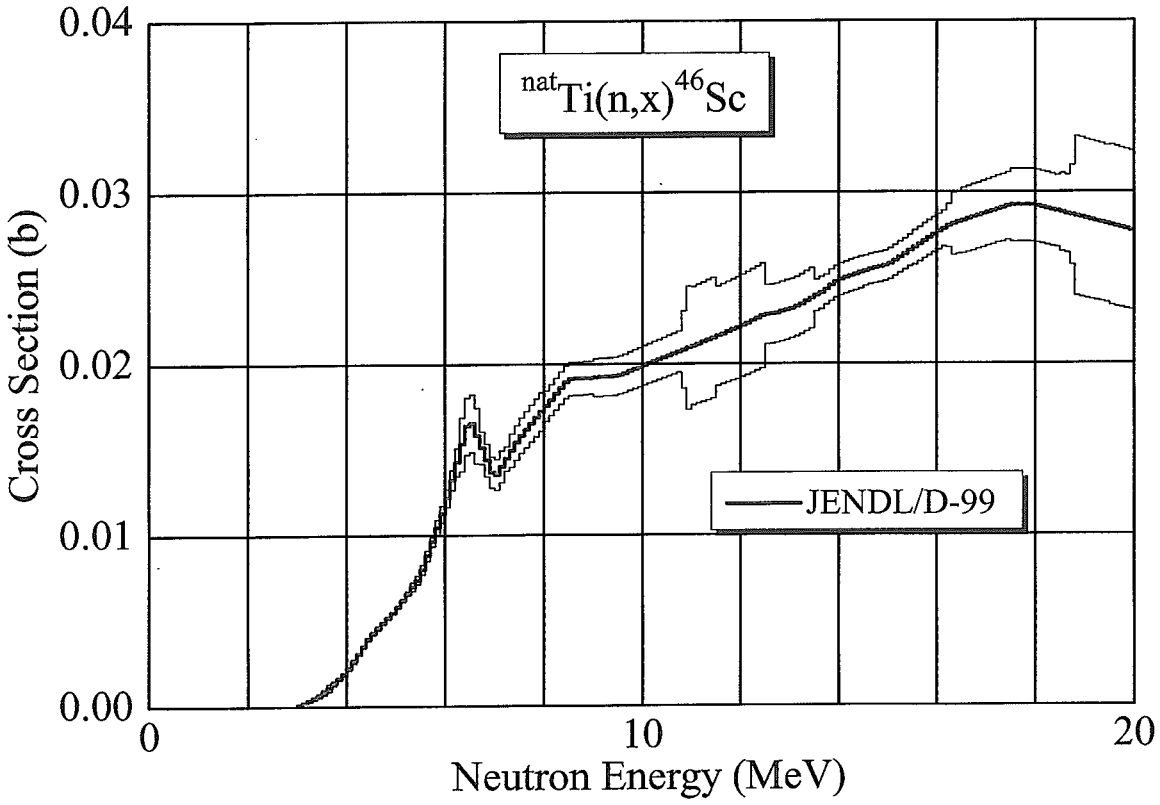

Fig. A.15 ^{nat}Ti(n, x)^{46}Sc cross section.

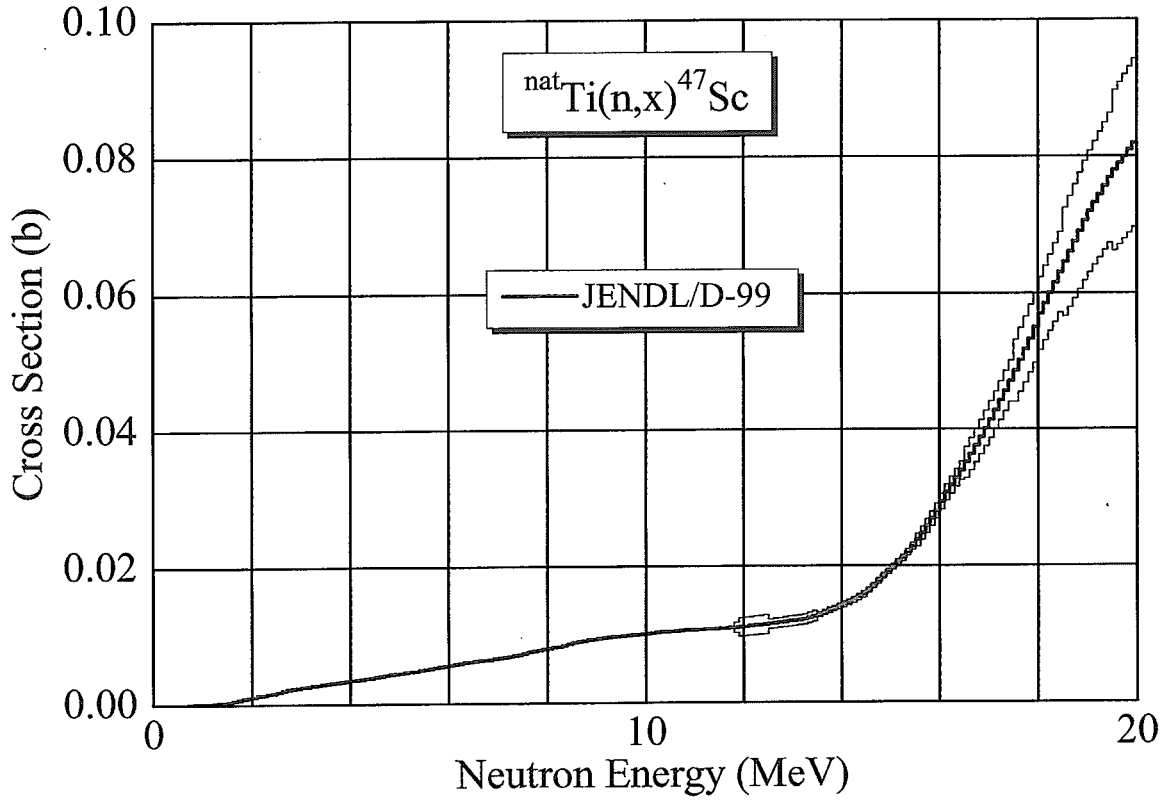

Fig. A.16 ^{nat}Ti(n, x)^{47}Sc cross section.

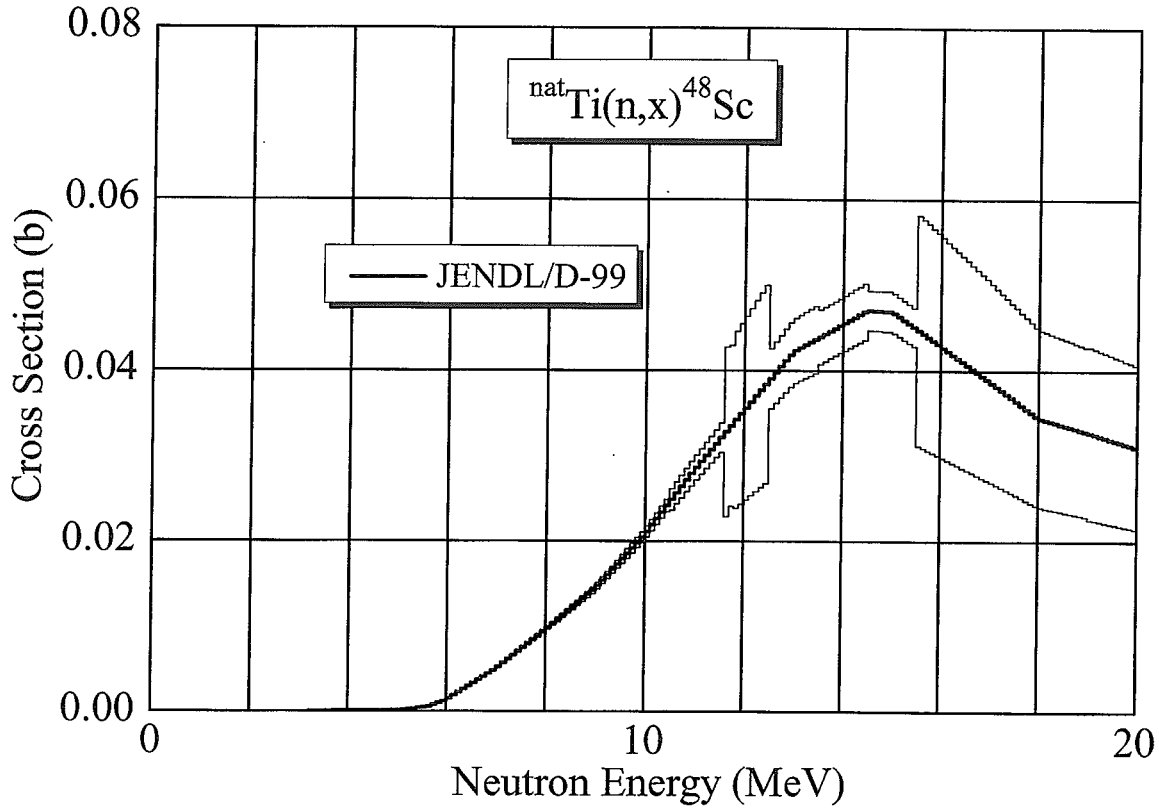

Fig. A.17 ^{nat}Ti(n, x)^{48}Sc cross section.

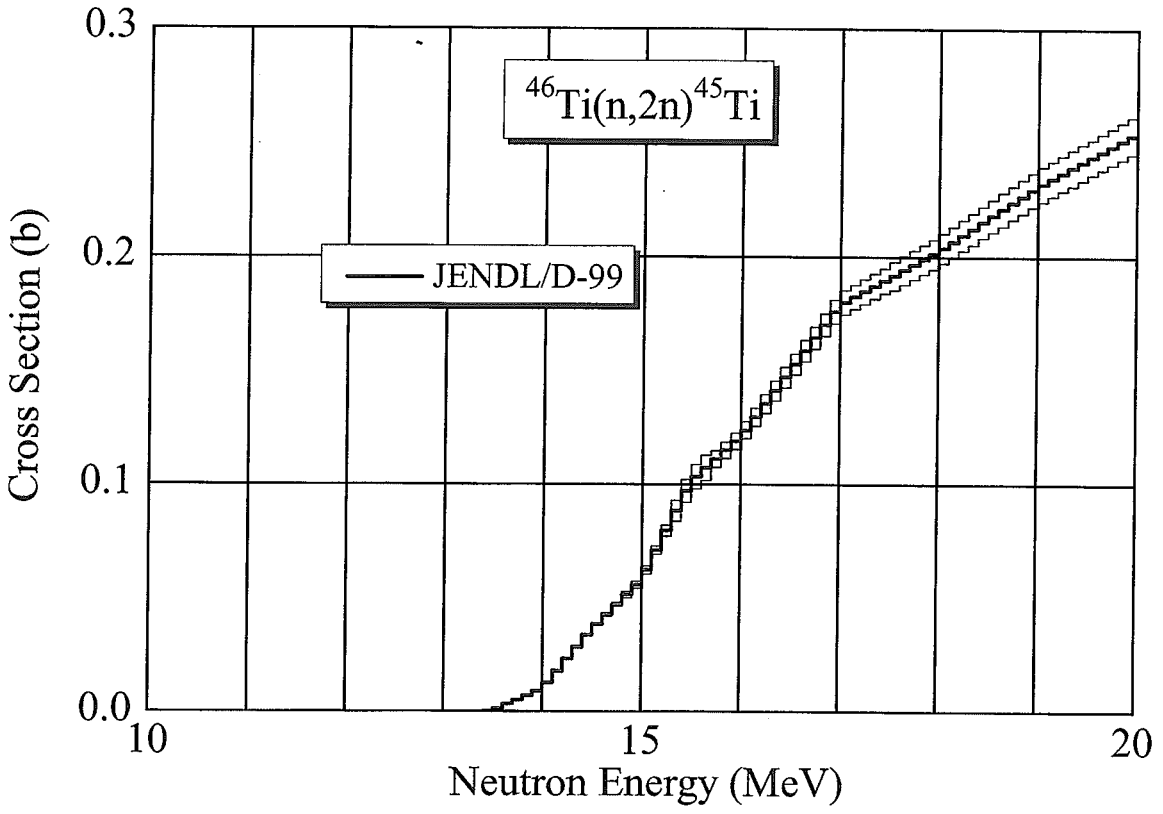

Fig. A.18 ^{46}Ti(n, 2n)^{45}Ti cross section.

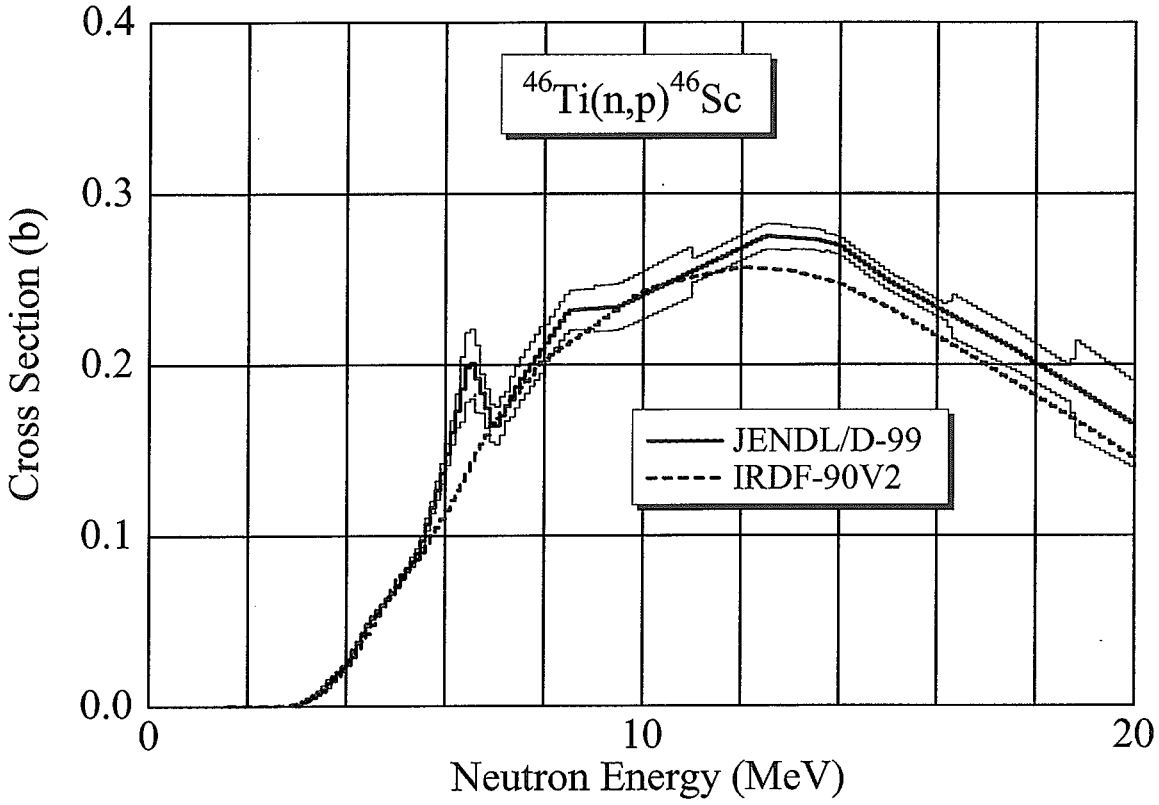

Fig. A.19 ^{46}Ti(n, p)^{46}Sc cross section.

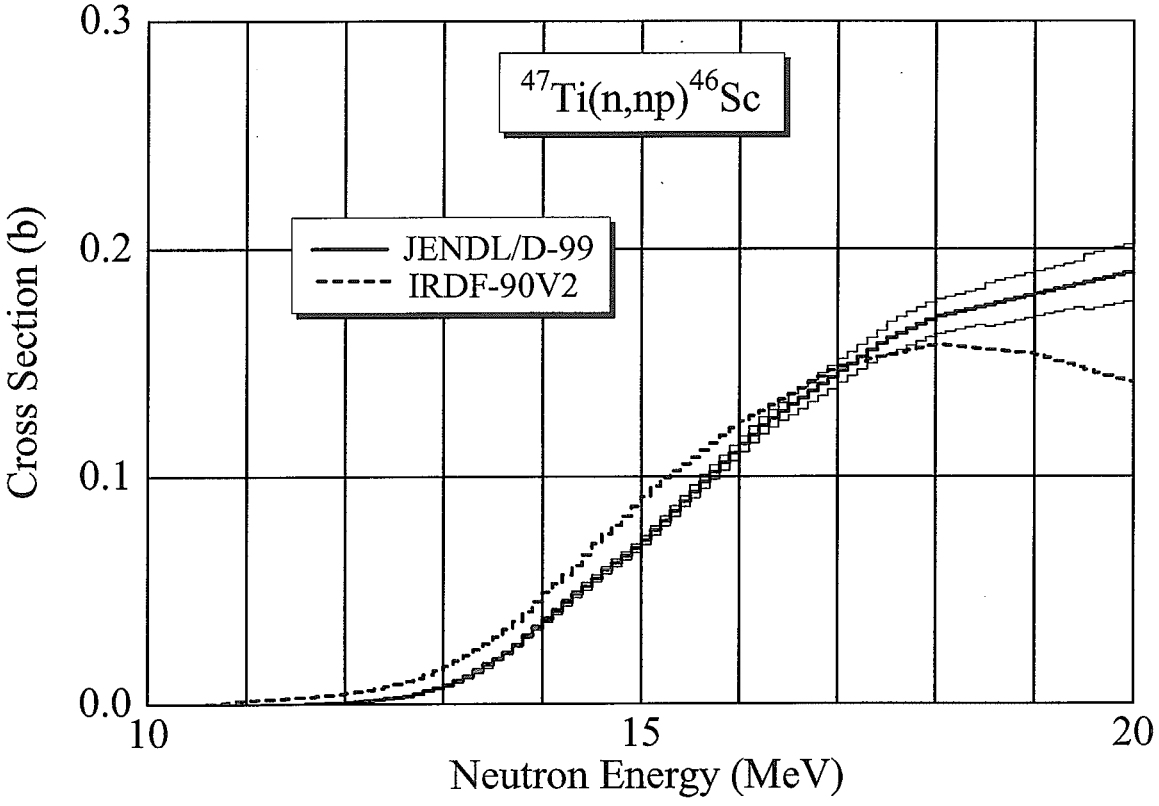

Fig. A.20 ^{47}Ti(n, np)^{46}Sc cross section.

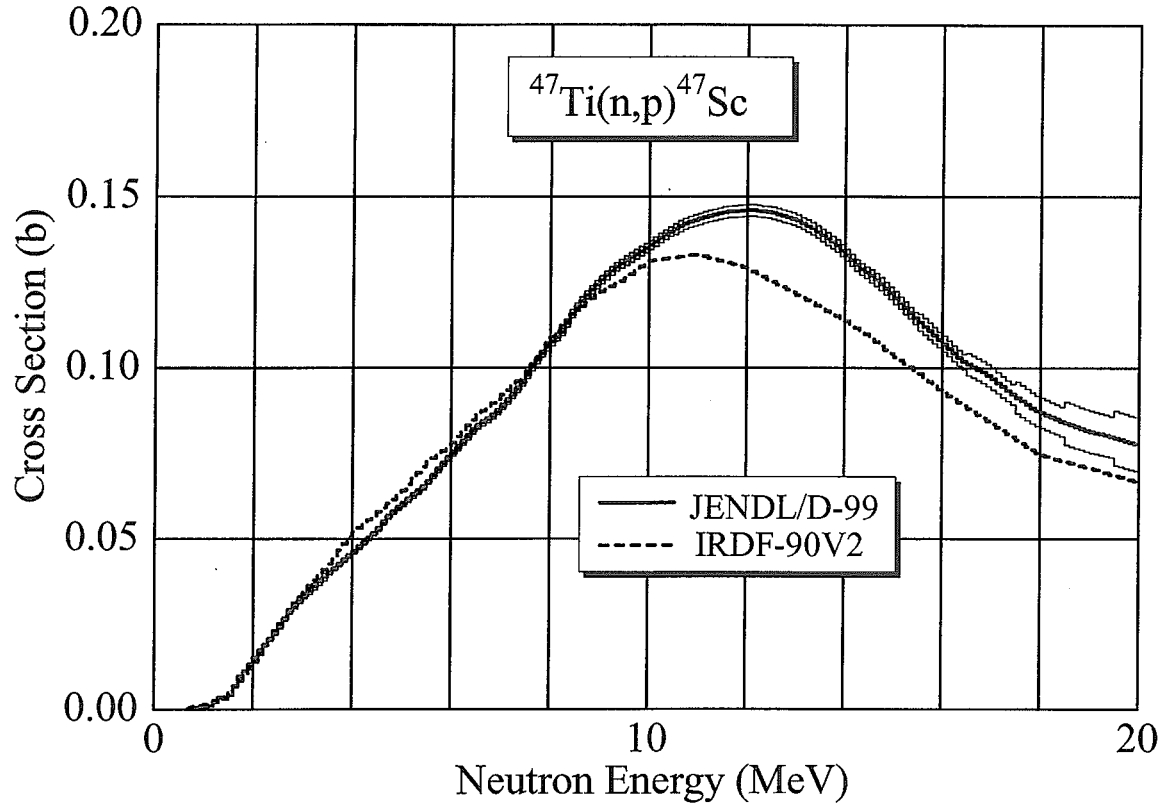

Fig. A.21 ^{47}Ti(n, p)^{47}Sc cross section.

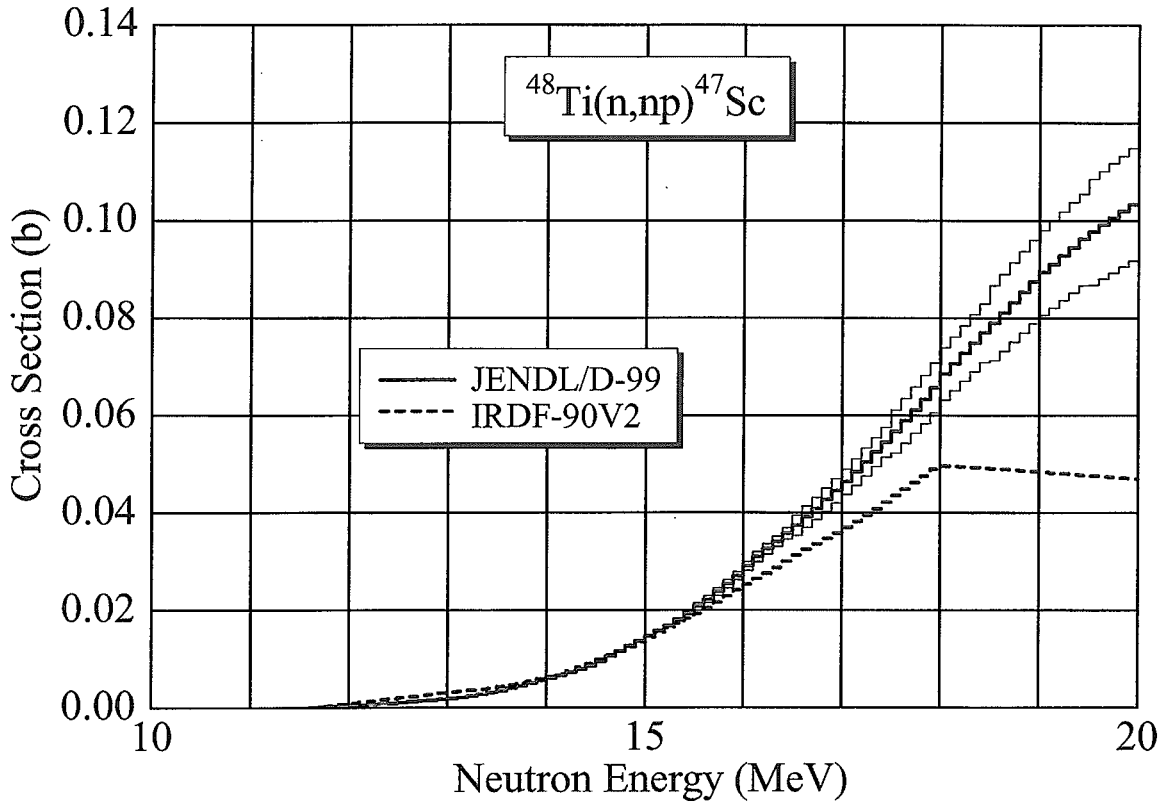

Fig. A.22 ^{48}Ti(n, np)^{47}Sc cross section.

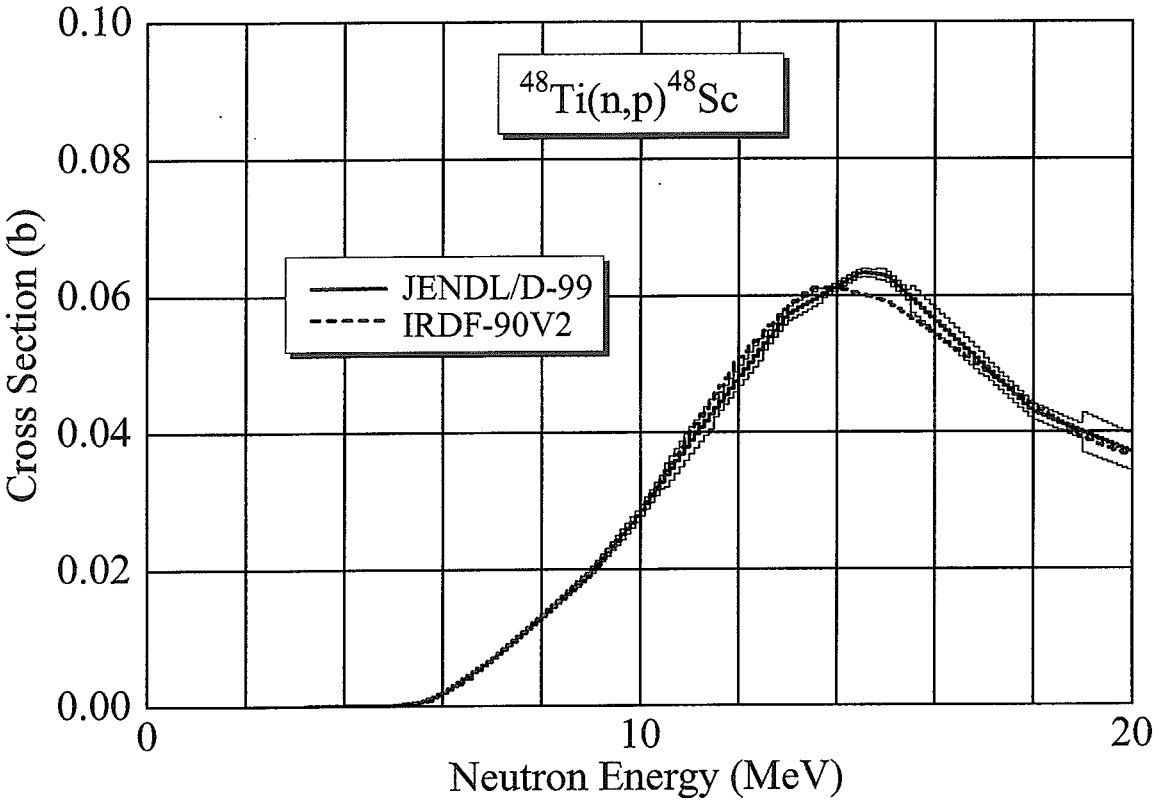

Fig. A.23 ^{48}Ti(n, p)^{48}Sc cross section.

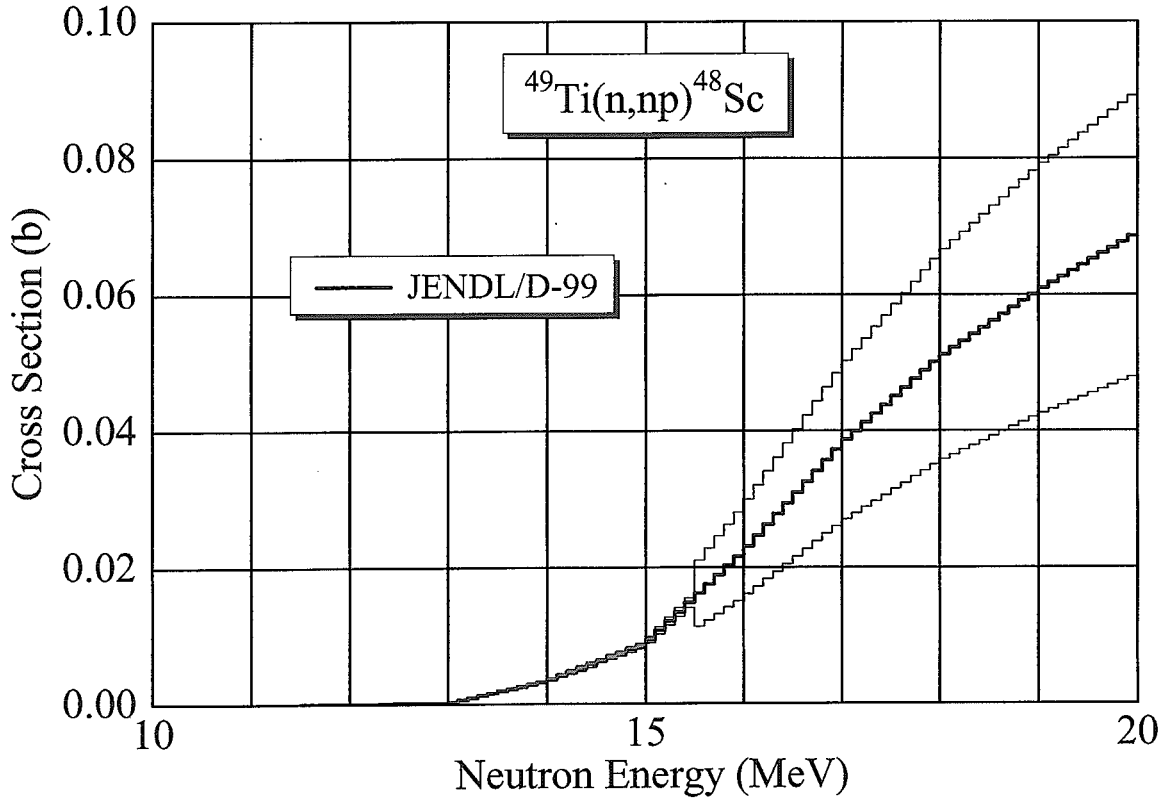

Fig. A.24 ^{49}Ti(n, np)^{48}Sc cross section.

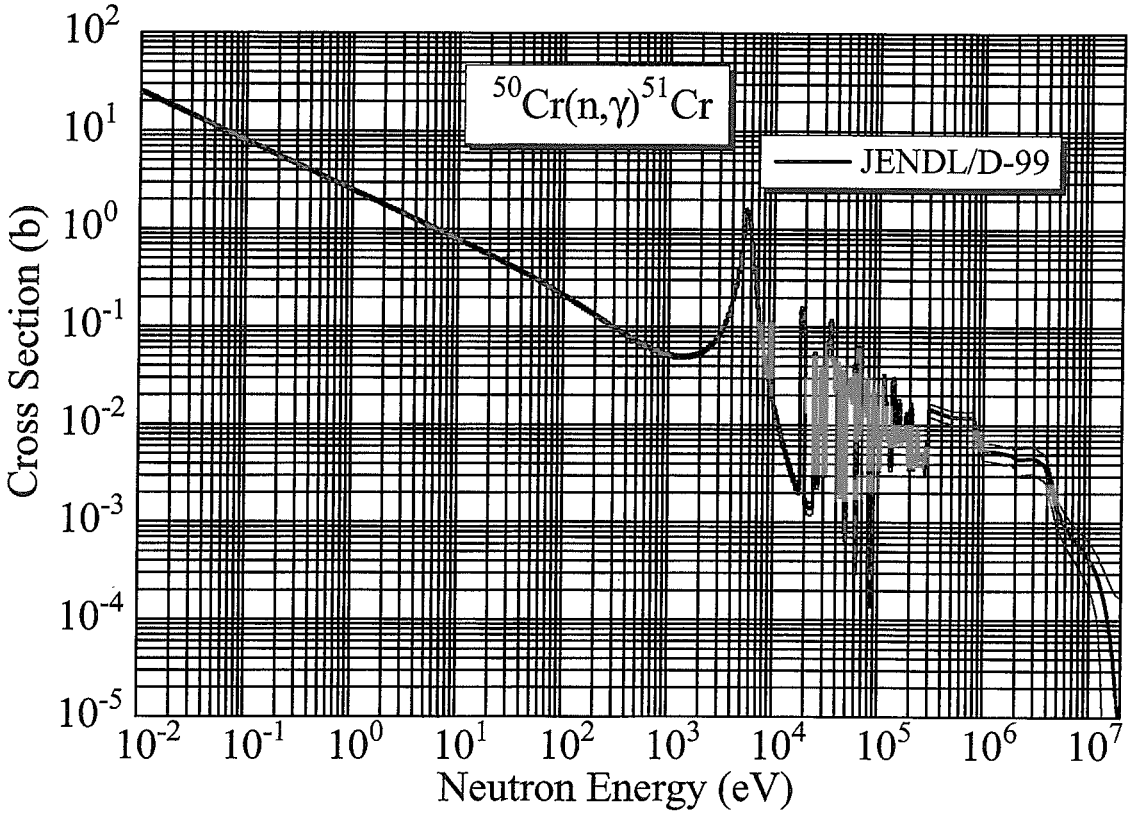

Fig. A.25 ^{50}Cr(n, γ)^{51}Cr cross section.

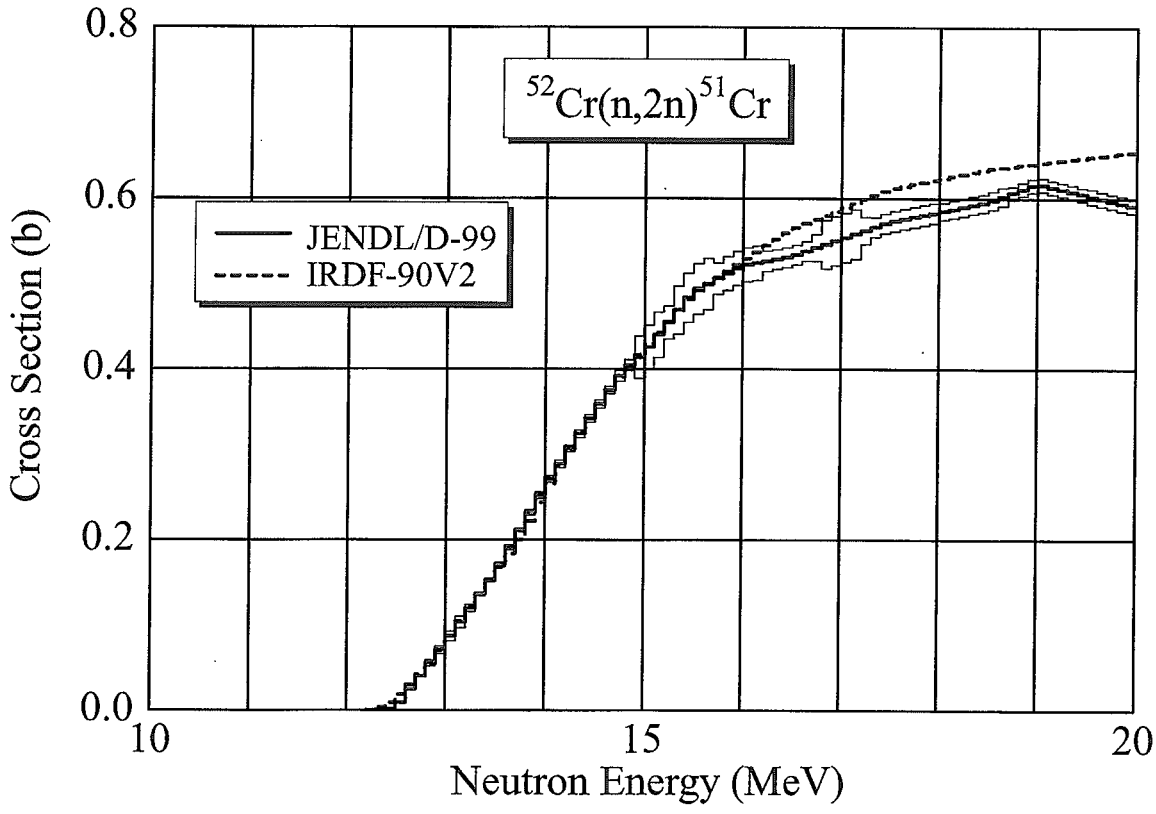

Fig. A.26 ^{52}Cr(n, 2n)^{51}Cr cross section.

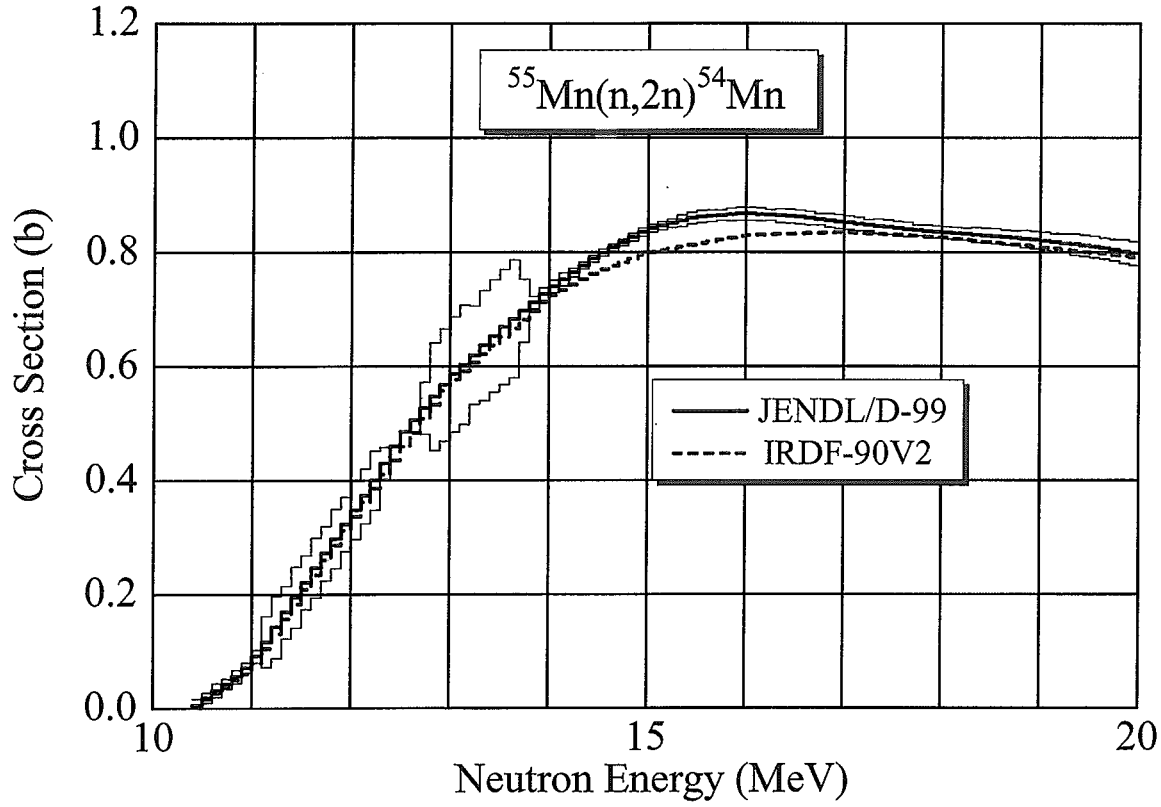

Fig. A.27 ^{55}Mn(n, 2n)^{54}Mn cross section.

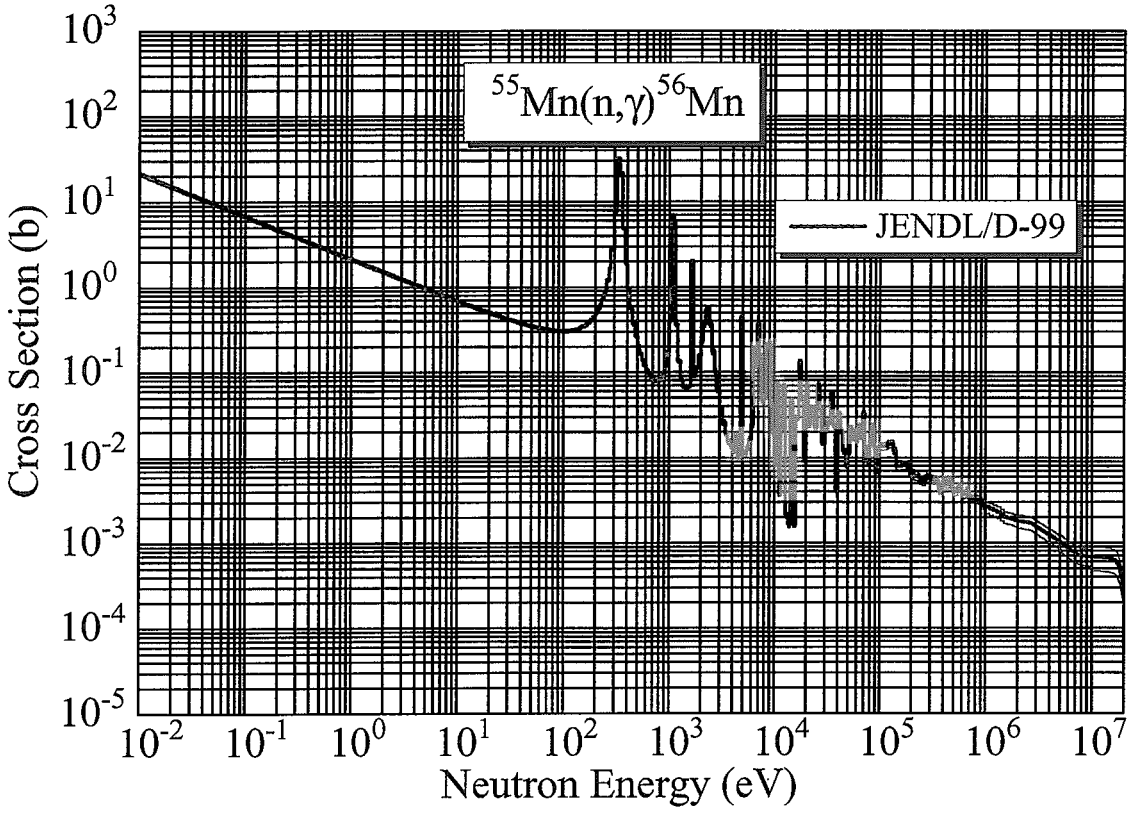

Fig. A.28 ^{55}Mn(n, γ)^{56}Mn cross section.

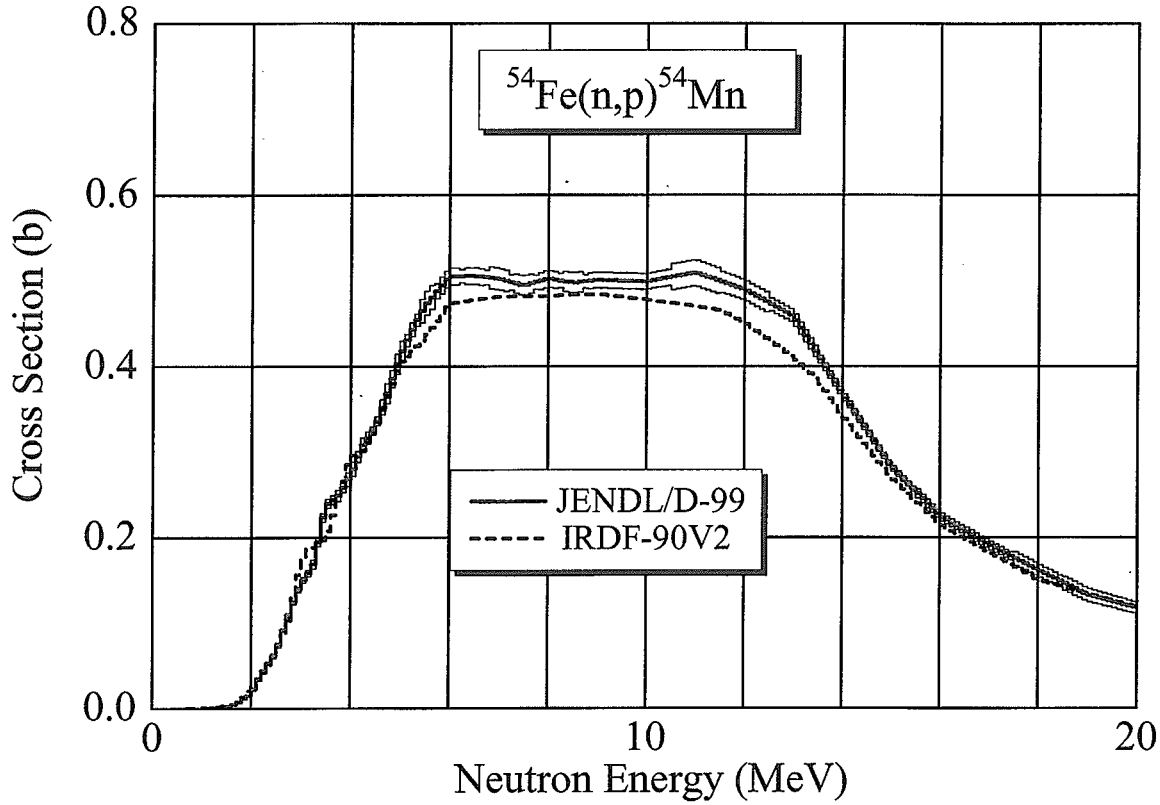

Fig. A.29 ^{54}Fe(n, p)^{54}Mn cross section.

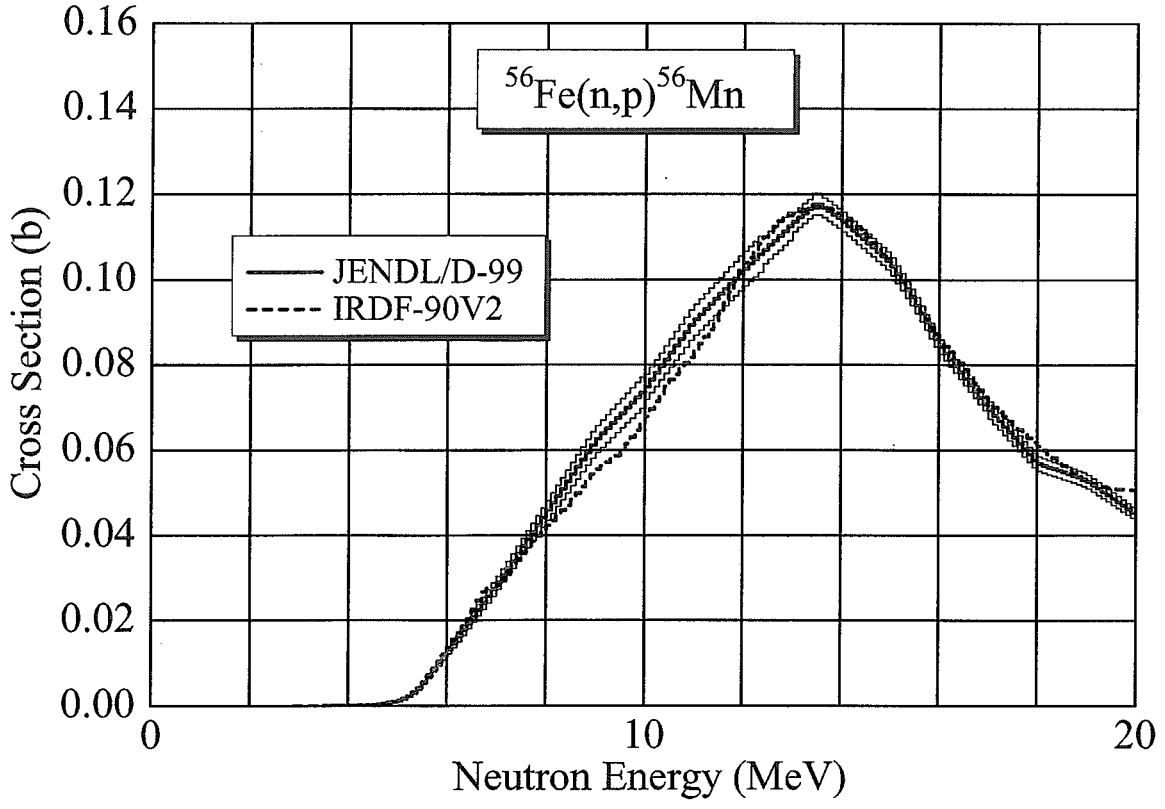

Fig. A.30 ^{56}Fe(n, p)^{56}Mn cross section.

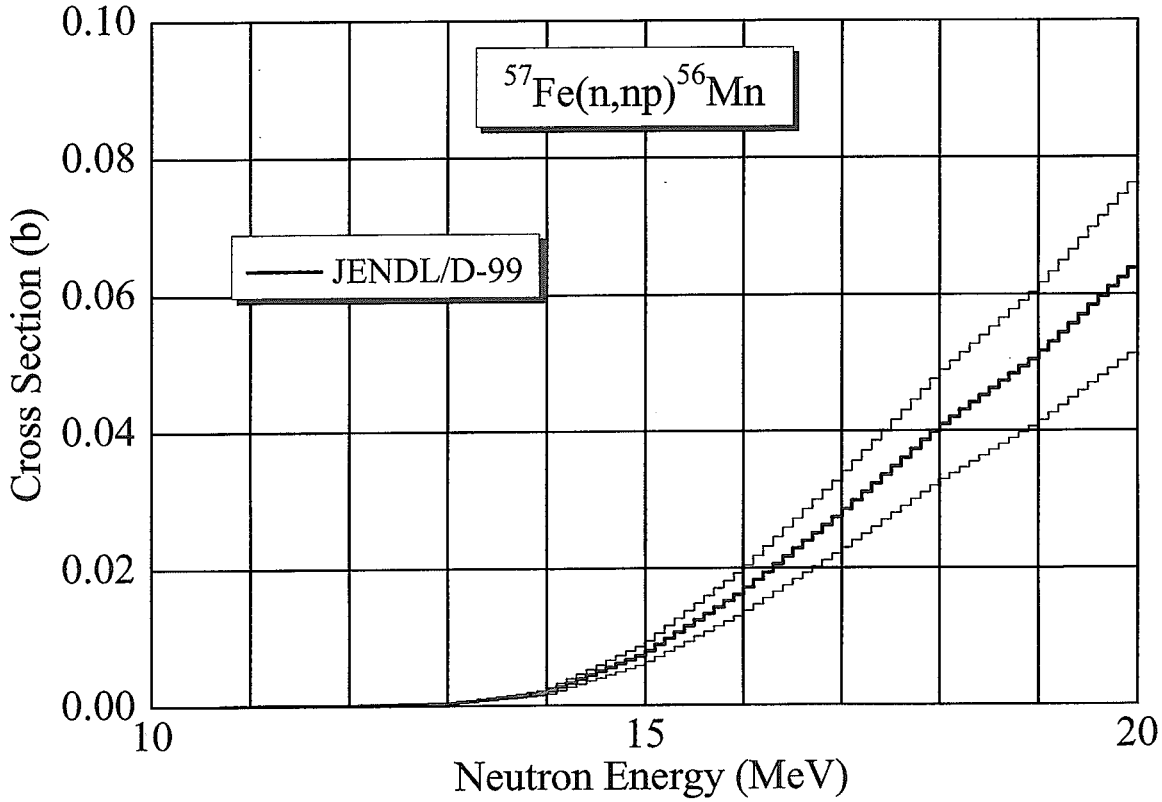

Fig. A.31 ^{57}Fe(n, np)^{56}Mn cross section.

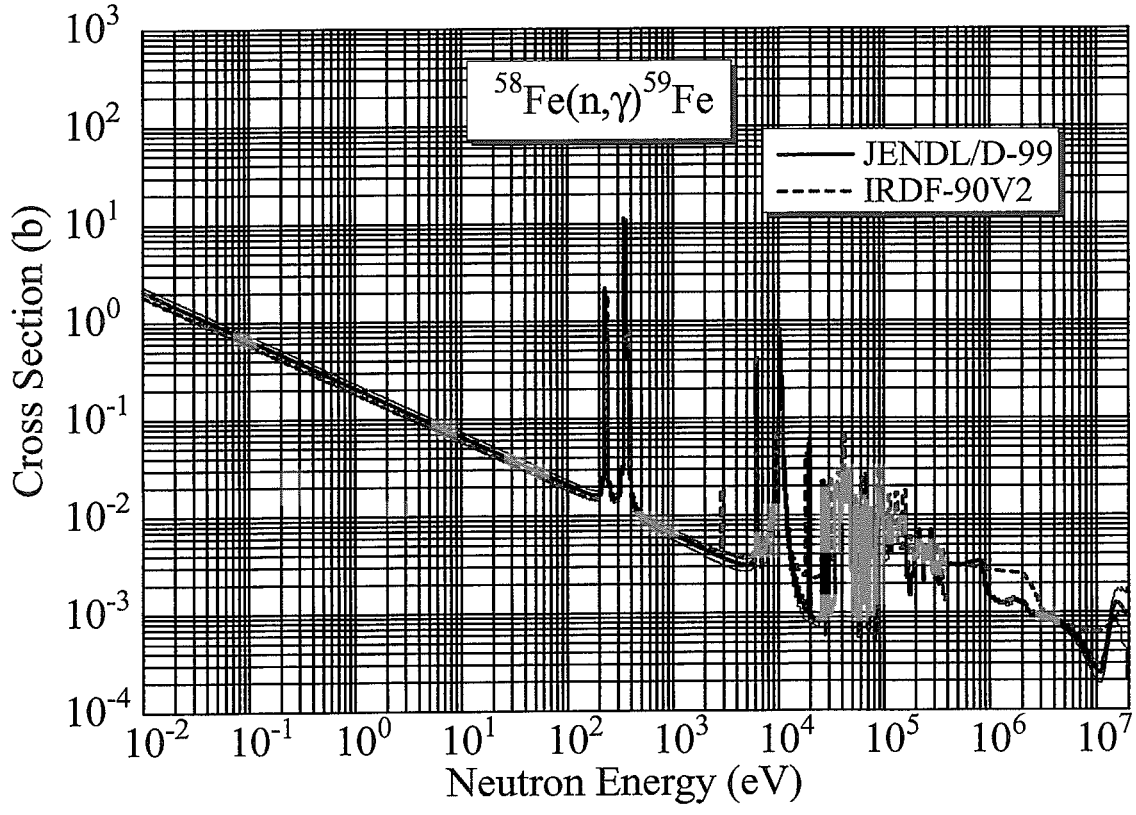

Fig. A.32 ^{58}Fe(n, γ)^{59}Fe cross section.

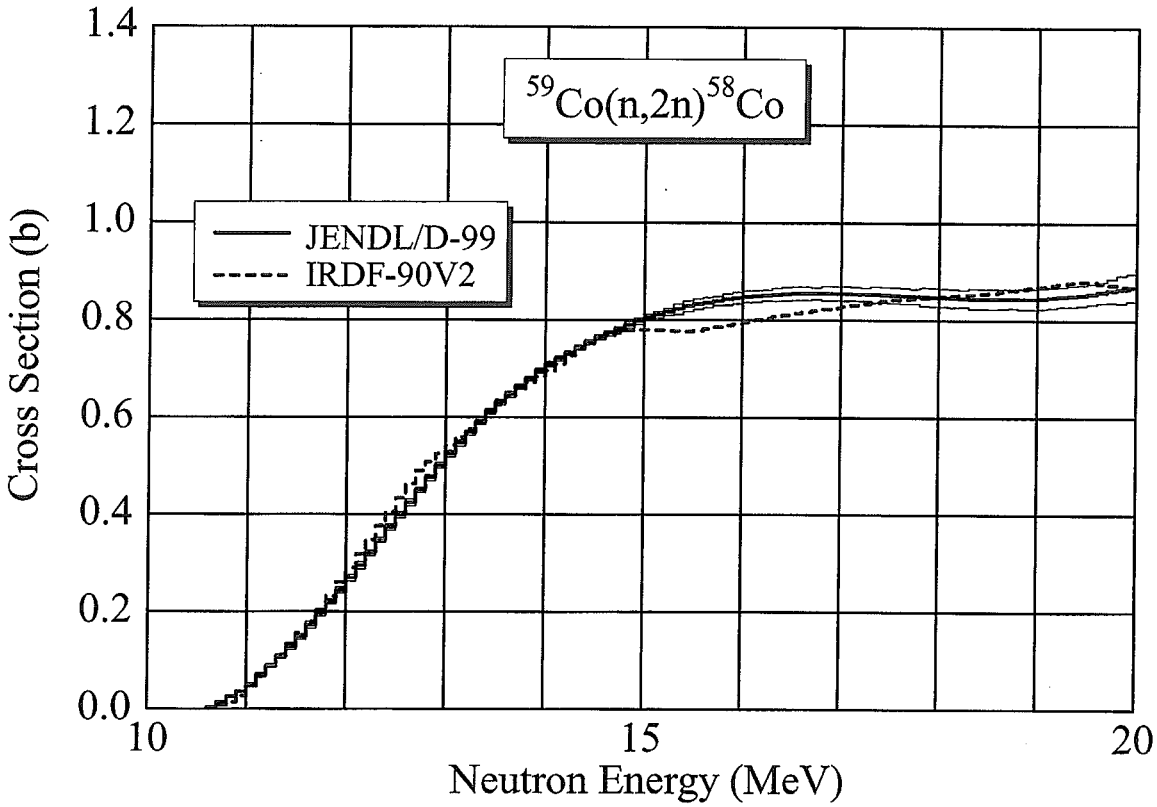

Fig. A.33 ^{59}Co(n, 2n)^{58}Co cross section.

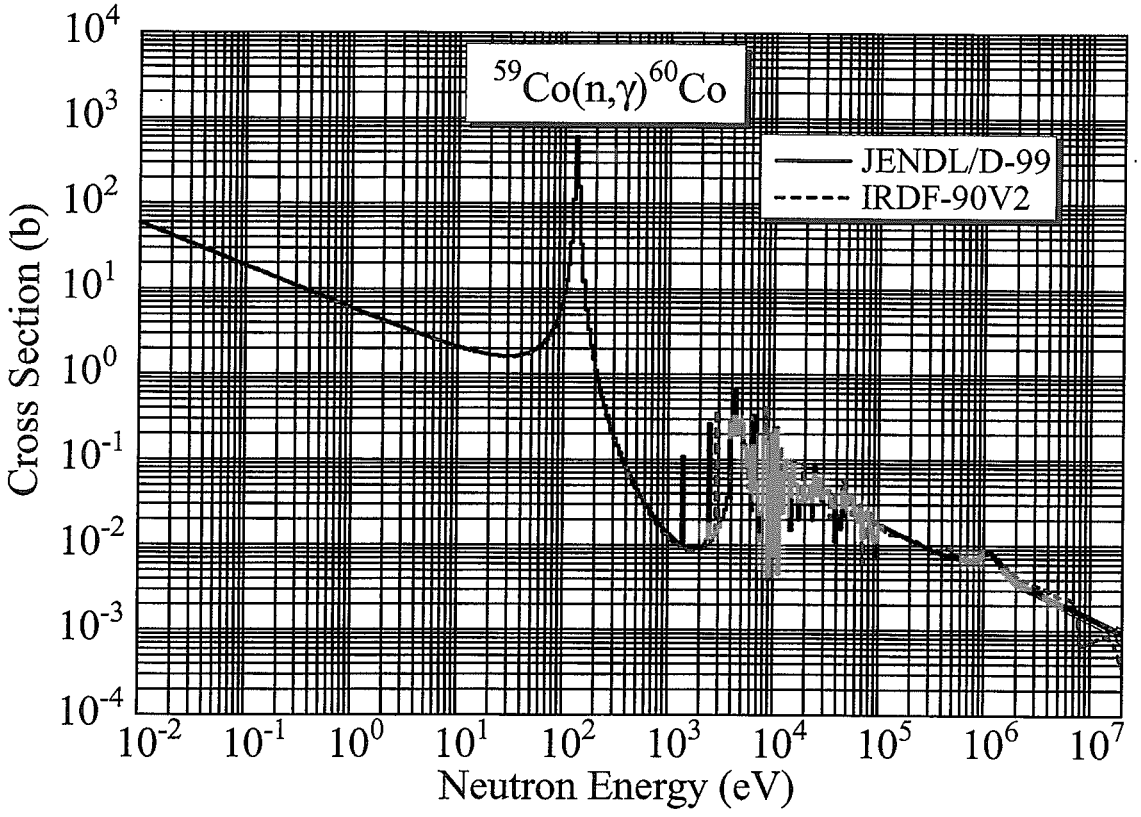

Fig. A.34 ^{59}Co(n, γ)^{60}Co cross section.

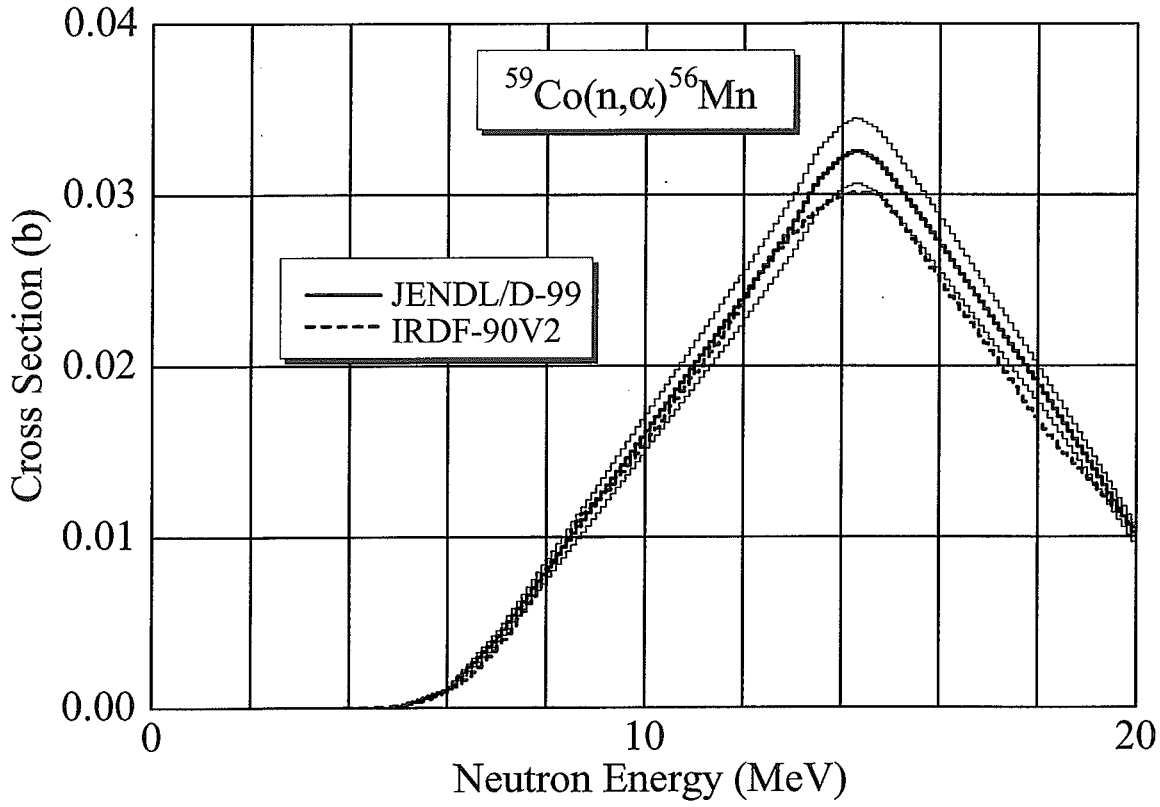

Fig. A.35 ^{59}Co(n, α)^{56}Mn cross section

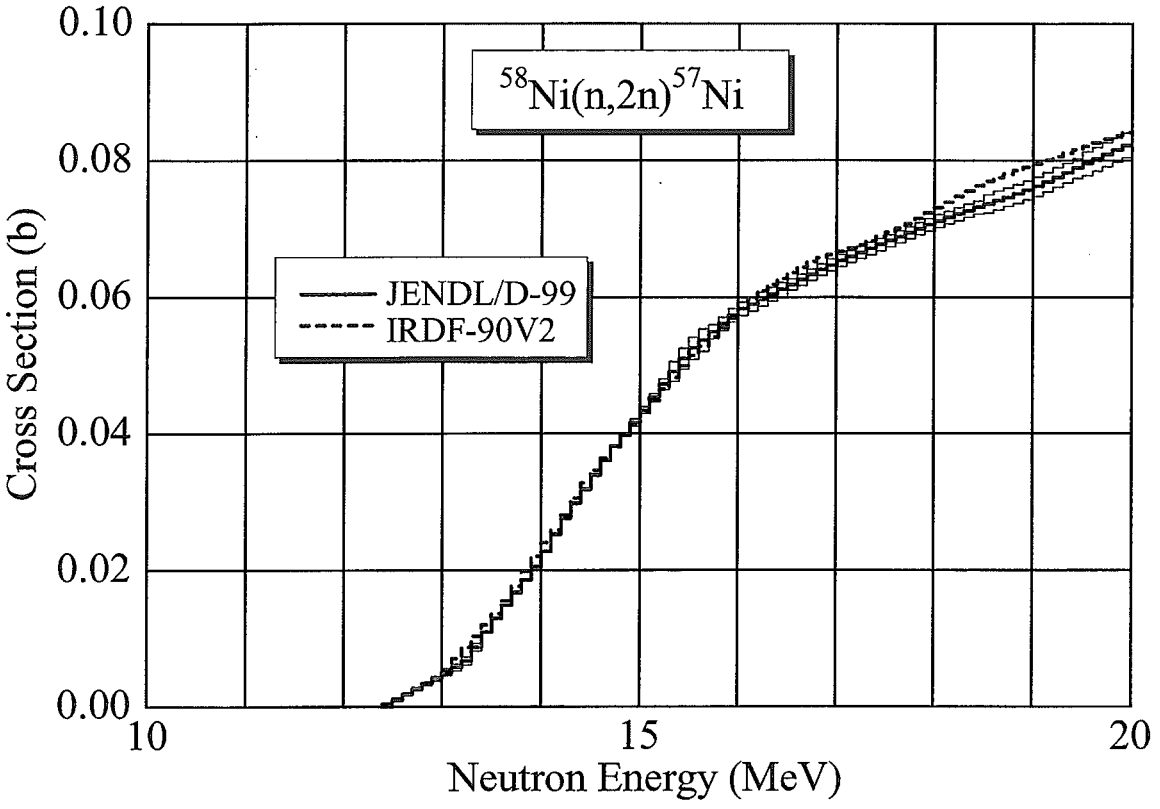

Fig. A.36 ^{58}Ni(n, 2n)^{57}Ni cross section.

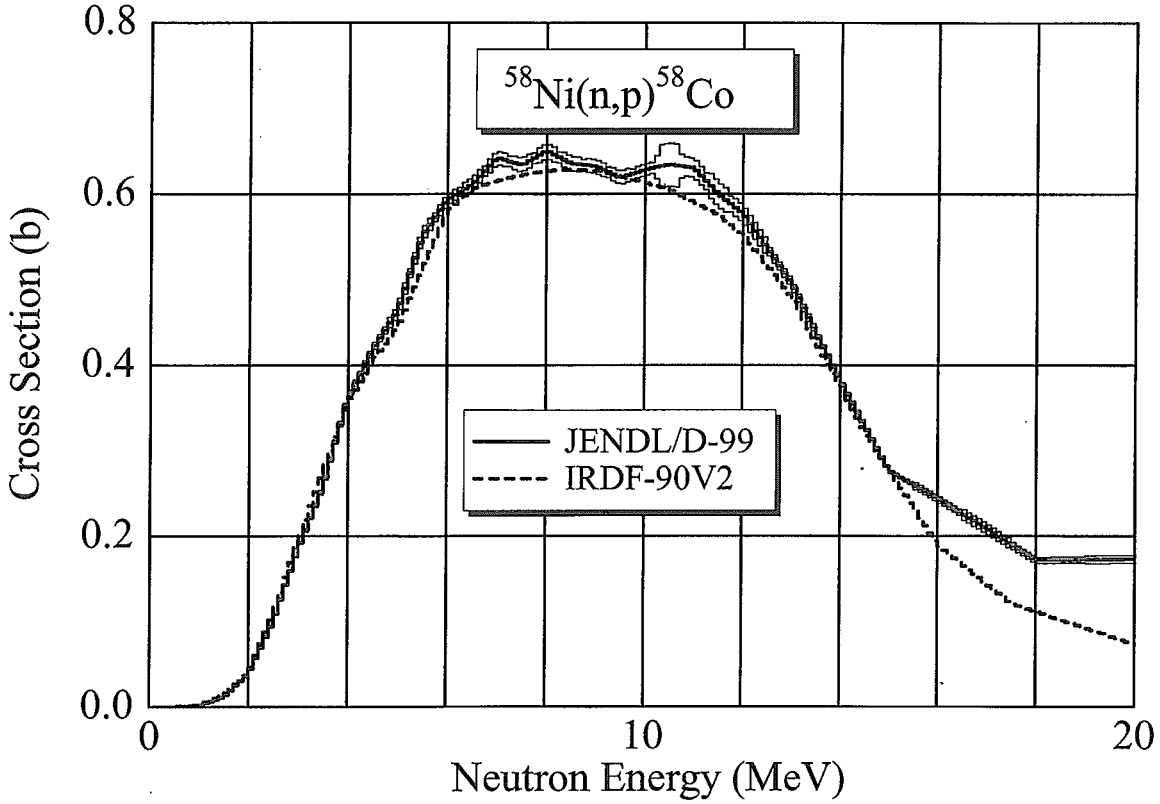

Fig. A.37 ^{58}Ni(n, p)^{58}Co cross section.

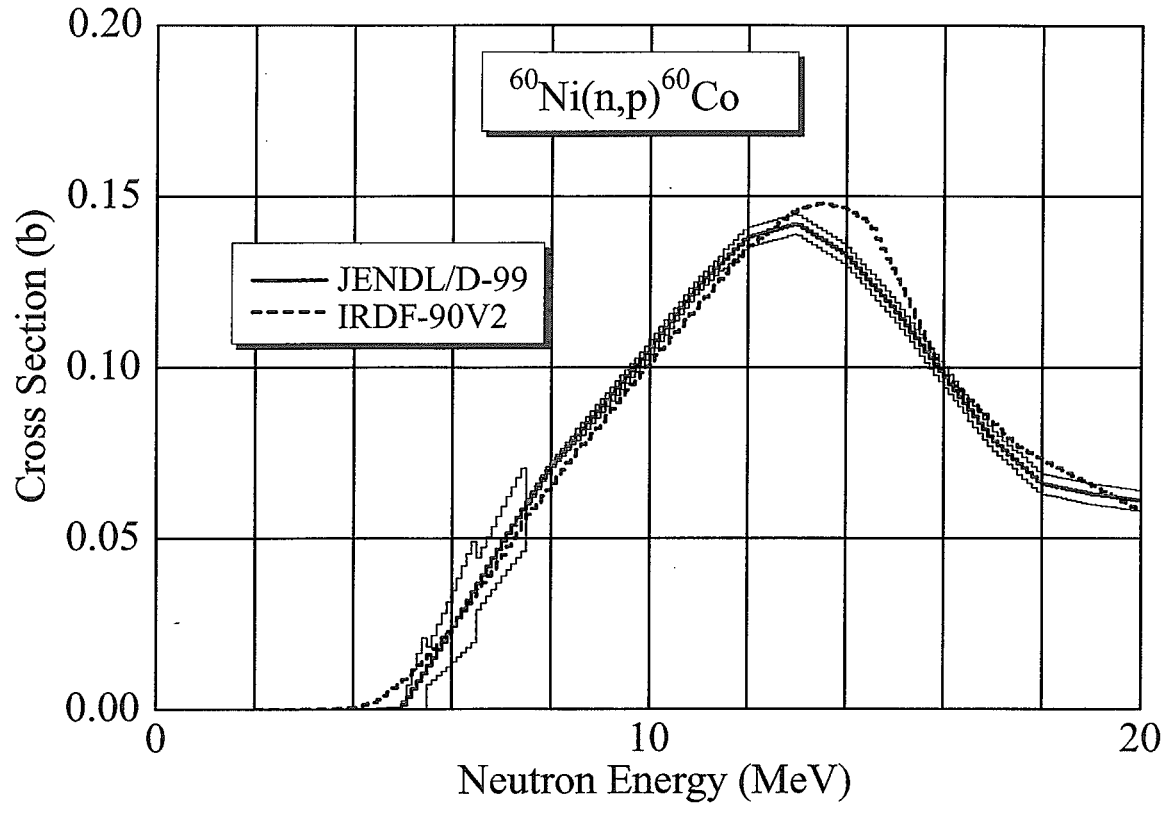

Fig. A.38 ^{60}Ni(n, p)^{60}Co cross section.

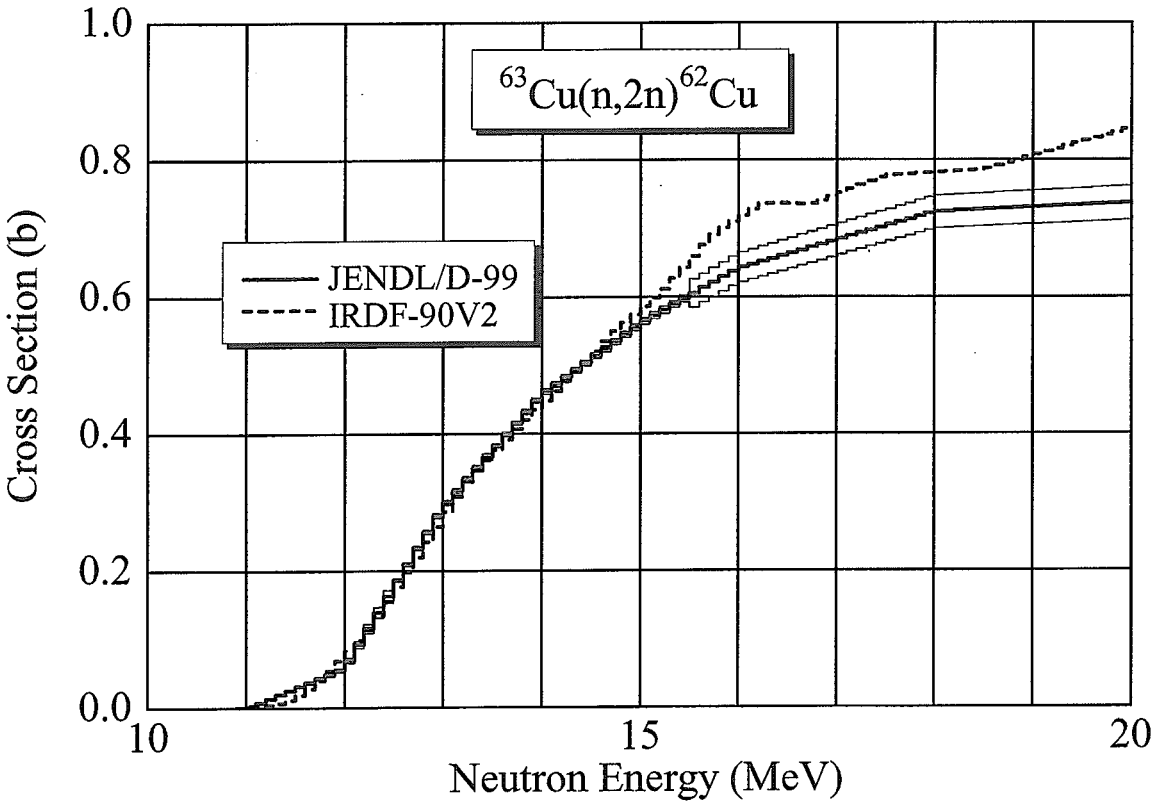

Fig. A.39 ^{63}Cu(n, 2n)^{62}Cu cross section.

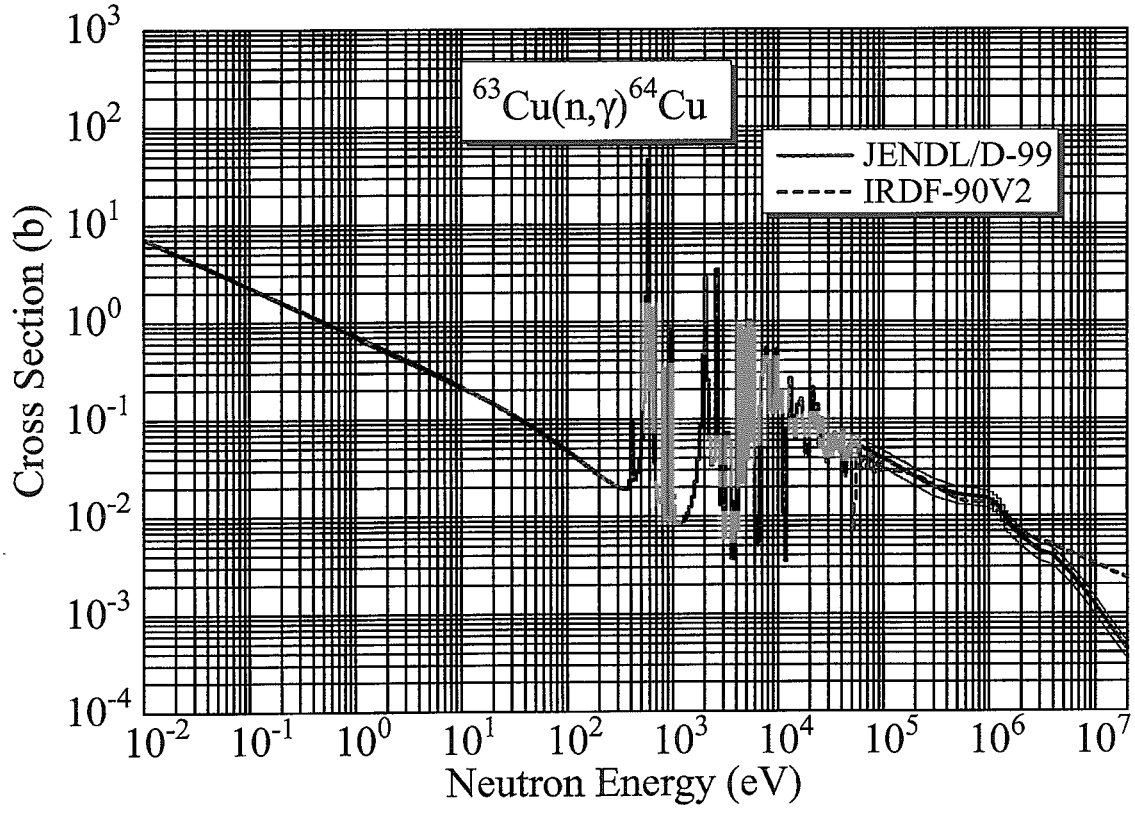

Fig. A.40 ^{63}Cu(n, γ)^{64}Cu cross section.

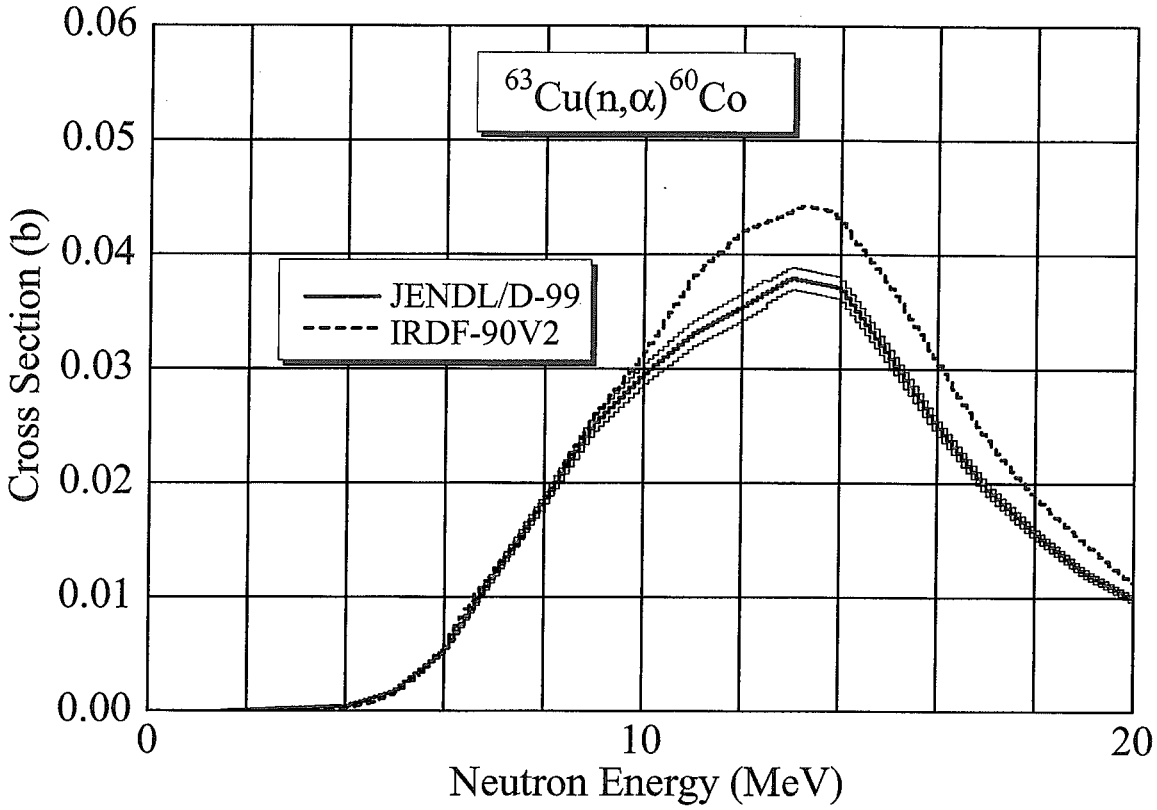

Fig. A.41 ^{63}Cu(n, α)^{60}Co cross section.

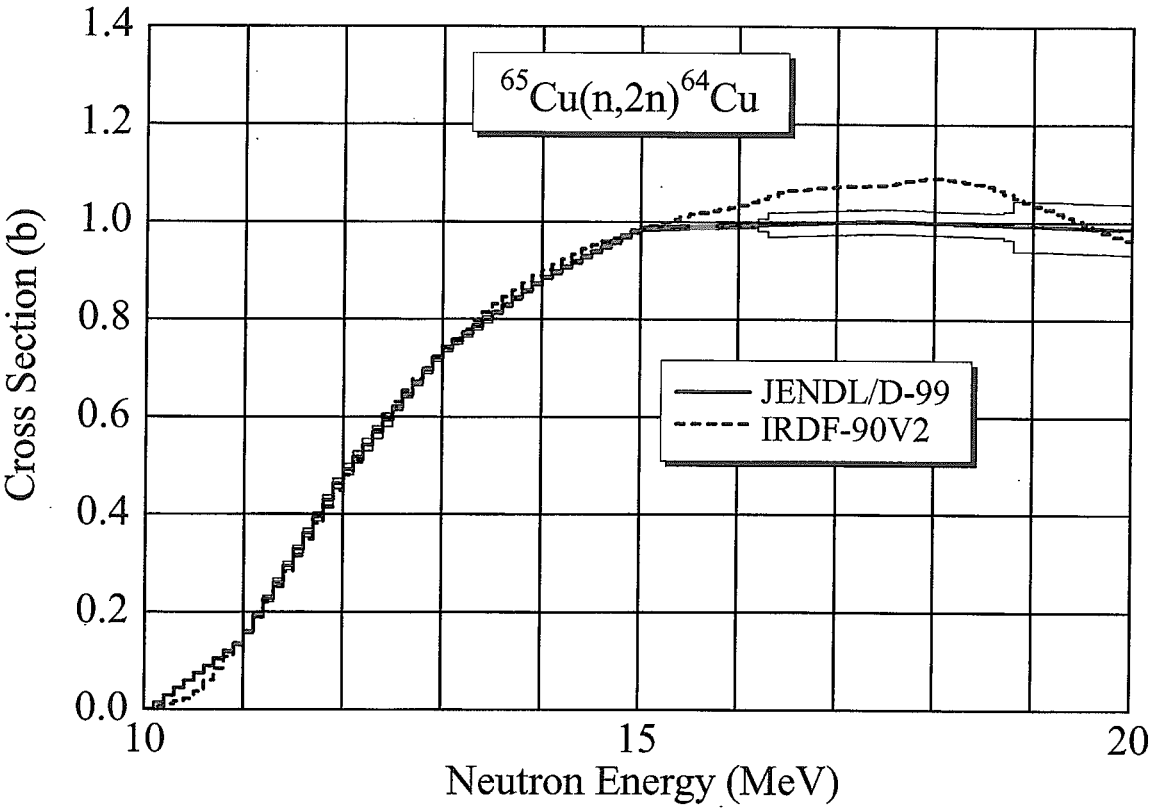

Fig. A.42 ^{65}Cu(n, 2n)^{64}Cu cross section.

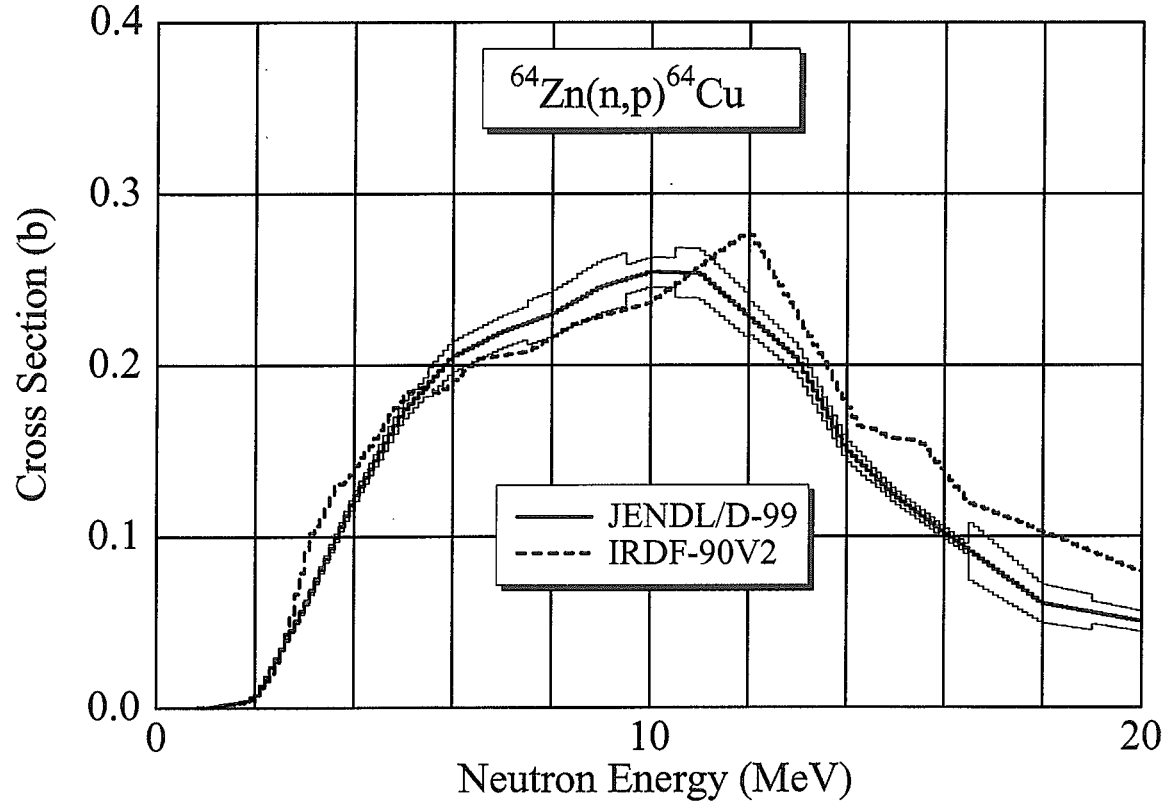

Fig. A.43 ^{64}Zn(n, p)^{64}Cu cross section.

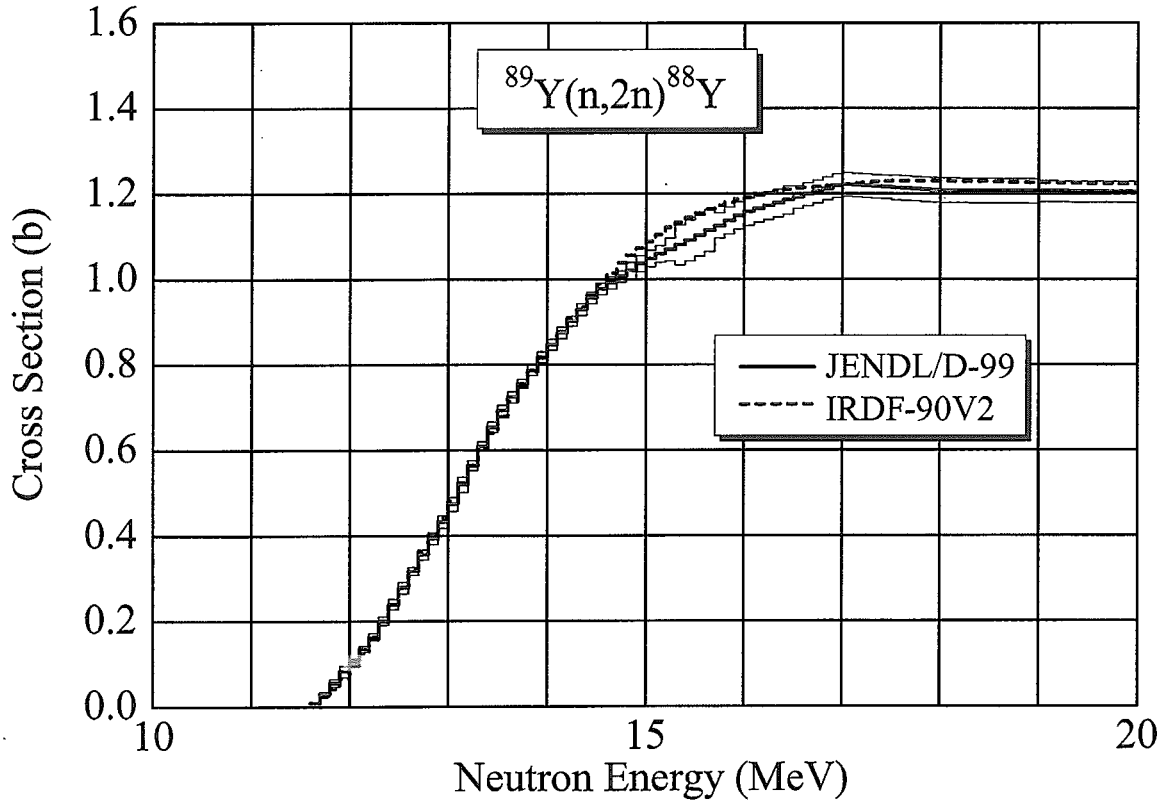

Fig. A.44 ^{89}Y(n, 2n)^{88}Y cross section.

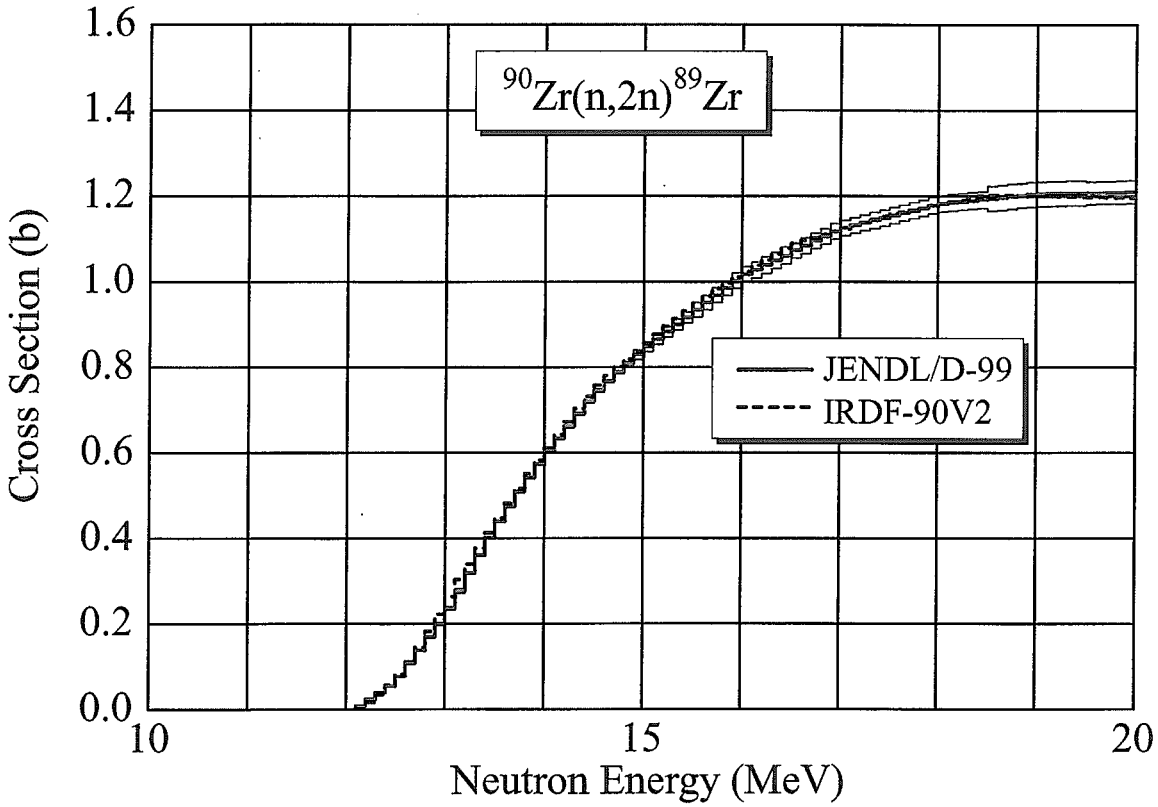

Fig. A.45 ^{90}Zr(n, 2n)^{89}Zr cross section.

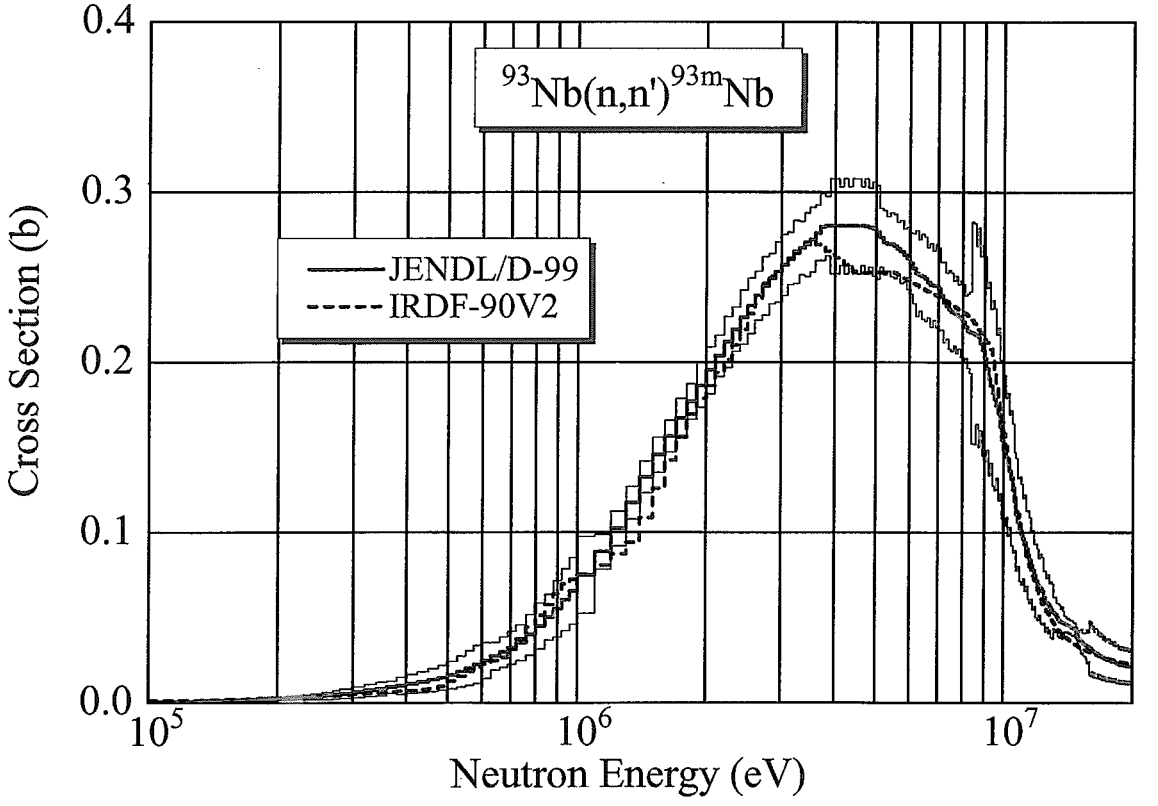

Fig. A.46 ^{93}Nb(n, n')^{93m}Nb cross section.

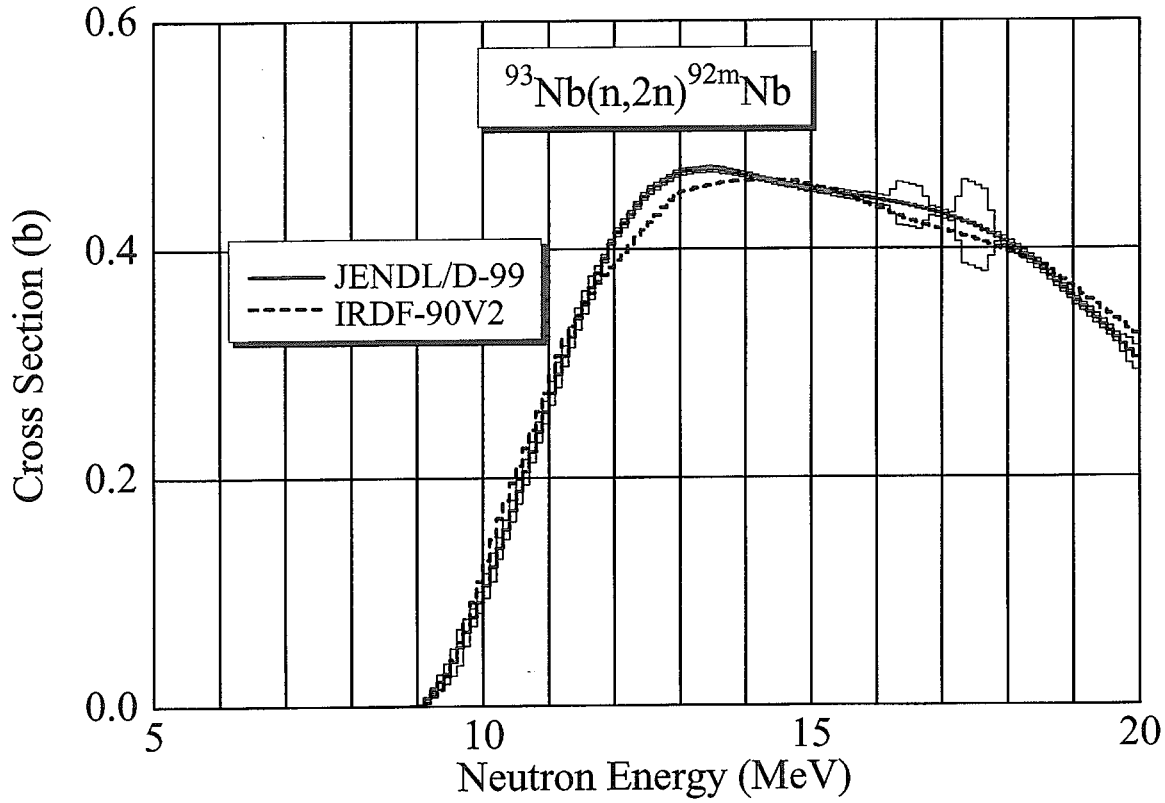

Fig. A.47 ^{93}Nb(n, 2n)^{92m}Nb cross section.

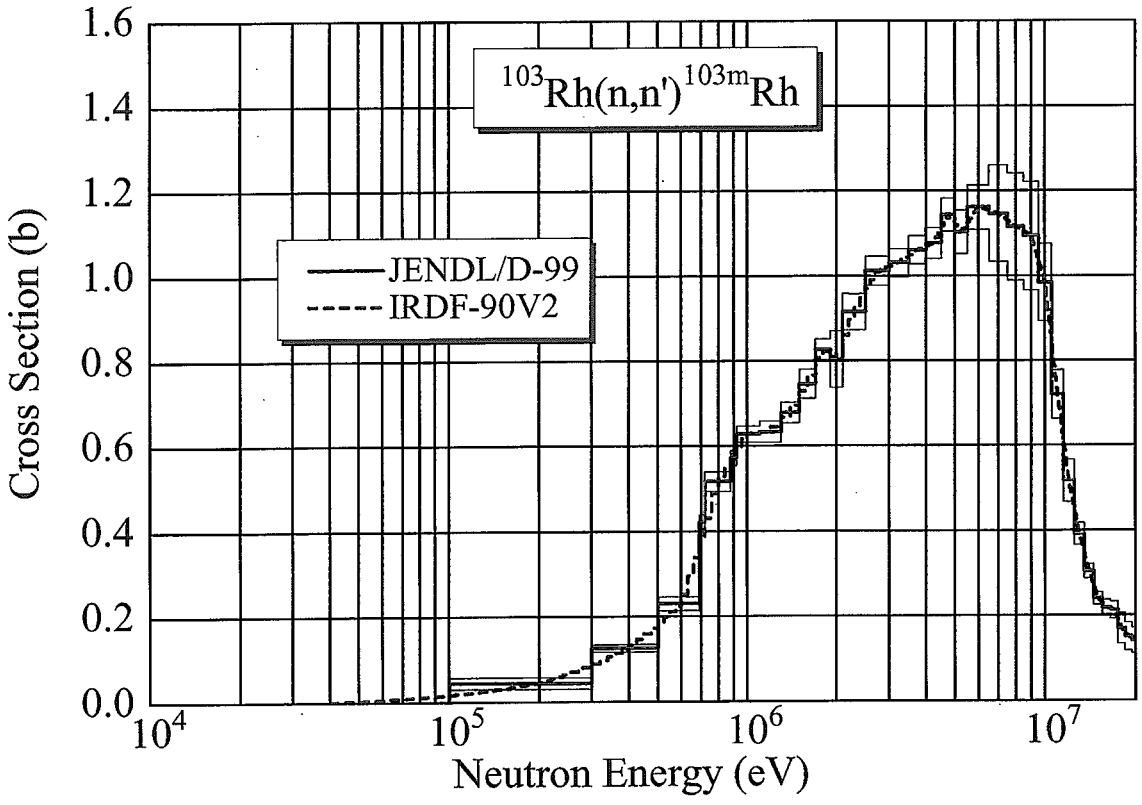

Fig. A.48 ^{103}Rh(n, n')^{103m}Rh cross section.

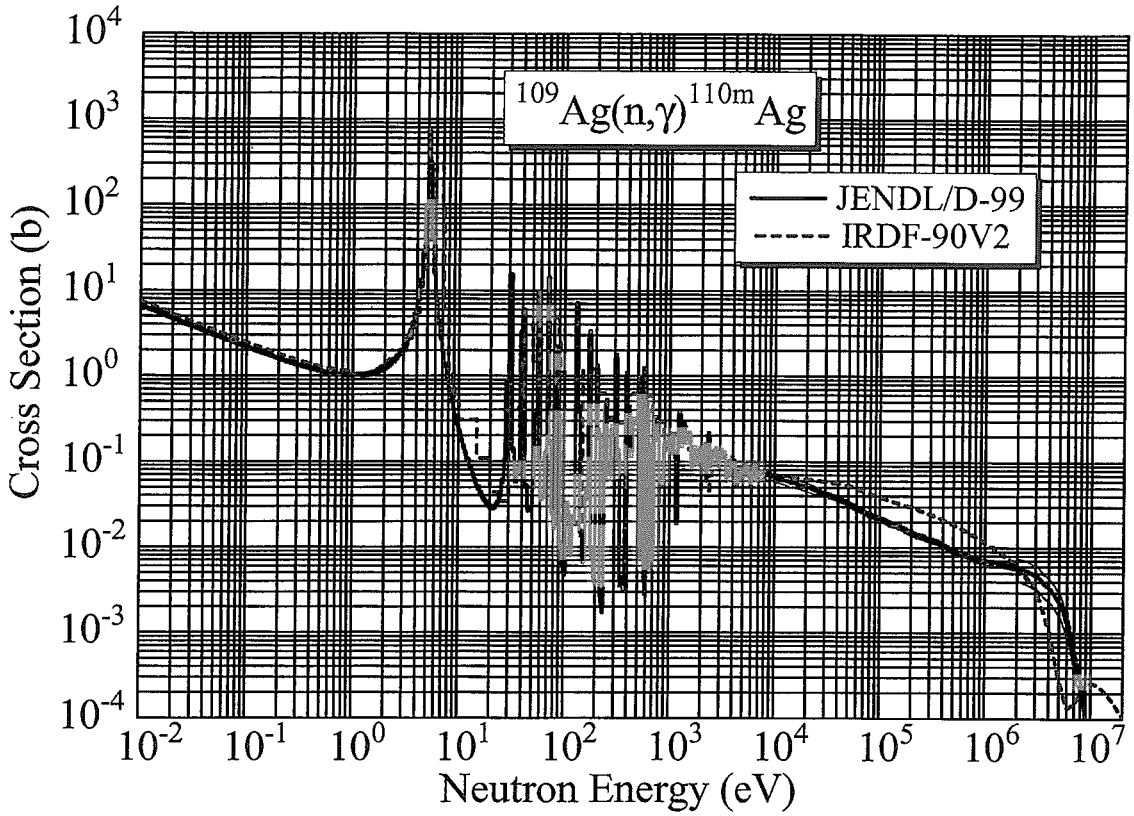

Fig. A.49 ^{109}Ag(n, γ)^{110m}Ag cross section.

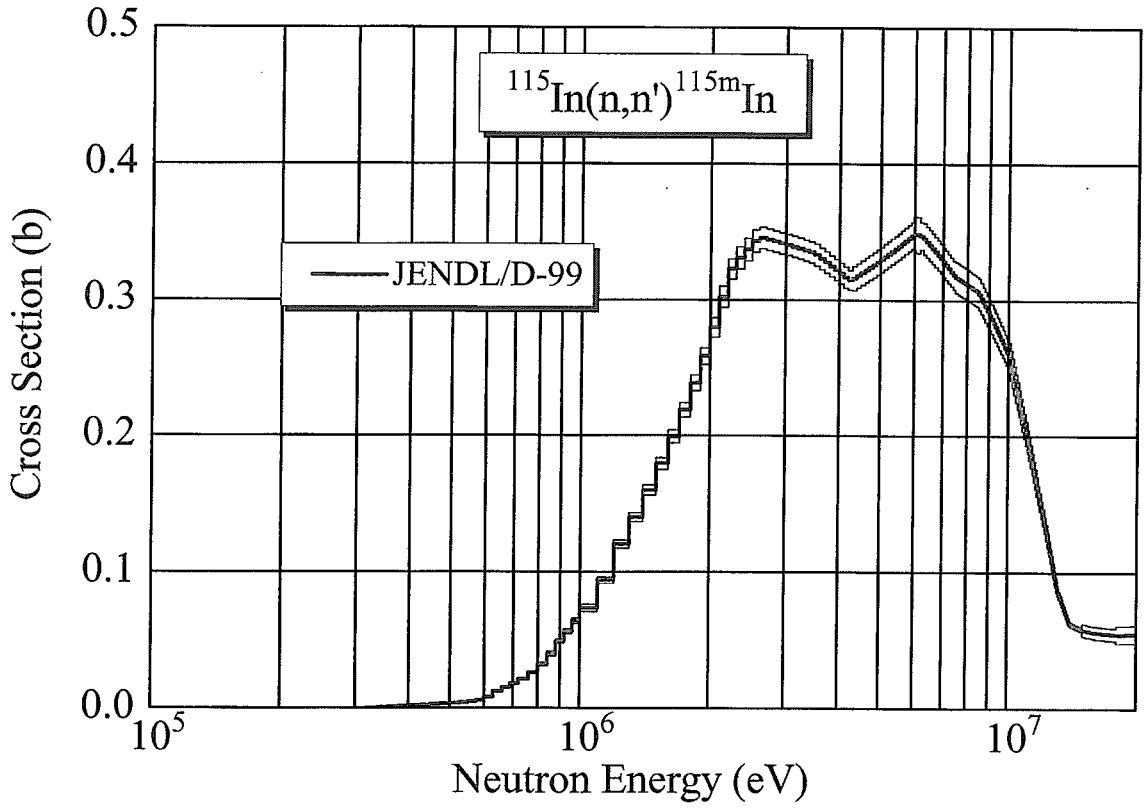

Fig. A.50 ^{115}In(n, n')^{115m}In cross section.

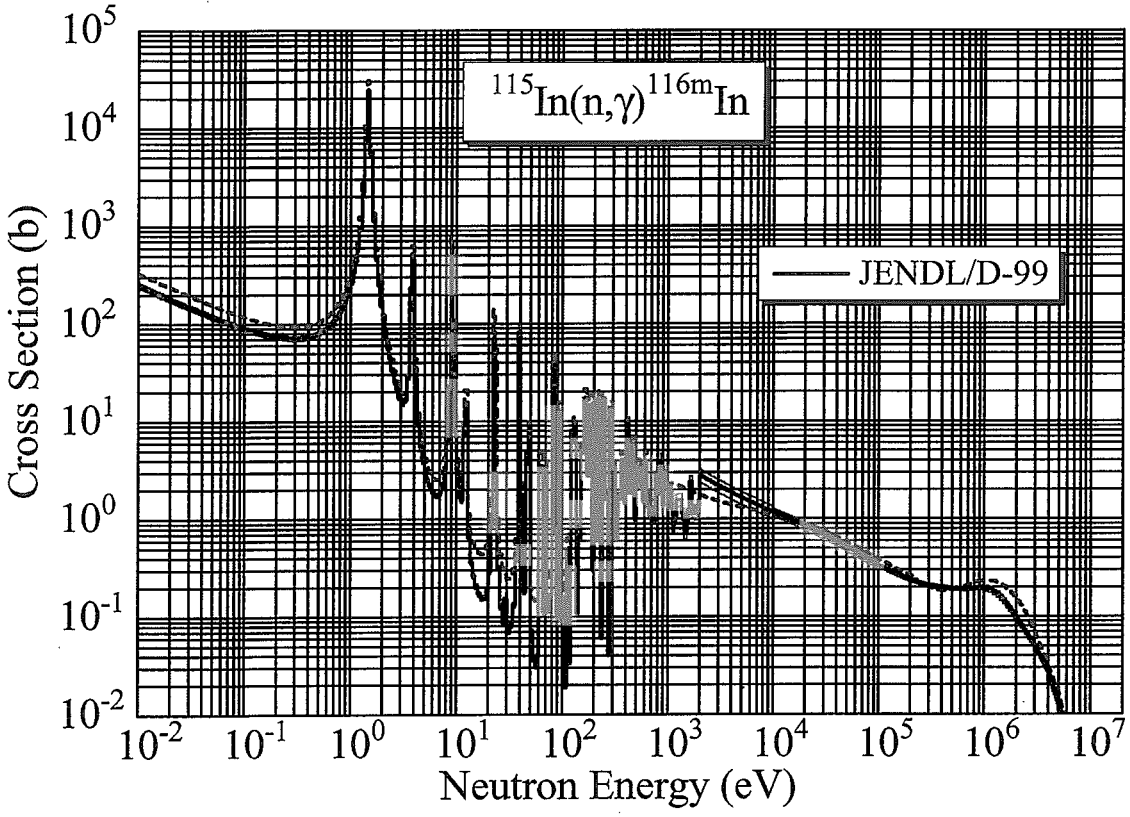

Fig. A.51 $^{115}In(n, \gamma)^{116m}In$ cross section.

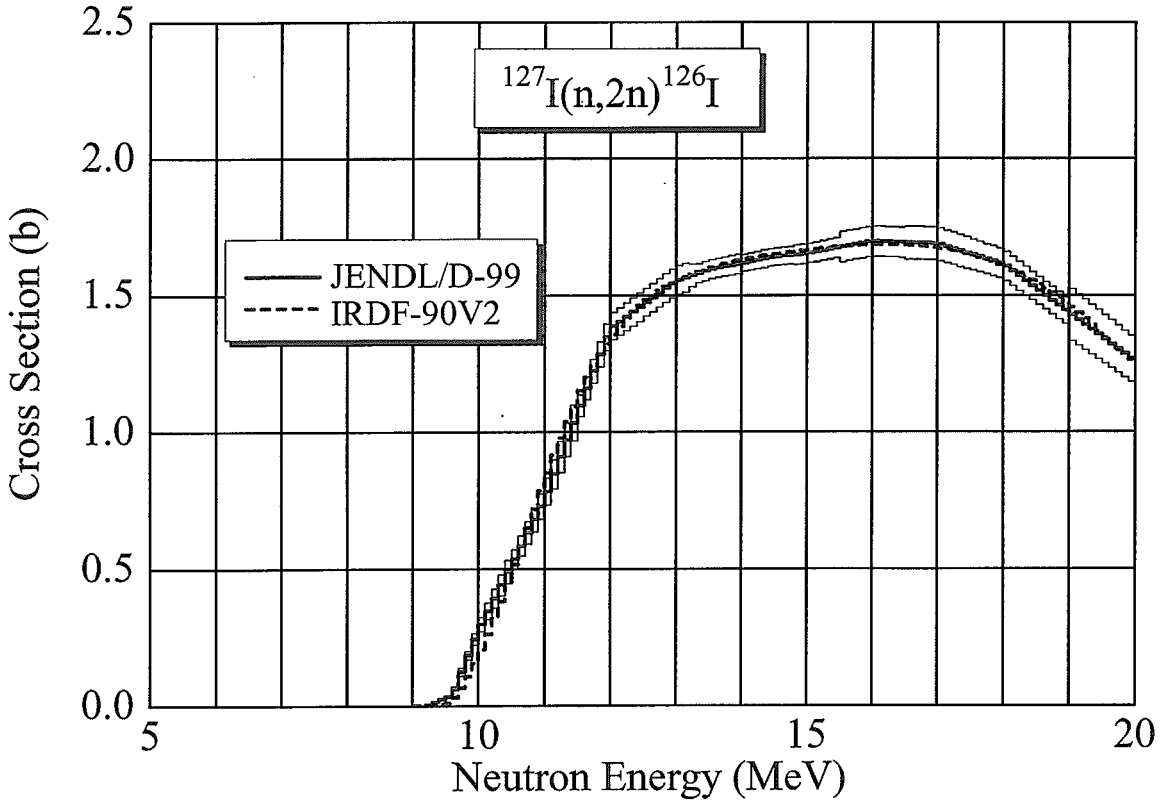

Fig. A.52 $^{127}I(n,2n)^{126}I$ cross section.

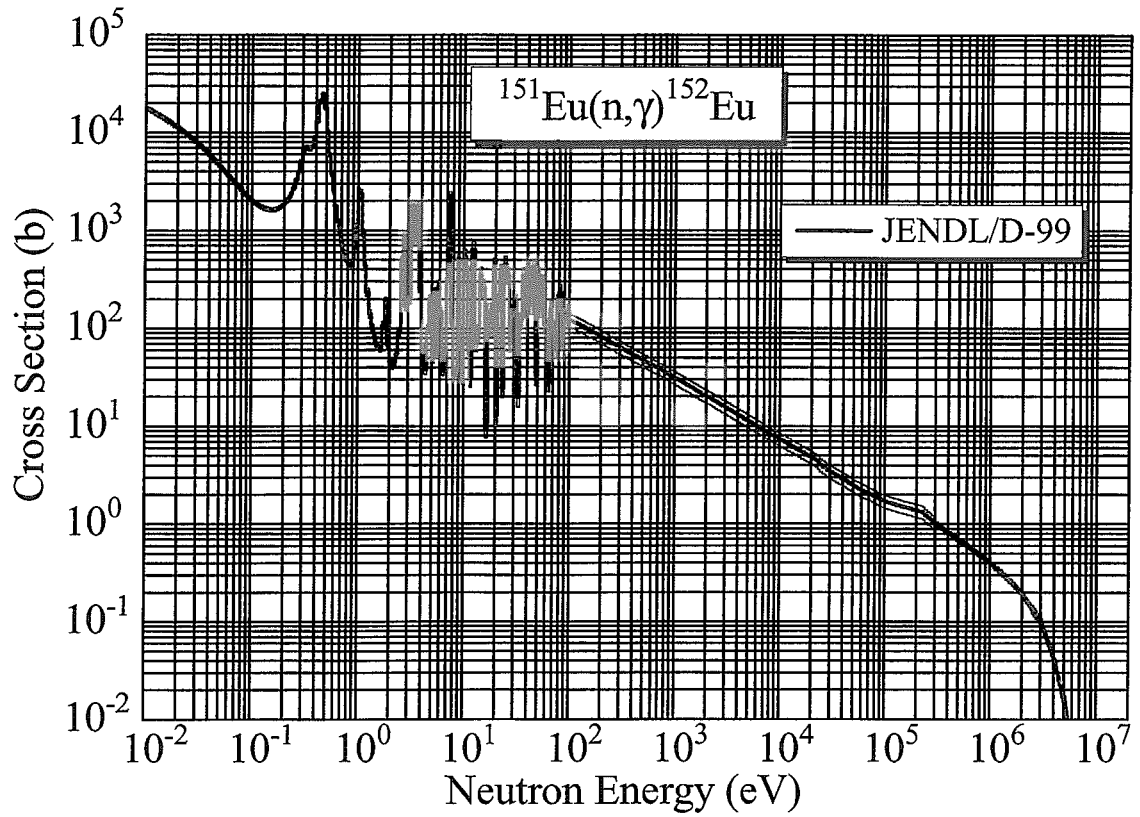

Fig. A.53 ^{151}Eu(n, γ)^{152}Eu cross section.

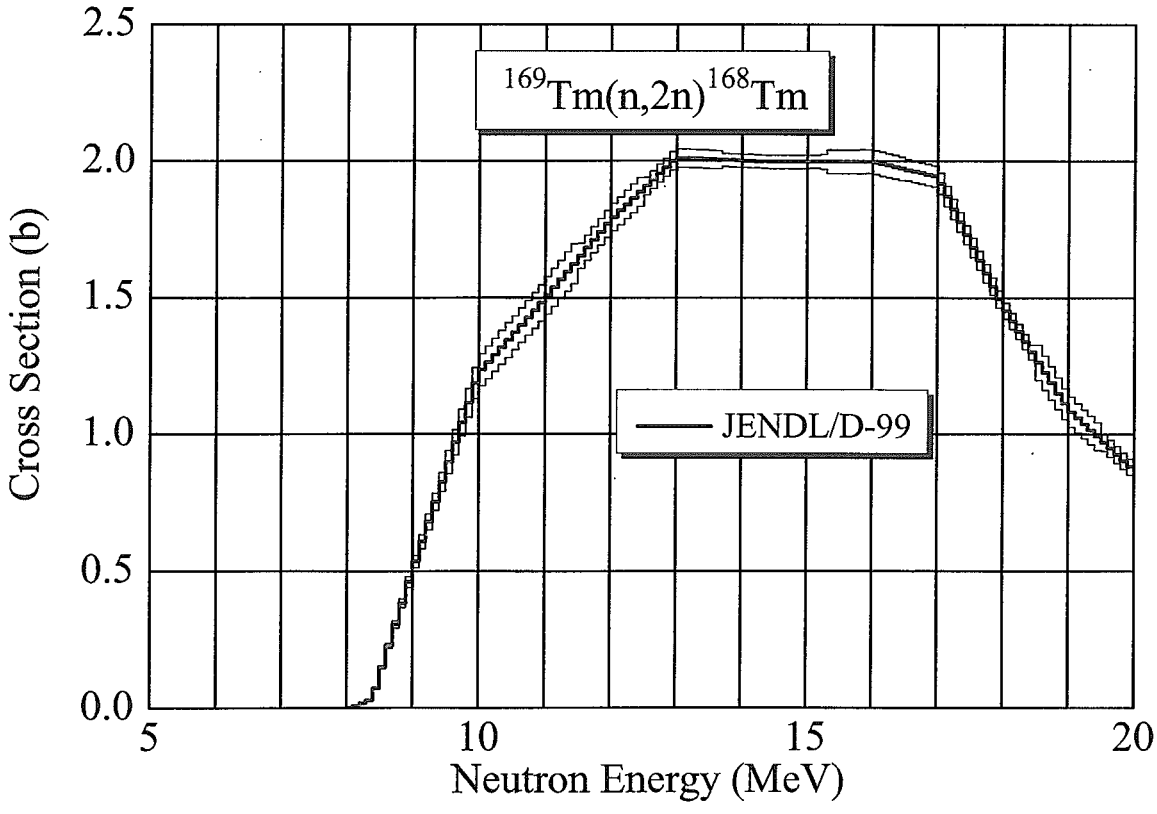

Fig. A.54 ^{169}Tm(n,2n)^{168}Tm cross section.

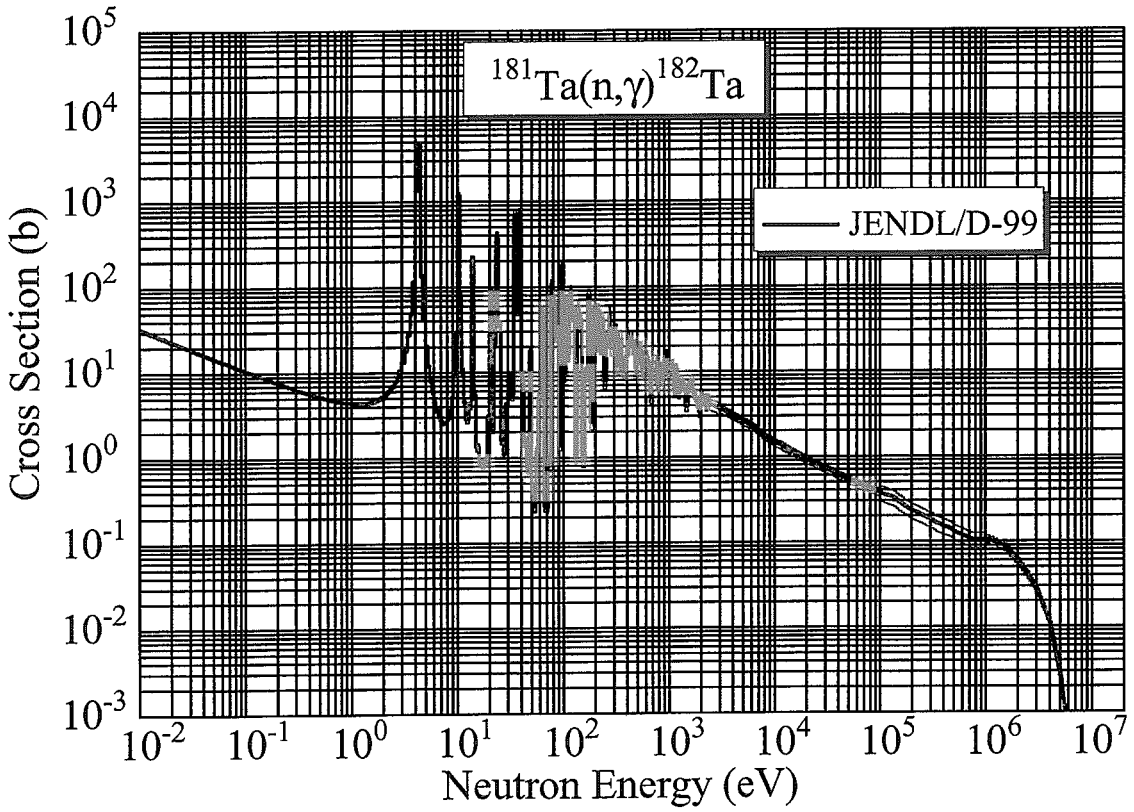

Fig. A.55 ^{181}Ta(n, γ)^{182}Ta cross section.

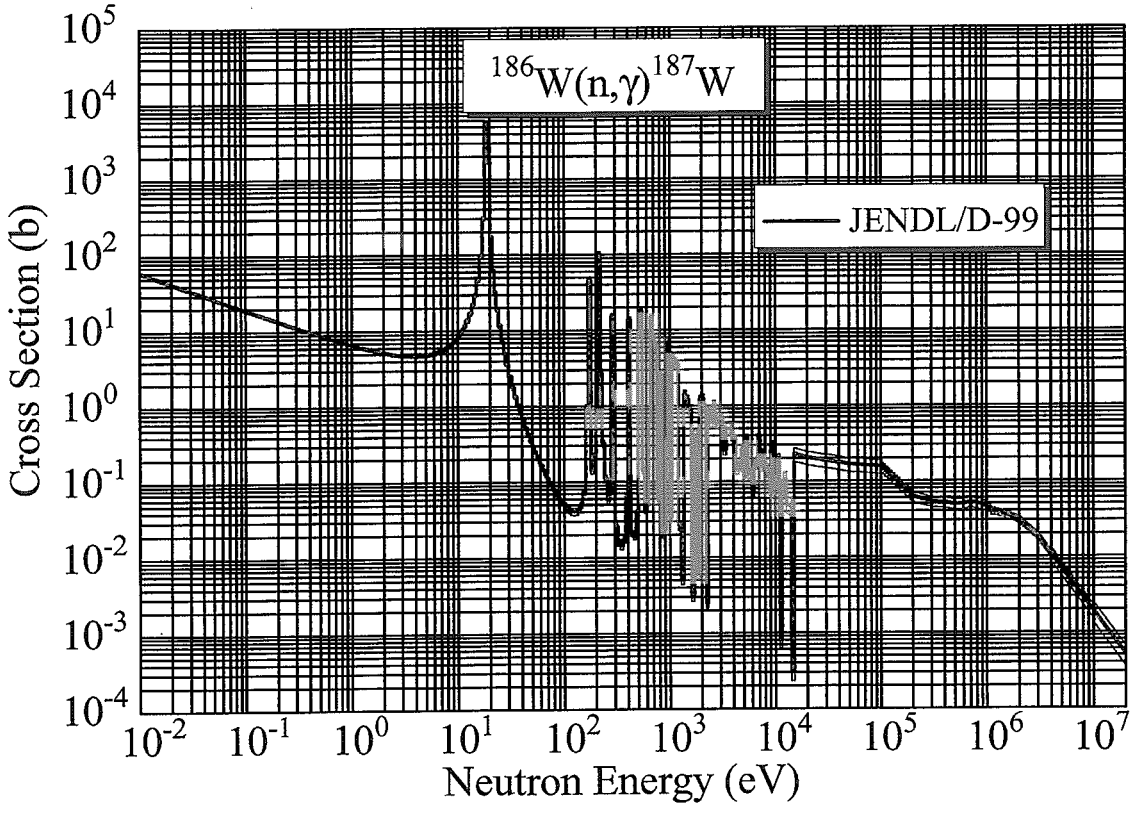

Fig. A.56 ^{186}W(n, γ)^{187}W cross section.

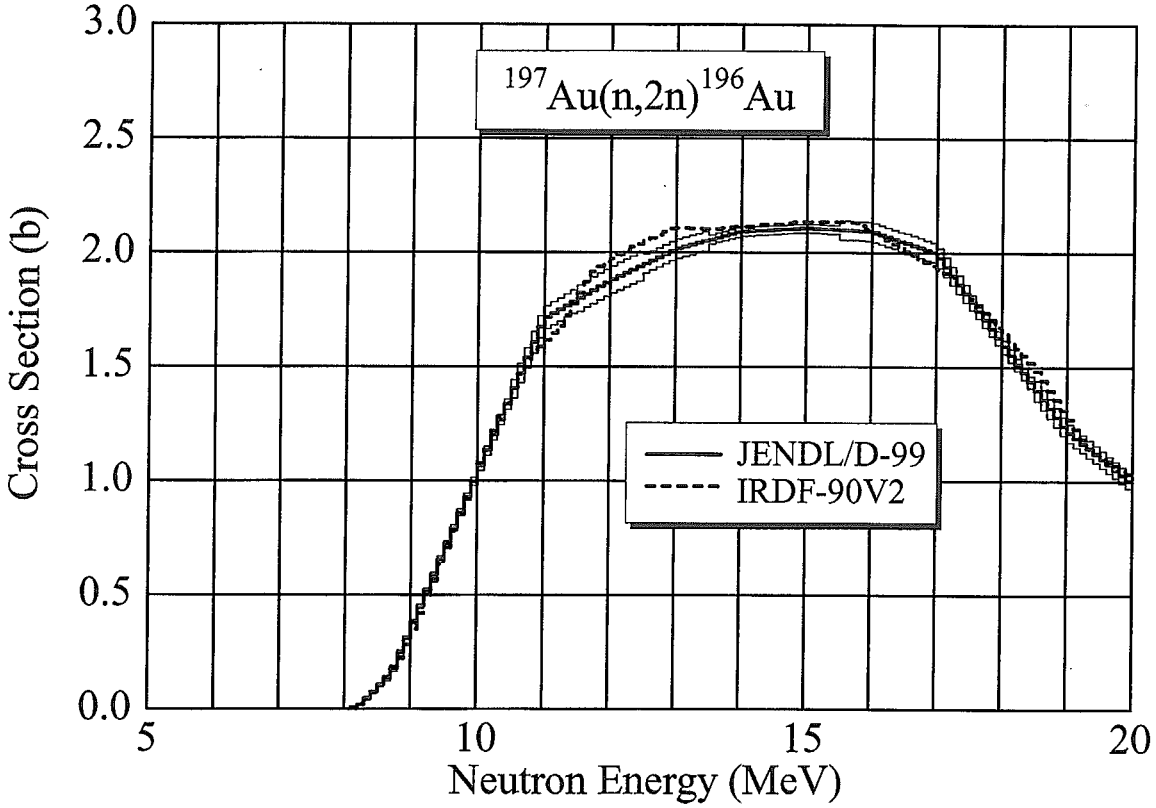

Fig. A.57 ^{197}Au(n, 2n)^{196}Au cross section.

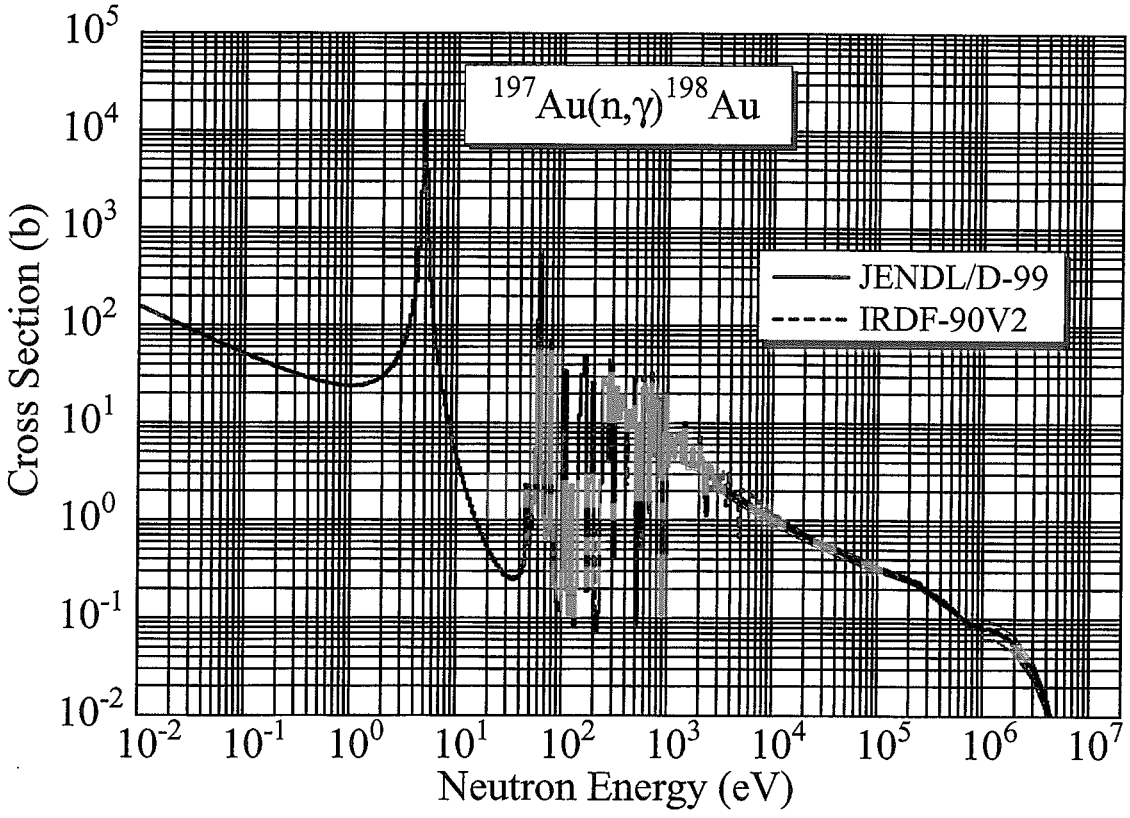

Fig. A.58 ^{197}Au(n, γ)^{198}Au cross section.

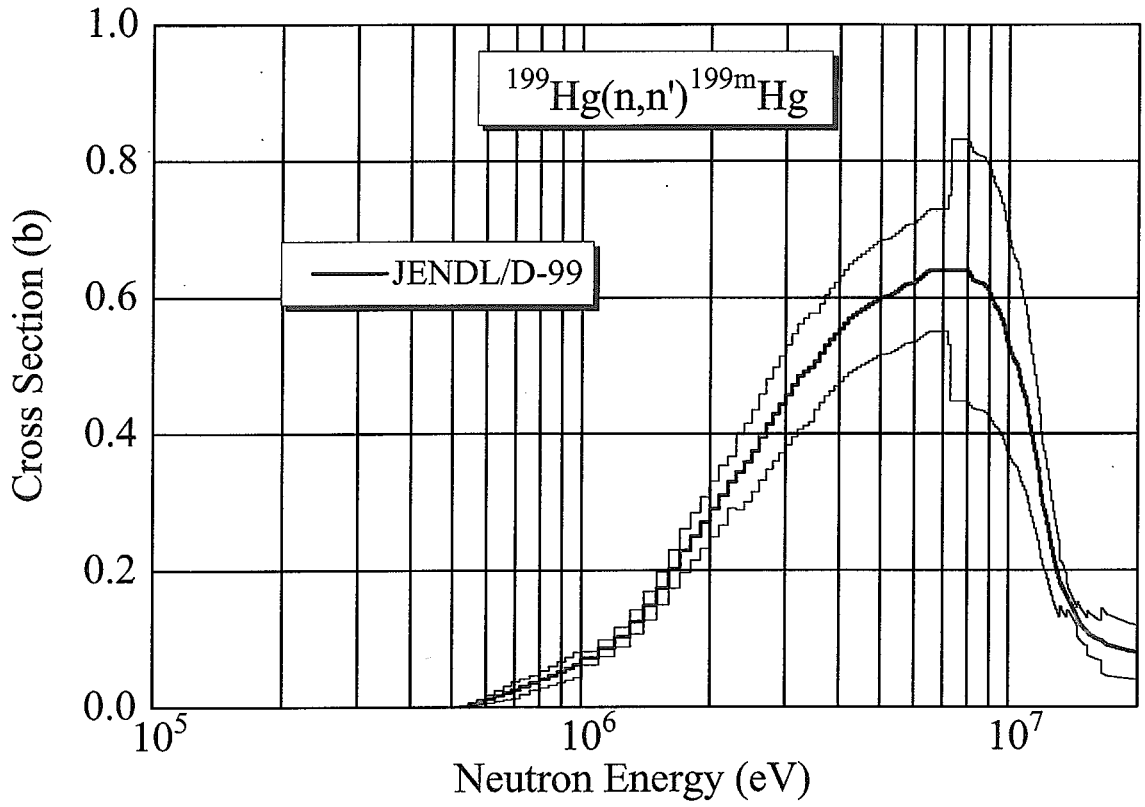

Fig. A.59 ^{199}Hg(n, n')^{199m}Hg cross section.

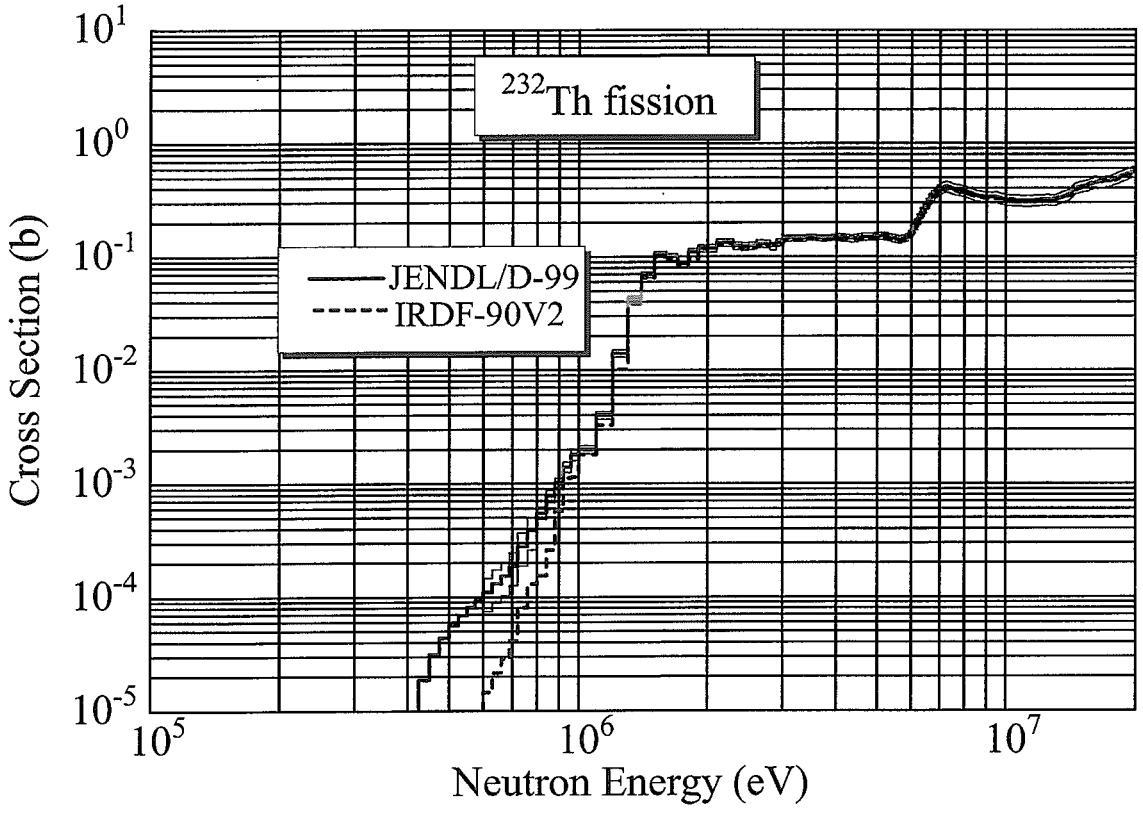

Fig. A.60 ^{232}Th fission cross section.

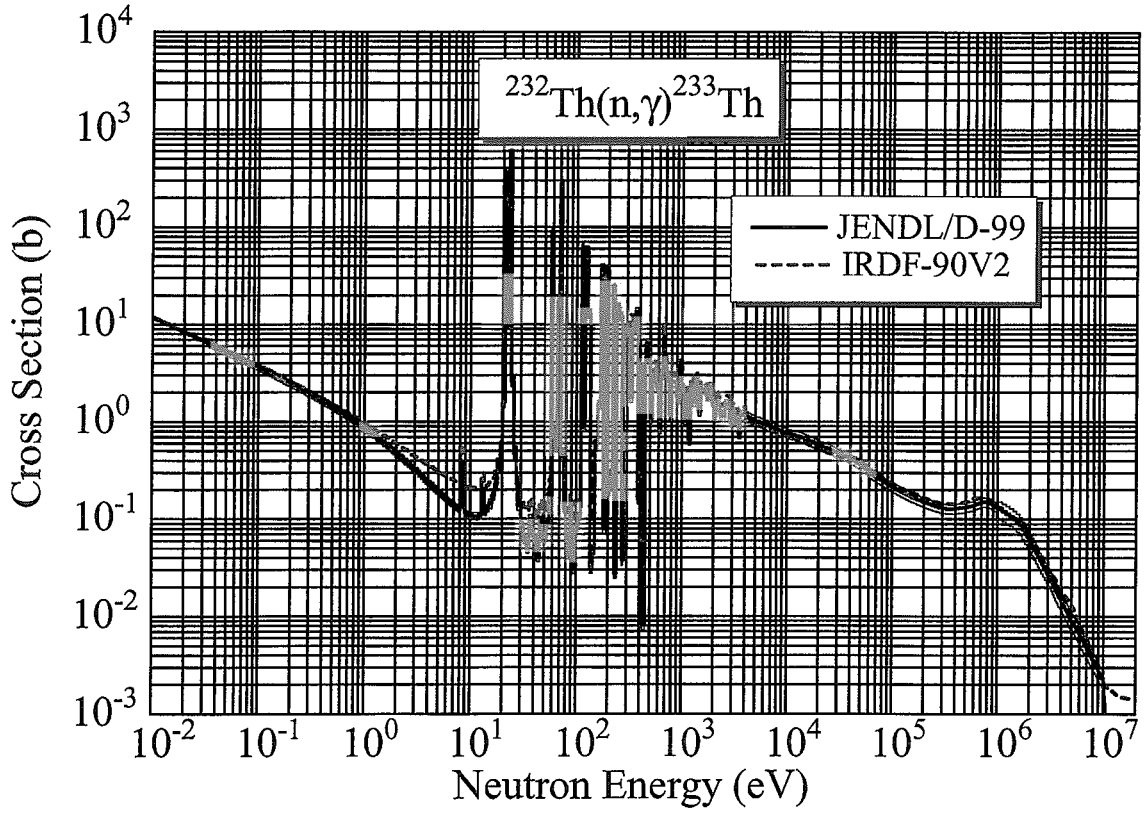

Fig. A.61 ^{232}Th(n, γ)^{233}Th cross section.

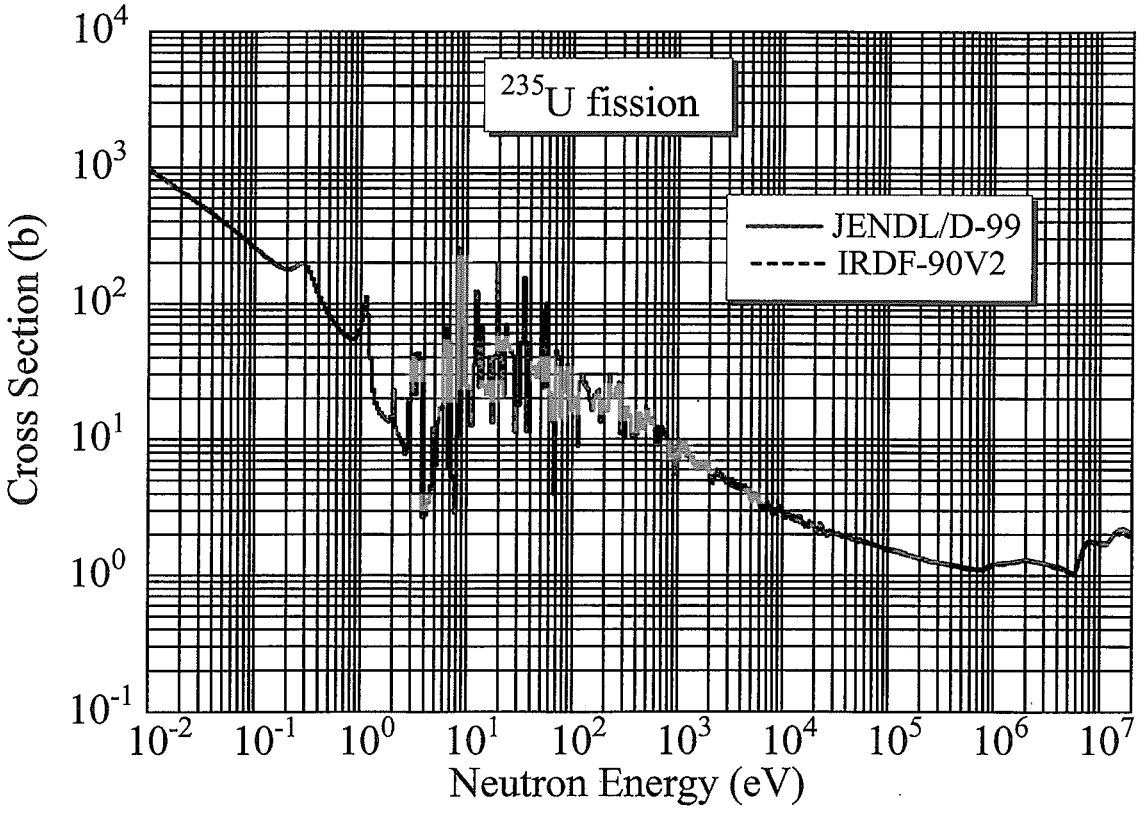

Fig. A.62 ^{235}U fission cross section.

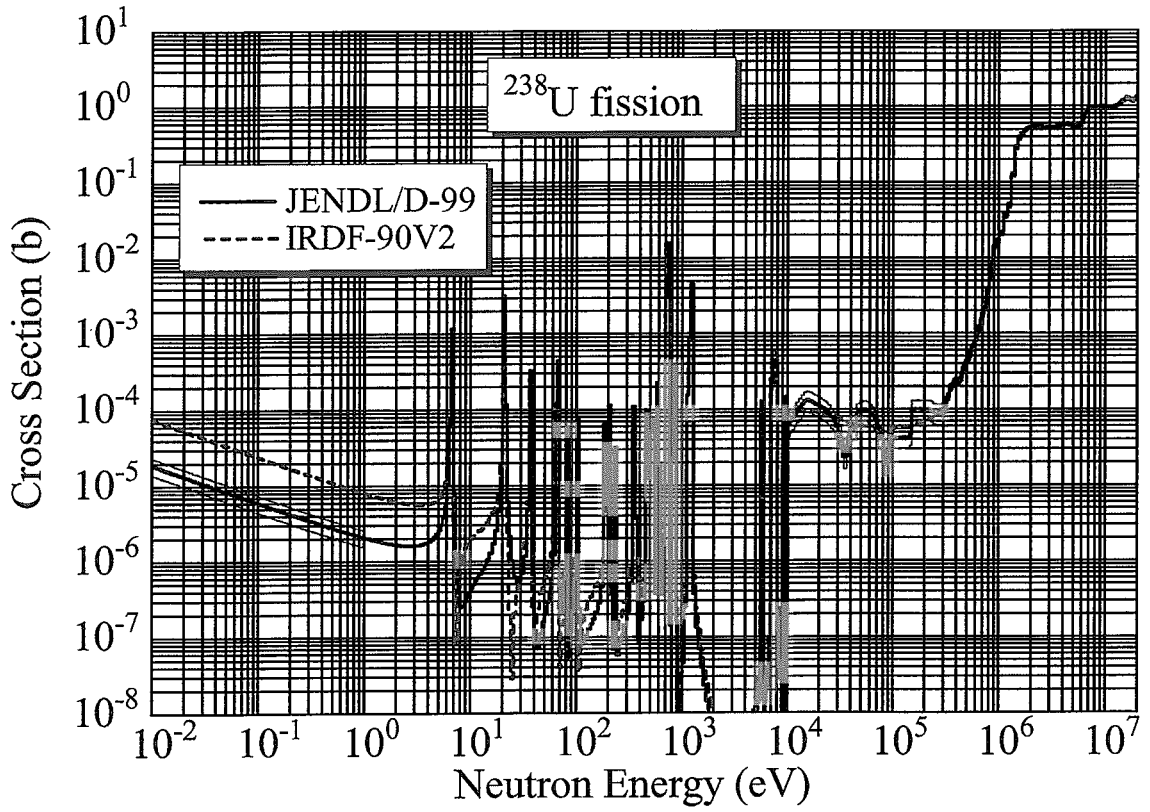

Fig. A.63 ^{238}U fission cross section.

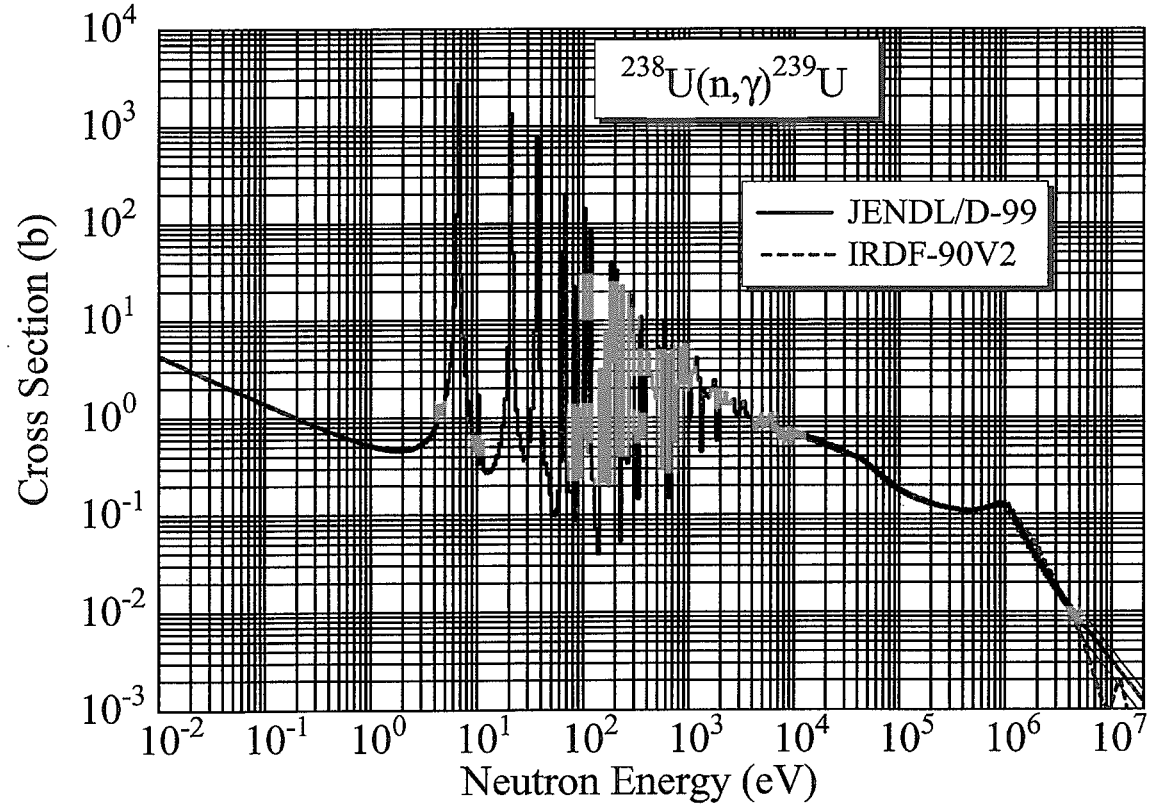

Fig. A.64 ^{238}U(n, γ)^{239}U cross section.

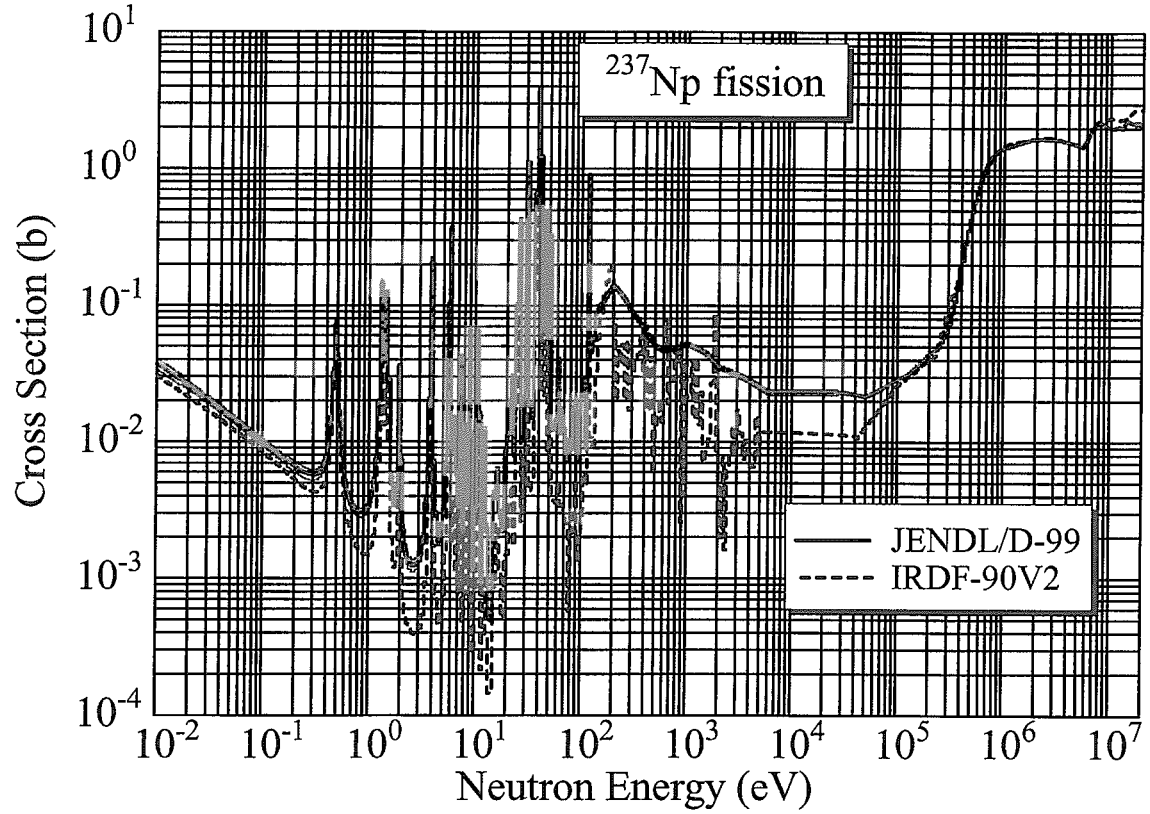

Fig. A.65 ^{237}Np fission cross section.

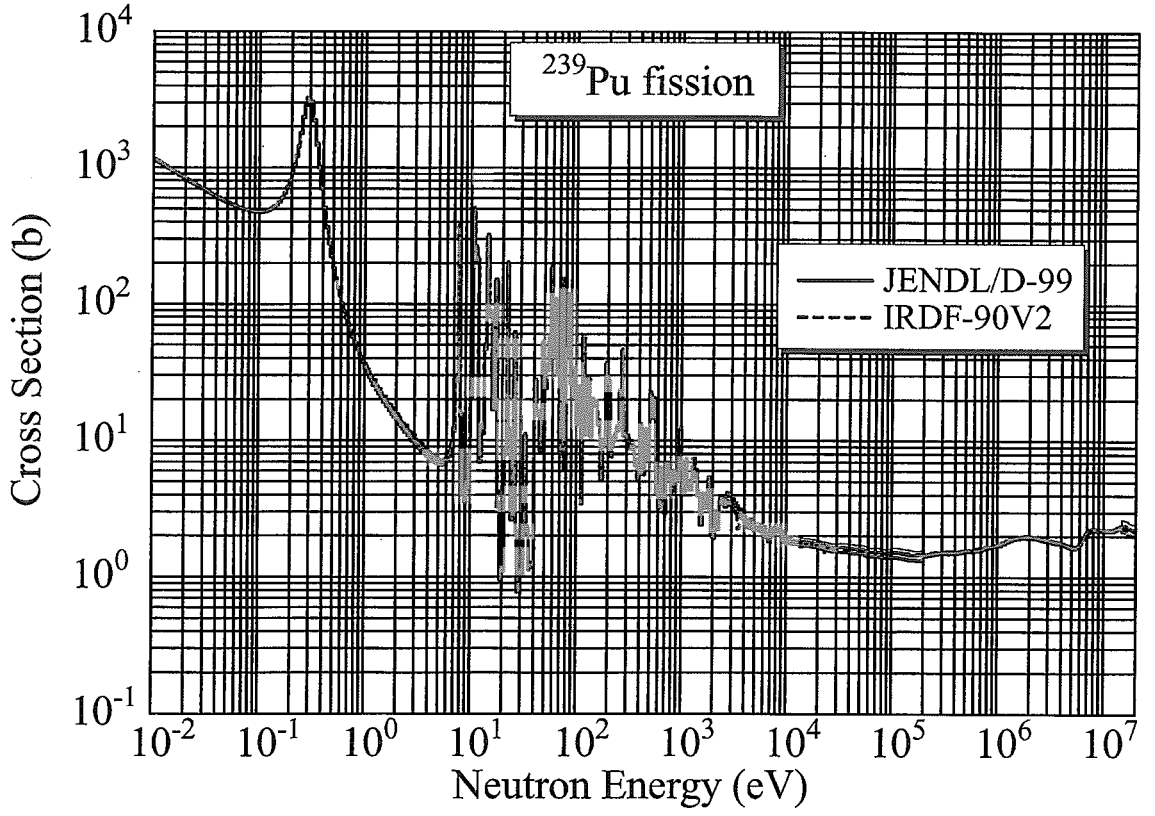

Fig. A.66 ^{239}Pu fission cross section.

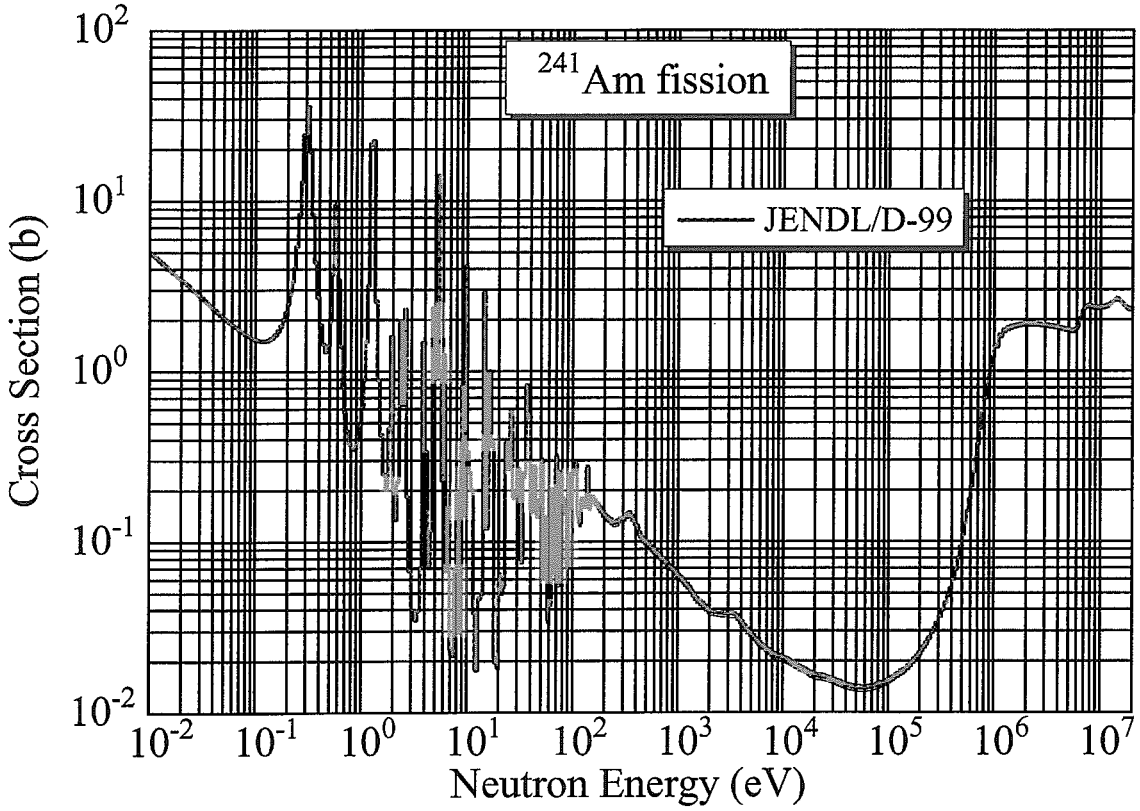

Fig. A.67 ^{241}Am fission cross section.

This is a blank page.

国際単位系 (SI) と換算表

表1　SI基本単位および補助単位

量	名称	記号
長さ	メートル	m
質量	キログラム	kg
時間	秒	s
電流	アンペア	A
熱力学温度	ケルビン	K
物質量	モル	mol
光度	カンデラ	cd
平面角	ラジアン	rad
立体角	ステラジアン	sr

表2　SIと併用される単位

名称	記号
分，時，日	min，h，d
度，分，秒	°，′，″
リットル	l，L
トン	t
電子ボルト	eV
原子質量単位	u

1 eV = 1.60218 × 10^{-19} J

1 u = 1.66054 × 10^{-27} kg

表3　固有の名称をもつSI組立単位

量	名称	記号	他のSI単位による表現
周波数	ヘルツ	Hz	s^{-1}
力	ニュートン	N	$m\cdot kg/s^2$
圧力，応力	パスカル	Pa	N/m^2
エネルギー，仕事，熱量	ジュール	J	N·m
工率，放射束	ワット	W	J/s
電気量，電荷	クーロン	C	A·s
電位，電圧，起電力	ボルト	V	W/A
静電容量	ファラド	F	C/V
電気抵抗	オーム	Ω	V/A
コンダクタンス	ジーメンス	S	A/V
磁束	ウェーバ	Wb	V·s
磁束密度	テスラ	T	Wb/m^2
インダクタンス	ヘンリー	H	Wb/A
セルシウス温度	セルシウス度	℃	
光束	ルーメン	lm	cd·sr
照度	ルクス	lx	lm/m^2
放射能	ベクレル	Bq	s^{-1}
吸収線量	グレイ	Gy	J/kg
線量当量	シーベルト	Sv	J/kg

表4　SIと共に暫定的に維持される単位

名称	記号
オングストローム	Å
バーン	b
バール	bar
ガル	Gal
キュリー	Ci
レントゲン	R
ラド	rad
レム	rem

1 Å = 0.1 nm = 10^{-10} m

1 b = 100 fm^2 = 10^{-28} m^2

1 bar = 0.1 MPa = 10^5 Pa

1 Gal = 1 cm/s^2 = 10^{-2} m/s^2

1 Ci = 3.7 × 10^{10} Bq

1 R = 2.58 × 10^{-4} C/kg

1 rad = 1 cGy = 10^{-2} Gy

1 rem = 1 cSv = 10^{-2} Sv

表5　SI接頭語

倍数	接頭語	記号
10^{18}	エクサ	E
10^{15}	ペタ	P
10^{12}	テラ	T
10^{9}	ギガ	G
10^{6}	メガ	M
10^{3}	キロ	k
10^{2}	ヘクト	h
10^{1}	デカ	da
10^{-1}	デシ	d
10^{-2}	センチ	c
10^{-3}	ミリ	m
10^{-6}	マイクロ	μ
10^{-9}	ナノ	n
10^{-12}	ピコ	p
10^{-15}	フェムト	f
10^{-18}	アト	a

（注）

1. 表1－5は「国際単位系」第5版，国際度量衡局 1985年刊行による。ただし，1 eVおよび1 uの値はCODATAの1986年推奨値によった。
2. 表4には海里，ノット，アール，ヘクタールも含まれているが日常の単位なのでここでは省略した。
3. barは，JISでは流体の圧力を表わす場合に限り表2のカテゴリーに分類されている。
4. EC閣僚理事会指令ではbar，barnおよび「血圧の単位」mmHgを表2のカテゴリーに入れている。

換　算　表

力	N(=10^5 dyn)	kgf	lbf
	1	0.101972	0.224809
	9.80665	1	2.20462
	4.44822	0.453592	1

粘度　1 Pa·s(N·s/m^2) = 10 P(ポアズ)(g/(cm·s))

動粘度　1 m^2/s = 10^4 St(ストークス)(cm^2/s)

圧力	MPa(=10 bar)	kgf/cm^2	atm	mmHg(Torr)	lbf/in^2(psi)
	1	10.1972	9.86923	7.50062 × 10^3	145.038
	0.0980665	1	0.967841	735.559	14.2233
	0.101325	1.03323	1	760	14.6959
	1.33322 × 10^{-4}	1.35951 × 10^{-3}	1.31579 × 10^{-3}	1	1.93368 × 10^{-2}
	6.89476 × 10^{-3}	7.03070 × 10^{-2}	6.80460 × 10^{-2}	51.7149	1

エネルギー・仕事・熱量	J(=10^7 erg)	kgf·m	kW·h	cal(計量法)	Btu	ft·lbf	eV
	1	0.101972	2.77778 × 10^{-7}	0.238889	9.47813 × 10^{-4}	0.737562	6.24150 × 10^{18}
	9.80665	1	2.72407 × 10^{-6}	2.34270	9.29487 × 10^{-3}	7.23301	6.12082 × 10^{19}
	3.6 × 10^6	3.67098 × 10^5	1	8.59999 × 10^5	3412.13	2.65522 × 10^6	2.24694 × 10^{25}
	4.18605	0.426858	1.16279 × 10^{-6}	1	3.96759 × 10^{-3}	3.08747	2.61272 × 10^{19}
	1055.06	107.586	2.93072 × 10^{-4}	252.042	1	778.172	6.58515 × 10^{21}
	1.35582	0.138255	3.76616 × 10^{-7}	0.323890	1.28506 × 10^{-3}	1	8.46233 × 10^{18}
	1.60218 × 10^{-19}	1.63377 × 10^{-20}	4.45050 × 10^{-26}	3.82743 × 10^{-20}	1.51857 × 10^{-22}	1.18171 × 10^{-19}	1

1 cal = 4.18605 J（計量法）
= 4.184 J （熱化学）
= 4.1855 J（15 °C）
= 4.1868 J（国際蒸気表）

仕事率　1 PS（仏馬力）
= 75 kgf·m/s
= 735.499 W

放射能	Bq	Ci
	1	2.70270 × 10^{-11}
	3.7 × 10^{10}	1

吸収線量	Gy	rad
	1	100
	0.01	1

照射線量	C/kg	R
	1	3876
	2.58 × 10^{-4}	1

線量当量	Sv	rem
	1	100
	0.01	1

（86年12月26日現在）